TAMPEREEN TEKNILLINEN YLIOPISTO
TAMPERE UNIVERSITY OF TECHNOLOGY

Katri Holm

Computational Modeling of IP_3 Receptor Function and Intracellular Mechanisms in Synaptic Plasticity

Julkaisu 1163 • Publication 1163

Tampere 2013

Tampereen teknillinen yliopisto. Julkaisu 1163
Tampere University of Technology. Publication 1163

Katri Holm

Computational Modeling of IP_3 Receptor Function and Intracellular Mechanisms in Synaptic Plasticity

Thesis for the degree of Doctor of Philosophy to be presented with due permission for public examination and criticism in Tietotalo Building, Auditorium TB109, at Tampere University of Technology, on the 22nd of November 2013, at 12 noon.

Tampereen teknillinen yliopisto - Tampere University of Technology
Tampere 2013

Supervisors	Adjunct Prof. Marja-Leena Linne Tampere University of Technology Finland
	Prof. Olli Yli-Harja Tampere University of Technology Finland
Reviewers	Dr. Volker Steuber University of Hertfordshire United Kindom
	Dr. Yann Le Franc University of Antwerp Belgium
Opponent	Assoc. Prof. Fidel Santamaria University of Texas at San Antonio United States

ISBN 978-952-15-3163-7 (printed)
ISBN 978-952-15-3218-4 (PDF)
ISSN 1459-2045

Abstract

Learning and memory in the brain have been shown to involve complex molecular interactions. In the field of computational neuroscience, mathematical modeling and computer simulations are combined with laboratory experiments to better understand the dynamics of these interactions. A vast number of computational models related to intracellular molecular mechanisms calls for means to compare them to each other. In this thesis, computational models and methods for understanding specific molecular mechanisms in synaptic plasticity, a phenomenon involved in learning, are studied and compared both quantitatively and qualitatively. The focus is set on the IP_3 receptor kinetics and the intracellular molecular mechanisms including processing of calcium ions in the postsynaptic neuron. Calcium has been shown to play an important role in different types of synaptic plasticity, only the mechanisms and dynamics for elevation of cytosolic calcium concentration vary. The IP_3 receptor, an intracellular calcium releasing channel, is one of the major factors responsible for the calcium elevation in neurons.

Firstly, the applicability of deterministic and stochastic approaches in modeling the IP_3 receptor kinetics, involving small number of molecules, is studied. In this case, the study shows that stochastic approach, especially Gillespie stochastic simulation algorithm, should be favored. Secondly, since a well-established model for IP_3 receptor function in neurons is lacking, this thesis provides not only tools for model comparison but also an insight to which model of the tens of models to choose. Using stochastic simulations, four IP_3 models are compared to experimental data to clarify how well they model the measured features in neurons. The results show that there are major differences in the statistical properties of the IP_3 receptor models although the models have originally been developed to describe the same phenomenon. Thirdly, this study shows that the models for postsynaptic signaling in synaptic plasticity are becoming more sophisticated by involving stochastic properties, incorporating electrophysiolocial properties of the entire neuron, or having diffusion of signaling molecules. Computational comparison of these models reveals that when using the same input, models describing the phenomenon in the same neuron type produce different

results.

One of the future goals of computational neuroscience is to find predictive computational models for biochemical and biophysical mechanisms of synaptic plasticity in different brain areas and cells of mammals. When describing a system of molecular events, the selection of modeling and simulation approach should be done carefully by keeping the properties of the modeled biological system in mind. Not only do theoreticians and modelers need to consider experimental findings, but the experimental progress could also be enhanced by using simulations to select the most promising experiments. As discussed in this thesis, attention paid to these issues should improve the utility of modeling approaches for investigating molecular mechanisms of synaptic plasticity. Only then is it possible to use the models to learn something new about the mammalian brain function.

Preface

The research for this thesis was carried out in the Department of Signal Processing at Tampere University of Technology, Finland during the years 2007-2012.

First of all, I wish to express my sincere gratitude to my supervisors Adjunct Prof. Marja-Leena Linne and Prof. Olli Yli-Harja for their guidance and support. I thank Marja-Leena for enabling great opportunities, teaching me science, and being inspiring. I also wish to thank Dr. Erik De Schutter for collaboration and for providing me the possibility to visit his research unit at Okinawa Institute of Science and Technology. I am grateful to all the collaborators and co-authors for their valuable contribution. I also want to thank the pre-examiners, Dr. Yann Le Franc and Dr. Volker Steuber, for their valuable comments on my thesis.

I wish to thank all my present and former colleagues in Computational Neuroscience Laboratory and Computational Systems Biology group. Special thanks go to Dr. Tiina Manninen, Dr. Eeva Toivari, Dr. Kaisa-Leena Aho, Heidi Teppola, M.Sc., and Riikka Havela, M.Sc., for their help and friendship. I also want to thank Dr. Tuula O. Jalonen for fruitful discussions.

I gratefully acknowledge the financial support from Tampere University of Technology President's Doctoral Programme, Tampere Doctoral Programme in Information Science and Engineering, Academy of Finland, Emil Aaltonen Foundation, Finnish Foundation for Technology Promotion, Otto A. Malm Foundation, and Finnish Cultural Foundation, Pirkanmaa Regional fund.

I owe gratitude to my parents, Raija and Heikki, and all the rest of my family for their help, their encouragement to find my own way in life and keeping my feet on the ground. Finally, my warmest thanks go to my husband, Mika, and my daughter, Aino, for their love.

Tampere, August 2013

Katri Holm, née Hituri

Abbreviations and symbols

N_a	Avogadro's constant
P_o	open probability
[A]	concentration of A, mol/l
AMPA	α-amino-3-hydroxy-5-methylisoxazole-4-propionic acid
AMPAR	AMPA receptor
ATP	adenosine triphosphate
Ca^{2+}	calcium ion
CA1	cornu ammonis 1
CaMKII	calcium/calmodulin-dependent protein kinase II
cAMP	cyclic adenosine monophosphate
CF	climbing fiber
CICR	Ca^{2+}-induced Ca^{2+} release
CME	chemical master equation
ER	endoplasmic reticulum
IP_3	inositol 1,4,5-trisphosphate
IP_3R	IP_3 receptor
LTD	long-term depression
LTP	long-term potentiation
NMDA	N-methyl-D-aspartate
NMDAR	NMDA receptor
ODE	ordinary differential equation

PF	parallel fiber
PIP_2	phosphatidylinositol 4,5-bisphosphate
PKA	protein kinase A
PLC	phospholipase C
PP1	protein phosphatase 1
RyR	ryanodine receptor
SBML	Systems Biology Markup Language
SDE	stochastic differential equation
SSA	stochastic simulation algorithm
STDP	spike-timing dependent plasticity
XML	Extensible Markup Language

Contents

List of Publications

The main contributions of this compound thesis are contained in the following publications (**Publications I–VI)**, which are referred to in the text by their Roman numerals. The publications are reproduced with permissions obtained from the publishers.

I. **Hituri K.** and Linne M.-L. (2013) Comparison of models for IP_3 receptor kinetics using stochastic simulations. *PLoS ONE* 8(4): e59618.

II. Manninen T.*, **Hituri K.***, Toivari E.*, and Linne M.-L. (2011) Modeling signal transduction in synaptic plasticity: evaluation and comparison of five models. *EURASIP Journal on Bioinformatics and Systems biology.* Volume 2011, Article ID 797250. *Equal contribution

III. Manninen T., **Hituri K.**, Hellgren Kotaleski J., Blackwell K.T., and Linne M.-L. (2010) Postsynaptic signal transduction models for long-term potentiation and depression. *Frontiers in Computational Neuroscience*, 4:152

IV. **Hituri, K.**, Achard, P., Wils, S., Linne, M.-L., and De Schutter, E. (2008) Stochastic modeling of inositol-1,4,5-trisphosphate receptors in Purkinje cell spine. In *Proceedings of 5^{th} International Workshop on Computational Systems Biology (WCSB08)*, Ahdesmäki, M., Strimmer, K., Radde, N., Rahnenführer, J., Klemm, K., Lähdesmäki, H., Yli-Harja, O. (eds.), pp. 57–60, Leipzig, Germany.

V. Intosalmi J., Manninen T., **Hituri K.**, Ruohonen K., and Linne M.-L (2008). Modeling of IP_3 receptor function using stochastic approaches. In *Proceedings of 5^{th} International Workshop on Computational Systems Biology (WCSB08)*, Ahdesmäki, M., Strimmer, K., Radde, N., Rahnenführer, J., Klemm, K., Lähdemäki, H., Yli-Harja, O. (eds.), pp. 69–72, Leipzig, Germany.

VI. Mäkiraatikka E., Manninen T., Saarinen A., Ylipää A., Teppola H., **Hituri K.**, Pettinen A., Yli-Harja O., and Linne M.-L. (2007) Stochastic simulation tools for cell signaling: Survey, evaluation and quantitative analysis. *Proceedings of the 2nd Conference on the Foundations of Systems Biology in Engineering (FOSBE2007)*, Allgöwer, F. and Reuss, M. (eds.), pp. 171–176, Stuttgart, Germany.

The author of this thesis, K. Holm (née Hituri), contributed to the **Publications I–VI** as follows. As the first author of **Publications I** and **IV**, K. Holm designed the study, implemented the models, performed simulations, and wrote the manuscripts. **Publication II** was jointly designed and written by T. Manninen, K. Holm, and E. Toivari. K. Holm participated in selection of the models, performed the simulations with two of the models, and wrote the corresponding parts of the manuscript. She also took part in designing the study, analyzing the results, making conclusions, and writing the manuscript. In **Publication III**, K. Holm participated in evaluation and categorization of the models, structuring of the article, and provided her expertise in cell biology and biochemistry, in addition to writing the manuscript as a part of the team. In **Publication V**, K. Holm provided the test case, participated in fine-tuning of the model, and commented on the manuscript. **Publication VI** was a result of collective effort, in which the authors evaluated, installed and tested different simulation tools and wrote corresponding parts of the manuscript. K. Holm participated in the evaluation of stochastic simulation tools, had a major role in preparation of the test case, and participated in analyzing the results and writing the manuscript.

Chapter 1

Introduction

1.1 Background and motivation

In the central nervous system, neurons communicate with each other using electrochemical signals. Each neuron uses complex systems of biochemical reactions to receive, process, and transmit information. Biochemical reactions are also involved in various other processes in neurons, such as maintaining homeostasis, providing energy, managing waste, and passing signals between different parts of the cell. Also gene expression is regulated by biochemical reactions through intracellular signal transduction pathways in a neuron.

The complex interactions in the brain can be studied using computational models of the observed phenomenona. Koch and Segev (1988) were one of the first to define the area of computational neuroscience. Recently Trappenberg (2010) has written a more concise definition for it: "Computational neuroscience is the theoretical study of the brain to uncover the principles and mechanisms that guide the development, organization, information processing, and mental abilities of the nervous system". Computational neuroscience can be seen as part of computational biology which provides models and tools for versatile research in all fields of biosciences. The development in computer hardware and architecture in addition to novel experimental methodology and increased amount of data has improved the possibilities to model and simulate the complex dynamics in cells, including the intracellular biochemical systems in neurons (Hellgren Kotaleski and Blackwell, 2010). Modeling and simulation, combined with experimental research, enable the study of the complex behavior of neurons. To understand the intrinsic dynamics of the neuron, the computational study of signal transduction networks is necessary, in addition to describing the electrophysiological behavior. In Hellgren Kotaleski and Blackwell (2010), dynamics is defined as time-dependent changes in the activity or quantity of a variable,

where the variable in context of biochemical systems refers to concentration of molecules or ions. In the same context, different from dynamics, kinetics studies the reaction rates of biochemical reactions and how the rates can be affected by chemical or physical factors (Hellgren Kotaleski and Blackwell, 2010).

In this thesis, the focus is on the models of inositol 1,4,5-trisphosphate (IP_3) receptor function and intracellular molecular mechanisms related to synaptic plasticity in postsynaptic neuron. Synaptic plasticity is the activity-dependent modification of the strength or efficacy of information transmission at synapses, and for over a century it has been proposed to play a central role in the capacity of the brain to incorporate transient experiences into long-lasting memory traces (Citri and Malenka, 2008). This thesis concentrates more particularly on postsynaptic mechanisms of two different forms of synaptic plasticity: long-term potentiation (LTP, long-term strengthening of a synapse) and long-term depression (LTD, long-term weakening of a synapse). Especially, in **Publication II** the focus is set on the synaptic plasticity in hippocampal CA1 pyramidal cells and striatal medium spiny neurons. More than a hundred molecules and ions, which are activated or affected in one way or another after neurotransmitter has bound to transmembrane receptors, are important in the synaptic plasticity (see, for example, Collins *et al.* (2005); Coba *et al.* (2009); Citri and Malenka (2008)). The complexity of the phenomenon makes the modeling challenging and multifaceted.

The development of a realistic model of neuron's biochemical system or even parts of it is not a straightforward task. Today, many researcher favor a data-driven approach (see also Janes and Yaffe (2006); De Schutter (2010*b*)) and develop biophysical models, instead of describing the experimentally observed phenomena in more theoretical manner using phenomenological approach. The reason for this might be that the community has realized the need for linking the phenomena and mechanisms with entities in computational models. Experimental data is required for describing the relationship of the concentration of molecules and ions and velocities of the reactions. Computational modeling as such provides the numerical means to describe the biological system but without parameter values defined using experimental data, a model lacks the dynamics. The model would be like a body without the muscles moving it. Many methods and tools, user-dependent and automated, for parameter estimation has been developed (see, for example, Moles *et al.* (2003); Wilkinson (2007)) and it is an own research area itself. In an ideal case, a model would be predictive, exhibiting emergent properties and could be used as a tool when designing the experiments further. The sparsity, diversity, and unavailability in data brings challenges to data-driven modeling and parameter estimation as also to the biological plausibility of the model. Large portion of the models describing both

synaptic plasticity and IP_3 receptor function have been developed using data-driven approach.

The computational models describing both postsynaptic signal transduction in synaptic plasticity (see **Publication III**) and IP_3 receptor function (for a review, see, for example, Sneyd and Falcke (2005)) are abundant. The models range from simple models with a single reversible reaction to detailed models with several hundred kinetic reactions. Roughly speaking there are two types of models, phenomenological and biophysical, for describing postsynaptic signal transduction in synaptic plasticity (Hellgren Kotaleski and Blackwell, 2010; **Publication III**). The diversity of models consolidates the fact that the underlying system is complex and can be approached from different angles. Not only the large amount and differences in complexity of the modeled phenomenon, but also the diversity in experimental data used in the model development, makes it difficult to compare the models and choose one to be used in research as such, or for further development. To help the model selection, methods for both quantitative and qualitative model comparison are needed. In **Publication III**, models of postsynaptic LTP and LTD are reviewed and compared in a quantitative manner. **Publication I** provides methodology and quantitative insight for the comparison of IP_3 receptor models and **Publication II** for models of LTP and LTD.

In addition to large amount of models, also the variety in modeling and simulation approaches and simulation tools has increased. There exist a number of different mathematical approaches to describe the dynamics of biochemical systems (see, for example, Turner *et al.* (2004); Hellgren Kotaleski and Blackwell (2010)) and also a great variety of tools implementing them (see, for example, Arkin (2001); Pettinen *et al.* (2005); Alves *et al.* (2006)). The selection of a right modeling and simulation approach is important in order to be able to draw biologically relevant conclusions based of the simulation results and selection of a right tool in order to make the modeling, simulation, and handling of the simulation results easy.

Stochasticity and noise have an important role in biological systems (Rao *et al.*, 2002). Especially in the context of signal transduction networks, stochasticity has been shown to have an impact on individual pathways and synaptic network properties (Bhalla, 2004*a*,*b*). It is known that not in all cases deterministic approaches give biologically valid results (Gillespie, 1976) and they are not always capable of modeling the random behavior observed with small numbers of molecules (Turner *et al.*, 2004; Barrio *et al.*, 2006; Choi *et al.*, 2010; Antunes and De Schutter, 2012; De Schutter, 2012), as concluded also in case of IP_3 receptor model in **Publication IV**. Stochastic modeling is therefore increasingly used for describing the dynamics of a biochemical system. The need for stochastic approaches is further addressed in Chapter 3.2.

1.2 Objectives of thesis

This doctoral thesis research belongs to the field of computational neuroscience and to some extent computational systems biology. In computational neuroscience, models describing various phenomena and, consequently, information processing in the nervous system are developed based on experimental evidence. The ultimate goal of the field is to understand how the nervous system and particularly how the brain works. The publications presented in this thesis were done in close collaboration with other researchers having different scientific backgrounds, such as biochemistry, chemistry, neuroscience, mathematics, and computer science.

This Ph.D. thesis research uses computational and theoretical sciences including applied mathematics to describe molecular level processes in the brain. The main goal of this work is to find a model for IP_3 receptor that is simple enough yet succeeds in reproducing experimental data from neurons satisfactorily. In addition to modeling work itself, also new approaches for model comparison need to be developed. A growing problem in computational neuroscience is the rapidly increasing amount of models describing the same or similar cell level phenomena, e.g. LTP or LTD, and, at the same time, lack of formal ways of comparing large models.

Specifically, this doctoral thesis aims to:

1. compare and analyze computational models for IP_3 receptor in quantitative manner by means of simulation,
2. compare and analyze computational models for postsynaptic signal transduction in synaptic plasticity both in qualitative manner and in quantitative manner by means of simulation,
3. study the effects of small number of molecules on IP_3 receptor function and, especially, to how the small number of molecules affects the selection of suitable, numerically correct modeling and simulation approach, and
4. evaluate and compare stochastic simulation tools intended for describing the time-series behavior of systems of biochemical reactions.

1.3 Outline of thesis

This thesis begins with an introduction to the context of the work in neuroscience and cell biology. Chapter 2 presents the concept of synaptic plasticity and the fundamental role of IP_3 receptor in synaptic plasticity. In Chapter

3, deterministic and stochastic approaches and tools for modeling and simulation are presented, in addition to summarizing the models developed to describe the IP_3 receptor and the postsynaptic signaling in synaptic plasticity and presenting the approaches to compare models used in this thesis. Chapter 4 summarizes the results and the conclusions of the original publications (**Publication I-VI**). Finally, the results of this thesis are discussed in Chapter 5.

Chapter 2

Synaptic Plasticity

In this thesis, the focus is set on studying models of a crucial parts of intracellular signal transduction networks in neurons related to learning and memory (see e.g. Figure 2.1). In cerebellum, IP_3 receptor has a crucial role as a coincidence detector of the two input signals to Purkinje cells and thus it is a key player in an electrophysiological phenomenon called long-term depression (LTD) of synaptic activity. IP_3 receptor is a ligand-gated calcium (Ca^{2+}) channel inside the cell, located on the endoplasmic reticulum (ER), and it contributes to calcium induced calcium release to cytosol, together with ryanodine receptors (RyRs). IP_3 receptor thus has also major role in calcium dynamics in other neurons. Ca^{2+} is an ubiquitous cellular messenger and, especially in neurons, dynamical changes in Ca^{2+} concentration are involved, among others, in plasticity and development (see, for example, reviews Libersat and Duch (2004); Michaelsen and Lohmann (2010)).

2.1 Molecular mechanisms of synaptic plasticity

Synaptic plasticity is the way neurons regulate the strength of information transmission in the brain and it has been proposed to play a central role in the capacity of the brain to incorporate transient experiences into persistent memory traces (Citri and Malenka, 2008). One of the first ones to propose synaptic plasticity was Dr. Hebb (Hebb, 1949): "When an axon of cell A is near enough to excite B and repeatedly or persistently takes part in firing it, some growth process or metabolic change takes place in one or both cells such that A's efficiency, as one of the cells firing B, is increased." Hebb's postulate is widely used, perhaps due to its simplicity, but has also quite limited capabilities (Sjöström *et al.*, 2008). The regulation of synaptic plasticity is activity-dependent, it happens at the molecular level in the synapse and can show either strengthening (potentiation) or weakening (depression) of

the synapse's efficacy (reviewed by Sjöström *et al.* (2008)). Depending on the activity of presynaptic and postsynatic neurons, surrounding glial cells, and even activity in the neuronal network level, the molecular organization and the length of the plastic modifications can vary and different types of synaptic plasticity can be observed. Short-term synaptic plasticity (for a recent review, see, for example, Klug *et al.* (2012)) can also be observed in addition to long-term synaptic plasticity which is of interest in this thesis.

It is important to realize that different forms of synaptic plasticity share a common biochemical background consisting at least of receptors, activation cascades of kinases and phosphatases in addition to calcium dynamics. To induce synaptic plasticity, there are several biochemical pathways activated in the postsynaptic neuron after the stimulation from the presynaptic neuron using glutamate (see Figure 2.1). Glutamate, together with depolarization of postsynaptic neuron, causes an elevation in cytosolic Ca^{2+} concentration which is turn induces activation cascade. Synaptic plasticity is modulated by various neuromodulators, such as dopamine and nitric oxide (Ito, 2002; Citri and Malenka, 2008; Hellgren Kotaleski and Blackwell, 2010) and also by astrocytes (Perea and Araque, 2007; Perea *et al.*, 2009; Henneberger *et al.*, 2010; Santello and Volterra, 2010; Henneberger *et al.*, 2010).

Different experimental procedures have been used to identify different types of synaptic plasticity (for a recent review, see Markram *et al.* (2011)). One of the plasticity forms is homeostatic plasticity (Turrigiano and Nelson, 2004; Turrigiano, 2011) which may be particularly important in the developing nervous system. In homeostatic plasticity, the excitability of the neuron is modified intrinsically, for example, by changing the proportions of different ion channel, which mechanistically differs from LTP and LTD.

Spike-timing dependent plasticity (STDP) has received considerable interest over the past years (Shouval *et al.*, 2010; Markram *et al.*, 2011). In STDP, LTP and LTD are presented by spike timing of presynaptic and postsynaptic neurons, presynaptic firing rate or presynaptic firing paired with postsynaptic holding potential (Graupner and Brunel, 2007). Basically, if the presynaptic neuron fires just a little before postsynaptic neuron, LTP is presented, and if the cells fire in opposite order, one sees LTD (Sjöström *et al.*, 2008). STDP was first effectively demonstrated by Markram *et al.* (1997).

One of the most studied forms of synaptic plasticity are the frequency-dependent long-term potentiation (LTP) and long-term depression (LTD) in cornu ammonis 1 (CA1) region of the hippocampus. Bliss and Lømo (1973) and Bliss and Gardner-Medwin (1973) were among the first ones to discover the "traditional", hippocampal LTP. Later, various different forms of LTP and LTD, varying in duration and molecular mechanisms, have been discovered in different parts of the brain (reviewed, for example, in Sjöström *et al.* (2008); Markram *et al.* (2011)). The duration of LTP is long which

means the phenomenon lasts at least an hour and up to days, weeks, and even months (Sjöström *et al.*, 2008). Experimentally, LTP is triggered with high-frequency stimulations, as LTD is with low-frequency stimulation in hippocampus. In LTP, the strength of synapse in a persistently increased meaning that the neuron fires action potentials easily. Typically, hippocampal LTP is triggered by the activation of N-methyl-D-aspartate (NMDA) receptors (NMDAR), which possibly also act as co-incidence detectors of pre- and postsynaptic firing (see, for example, Malenka and Bear (2004); Citri and Malenka (2008); Sjöström *et al.* (2008)). The activation of NMDARs triggers Ca^{2+} influx, which in turn lead to activation of different kinases, such as calcium/calmodulin-dependent protein kinase II (CaMKII), and phosphatases, such as protein phosphatase 1 (PP1), and cascades of them (see Figure 2.1). Kinases and phosphatases and phosphorylation-dephosphorylation cycles caused by them have been studied also using models (reviewed in **Publication III**) and have been suggested to act as the mechanism for information storage in neurons (Delord *et al.*, 2007). There has been debate whether LTP or even synaptic plasticity could be the actual mechanism for learning in the mammalian brain (Sjöström *et al.*, 2008; Bramham, 2010). Despite this, valuable understanding of neurons' behavior has been collected.

In addition to hippocampus, LTD, specifically the non-NMDAR-dependent plasticity has been first observed in cerebellar Purkinje cells (Ito *et al.*, 1982; Konnerth *et al.*, 1992). In Purkinje cells, LTD is induced by the simultaneous stimuli from parallel fibers (PFs, axons of granule cells) and climbing fiber (CF) originating from outside of cerebellum, the inferior olive. At the molecular level, cerebellar LTD, in addition to NMDAR-dependent LTD, are due to the phosphorylation and removal of α-amino-3-hydroxy-5-methylisoxazole-4-propionic acid (AMPA) receptors (AMPAR) from the plasmamembrane (Beattie *et al.*, 2000; Ito, 2002) as opposite to hippocampal LTP where AMPARs are inserted to plasmamembrane after phosphorylation. However, before AMPA receptors are removed a large amount of biochemical reactions, including phosphorylations and dephosphorylations, need to occur (Ito, 2002). The signal transduction network involved in LTD induction, or more particularly, the pathways activated after the two stimulating inputs, PF and CF, in Purkinje cells is quite well understood (reviewed in Ito (2002)).

2.2 Intracellular calcium dynamics

Both experimental and theoretical studies have shown that intracellular signaling, especially changes in intracellular Ca^{2+} concentration, plays an important role in the function of neurons and other cells. Both LTP and LTD

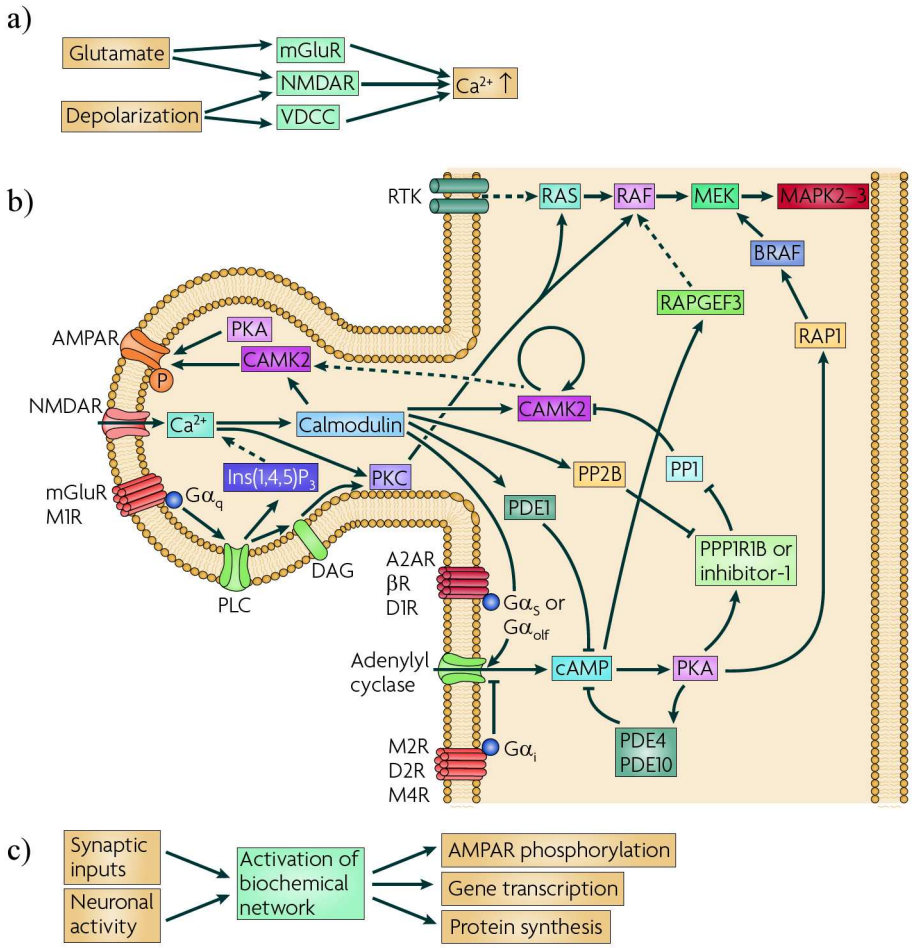

Figure 2.1. Signal transduction pathways activated in synaptic plasticity. (a) Glutamate, together with depolarization of postsynaptic neuron, causes an elevation in cytosolic Ca^{2+} concentration, (b) Elevated Ca^{2+} concentration causes signaling cascade to activate, (c) Synaptic inputs, together with neuronal activity activated biochemical network which affect the cell in multiple levels. $\rightarrow$ positive effect/activation, $\dashrightarrow$ indirect positive effect/activation, $\dashv$ negative effect/inhibition. Adapted by permission from Macmillan Publishers Ltd: Nature Reviews Neuroscience (Hellgren Kotaleski and Blackwell, 2010), copyright (2010).

are dependent on elevation of cytosolic Ca^{2+} concentrations. Short and strong postsynaptic Ca^{2+} elevation induce LTP and smaller and longer elevation trigger LTD (Sjöström *et al.*, 2008). Therefore, it is important to study the dynamics (i.e. the time course behavior) of the complex signaling

events in neurons (Franks and Sejnowski, 2002; De Schutter and Smolen, 1998).

Ca^{2+} is an important intracellular messenger and it regulates a great variety of neuronal processes like excitability, associativity, neurotransmitter release, synaptic plasticity, and gene expression (for a review, see, for example, Berridge (1998)). At rest, the cytosolic Ca^{2+} concentration is kept low and after stimulus it is released from outside the cell through ion channels, such as NMDARs or voltage-gated Ca^{2+} channels, and from intracellular stores, i.e. ER and mitochondria. Also different kind of buffers, such as parvalbumin or calbindin, regulate the Ca^{2+} levels. IP_3 receptors and RyRs release Ca^{2+} from ER but their dynamics differ. RyRs act on fast time-scale as IP_3 receptors on slower time-scale. In neurons, Ca^{2+} is an active player in various signal transduction pathways in synapses, thus modifying the properties of neurons over time. An increase in postsynaptic intracellular Ca^{2+} concentration is required for induction of both LTP and LTD (Lynch *et al.*, 1983; Malenka *et al.*, 1988; Konnerth *et al.*, 1992; Miyata *et al.*, 2000). A rise in Ca^{2+} concentration triggers the activation of many intracellular enzymes, mainly kinases and phosphatases (see Figure 2.1). As in other cell, in neurons the Ca^{2+} is originated from extracellular or intracellular sources.

Ca^{2+} has been shown to have an important role not only in healthy cells but in cells whose functioning has been disturbed. Ca^{2+} is also related to development (see, for example, Michaelsen and Lohmann (2010)) and degeneration of neurons (see, for example, Banerjee and Hasan (2005); Wojda *et al.* (2008); Foskett (2010)). The calcium dynamics in neurons have been shown to be altered in Down syndrome (Cárdenas *et al.*, 1999) and in many neurological disorders including, for example, Alzheimer's disease and Parkinson's disease (for a review, see Missiaen *et al.* (2000); Foskett (2010); Tanaka *et al.* (2013)). Computational modeling provides tools to understand the complex molecular events inside the cell leading to pathological conditions.

2.3 Inositol 1,4,5-trisphosphate receptor

One of the most important factors in calcium dynamics in neurons is the IP_3. This protein, a ligand binding intracellular calcium channel, is responsible for releasing calcium from endoplasmic reticulum to cytosol (marked as $Ins(1,4,5)P_3$ in Figure 2.1). IP_3 receptors are mainly expressed on ER but have also been found to mediate the Ca^{2+} release from other organelles like nuclear envelope, Golgi apparatus, and secretory vesicles (Foskett *et al.*, 2007). In some cell types, for example in DT40 cells, IP_3 receptors have been found in the plasma membrane (Taylor *et al.*, 2004). It has also been

observed that IP_3 receptors are spatially organized in high density clusters (Banerjee and Hasan, 2005).

2.3.1 Structure and regulation of IP_3 receptor

IP_3 receptor is a large protein ($\sim$1 MDa) consisting of four subunits each of which has a single IP_3 binding site. Based on the sequence analysis and structural studies it is known that each of the subunits has one IP_3 binding site and the binding is stoichiometric (Foskett *et al.*, 2007). Each IP_3 receptor type (1, 2, or 3) has slightly different steady-state and kinetic properties and is expressed in different proportions in different tissues. For example, in neurons the type 1 is the most abundant (Sharp *et al.*, 1999). In general, all types of IP_3 receptor have the similar type of function and same factors regulate (IP_3 and Ca^{2+}) or modify (ATP, calmodulin) the function. The structure of IP_3 receptor has been lately studied also in more detail with molecular dynamics simulations (Ida and Kidera, 2013). The structure and function of IP_3 receptor have been reviewed, for example, by Foskett *et al.* (2007) and Taylor and Tovey (2010).

IP_3R is activated and opened by both IP_3 and Ca^{2+}. Ca^{2+} also acts as the inhibitor of IP_3 receptor in higher concentrations. IP_3 is produced from phosphatidylinositol 4,5-bisphosphate (PIP_2) by phospholipase C (PLC). After a cell is stimulated (for example by glutamate in neurons) certain G protein-linked receptors are activated. These, in turn, can activate PLC. ER acts as a Ca^{2+} store, and while open, IP_3 receptor can release Ca^{2+} from ER lumen to the cytosol. Transient rises or oscillations in Ca^{2+} concentration can then activate various enzymes and even induce changes in the transcriptional level.

Several or all of the subunits of IP_3 receptor need to bind IP_3 to achieve stable open state (Marchant and Taylor, 1997; Taylor *et al.*, 2004). All the details of the co-operation of the two regulators (IP_3 and Ca^{2+}) are not yet fully understood, but it is known that binding of IP_3 has two important consequences. It inhibits the binding of Ca^{2+} to an inhibitory site and permits Ca^{2+} to bind to activating site (sequential binding) (Taylor *et al.*, 2004), where the latter promotes the opening of an ion channel. Because IP_3 receptor is regulated by Ca^{2+}, it can respond to its own activity and affect also the activities of nearby IP_3 receptors (Taylor *et al.*, 2004). This causes Ca^{2+} sparks, which are sudden localized increases in cytosolic Ca^{2+} concentration, also called as puffs. One of the most important cellular functions IP_3 receptor has is Ca^{2+}-induced Ca^{2+} release (CICR), where release of a small amount of Ca^{2+} causes a larger release (Rizzuto, 2001). This phenomenon is enhanced by the short distance between clustered IP_3 receptors. Sparks have been found in many types of cells including neurons (Melamed-Book *et al.*, 1999).

2.3.2 The role of IP_3 receptor in the brain

In addition to RyRs, IP_3 receptors contribute to CICR in brain cells. As an exception, RyRs are not expressed in cerebellar Purkinje cell spine and thus the role of IP_3 receptor in local Ca^{2+} dynamics is pronounced (Walton *et al.*, 1991; Barbara, 2002). The IP_3 receptors are highly expressed in Purkinje cell spines (Sharp *et al.*, 1999) and have a major role in cerebellar LTD (Ito, 2001) and in maintenance of spine morphology and synapses in Purkinje cells (Sugawara *et al.*, 2013). IP_3 receptor has been shown to act as a coincidence detector of the PF and the CF inputs both experimentally (Wang *et al.*, 2000; Sarkisov and Wang, 2008) and computationally (Doi *et al.*, 2005). In addition to neurons, the findings of Tanaka *et al.* (2013) suggest that IP_3-mediated astrocytic Ca^{2+} signaling correlates with the formation of functional tripartite synapses in the hippocampus.

IP_3 receptor has been associated with multiple neurological diseases (Foskett, 2010) which is not a surprise because of its ubiquitous expression and involvement in variety of cellular function. However, there are only few diseases linked directly to mutations in IP_3 receptor gene: spinocerebellar ataxias 15 and 16 (see, for a review, Foskett (2010)). Not only mutations in the IP_3 receptor gene itself can cause disease, but mutations in other genes in diseases such as Huntington's disease, Alzheimer's disease, and some spinocerebellar ataxias also influence on the IP_3 receptor function. Recently, for example, Demuro and Parker (2013) have shown that intracellular Aβ oligomers affect IP_3-mediated Ca^{2+} and consequent liberation of Ca^{2+} from the endoplasmic reticulum is cytotoxic, potentially representing a pathological mechanism in Alzheimer's disease. The effect might further be aggravated by mutations in presenilin proteins to promote opening of IP_3 receptors (Demuro and Parker, 2013).

The experimental data on IP_3 receptors in neurons that could be used in quantitative modeling is limited or not publicly available. In most of the cases some data can be found in the publications but the raw data, which would have been valuable, for example, in the present work, is not available. Next the data that can be found in the literature is discussed. Bezprozvanny *et al.* (1991) are one of the first ones to report that the open probability of IP_3 receptor isolated from canine cerebellum is dependent on cytosolic $[Ca^{2+}]$ and this dependence is bell-shaped with maximum reached around 250 nM while $[IP_3] = 2\ \mu$M. The open probability is also dependent on cytosolic $[IP_3]$, but this dependence is not bell-shaped but s-shaped instead (Watras *et al.*, 1991; Marchenko *et al.*, 2005; Taufiq-Ur-Rahman *et al.*, 2009).

Few articles report the mean open time of native cerebellar IP_3 receptor: 2.9 ms $\pm$ 0.2 ms for canine IP_3 receptor (Bezprozvanny and Ehrlich, 1994) and 4.2 $\pm$ 0.5 ms for rat IP_3 receptor (Kaznacheyeva *et al.*, 1998). In addition to this, it is shown that the open and closed time distributions follow the

exponential distribution (Bezprozvanny and Ehrlich, 1994; Kaftan *et al.*, 1997; Kaznacheyeva *et al.*, 1998; Moraru *et al.*, 1999). Experimental data by Khodakhah and Ogden (1995) and Fujiwara *et al.* (2001) indicate that the IP_3 affinity of the receptor is about five times lower *in vivo* than in the constructed lipid bilayers. To make the simulation results comparable with the experimental results, both 2 μM and 10 μM concentrations of IP_3 were used in the simulations in **Publication I**.

Chapter 3

Methods for Modeling and Simulation

Computational modeling provides powerful tools for describing biochemical reaction systems in neurons (Bhalla and Iyengar, 1999; Eungdamrong and Iyengar, 2004; Hellgren Kotaleski and Blackwell, 2010). To reveal the emergent properties of these system, the time-evolution of the systems is simulated. Thus it is possible to reach a better understanding on the mechanisms underlying, for example, synaptic plasticity in neurons. In this Chapter, the methodology for modeling and simulation of a system of biochemical reactions is described. In addition, the approaches used for model comparison in this work are presented.

3.1 Deterministic approach

To reach a system-level understanding of the behavior of a neuron, it is necessary to model the time evolution of the system in a quantitative manner. The dynamics, or in other words, the time-series behavior of concentrations of chemically reacting species, ie. molecules or ions, can be calculated with *deterministic* approach by solving a set of ordinary differential equations (ODEs). It is possible to describe the time dependent change in concentration with ODEs based on the law of mass action or any other mathematical description, such as Michaelis-Menten kinetics. In computational neuroscience, a widely used Hodgkin-Huxley model (Hodgkin and Huxley, 1952) is a system of ODEs that is used to describe the electrical properties of a neuron. Here the formulation of ODEs based on the law of mass action is described in more detail.

Let us assume, that there are two types of molecules, IP_3 receptor (R) and IP_3, available in the cytosol. The reaction where R binds IP_3 molecule and a

receptor-ligand (RI) complex is formed, is described with following reaction equation:

$$\mathrm{R} + \mathrm{IP_3} \underset{k_b}{\overset{k_f}{\rightleftharpoons}} \mathrm{RI} \tag{3.1}$$

The reaction is reversible as the RI complex can dissociate back to IP_3 receptor and IP_3. k_f is the forward rate constant and k_b the backward rate constant. The constants define the speed of the forward and backward reactions, as also the chemical equilibrium of the reaction. Many times it is possible to define a value for dissociation constant, K_d, of a protein-ligand complex in laboratory experiments. This information can be used in some extent also in modeling as K_d is the ratio of the backward and forward reaction constants (Equation 3.2).

$$K_d = \frac{[\mathrm{R}][\mathrm{IP_3}]}{[\mathrm{RI}]} = \frac{k_b}{k_f} \tag{3.2}$$

The change in the concentration of receptor-ligand complex, [RI], over time can be described using ODE as presented in Equation 3.3 and as the negative of this for [R] and [IP_3] (Equation 3.4).

$$\frac{d[\mathrm{RI}]}{dt} = k_f[\mathrm{R}][\mathrm{IP_3}] - k_b[\mathrm{RI}] \tag{3.3}$$

$$\frac{d[\mathrm{R}]}{dt} = \frac{d[\mathrm{IP_3}]}{dt} = k_b[\mathrm{RI}] - k_f[\mathrm{R}][\mathrm{IP_3}] \tag{3.4}$$

A general chemical reaction can be presented as

$$a\mathrm{A} + b\mathrm{B} \underset{k_b}{\overset{k_f}{\rightleftharpoons}} c\mathrm{C} + d\mathrm{D}, \tag{3.5}$$

where lower case letters declare stoichiometric ratios, ie. the number of reacting chemical species. For the general reaction, when the reaction rate v is

$$v = k_f[\mathrm{A}]^a[\mathrm{B}]^b - k_b[\mathrm{C}]^c[\mathrm{D}]^d, \tag{3.6}$$

the rates for concentration change of each species are

$$\frac{\mathrm{d}[\mathrm{A}]}{\mathrm{d}t} = -av, \frac{\mathrm{d}[\mathrm{B}]}{\mathrm{d}t} = -bv, \frac{\mathrm{d}[\mathrm{C}]}{dt} = cv, \frac{\mathrm{d}[\mathrm{D}]}{dt} = dv \tag{3.7}$$

If the initial concentrations for the reacting species (ie. the initial conditions) and rate constant (i.e. parameters) of the model are known, using the same input the model will always produce the same output when using deterministic approach.

When modeling a dynamical system with a set of ODEs, the reactions are usually assumed to happen in a constant temperature and volume which is a spatially homogeneous mixture. In this well-stirred system, the chemical species are randomly and uniformly distributed throughout the volume. The exact location of the chemical species is not defined, but instead they are considered to be everywhere and always available for the reaction. In biological systems this would mean that the diffusion is faster than the actual occurring reactions.

The ODE models have to be numerically solved because they very often contain more than a few chemical species and chemical reactions. Thus it becomes mathematically difficult to solve them analytically. There are many different methods for solving a system of ODEs numerically (presented, for example, in Ermentrout and Rinzel (2010)). The simplest and easiest solving method is Euler method. Commonly used improvement for it is Runge-Kutta method. In this work, the deterministic approach was used for simulation in **Publication II**.

3.2 Stochastic approach

It is important to realize that the assumptions underlying the deterministic ODE model are problematic when applied to modeling biochemical reactions in a cell. The cell is tightly packed and highly compartmentalized thus the small volumes of compartments lead to large concentrations even with small number of molecules and ions.

In the deterministic approach, the dynamics of a reaction system is a continuous process and it is applicable to many biological systems. A physically more realistic approach would be to describe the process as a *stochastic*, because the collisions of chemical species, and thus also the reactions, happen in a random manner and cause fluctuations in the system. This means that collisions of reacting species and the chemical reactions are stochastic in nature.

Stochastic approach is always valid whenever the deterministic approach is valid, but when the deterministic is not, the stochastic might sometimes be valid (Gillespie, 1976). When considering systems with small numbers of molecules, the deterministic approaches do not always give biologically valid results and are not capable of capturing the stochastic behavior observed in biological system (Gillespie, 1977; Turner *et al.*, 2004; Barrio *et al.*, 2006;

Choi *et al.*, 2010). This leads to a situation where the deterministic approach gives unrealistic results in some cases. This is especially of concern when dealing with systems having small number of molecules such as the dendritic spines in neurons. The average volume of a spine is 1 fl (Harris and Stevens, 1988) and resting level concentration of Ca^{2+} is 0.1 μM, which means that then there are about 60 calcium ions in one spine. Turner *et al.* (2004) conclude that if the number of molecules is under 100, stochastic approach should be used for modeling and simulation. On the other hand, 10^3–10^5 molecules have been also considered low and thus call for stochastic approach in modeling (Perc *et al.*, 2006).

As concluded in **Publication IV**, the need for stochastic modeling and simulation methods is clearly evident especially in situations when small number of molecules are involved as in dendritic spines of the cerebellar Purkinje cell. It has also been shown that taking the stochasticity into account in cellular systems with large number molecules also matters. Skupin *et al.* (2008, 2010) shows how intracellular Ca^{2+} oscillations are sequences of random Ca^{2+} spikes despite of the involvement of large amount molecules in spike generation. First, they conclude that the information transfer is not prevented although there are randomness in the spike trains (Skupin *et al.*, 2008). Later, Skupin *et al.* (2010) show that this randomness arises from the stochastic state transitions of individual IP_3 receptors (Ca^{2+} release channels). Perc *et al.* (2008) have shown that intracellular Ca^{2+} oscillations in hepatocytes are of stochastic nature as well.

The system of chemical reactions, excluding the diffusion, can be modeled in a stochastic manner with chemical master equation (CME) (McQuarrie, 1967; Gillespie, 1992). In most cases, the CME is mathematically analytically intractable, impossible to solve. Gillespie (1976, 1977) has introduced a stochastic simulation algorithm (SSA) which numerically simulates the discrete Markov process which is described by the CME. SSA is described in more detail in Chapter 3.3.

The SSA can be, in the case of large systems, heavy and time consuming from computational point of view and sometimes practically impossible to use with current computational power. This has lead into a development of stochastic approaches, such as stochastic differential equations (SDEs), to describe the cellular and neuronal functions (see, for example, Manninen *et al.* (2006); Saarinen *et al.* (2006)). These approaches are described and applied in more detail, for example, in Manninen (2007) and Intosalmi (2012). A system of SDEs is faster to simulate with appropriate methods (solved, for example, using Euler-Maryama methods) than equivalent system with SSA and for that reason in some cases it would be necessary to use SDEs. SDEs are also applicable to systems which are not based on the law of mass-action, but on other types of differential equations such as, for example, Hodgkin-Huxley equations (Hodgkin and Huxley, 1952) that describes the

bioelectrical properties of neuron's plasmamembrane or Michaelis-Menten equation describing enzyme kinetics. The SDEs have their limitations, for example, when considering a system with only few molecules or ions. The SDE model can become unstable and produce negative concentrations which is unrealistic in biological sense although still mathematically correct (see, for example, Manninen (2007)).

In **Publication V**, stochastic differential equations are used as one stochastic method when evaluating the suitability of different stochastic approaches in modeling IP_3 receptors in small volumes. It is concluded that, because of the possibility of a unstable model, SSA is a better method for simulating the IP_3 receptor model.

3.3 Gillespie stochastic simulation algorithm

Gillespie stochastic simulation algorithm (SSA) is an event-driven algorithm for numerically simulating well-stirred system of reacting chemical species which is described by CME. SSA does not make approximation and has been shown to simulates the CME exactly (Gillespie, 1977). In the algorithm, the chemical species are treated in a discrete manner, ie. as the number of species instead of a concentration. In the SSA, it is assumed that the number of molecular collisions greatly outnumber the occurring reactions. In reversible reactions, both the forward and backward reactions are handled as separate, unidirectional, reactions. Basically, what SSA does is that it generates two random numbers and uses them to determine after what time the next reaction will occur and which reaction it is. Using this information it advances to the next time point, and updates the number of molecules and ions involved in the reaction that occurred. The SSA then generates the random numbers again to calculate the state of the system in the next step. The unit-interval uniform distribution is used for the random number generation.

In SSA, stochastic reaction parameter, c_μ, is used instead of rate constants, k_μ, in deterministic approach (see Equation 3.5). c_μ deals with number of molecules and not molar concentrations as the k_μ. Stochastic reaction parameter c_μ describes the probability of a reaction R_μ to happen in discrete number of molecules per unit of time $(1/s)$. The derivation of c_μ is not straightforward but can be approximated using the k_μ. For example, for the first-order reaction, $S_1 \rightarrow S_2$, the $c_\mu = k_\mu$ and for the second order reaction, $S_1 + S_2 \rightarrow S_3$, $c_\mu = k_\mu / N_a V$, where N_a is the Avogadro's constant and V the volume of the system (Gillespie, 1976).

Let us assume a biochemical reaction systems, including N molecules or ions $\{S_1, ..., S_n\}$, M reactions $\{R_1, ..., R_\mu\}$, and thus M stochastic reaction

parameters $\{c_1, ..., c_\mu\}$. The state of the system is described with a vector $\mathbf{x}(t) = (x_1(t), ..., x_n(t))$, where x_n(t) is the number of S_n molecules at time point t. At time point 0 ($t = 0$), the system is in state $\mathbf{x}_0$, which is defined by the user.

The reactions are governed by the propensity function a_j. When the system is at a state $\mathbf{x}(t)$, the probability, that one reaction R_j of all M reactions occurs in the next infinitesimal time interval dt, is calculated with

$$a_j(\mathbf{x}(\mathrm{t}))dt = c_j h_j dt, \tag{3.8}$$

where h_j is the number of distinct reactant combinations for reaction R_j at time t. For example, for reaction $S_1 + S_2 \rightarrow S_3$ at $t = 0$, the $a_1 = c_1 x_1(0) x_2(0)$. Here it can be seen that the probabilities are proportional to the number of molecules or ions.

The zero propensity a_0 is the sum of all propensities and describes the probability that any reaction will occur in the next infinitesimal time step.

$$a_0 = \sum_{j=1}^{M} a_j = \sum_{j=1}^{M} c_j h_j \tag{3.9}$$

The SSA can be described with the following five steps:

1. In the initialization step, define the initial conditions, the initial number of molecules and ions x_0 and values for rate parameters $c_1, ...c_\mu$ and initialize the state of the system, $\mathbf{x} = \mathbf{x}_0$. Set also the time variable and the reaction number counter to 0 and initialize random number generator.

2. Calculate the probabilities for each reactions with the propensity function $a_j = h_j c_j$ $(j = 1, ..., M)$ and compute the $a_0(\mathbf{x})$.

3. Generate a random number, r_1, and calculate the τ using the equation

$$\tau = \frac{1}{a_0(\mathbf{x})} ln \frac{1}{r_1} \tag{3.10}$$

   If the $t + \tau > t_{end}$, the algorithm is stopped.

4. Generate another random number, r_2. Choose the next occurring reaction, R_i, by finding the index i using the following criteria

$$\sum_{i=1}^{j-1} a_i < r_2 a_0(\mathbf{x}) \leq \sum_{i=1}^{j} a_i \tag{3.11}$$

5. Update the number of molecules involved in a reaction R_i, set time, $t = t + \tau$, and return to step 2.

The algorithm presented here is the direct method (Gillespie, 1976). Later, computationally more efficient versions of SSA and versions with other improvements have been developed (see, for a review, Gillespie (2007)). For example, Gibson and Bruck (2000) developed the next reaction methods and Gillespie (2001) a τ-leap method.

3.4 Simulation tools

Once a mathematical model for a biochemical system has been developed, it needs to be implemented as a computer algorithm for numerical simulations. It can be done, for example, using a general computing environment such as MATLAB® or with a programming language such as C++ or Python. In the field of computational neuroscience, the trend is more and more towards using specialized simulation tools for the purpose. Simulation tools have been developed since they have obvious advantages compared to programming languages. First of all, with tools there is no requirement for such advanced programming skills as using, for example, C++. This lowers the threshold for using tools. When using programming language, one has to, in addition to the model itself, also implement the simulation method, ie. numerical integration algorithms. Tools implicitly interpret some selected laws for modeling and most common algorithms for simulation methods. Their functions have been tested and one should be able to just use them for specific purposes. Testing the simulation methods and other functions and features, in addition to benchmarking a tool, is laborious and an area of research itself.

When using the simulation tool, the model must be described in a language that the simulator understands. Many times the situation is such that the simulator uses a special language just designed for the specific simulator. This limits the use of the model to that tool if one is not ready to implement the model to another tool. Systems Biology Markup Language (SBML) (Hucka *et al.*, 2004), NeuroML (Gleeson *et al.*, 2010), and NineML (Raikov *et al.*, 2011) are tool-independent description languages and they have been developed to increase the interoperability of tools and to help sharing of models.

Many simulation tools have been developed and made publicly available for modeling different phenomena of neurons. For the past ten years the trend has been that different research groups develop their own tool according to their own research questions and requests. This also became evident in the course of this thesis work. When comparing and reviewing models

for postsynaptic signal transduction in synaptic plasticity in **Publication III**, the study revealed that the models had been simulated in 22 different simulation environments. It is obvious that different research aspects need different kind of simulation methods, analysis tools, and features for their research purposes. Fortunately, currently existing tools are developed further and increasing amount of resources are allocated to interoperability of different simulators since, in computational neuroscience, it is often necessary to use several different software tools in order to carry out various forms of simulations and data analysis. Examples of research project promoting interoperability include, for example, PyNN (Davison *et al.*, 2008), NeuroML (Gleeson *et al.*, 2010), MUSIC (Djurfeldt *et al.*, 2010), and NineML (Raikov *et al.*, 2011). Many of these rely on XML (Extensible Markup Language) and there has been discussion about the limitations of XML-based languages (Raikov and De Schutter, 2012*a*) and a layer-oriented approach has been suggested (Raikov and De Schutter, 2012*b*).

Different tools have different features, for example, simulation methods, methods for model analysis, and saving or visualizing the results. There has been some studies comparing the simulation tools for systems of biochemical reactions (see, for example, Pettinen *et al.* (2005); Alves *et al.* (2006)). In **Publication VI** stochastic simulations tools supporting SBML are studied. The compared tools all use Gillespie SSA for simulation but other features such as support for both SBML import and export, user interface (graphical or command line), and tools for sensitivity analysis differ. Also the ease of installation, general usability, and availability and quality of instruction manual vary. The study concludes that all the simulators produce similar simulation results and that the selection of the tool depends on the user's requirements for different features.

The systems of biochemical reactions can be simulated using various tools. For instance, some of most well known simulators, incorporating both reactions and diffusion, include MesoRD (Hattne *et al.*, 2005), MCell (Kerr *et al.*, 2008), Smoldyn (Andrews *et al.*, 2010), STEPS (Wils and De Schutter, 2009; Hepburn *et al.*, 2012), and NeuroRD (Oliveira *et al.*, 2010). In this work, STEPS (STochastic Engine for Pathway Simulation) (Wils and De Schutter, 2009; Hepburn *et al.*, 2012) was selected to be used as a tool to simulate IP_3 receptor models in **Publications I** and **IV**. STEPS was not included in the **Publication VI** because it was not publicly available at the time. Currently, STEPS is freely available and also supports SBML import. STEPS is used through a Python interface and thus suitable Python packages can be used for analysis or visualization of the simulation results. STEPS is also platform independent and thus users can run it in an operating system best suitable for their purposes. It uses Gillespie SSA for simulation and, consequently, models based on the law of mass action can be implemented to STEPS. During the course of this thesis work, STEPS was further devel-

oped and various versions of the tool were used. The final simulations for **Publication I** were run using the STEPS version 1.1.2. Currently, version 2.0.0. is available (http://sourceforge.net/projects/steps/files, accessed 17 Apr, 2013) and it also supports simulating the electric potential across a membrane (The STEPS developers, 2013).

STEPS tackles the problem of cell's compartmentalization and diffusion using a voxel-based method. A stochastic reaction-diffusion can be simulated using two different approaches: particle-based or voxel-based methods. In the particle-based approach, the path and velocity of each molecule is followed and reactions are based on collisions of molecules whose paths encounter. This approach is used, for example, in MCell (Kerr *et al.*, 2008) and Smoldyn (Andrews *et al.*, 2010). Particle-based approach is physicochemically adequate as it keeps track on each of the molecules but, at the same time, the tracking makes it computationally heavy.

In the voxel-based approach, the volume is divided into subvolumes, voxels, which are considered as well-mixed systems. In this approach, the diffusion is modeled as first-order reaction of the diffusion molecules from one voxel to another. In addition to normal chemical reactions in the system, the 'diffusion reactions' can be simulated with Gillespie SSA, thus also making the diffusion stochastic. This approach is computationally lighter than particle-based approach. In this work, the diffusion was not included, since only the kinetics of IP_3 receptor was studied. The IP_3 receptor models in **Publications I** and **IV** have two compartments, cytosol and ER lumen, and a surface, ER membrane, between them. The IP_3 receptor was placed on the surface. Although diffusion is not used, STEPS was a good choice for the studies to make the incorporation of diffusion easy in the future, for example, if the models are used as a part of larger models for signal transduction.

STEPS has been computationally compared to two other similar simulation tools, Smoldyn (Andrews *et al.*, 2010) and MesoRD (Hattne *et al.*, 2005) in the original publication (Hepburn *et al.*, 2012). To compare the voxel-based method to particle-based method, STEPS was compared with Smoldyn. The results indicated that voxel-based approach is faster to simulate and as the number of molecules increases the difference is emphasized. The comparison with MesoRD was done to test the efficiency of the reaction-diffusion algorithm in different conditions, ie. in the case of high and low number of molecules and different numbers of subvolumes. Both STEPS and MesoRD use the voxel-based approach and thus a direct comparison of the tools was possible. Throughout the tests, STEPS was shown to run the simulations at least 4-5 times faster than MesoRD and thus perform better in all tested conditions.

3.5 Comparison of models

One goal of this thesis is to screen, test and compare models for IP_3 receptor and postsynaptic signal transduction in synaptic plasticity. Comparison and validation of computational models for biochemical systems is a challenging task. Many times, due to their large size and nonlinear properties, as well as lack of experimental data (Hellgren Kotaleski and Blackwell, 2010; De Schutter, 2010*a*), simple mathematical tools cannot be used to compare complex models. When a new model is published, it is important to define model's context and relation to other models. This is not often done and is left to the reader to figure out, although the model authors are the experts of their model. Not only is the lack of data to be used in comparison a problem, but it is often also unclear which data or subset of data was used when constructing the model originally. Equally important would be to clearly justify the need for a new model, especially if models for the same phenomenon already exist and explicitly define the questions the model is supposed to give answers to. Models are not always made publicly available or described comprehensively as they should to advance the reusability. Inclusion of all the mentioned things add value to model and improve model's usability and reproducibility.

3.5.1 Models for postsynaptic signal transduction in synaptic plasticity

Synaptic plasticity has received considerable attention over the past decades. Intensive experimental and computational work has been performed to understand how mammals and non-mammals are able to learn and store memories and what are the molecular level mechanisms behind learning and memory (see, for example, Markram *et al.* (2011)).

Consequently, there exists a vast number of models for LTP and LTD (see, for example, **Publication III**). The models vary from detailed molecular level models to more phenomenological ones describing synaptic plasticity from elaborate to a more abstract level. The use of previous models in future studies is in many cases difficult as no benchmarking or comparison of models have been made. Altogether 117 of these models, published by the end of the year 2009, are reviewed in **Publication III**. The purpose of the study was to make qualitative evaluation of existing models to ease the selection of models for future work.

Three out of the 117 models (d'Alcantara *et al.*, 2003; Hayer and Bhalla, 2005; Lindskog *et al.*, 2006) and two more recent ones (Kim *et al.*, 2010; Nakano *et al.*, 2010) were selected for more detailed comparison where computer simulations were used to analyze the model behavior (**Publication**

II). The selection of models was made based on few criteria, of which the most important was that the model should be publicly available, for example, in an open-access database. These five models are developed to descibe either the LTP alone, or LTP and LTD together.

After 2009, several new models for postsynaptic signal transduction in synaptic plasticity have been published. For example, Nakano *et al.* (2010) have published a model describing the induction of LTP and LTD in striatal medium spiny neuron and demonstrates the mechanisms involved in bidirectional regulation of corticostriatal synapses by Ca^{2+} and dopamine. A model for synaptic plasticity, more precisely LTP, in hippocampal CA1 pyramidal neurons by Kim *et al.* (2010) studies the temporal sensitivity of protein kinase A (PKA) and describes the interactions of Ca^{2+} and cyclic adenosine monophosphate (cAMP) signaling pathways. The model is based on biochemical measurements of PKA and CaMKII which have important role in synaptic signaling (Kim *et al.*, 2010). Antunes and De Schutter (2012) have published a model describing Ca^{2+} dependent LTD and mechanisms for AMPA receptor trafficking. The model is strongly based on experimental data. Antunes and De Schutter (2012) show that the stochastic signaling network mediates induction of cerebellar long-term depression. These models presented here as examples are relatively complex and involve tens and some even hundreds of variables.

3.5.2 IP_3 receptor models

As IP_3 receptor has a major role in Ca^{2+} dynamics of neurons and other cells, many models describing its function has been developed. For **Publication I**, existing models of IP_3 receptor were carefully studied to assess their suitability to describe electrophysiologically measured kinetics of type 1 IP_3 receptor in neurons. After a careful analysis, four IP_3 receptor models (Figure 3.1) out of 20 models (De Young and Keizer, 1992; Othmer and Tang, 1993; Bezprozvanny and Ehrlich, 1994; Li and Rinzel, 1994; Kaftan *et al.*, 1997; Laurent and Claret, 1997; Swillens *et al.*, 1998; Moraru *et al.*, 1999; LeBeau *et al.*, 1999; Sneyd and Dufour, 2002; Shuai and Jung, 2002; Dawson *et al.*, 2003; Mak *et al.*, 2003; Falcke, 2003; Fraiman and Dawson, 2004; Diambra and Guisoni, 2005; Hernjak *et al.*, 2005; Ullah and Jung, 2006; Haeri *et al.*, 2007; Gin *et al.*, 2009*b*) were selected and implemented to a simulation tool STEPS. After simulation, the results were compared with experimental data. After the completion of the study in **Publication I**, at least one new model of IP_3 receptor kinetics has been published; Siekmann *et al.* (2012) have published a model accounting for experimentally shown mode changes in the activity.

Many quantitative models, as well as qualitative and more phenomenological ones, have been proposed for the behavior of IP_3 receptor. There are models

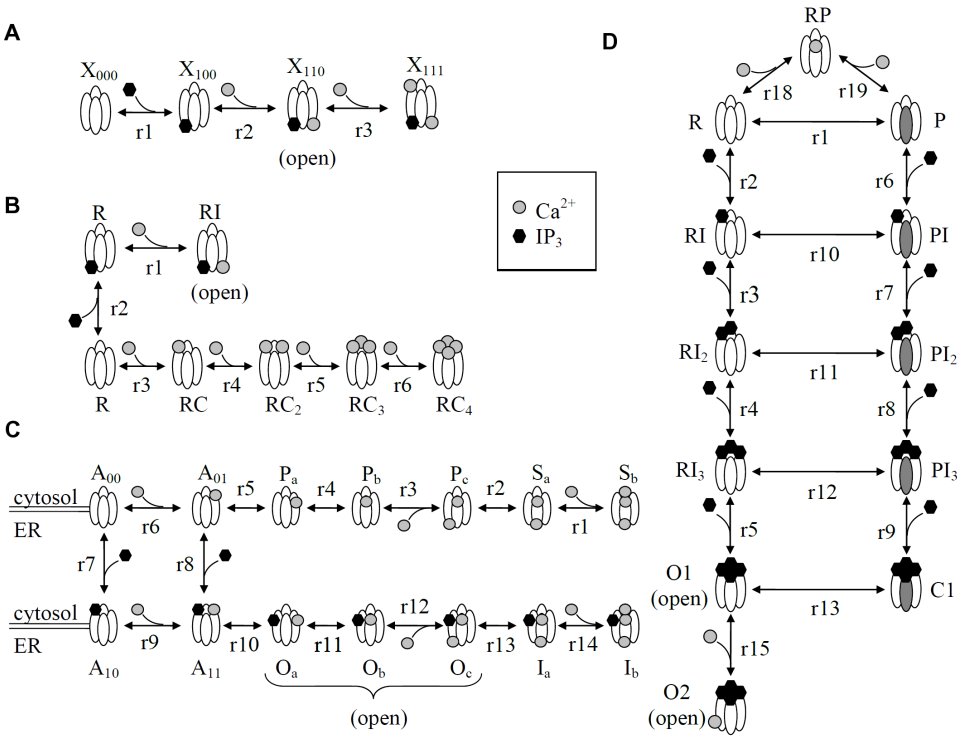

Figure 3.1. Schematic representation of the states and transitions of the four IP_3R models compared in **Publication I**. (a) Othmer and Tang (1993) (forward direction of a reaction is to the right) (b) Doi *et al.* (2005) (forward direction of a reaction is to the right or up), (c) Fraiman and Dawson (2004) (forward direction of a reaction is to the right or down) (d) Dawson *et al.* (2003) (forward direction of a reaction is the to the direction of binding a ligand or in the plain state transitions from left to the right). Adapted from Hituri and Linne, (2013).

presented for different types of IP_3 receptor (type 1, 2, and 3) (Foskett *et al.*, 2007) and IP_3 receptor in different animals, tissues and cells (for example, *Xenopus* oocyte (Falcke, 2003), cerebellar cells (De Young and Keizer, 1992), pancreatic acinar cells (LeBeau *et al.*, 1999) and hepatic cells (Dufour *et al.*, 1997)). Probably, the most well-know IP_3 receptor model is the model of De Young and Keizer (1992). Some models for IP_3 receptor have been compared either analytically or by means of simulation (Tang *et al.*, 1996; Mak *et al.*, 2003; Sneyd *et al.*, 2004; Shuai *et al.*, 2009) and reviewed (Schuster *et al.*, 2002; Sneyd and Falcke, 2005). All the models have been important in understanding some property or behavior of IP_3 receptors. Next the findings of the comparative studies are briefly presented.

The comparative study of Tang *et al.* (1996) presents reduced versions of four models: Othmer and Tang (1993), Bezprozvanny and Ehrlich (1994), De Young and Keizer (1992), and Atri *et al.* (1993). Tang *et al.* (1996) reduced all the four models to a single gating equation that is linear in the gating variable and has coefficients that depend on the IP_3 concentration and cytosolic Ca^{2+} concentration. They also re-estimated the model parameters and compared steady-state channel behavior of the models to experimental data by Bezprozvanny *et al.* (1991) and Watras *et al.* (1991) and time-dependent responses of Ca^{2+} dynamics to experimental data by Zhao *et al.* (1990). Tang *et al.* (1996) conclude that all the models reproduce the experimental data (Bezprozvanny *et al.*, 1991; Watras *et al.*, 1991) satisfactorily. Of the models compared in Tang *et al.* (1996), Bezprozvanny and Ehrlich (1994) is a variation of the binding scheme of Othmer and Tang (1993) with additional open state and transition to this state. Both models (Othmer and Tang, 1993; Bezprozvanny and Ehrlich, 1994) adequately explain the electrophysiologically recorded data (Bezprozvanny and Ehrlich, 1994) from canine cerebellar IP_3 receptors isolated in microsomes and fused to lipid bilayer (Tang *et al.*, 1996).

Mak *et al.* (2003) compare (in the Supplemental Material of the publication) several allosteric models of IP_3 receptor in ascending order of complexity to find out the simplest model that can account for the regulation by IP_3 concentration and Ca^{2+} concentration of homotetrameric IP_3 receptor. For parameter estimation and verification of the model behavior, Mak *et al.* (2003) have used their own experimental measurements on type 1 and type 3 rat IP_3 receptors expressed in *Xenopus* oocytes. They conclude that the four plus two conformation MWC-based model (Monod *et al.*, 1965) is the simplest model that adequately accounted for their observations on IP_3 receptor regulation. It should be noted that the models compared by Mak *et al.* (2003) can be implemented into simulator like STEPS (see Chapter 3.4) but this would require making assumptions about the absolute values of the forward and backward rate constants, given that the models where only dissociation constants (i.e. ratios of rate constants) are given correspond to a whole family of models with different rate constants.

Sneyd *et al.* (2004) present a comparison of three models: De Young and Keizer (1992), Sneyd and Dufour (2002), and Dawson *et al.* (2003). In their study, Sneyd *et al.* (2004) re-estimed the parameters of each model using Bayesian methods and data from hepatic microsomes (Dufour *et al.*, 1997). Although the model of Sneyd and Dufour (2002) gives the best fit to the data and the model of Dawson *et al.* (2003) the worst, Sneyd and Dufour (2002) do not make a clear conclusion which of the models best describes the behavior of IP_3 receptor. All the models are concluded to have both pros and cons and it is more a matter of application which one of the models to select.

In their extensive review, Sneyd and Falcke (2005) introduce over ten mathematical and schematical models of IP_3 receptor presented by that time and compare them in a qualitative manner to each other and also to models of ryanodine receptor. Shuai *et al.* (2009) study models of IP_3 receptor. They have fitted models containing 20 states to models with four 13-state subunits and used experimental data from patch clamp recordings of IP_3 receptor on nuclear membranes of *Xenopus* oocytes. Their results support the hypothesis that IP_3 receptor binds Ca^{2+} and IP_3 sequentially, not independently, and that the ion channel opens through a conformational transition from a closed state to an active state.

None of the previous comparative studies have concentrated on finding a model for IP_3 receptor particularly in neurons although there are few studies utilizing different IP_3 receptor models when modeling Ca^{2+} events in neuronal cells (Fiala *et al.*, 1996; De Schutter and Smolen, 1998; Doi *et al.*, 2005; Hernjak *et al.*, 2005; Peercy, 2008) or in general (see, for example, Mishra and Bhalla (2002); Williams *et al.* (2008)). De Schutter and Smolen (1998) have used the IP_3 receptor model of Li and Rinzel (1994) as a part of their model for Ca^{2+} dynamics in cerebellar Purkinje cell. In the minimal model of Li and Rinzel (1994), the fraction of open receptors is defined, according to the Hodgkin-Huxley formalism, as a function of the state of activation and inactivation particles. Mishra and Bhalla (2002) have used the model of Othmer and Tang (1993) as a part of their model for inositol phosphate metabolism.

There exist tens of computational models for the function of IP_3 receptor. It is inevitable to think whether all models are really necessary and if they contributed in finding something novel which already existing models were not capable of capturing. After going though the IP_3 receptor models one cannot discard that they have been developed using experimental data but usually different data every time. Despite this, the many models of IP_3 receptor function are nice examples of data-driven modeling work.

3.5.3 Qualitative approach to comparison of models

In this thesis, computational models are compared in **Publications I** (IP_3 receptor models), **II**, and **III** (models for postsynaptic signal transduction in synaptic plasticity). Due to the vast number of models describing LTP and LTP, a qualitative approach for model comparison is the only reasonable approach to take. Despite the fact that the models describe similar phenomena, quantitative approach would be impossible because of the size of models, molecules, inputs, and outputs are very different. Many times the computational implementation of the models are not publicly available and the description of the model in the original paper is not comprehensive

and which many times makes model reproduction impossible. In **Publication III**, the models for LTP and LTD are *categorized in two ways*, first the models are divided into three groups based on the phenomenon they present (LTP, LTD and dual LTP/LTD) and, second, they are categorized based on the level they model postsynaptic signal transduction. The established categories are models for single pathways, models for calcium mechanisms or simplified intracellular processes, and models for signaling networks. Models for single pathways have at most one kinase as a model variable and do not include any receptors, ion channels, or pumps. In most of the cases, these models contain one pathway involving calmodulin and CaMKII and also sometimes phosphatases. Models for calcium mechanisms or simplified intracellular processes include postsynaptic Ca^{2+} buffers together with ion channels, receptors, or pumps, or simplified intracellular processes. Models for signaling networks include interactions between at least two pathways and thus many times have several protein kinases and phosphatases, in addition to pumps, ion channels, and receptors.

3.5.4 Quantitative approach to comparison of models

This work presents two *simulation based approaches* for model comparison (**Publications I** and **II**). Previously, IP_3 receptor models have been compared with computational means in several studies (Tang *et al.*, 1996; Mak *et al.*, 2003; Sneyd *et al.*, 2004; Shuai *et al.*, 2009; Gin *et al.*, 2009*b*). In some of these studies (Sneyd *et al.*, 2004; Shuai *et al.*, 2009; Gin *et al.*, 2009*b*), the model parameters have been re-estimated using experimental data, original data from electrophysiological experiments, and then the model outcomes have been compared to the same data. Sneyd *et al.* (2004) and Gin *et al.* (2009*b*) used Bayesian methods (see, for example, Girolami (2008); Gin *et al.* (2009*a*)) for parameter estimation. In this work, a different kind of approach is taken. In **Publication I**, the original parameter values are used and the stochastic simulations were designed in such a way that they replicate outcomes of experimental measurements done with IP_3 receptor. The statistical properties of the simulated results are compared to corresponding experimental data found in literature. This experimental data used for comparison in the present work is mainly different from the data for which the models were originally based on.

In **Publication II** models for postsynaptic signaling in synaptic plasticity are also compared using simulation based approach. Simulation based approach is one of the few approaches that can be used to compare large biochemical models of intracellular origin in quantitative manner. The structure of these networks many times differ and the models are nonlinear. In **Publication II**, each of the five models describing LTP and/or LTD (d'Alcantara *et al.*, 2003; Hayer and Bhalla, 2005; Lindskog *et al.*, 2006; Kim *et al.*, 2010;

Nakano *et al.*, 2010) are simulated with the same kind of stimuli in six different initial conditions. In this study, the time-course of concentrations for active CaMKII and PP1, as as well as the model outputs used in original publications, are compared to each other.

Chapter 4

Summary of Results

In this thesis, computational models for IP_3 receptor and postsynaptic signaling in synaptic plasticity are compared in addition to comparison of simulation methods and tools in order to provide means for better describing certain phenomena in the brain. This thesis in based on six publications. Next, the obtained results and most important conclusions are presented in brief.

4.1 Comparison of simulation methods and tools

There is a large variety of stochastic and deterministic simulation tools available for simulating biochemical reaction systems. **Publication VI** presents an evaluation and comparison of 12 simulation tools. Previously, few surveys of simulation tools has been published (Pettinen *et al.*, 2005; Alves *et al.*, 2006) but an evaluation of tools from the point of view of stochasticity with more quantitative approach was lacking. First, existing stochastic simulation tools supporting SBML were examined briefly and of them were selected the tools which use Gillespie SSA and are freely downloadable. A model describing the expression of the gene coding the luciferase enzyme (Kierzek *et al.*, 2001) and the function of the enzyme (Brovko *et al.*, 1994) was used as a test in the study. Only in three of the 12 evaluated tools it was possible to simulate the model. It was concluded that the user-friendliness and applicability of tools vary. A MATLAB® implementation of the test case model was used as reference in simulations. The results show that the outcomes of the simulations in different tools are similar based on the p-values of Kolmogorov-Smirnov test (see Table 5 in **Publication VI**) and thus the user can choose the one of these tools which has the most suitable feature's for the user's needs. Properties related to these features of the models are listed in Figure 1 in **Publication VI**.

Stochasticity can be taken into account in a biochemical reaction system with several different approaches. In **Publication V**, stochastic differential equation (SDE) approach is compared to Gillespie SSA and to deterministic (ODE) approach to see which of the approaches best suites for describing the function of IP_3 receptor in a small volume. The simulation results show that there is a possibility of negative concentrations and thus risk of unstable model when using SDE. Simulation results of fairly stable, modified SDE model converge on the deterministic result, while simulation results from simulations with Gillespie SSA are clearly different from the deterministic results (see Figure 2 in **Publication V**). The results indicate that it is thus preferable to use Gillespie SSA when simulating systems with small number of molecules.

In the **Publication IV**, the effects of stochasticity on IP_3 receptor in a small volume, Purkinje cell spine, is studied by comparing deterministic and stochastic simulation (Gillespie SSA) methods by simulating two models for IP_3 receptor (Fraiman and Dawson, 2004; Doi *et al.*, 2005). There are significant differences between the deterministic and stochastic responses when small initial concentrations for IP_3 and Ca^{2+} are used. The average of several stochastic simulations is different from the deterministic one (for example, see Figure 4.1). The simulations in **Publication IV** show that deterministic simulations of IP_3 receptor activation do not produce realistic results under all conditions.

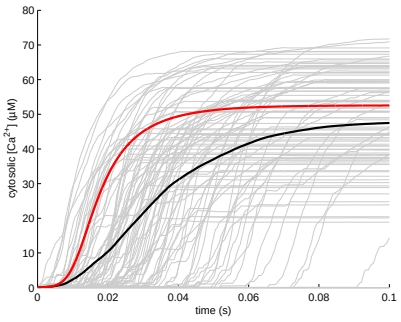

Figure 4.1. Time evolution of cytosolic Ca^{2+} concentration of the model of Doi *et al.* (2005) simulated with deterministic and stochastic simulation methods. Grey: individual stochastic runs, Black: average of 100 stochastic runs, Red: deterministic solution.

Table 4.1. Models compared or used as test cases in **Publications I-VI**

Publication	Model
I	4 IP_3 receptor models
II	5 models for LTP and LTD
III	117 models for LTP and LTD
IV	IP_3 receptor model of Fraiman and Dawson (2004) and Doi *et al.* (2005)
V	IP_3 receptor model of Doi *et al.* (2005)
VI	Firefly luciferase pathway

4.2 Comparison of models

In the field of computational neuroscience, models have been developed already for few decades which means that the number of models in fairly large. Many times models are created *de novo*, from scratch, and fortunately quite often using data-driven approach. Very rarely new models are compared to the existing ones, at least not in a quantitative manner which might be partly due to the lack of methods to compare them. Comparison is also difficult if previous models are not comprehensively described in the original publication or the models are not available in public database. In many cases, simulations would be the most evident option for model comparison due to the complexity and size of the models. At least, the comparison to experimental time-course data many times requires simulations.

Comparison of biochemical models is difficult even if they describe the same phenomenon. In this work, three separate studies have been made to compare computational models of synaptic plasticity and associated phenomena. One study is performed in a qualitative manner only, due to large number of models involved. Two studies are performed in quantitative manner, using simulation based approach, to compare the models. The results of these studies are summarized below.

In **Publication I**, four models for IP_3 (Othmer and Tang, 1993; Dawson *et al.*, 2003; Fraiman and Dawson, 2004; Doi *et al.*, 2005) receptor are compared. The models are simulated with stochastic means (Gillespie SSA). The results show major differences in the statistical properties of the model functioning. It is concluded that the statistical properties of the model of Fraiman and Dawson (2004) is the most similar to the ones obtained in wet-lab experiments. For open probability (P_o) as a function of Ca^{2+}, three of the models, as model of Dawson *et al.* (2003) being exception, produced a bell-shaped curve (Figure 4.2(a)) shown in wet-lab experiments (Bezprozvanny *et al.*, 1991). The open probability of IP_3 receptor is also dependent on cytosolic IP_3 concentration. The open probability curves of the models

obtained in simulations are shown in Figure 4.2(b). Also in this case, P_os for all the models except the model of Dawson *et al.* (2003) follow the s-shape that is reported in experimental studies (Watras *et al.*, 1991; Marchenko *et al.*, 2005; Taufiq-Ur-Rahman *et al.*, 2009). In **Publication I**, it was also studied how the dependence of P_o on Ca^{2+} concentration changes when the IP_3 concentration is increased (Figure 3 in **Publication I**) as it has been shown in experiments by Kaftan *et al.* (1997) that the bell-shaped Ca^{2+}-dependence curve moves upward and to the right when IP_3 concentration is increased. None of the models were able to reproduce the results presented by Kaftan *et al.* (1997).

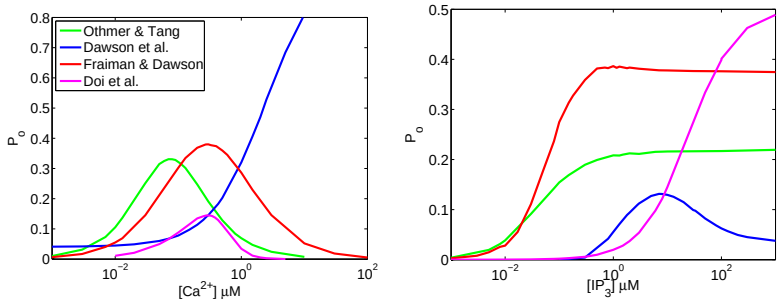

(a) (b)

Figure 4.2. Open probability of IP_3R as a function of (a) cytosolic Ca^{2+} concentration ($IP_3 = 10$ μM) and (b) cytosolic IP_3 concentration ($Ca^{2+} = 0.25$ μM). Green: Othmer and Tang (1993), Blue: Dawson *et al.* (2003), Red: Fraiman and Dawson (2004), Magenta: Doi *et al.* (2005). Adapted from Hituri and Linne (2013).

Simulations in **Publication I** also showed the mean open time of the model of Fraiman and Dawson (2004) is 2.5 ms. This values is close to the experimentally obtained values for neuronal IP_3 receptor (2.9 ms (Bezprozvanny and Ehrlich, 1994), and 4.2 ms (Kaznacheyeva *et al.*, 1998)). The mean open times obtained for the other models are an order of magnitude smaller (0.5 ms for Dawson *et al.* (2003) and Doi *et al.* (2005)) or greater (460 ms, Othmer and Tang (1993)). The open time distribution of the model of Fraiman and Dawson (2004) is the closest to experimentally (Kaznacheyeva *et al.*, 1998) obtained distribution (see Figures 4.3(a), 4.3(b)). The same applies also to the closed time distributions (see Figures 4.3(c), 4.3(d)).

In **Publication III** 117 models for postsynaptic signal transduction in synaptic plasticity are reviewed by categorizing and listing their characteristics. Firstly, the main characteristics of the models are listed in three tables, LTP models in Table 2, LTP models in Table 3, and dual LTP and LTD models in Table 4 in **Publication III**. Secondly, a new categorization

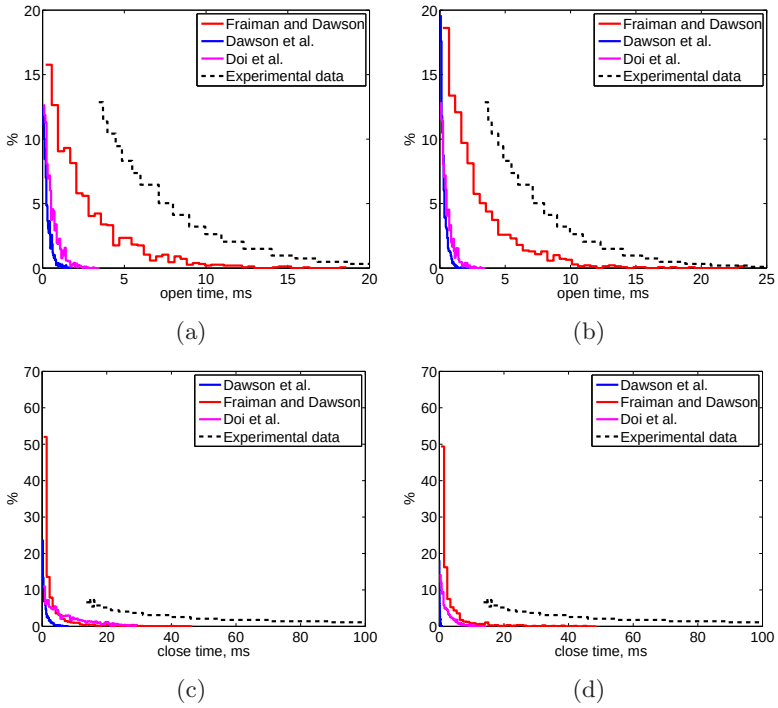

Figure 4.3. Distribution of IP_3R open (c,d) and closed times (e,f) for different models in simulation conditions $[Ca^{2+}] = 0.2$ μM, $[IP_3] = 2$ μM. Blue: Dawson *et al.* (2003), Red: Fraiman and Dawson (2004), Magenta: Doi *et al.* (2005), Black: Experimental data from Kaznacheyeva *et al.* (1998). Adapted from Hituri and Linne (2013).

system is established for these kind of models and the models are divided into the following categories: (A) models for single pathways, (B) models for calcium mechanisms or simplified intracellular processes, and (C) models for signaling networks. Models in category A, models for single pathways, involve at most one kinase as a model variable and do not include any receptors, ion channels, or pumps on the plasma membrane. Typically these models contain one pathway involving calmodulin and CaMKII and sometimes phosphatases in addition. Models in category B, models for calcium mechanisms or simplified intracellular processes, include postsynaptic Ca^{2+} buffers together with ion channels, receptors, or pumps, or simplified intracellular processes. Models in category C, signaling networks, include interactions between at least two pathways and thus often have several protein kinases and phosphatases. These models can also include pumps, ion channels, and receptors. The characteristics of the models are presented in Tables 5-7 in **Publication III** for each category, respectively.

The results in **Publication III** show that year after year the models are becoming increasingly complex and sophisticated, by including stochastic properties, integrating with electrophysiological properties of whole neurons, and incorporating diffusion of molecules (see Figure 3 in **III**). The study also revealed that only 26 of the 117 models were provided in a database or by other open-access means.

If a model is freely available in a database and it is described in language that current simulators can read or it is comprehensively described in the original publication, and thus possible to implement, it may be possible to computationally compare the model to other similar ones. Unfortunately many times these conditions are not fulfilled. For **Publication II**, we were able to find five fairly recent models (d'Alcantara *et al.*, 2003; Hayer and Bhalla, 2005; Lindskog *et al.*, 2006; Kim *et al.*, 2010; Nakano *et al.*, 2010) that were suitable for our comparative study on models for postsynaptic LTP/LTD (for selection criteria, see p. 3 in **Publication II**). To my best knowledge, **Publication II** is the first computational comparison of models for postsynaptic signal transduction in synaptic plasticity and the first one to take a step towards finding a general setup for quantitative model comparison. The models were simulated using deterministic approach and using same kind of input and total concentrations of key enzymes CaMKII and PP1 were varied.

When using exactly the same input, models produce varying responses but yet there also are similarities. In models by d'Alcantara *et al.* (2003), Kim *et al.* (2010), Lindskog *et al.* (2006), and Nakano *et al.* (2010) values of active [CaMKII] and active [PP1] follow the initial value: higher initial value results in higher output value. In the generic model by Hayer and Bhalla (2005) the active [CaMKII] is dependent on $[PP1]_{tot}$. Models by d'Alcantara *et al.* (2003) and Nakano *et al.* (2010) produced similar results even though they describe the phenomenon in different types of neurons. Simulation results also show that the end point concentrations of active CaMKII in the models by Hayer and Bhalla (2005) and Kim *et al.* (2010) are much higher than with the other three models. The peak and end point concentrations of PP1 are similar in all the models. These results are presented in Figure 3 and Table 5 in **Publication II** .

Chapter 5

Discussion

In this thesis, a variety of computational models and methods in the field of computational neuroscience were compared and evaluated. Models of interest describe intracellular phenomena related to synaptic plasticity and more specific mechanisms such as IP_3 receptor function in neurons. Based on the results, several conclusions were made both on the quality and usability of the models. This chapter is devoted to discussion of these results.

Numerous computational models have been developed to describe synaptic plasticity, a phenomenon considered important in learning and formation of memory (Markram *et al.*, 2011). In this work, a large amount of models for the postsynaptic signal transduction in synaptic plasticity and the IP_3 receptor function are studied. The studies, included in this work, revealed that many of the models are neither constructed nor validated based on previous models. Instead, they are rebuild from scratch (so called *de novo* methodology; see Cannon *et al.* (2007)). The lack of studies comparing the models, indicates that the comparison is challenging. This thesis provides detailed insight into model comparison and tools for simulation in order to help researchers to choose a suitable model for future work.

The quality of a model is dependent on several factors but probably the most important criteria is whether the model can address a question which is biologically relevant and of general scientific interest. Data for model construction and fine-tuning would ideally be acquired from the same neuronal type as the model is built for. Now, in many cases, the modelers just use data from various sources as nothing else is available. Many times the original, experimental data used in modeling is neither refered nor described properly and difficult to track later on. Another criteria could be whether a model can be used to make verifiable predictions. Thus the model could be seen useful and it might be possible to enhance experimental progress by using simulations to select the most promising experiments.

Three of the publications (**Publication I–III**) deal with assessing the quality of the previously developed models and their suitability in future modeling work. In **Publication III**, the emphasis was set on evaluating the model components and on the significance of the models rather than on comparison of the actual simulated model responses as in **Publications I** and **II**. The comparison of model responses is complicated as all models need to be implemented and simulated before a comparative analysis can be performed. This is not only time consuming, but many times impossible as many of the models are not described in sufficient detail or provided in model databases or by other open-access means. According to **Publication III**, only 26 of the 117 models for postsynaptic signal transduction in synaptic plasticity, more precisely in LTP and LTD, are publicly available (see Table 8 in **Publication III**). Qualitative comparison is also many times difficult since only a few publications provide a graphical illustration of the model components, in many cases it is complicated to decipher the model input or stimulus, or the model is otherwise insufficiently described in the original publication.

A quantitative comparison of models in this thesis revealed major differences in the statistical properties of the four IP_3 receptor models (**Publication I**). Four major reasons, why the selected models behave differently to each other, are identified: 1) the structure and parameter values differ between the models, 2) experimental data that was used in the model development vary, 3) different data handling procedures have been used when developing the models, and 4) model developers did not use automated parameter estimation methods. Although only one of the IP_3 models, the model of Fraiman and Dawson (2004), satisfactorily reproduces the experimental findings, the study offers an important step towards a new, predictive model of IP_3 receptor that will be required in larger scale modeling of neuronal intracellular processes.

In **Publication II**, the quantitative comparison showed that, when using exactly the same input, the responses of different models describing the LTP/LTD in the very same type of a neuron. The difference may partly be explained by the fact that some models had been constructed to answer relatively specific questions and that simulation setup used in **Publication II** might be out the models capabilities.

As concluded in the **Publication II** and **III**, there are some minimum criteria for published model in order to it be useful for other scientist. The following criteria are a combined collection of those presented in **Publication II** and **III**. All models should (1) be described in sufficient detail including equations, inputs, outputs, compartments, variables, constants, parameters, and initial conditions, (2) have adequate metadata and citations related to the experimental data used, (3) explain set of features describing the overall behavior of the modeled system, (4) be compared to previous

models at least to some extent, (5) be formulated using common description language, and (6) provided in a model database. There are several model databases available to store models and metadata for future use, for example, the BioModels database (Le Novére *et al.*, 2006; Li *et al.*, 2010), ModelDB (Migliore *et al.*, 2003; Hines *et al.*, 2004), DOQCS (Sivakumaran *et al.*, 2003), and Open Source Brain (Gleeson *et al.*, 2012). The value of the models for understanding molecular mechanisms of synaptic plasticity would enhance further with more complete descriptions and sharing of the published models. The IP_3 receptor models implemented in **Publication I** have been made publicly available and can be found from ModelDB (Migliore *et al.*, 2003; Hines *et al.*, 2004).

In addition to minimum criteria to publish models, there are other challenges that the field of computational neuroscience should address. One of these challenges is related to the lack of time-series functional data in general, and the access to original raw data. In addition, the existing bioinformatics and other databases contain a lot of information on the structure of ion channels and receptor-channel complexes of neural origin (see, for example, The Protein Database (2013), The Protein Data Bank (PDB) (2013), Human Protein Reference Database (2013), and IUPHAR Database (Sharman *et al.*, 2013)). However, the electrophysiological measurements to record the activity of these ion channels and ion channel-receptor complexes are not, in general, available in public databases. A lot of such functional data has benn produced and published over the past 25 years. The reason for not having the raw data available is the lack of suitable databases and storage space. Electrophysiological data would be extremely useful in developing detailed biophysical models for ion channel kinetics and modulation of channel functions by various intra- and extracellular factors. Electrophysiological data on ion channel function would also be very useful source of information when developing multi-scale models of neural functions in the future. Electrophysiological data measured on IP_3 receptor is not either currently available in any public database and as the years pass by it becomes extremely hard to acquire the data from its original sources.

The problem of publicly unavailable data has been discussed already over ten years ago and is not limited just to measurements of ion channels but to all neuroscience data (Amari *et al.*, 2002; Cannon *et al.*, 2002). De Schutter (2010*a*), for instance, has suggested one solution in which data publishing should be totally distinguished from paper publishing. Fortunately, some improvement to the situation have been made. The CARMEN project (CARMEN project, 2013) aims to create an environment for sharing collaborative exploitation of neurophysiology experiment data and algorithms using distributed computing technology and Ranjan *et al.* (2011) have established an information management framework for ion channel information that hopefully will make more and more experimental data accessible in the

future. Furthermore, NeuroMorpho.Org (Ascoli, 2006; Ascoli *et al.*, 2007) contains digitally reconstructed neurons published in articles.

This thesis also addresses the usability of simulation tools and methods in context of models for systems of biochemical reactions. Based on the studies in this thesis, it is important to put more emphasis on better guiding the selection of simulation tool and methods. In addition to increasing amount of models, the number of tools to simulate them is increasing. **Publication VI** contributes to developing better modeling and simulation tools by evaluating stochastic simulation tools for cellular signaling. According to the study, the outcomes of the simulations do not differ between the simulation tools compared and thus the user can freely select the tool according to the features needed. The study also concludes that multiple features are included in the tool in the expense of user-friendliness.

Additional attention should also be put to the selection of modeling and simulation methods in order to better capture the special characteristics of nervous tissue in the models. Depending on the previous dynamic state of a neuron, the information that the neuron receives through synapses from other neurons, and the modulatory effects of glial cells the neuron reaches its next dynamic state. This special way of working of the nervous system, as well as randomness and fluctuations inherently present in the system, has to be better taken into account in computational modeling in the future. Most of the previously developed models that were used in **Publication I** and **III** are deterministic, although many events in biology are stochastic in nature and stochastic methods have recently been applied and developed more and more. As also shown in this thesis, the stochastic approach, in general, gives more realistic results than the deterministic one, because it allows to take the randomness and fluctuations naturally present in the system into account. Specifically, the simulations in **Publications IV** and **V** show that when the numbers of molecules in the system are small, realistic results can be obtained only using stochastic modeling approaches. Special attention should thus be put to the selection of stochastic approach.

More attention should be put to the development and comparison of new simulation methods as well. In this thesis, when comparing different stochastic modeling methods In **Publication V**, it is concluded that stochastic differential equation modeling might lead to an unstable model when the numbers of molecules are small. Thus the Gillespie SSA is a better choice in this special modeling case. Similar concern should be used when using the Michaelis-Menten kinetics and stochastic algorithm to solve the equations computationally. Michaelis-Menten formulation is a quasi-steady-state approximation of the underlying enzymatic reactions. Recently, Agarwal *et al.* (2012) have questioned the validity of this quasi-steady-state approach approximation when applied to stochastic systems. Agarwal *et al.* (2012) show that the stochastically simulated results of the approximated system do not

accurately give the same outcome as the underlying enzymatic reactions. Thus when making decisions about the stochastic approach to be used in a study, the selection of modeling method and stochastic simulation approach should be made carefully. Stochastic approaches for modeling and simulation are important because very small numbers of molecules can have a dramatic effect on either strengthening or weakening the synapses and these effects should be taken into account (Skupin *et al.*, 2008). This thesis strongly advocates for stochastic approach for models based on the law of mass action.

The field of computational neuroscience is moving towards data-driven modeling and development of models with finer biochemical and biophysical details. As more and more details are discovered about the synaptic plasticity, it seems inevitable that the number of variables in models increase meaning that the models grow bigger in size. In the future, the increase in experimental data will also emphasize the significance of data-driven modeling approach. The reduction of model complexity might be an important research area in the future. Simplified models that capture relevant aspects of dynamics could be embedded, for example, into biologically-inspired neuronal network models when the activity of individual neurons is modeled in more detail. Since the brain is an organ with multiple levels of organization, multi-scale modeling approach for modeling its function would be beneficial. For example, a recently initiated large project, The Human Brain Project (HBP-PS Consortium, 2012), aims to contribute to multi-scale modeling of the mammalian brain. There are still a lot of open question and challenges in multi-scale modeling. They are reviewed from the point of view of computational biology by Southern *et al.* (2008). Inevitably, computational modeling and massive data-driven simulations will be the future of neuroscience to reveal new aspects of the brain and to better understand the role of neurons, glial cells, and molecules in health and disease.

Bibliography

Agarwal, A., Adams, R., Castellani, G. C. and Shouval, H. Z. (2012) On the precision of quasi steady state assumptions in stochastic dynamics. *J. Chem. Phys.,* 137, 044105.

Alves, R., Antunes, F. and Salvador, A. (2006) Tools for kinetic modeling of biochemical networks. *Nature Biotech.,* 24(6), 667–672.

Amari, S., Beltrame, F., Bjaalie, J., Dalkara, T., De Schutter, E., Egan, G., Goddard, N., Gonzalez, C., Grillner, S., Herz, A. *et al.* (2002) Neuroinformatics: the integration of shared databases and tools towards integrative neuroscience. *J. Integr. Neurosci.,* 1, 117–128.

Andrews, S. S., Addy, N. J., Brent, R. and Arkin, A. P. (2010) Detailed simulations of cell biology with Smoldyn 2.1. *PLoS Comput. Biol.,* 6(3), e1000705.

Antunes, G. and De Schutter, E. (2012) A stochastic signaling network mediates the probabilistic induction of cerebellar long-term depression. *J. Neurosci.,* 32(27), 9288–9300.

Arkin, A. P. (2001) Synthetic cell biology. *Curr. Opin. Biotech.,* 12(6), 638–644.

Ascoli, G. A. (2006) Mobilizing the base of neuroscience data: the case of neuronal morphologies. *Nature Rev. Neurosci.,* 7(4), 318–324.

Ascoli, G. A., Donohue, D. E. and Halavi, M. (2007) NeuroMorpho. Org: a central resource for neuronal morphologies. *J. Neurosci.,* 27(35), 9247–9251.

Atri, A., Amundson, J., Clapham, D. and Sneyd, J. (1993) A single-pool model for intracellular calcium oscillations and waves in the Xenopus laevis oocyte. *Biophys. J.,* 65(4), 1727–1739.

Banerjee, S. and Hasan, G. (2005) The $InsP_3$ receptor: its role in neuronal physiology and neurodegeneration. *Bioessays,* 27(10), 1035–1047.

Barbara, J. (2002) IP_3-dependent calcium-induced calcium release mediates bidirectional calcium waves in neurones: functional implications for synaptic plasticity. *Biochim. Biophys. Acta - Proteins & Proteomics,* 1600(1-2), 12–18.

Barrio, M., Burrage, K., Leier, A. and Tian, T. (2006) Oscillatory regulation of Hes1: discrete stochastic delay modelling and simulation. *PLoS Comput. Biol.,* 2(9), e117.

Beattie, E. C., Carroll, R. C., Yu, X., Morishita, W., Yasuda, H., von Zastrow, M. and Malenka, R. C. (2000) Regulation of AMPA receptor endocytosis by a signaling mechanism shared with LTD. *Nature Neurosci.,* 3(12), 1291–1300.

Berridge, M. (1998) Neuronal calcium cignaling. *Neuron,* 21, 13–26.

Bezprozvanny, I. and Ehrlich, B. (1994) Inositol (1,4,5)-trisphosphate ($InsP_3$)-gated Ca channels from cerebellum: conduction properties for divalent cations and regulation by intraluminal calcium. *J. Gen. Phys.,* 104, 821–856.

Bezprozvanny, I., Watras, J. and Ehrlich, B. (1991) Bell-shaped calcium-response curves of $Ins(1,4,5)P_3$- and calcium-gated channels from endoplasmic reticulum of cerebellum. *Nature,* 351, 751–754.

Bhalla, U. and Iyengar, R. (1999) Emergent properties of networks of biological signaling pathways. *Science,* 283, 381–387.

Bhalla, U. S. (2004*a*) Signaling in small subcellular volumes. I. stochastic and diffusion effects on individual pathways. *Biophys. J.,* 87(2), 733–744.

Bhalla, U. S. (2004*b*) Signaling in small subcellular volumes. II. stochastic and diffusion effects on synaptic network properties. *Biophys. J.,* 87(2), 745–753.

Bliss, T. V. and Gardner-Medwin, A. (1973) Long-lasting potentiation of synaptic transmission in the dentate area of the unanaesthetized rabbit following stimulation of the perforant path. *J. Physiol.,* 232(2), 357.

Bliss, T. V. and Lømo, T. (1973) Long-lasting potentiation of synaptic transmission in the dentate area of the anaesthetized rabbit following stimulation of the perforant path. *J. Physiol.,* 232(2), 331–356.

Bramham, C. R. (2010) LTP≠ learning: lessons from short-term plasticity. *Front. Behav. Neurosci.,* 4.

Brovko, L., Gandelman, O., Polenova, T. and Ugarova, N. (1994) Kinetics of bioluminescence in the firefly luciferin-luciferase. *Biochem. (Moscow),* 59, 19–201.

Cannon, R., Howell, F., Goddard, N. and De Schutter, E. (2002) Non-curated distributed databases for experimental data and models in neuroscience. *Network: Computation in Neural Systems,* 13(3), 415–428.

Cannon, R. C., Gewaltig, M.-O., Gleeson, P., Bhalla, U. S., Cornelis, H., Hines, M. L., Howell, F. W., Muller, E., Stiles, J. R., Wils, S. *et al.* (2007) Interoperability of neuroscience modeling software: current status and future directions. *Neuroinformatics,* 5(2), 127–138.

Cárdenas, A., Rodríguez, M., Cortés, M., Alvarez, R., Wei, W., Rapoport, S., Shimahara, T., Caviedes, R. and Caviedes, P. (1999) Calcium signals in cell lines derived from the cerebral cortex of normal and trisomy 16 mice. *NeuroReport,* 10(2), 363–369.

CARMEN project (2013). http://www.carmen.org.uk/, [Online], Accessed August 6, 2013.

Choi, T., Maurya, M., Tartakovsky, D. and Subramaniam, S. (2010) Stochastic hybrid modeling of intracellular calcium dynamics. *J. Chem. Phys.,* 133, 165101.

Citri, A. and Malenka, R. (2008) Synaptic plasticity: multiple forms, functions, and mechanisms. *Neuropsychopharmacol.,* 33(1), 18–41.

Coba, M. P., Pocklington, A. J., Collins, M. O., Kopanitsa, M. V., Uren, R. T., Swamy, S., Croning, M. D., Choudhary, J. S. and Grant, S. G. (2009) Neurotransmitters drive combinatorial multistate postsynaptic density networks. *Sci. Signal.,* 2(68), ra19.

Collins, M. O., Yu, L., Coba, M. P., Husi, H., Campuzano, I., Blackstock, W. P., Choudhary, J. S. and Grant, S. G. (2005) Proteomic analysis of in vivo phosphorylated synaptic proteins. *Sci. Signal.,* 280(7), 5972.

d'Alcantara, P., Schiffmann, S. N. and Swillens, S. (2003) Bidirectional synaptic plasticity as a consequence of interdependent Ca^{2+}-controlled phosphorylation and dephosphorylation pathways. *Eur. J. Neurosci.,* 17(12), 2521–2528.

Davison, A. P., Brüderle, D., Eppler, J., Kremkow, J., Muller, E., Pecevski, D., Perrinet, L. and Yger, P. (2008) PyNN: a common interface for neuronal network simulators. *Front. Neuroinf.,* 2(11).

Dawson, A., Lea, E. and Irvine, R. (2003) Kinetic model of the inositol trisphosphate receptor that shows both steady-state and quantal patterns of Ca^{2+} release from intracellular stores. *Biochem. J.,* 370(2), 621.

De Schutter, E. (2010*a*) Data publishing and scientific journals: the future of the scientific paper in a world of shared data. *Neuroinformatics,* 8(3), 151–153.

De Schutter, E., ed. (2010*b*) *Computational modeling methods for neuroscientists.* The MIT Press.

De Schutter, E. (2012). The importance of stochastic signaling processes in the induction of long-term synaptic plasticity.

De Schutter, E. and Smolen, P. (1998) *Calcium dynamics in large neuronal models.* Cambridge, MA: MIT Press 2nd edition, 211–250.

De Young, G. and Keizer, J. (1992) A single-pool inositol 1,4,5-trisphosphate-receptor-based model for agonist-stimulated oscillations in Ca^{2+} concentration. *Proc. Natl. Acad. Sci. U.S.A.,* 89(20), 9895–9899.

Delord, B., Berry, H., Guigon, E. and Genet, S. (2007) A new principle for information storage in an enzymatic pathway model. *PLoS Comput. Biol.,* 3(6), e124.

Demuro, A. and Parker, I. (2013) Cytotoxicity of intracellular Aβ42 amyloid oligomers involves Ca^{2+} release from the endoplasmic reticulum by stimulated production of inositol trisphosphate. *J. Neurosci.,* 33(9), 3824–3833.

Diambra, L. and Guisoni, N. (2005) Modeling stochastic Ca^{2+} release from a cluster of IP_3-sensitive receptors. *Cell Calcium,* 37(4), 321–332.

Djurfeldt, M., Hjorth, J., Eppler, J. M., Dudani, N., Helias, M., Potjans, T. C., Bhalla, U. S., Diesmann, M., Kotaleski, J. H. and Ekeberg, O. (2010) Run-time interoperability between neuronal network simulators based on the MUSIC framework. *Neuroinformatics,* 8(1), 43–60.

Doi, T., Kuroda, S., Michikawa, T. and Kawato, M. (2005) Inositol 1,4,5-trisphosphate-dependent Ca^{2+} threshold dynamics detect spike timing in cerebellar Purkinje cells. *J. Neurosci.,* 25(4), 950–961.

Dufour, J., Arias, I. and Turner, T. (1997) Inositol 1,4,5-trisphosphate and calcium regulate the calcium channel function of the hepatic inositol 1,4,5-trisphosphate receptor. *J. Biol. Chem.,* 272(5), 2675–2681.

Ermentrout, B. and Rinzel, J. (2010) Differential equations. In *Computational modeling methods for neuroscientists.* The MIT Press.

Eungdamrong, N. and Iyengar, R. (2004) Modeling cell signaling networks. *Biol. Cell,* 96(5), 355–362.

Falcke, M. (2003) On the role of stochastic channel behavior in intracellular Ca^{2+} dynamics. *Biophys. J.,* 84(1), 42–56.

Fiala, J. C., Grossberg, S. and Bullock, D. (1996) Metabotropic glutamate receptor activation in cerebellar purkinje cells as substrate for adaptive

timing of the classically conditioned eye-blink response. *J. Neurosci.,* 16(11), 3760–3774.

Foskett, J. (2010) Inositol trisphosphate receptor Ca^{2+} release channels in neurological diseases. *Pflugers Arch. Eur. J. Physiol.,* 460(2), 481–494.

Foskett, J. K., White, C., Cheung, K.-H. and Mak, D.-O. D. (2007) Inositol trisphosphate receptor Ca^{2+} release channels. *Physiol. Rev.,* 87(2), 593–658.

Fraiman, D. and Dawson, S. P. (2004) A model of IP_3 receptor with a luminal calcium binding site: stochastic simulations and analysis. *Cell Calcium,* 35(5), 403–413.

Franks, K. M. and Sejnowski, T. J. (2002) Complexity of calcium signaling in synaptic spines. *BioEssays,* 24(12), 1130–1144.

Fujiwara, A., Hirose, K., Yamazawa, T. and Iino, M. (2001) Reduced IP_3 sensitivity of IP_3 receptor in Purkinje neurons. *Neuroreport,* 12(12), 2647–2651.

Gibson, M. A. and Bruck, J. (2000) Efficient exact stochastic simulation of chemical systems with many species and many channels. *J. Phys. Chem. A,* 104(9), 1876–1889.

Gillespie, D. T. (1976) A general method for numerical simulating the stochastic time evolution of coupled chemical reactions. *J. Comp. Phys.,* 22, 403–434.

Gillespie, D. T. (1977) Exact stochastic simulation of coupled chemical reactions. *J. Phys. Chem.,* 81(25), 2340–2361.

Gillespie, D. T. (1992) A rigorous derivation of the chemical master equation. *Physica A,* 188(1), 404–425.

Gillespie, D. T. (2001) Approximate accelerated stochastic simulation of chemically reacting systems. *J. Chem. Phys.,* 115, 1716.

Gillespie, D. T. (2007) Stochastic simulation of chemical kinetics. *Annu. Rev. Phys. Chem.,* 58, 35–55.

Gin, E., Falcke, M., Wagner, L., Yule, D. and Sneyd, J. (2009*a*) Markov chain Monte Carlo fitting of single-channel data from inositol trisphosphate receptors. *J. Theor. Biol.,* 257(3), 460–474.

Gin, E., Falcke, M., Wagner, L. *et al.* (2009*b*) A kinetic model of the inositol trisphosphate receptor based on single-channel data. *Biophysical journal,* 96(10), 4053.

Girolami, M. (2008) Bayesian inference for differential equations. *Theor. Comput. Sci.,* 408(1), 4–16.

Gleeson, P., Crook, S., Cannon, R. C., Hines, M. L., Billings, G. O., Farinella, M., Morse, T. M., Davison, A. P., Ray, S., Bhalla, U. S. *et al.* (2010) NeuroML: a language for describing data driven models of neurons and networks with a high degree of biological detail. *PLoS Comput. Biol.,* 6(6), e1000815.

Gleeson, P., Piasini, E., Crook, S., Cannon, R., Steuber, V., Jaeger, D., Solinas, S., D'Angelo, E. and Silver, R. A. (2012) The Open Source Brain Initiative: enabling collaborative modelling in computational neuroscience. *BMC Neurosci.,* 13, 1–2.

Graupner, M. and Brunel, N. (2007) STDP in a bistable synapse model based on CaMKII and associated signaling pathways. *PLoS Comput. Biol.,* 3(11), e221.

Haeri, H., Hashemianzadeh, S. and Monajjemi, M. (2007) A kinetic Monte Carlo simulation study of inositol 1,4,5-trisphosphate receptor (IP3R) calcium release channel. *Comp. Biol. Chem.,* 31(2), 99–109.

Harris, K. M. and Stevens, J. K. (1988) Dendritic spines of rat cerebellar Purkinje cells: serial electron microscopy with reference to their biophysical characteristics. *J. Neurosci.,* 8, 4455–4469.

Hattne, J., Fange, D. and Elf, J. (2005) Stochastic reaction-diffusion simulation with mesord. *Bioinformatics,* 21(12), 2923–2924.

Hayer, A. and Bhalla, U. S. (2005) Molecular switches at the synapse emerge from receptor and kinase traffic. *PLoS Comput. Biol.,* 1(2), e20.

HBP-PS Consortium (2012). The Human Brain Project - A Report to the European Commission, April 2012, Lausanne (http://www.humanbrainproject.eu/).

Hebb, D. O. (1949) *The organization of behavior: A neuropsychological theory.* Wiley.

Hellgren Kotaleski, J. and Blackwell, K. (2010) Modelling the molecular mechanisms of synaptic plasticity using systems biology approaches. *Nat. Rev. Neurosci.,* 11(4), 239–251.

Henneberger, C., Papouin, T., Oliet, S. H. and Rusakov, D. A. (2010) Long-term potentiation depends on release of d-serine from astrocytes. *Nature,* 463(7278), 232–236.

Hepburn, I., Chen, W., Wils, S. and De Schutter, E. (2012) STEPS: efficient simulation of stochastic reaction-diffusion models in realistic morphologies. *BMC Syst. Biol.,* 6(35), 1752–0509.

Hernjak, N., Slepchenko, B., Fernald, K., Fink, C., Fortin, D., Moraru, I., Watras, J. and Loew, L. (2005) Modeling and analysis of calcium signaling events leading to long-term depression in cerebellar Purkinje cells. *Biophys. J.,* 89(6), 3790–3806.

Hines, M. L., Morse, T., Migliore, M., Carnevale, N. T. and Shepherd, G. M. (2004) ModelDB: a database to support computational neuroscience. *J. Comput. Neurosci.,* 17(1), 7–11.

Hodgkin, A. L. and Huxley, A. F. (1952) A quantitative description of membrane current and its application to conduction and excitation in nerve. *J. Physiol.,* 117(4), 500–544.

Hucka, M., Finney, A., Bornstein, B. J., Keating, S. M., Shapiro, B. E., Matthews, J., Kovitz, B. L., Schilstra, M. J., Funahashi, A., Doyle, J. C. *et al.* (2004) Evolving a lingua franca and associated software infrastructure for computational systems biology: the Systems Biology Markup Language (SBML) project. *Systems Biol.,* 1(1), 41–53.

Human Protein Reference Database (2013). http://www.hprd.org/, [Online], Accessed May 17, 2013.

Ida, Y. and Kidera, A. (2013) The conserved Arg241-Glu439 salt bridge determines flexibility of the inositol 1, 4, 5-trisphosphate receptor binding core in the ligand-free state. *Proteins: Structure, Function, and Bioinformatics,*.

Intosalmi, J. (2012). *Stochastic Modeling and Analysis of Time Evolution for Biochemical Systems*. PhD thesis, Tampere University of Technology.

Ito, M. (2001) Cerebellar long-term depression: characterization, signal transduction, and functional roles. *Physiol. Rev.,* 81(3), 1143–1195.

Ito, M. (2002) The molecular organization of cerebellar long-term depression. *Nature Rev. Neurosci.,* 3(11), 896–902.

Ito, M., Sakurai, M. and Tongroach, P. (1982) Climbing fiber induced depression of both mossy fiber responsiveness and glutamate sensitivity of cerebellar Purkinje cells. *J. Physiol.,* 324(1), 113–124.

Janes, K. A. and Yaffe, M. B. (2006) Data-driven modelling of signal-transduction networks. *Nat. Rev. Mol. Cell Biol.,* 7(11), 820–828.

Kaftan, E., Ehrlich, B. and Watras, J. (1997) Inositol 1,4,5-trisphosphate ($InsP_3$) and calcium interact to increase the dynamic range of $InsP_3$ receptor-dependent calcium signaling. *J. Gen. Physiol.,* 110(5), 529–538.

Kaznacheyeva, E., Lupu, V. D. and Bezprozvanny, I. (1998) Single-channel properties of inositol (1,4,5)-trisphosphate receptor heterologously expressed in HEK-293 cells. *J. Gen. Physiol.,* 111(6), 847–856.

Kerr, R. A., Bartol, T. M., Kaminsky, B., Dittrich, M., Chang, J.-C. J., Baden, S. B., Sejnowski, T. J. and Stiles, J. R. (2008) Fast monte carlo simulation methods for biological reaction-diffusion systems in solution and on surfaces. *SIAM J. Sci. Comput.,* 30(6), 3126–3149.

Khodakhah, K. and Ogden, D. (1995) Fast activation and inactivation of inositol trisphosphate-evoked Ca^{2+} release in rat cerebellar Purkinje neurones. *J. Physiol.,* 487(2), 343.

Kierzek, A. M., Zaim, J. and Zielenkiewicz, P. (2001) The effect of transcription and translation initiation frequencies on the stochastic fluctuations in prokaryotic gene expression. *J. Biol. Chem.,* 276(11), 8165–8172.

Kim, M. S., Huang, T., Abel, T. and Blackwell, K. T. (2010) Temporal sensitivity of protein kinase A activation in late-phase long term potentiation. *PLoS Comput. Biol.,* 6(2), e1000691.

Klug, A., Borst, J. G. G., Carlson, B. A., Kopp-Scheinpflug, C., Klyachko, V. A. and Xu-Friedman, M. A. (2012) How do short-term changes at synapses fine-tune information processing? *J. Neurosci.,* 32(41), 14058–14063.

Koch, C. and Segev, I. (1988) *Methods in neuronal modeling: From synapses to networks.* MIT Press.

Konnerth, A., Dreessen, J. and Augustine, G. J. (1992) Brief dendritic calcium signals initiate long-lasting synaptic depression in cerebellar Purkinje cells. *Proc. Natl. Acad. Sci. U.S.A.,* 89, 7051–7055.

Laurent, M. and Claret, M. (1997) Signal-induced ca^{2+} oscillations through the regulation of the inositol 1, 4, 5-trisphosphate-gated ca^{2+} channel: an allosteric model. *J. Theor. Biol.,* 186(3), 307–326.

Le Novére, N., Bornstein, B., Broicher, A., Courtot, M., Donizelli, M., Dharuri, H., Li, L., Sauro, H., Schilstra, M., Shapiro, B. *et al.* (2006) BioModels Database: a free, centralized database of curated, published, quantitative kinetic models of biochemical and cellular systems. *Nucleic Acids Res.,* 34(suppl 1), D689–D691.

LeBeau, A., Yule, D., Groblewski, G. and Sneyd, J. (1999) Agonist-dependent phosphorylation of the inositol 1, 4, 5-trisphosphate receptor. *J. Gen. Physiol.,* 113(6), 851.

Li, C., Donizelli, M., Rodriguez, N., Dharuri, H., Endler, L., Chelliah, V., Li, L., He, E., Henry, A., Stefan, M. I., Snoeand, J. L., Hucka, M., Le Novére, N. and Laibe, C. (2010) BioModels Database: an enhanced, curated and annotated resource for published quantitative kinetic models. *BMC Syst. Biol.,* 4(1), 92.

Li, Y. and Rinzel, J. (1994) Equations for $Insp_3$ receptor-mediated $[Ca^{2+}]_i$ oscillations derived from a detailed kinetic model: a Hodgkin-Huxley like formalism. *J. Theor. Biol.,* 166(4), 461–473.

Libersat, F. and Duch, C. (2004) Mechanisms of dendritic maturation. *Mol. Neurobiol.,* 29(3), 303–320.

Lindskog, M., Kim, M., Wikström, M. A., Blackwell, K. T. and Hellgren Kotaleski, J. (2006) Transient calcium and dopamine increase PKA activity and DARPP-32 phosphorylation. *PLoS Comput. Biol.,* 2(9), e119.

Lynch, G., Larson, J., Kelso, S., Barrionuevo, G. and Schottler, F. (1983) Intracellular injections of EGTA block induction of hippocampal long-term potentiation. *Nature,* 305(5936), 719–721.

Mak, D., McBride, S. and Foskett, J. (2003) Spontaneous channel activity of the inositol 1,4,5-trisphosphate ($InsP_3$) receptor ($InsP_3R$). Application of allosteric modeling to calcium and $InsP_3$ regulation of $InsP_3R$ single-channel gating. *J. Gen. Physiol.,* 122(5), 583.

Malenka, R. C. and Bear, M. F. (2004) LTP and LTD: an embarrassment of riches. *Neuron,* 44(1), 5–21.

Malenka, R. C., Kauer, J. A., Zucker, R. S., Nicoll, R. A. *et al.* (1988) Postsynaptic calcium is sufficient for potentiation of hippocampal synaptic transmission. *Science,* 242(4875), 81–84.

Manninen, T. (2007). *Stochastic Methods for Modeling Intracellular Signaling.* PhD thesis, Tampere University of Technology.

Manninen, T., Linne, M.-L. and Ruohonen, K. (2006) A novel approach to model neuronal signal transduction using stochastic differential equations. *Neurocomputing,* 69, 1066–1069.

Marchant, J. S. and Taylor, C. W. (1997) Cooperative activation of IP_3 receptors by sequential binding of IP_3 and Ca^{2+} safeguards against spontaneous activity. *Curr. Biol.,* 7, 510–518.

Marchenko, S., Yarotskyy, V., Kovalenko, T., Kostyuk, P. and Thomas, R. (2005) Spontaneously active and $InsP_3$-activated ion channels in cell nuclei from rat cerebellar Purkinje and granule neurones. *J. Physiol.,* 565(3), 897–910.

Markram, H., Gerstner, W. and Sjöström, P. J. (2011) A history of spike-timing-dependent plasticity. *Front. Syn. Neurosci.,* 3.

Markram, H., Lübke, J., Frotscher, M. and Sakmann, B. (1997) Regulation of synaptic efficacy by coincidence of postsynaptic APs and EPSPs. *Science,* 275(5297), 213–215.

McQuarrie, D. A. (1967) Stochastic approach to chemical kinetics. *J. Appl. Probab.,* 4(3), 413–478.

Melamed-Book, N., Kachalsky, S. G., Kaiserman, I. and Rahamimoff, R. (1999) Neuronal calcium sparks and intracellular calcium "noise". *Proc. Natl. Acad. Sci. U.S.A.,* 96(26), 15217–15221.

Michaelsen, K. and Lohmann, C. (2010) Calcium dynamics at developing synapses: mechanisms and functions. *Eur. J. Neurosci.,* 32(2), 218–223.

Migliore, M., Morse, T. M., Davison, A. P., Marenco, L., Shepherd, G. M. and Hines, M. L. (2003) ModelDB: making models publicly accessible to support computational neuroscience. *Neuroinformatics,* 1(1), 135–139.

Mishra, J. and Bhalla, U. (2002) Simulations of inositol phosphate metabolism and its interaction with InsP3-mediated calcium release. *Biophys. J.,* 83(3), 1298–1316.

Missiaen, L., Robberecht, W., Bosch, L., Callewaert, G., Parys, J., Wuytack, F., Raeymaekers, L., Nilius, B., Eggermont, J. and Smedt, H. D. (2000) Abnormal intracellular ca^{2+} homeostasis and disease. *Cell Calcium,* 28(1), 1–21.

Miyata, M., Finch, E. A., Khiroug, L., Hashimoto, K., Hayasaka, S., Oda, S. I., Inouye, M., Takagishi, Y., Augustine, G. J. and Kano, M. (2000) Local calcium release in dendritic spines required for long-term synaptic depression. *Neuron,* 28, 233–244.

Moles, C. G., Mendes, P. and Banga, J. R. (2003) Parameter estimation in biochemical pathways: a comparison of global optimization methods. *Genome research,* 13(11), 2467–2474.

Monod, J., Wyman, J. and Changeux, J. (1965) On the nature of allosteric transitions: a plausible model. *J. Mol. Biol.,* 12, 88.

Moraru, I., Kaftan, E., Ehrlich, B. and Watras, J. (1999) Regulation of Type 1 Inositol 1,4,5-Trisphosphate-gated Calcium channels by $Insp_3$ and Calcium. Simulation of Single Channel Kinetics Based on Ligand Binding and Electrophysiological Analysis. *J. Gen. Physiol.,* 113(6), 837–849.

Nakano, T., Doi, T., Yoshimoto, J. and Doya, K. (2010) A kinetic model of dopamine- and calcium-dependent striatal synaptic plasticity. *PLoS Comput. Biol.,* 6(2), e1000670.

Oliveira, R., Terrin, A., Di Benedetto, G., Cannon, R., Koh, W., Kim, M., Zaccolo, M. and Blackwell, K. (2010) The role of type 4 phosphodiesterases in generating microdomains of cAMP: large scale stochastic simulations. *PLoS One,* 5(7), e11725.

Othmer, H. G. and Tang, Y. (1993) *Oscillations and waves in a model of calcium dynamics* Experimental and Theoretical Advances in Biological Pattern Formation. London: Plenum Press 295–319.

Peercy, B. (2008) Initiation and propagation of a neuronal intracellular calcium wave. *J. Comp. Neurosci.,* 25(2), 334–348.

Perc, M., Gosak, M. and Marhl, M. (2006) From stochasticity to determinism in the collective dynamics of diffusively coupled cells. *Chem. Phys. Lett.,* 421(1), 106–110.

Perc, M., Green, A. K., Dixon, C. J. and Marhl, M. (2008) Establishing the stochastic nature of intracellular calcium oscillations from experimental data. *Biophys. Chem.,* 132(1), 33–38.

Perea, G. and Araque, A. (2007) Astrocytes potentiate transmitter release at single hippocampal synapses. *Sci. Signal.,* 317(5841), 1083.

Perea, G., Navarrete, M., Araque, A. *et al.* (2009) Tripartite synapses: astrocytes process and control synaptic information. *Trends in Neurosci.,* 32(8), 421.

Pettinen, A., Aho, T., Smolander, O.-P., Manninen, T., Saarinen, A., Taattola, K.-L., Yli-Harja, O. and Linne, M.-L. (2005) Simulation tools for biochemical networks: evaluation of performance and usability. *Bioinformatics,* 21, 357–363.

Raikov, I., Cannon, R., Clewley, R., Cornelis, H., Davison, A., De Schutter, E., Djurfeldt, M., Gleeson, P., Gorchetchnikov, A., Plesser, H. E. *et al.* (2011) NineML: the network interchange for neuroscience modeling language. *BMC Neurosci.,* 12(Suppl 1), P330.

Raikov, I. and De Schutter, E. (2012*a*) The promise and shortcomings of XML as an interchange format for computational models of biology. *Neuroinformatics,* 10(1), 1–3.

Raikov, I. and De Schutter, E. (2012*b*) The layer-oriented approach to declarative languages for biological modeling. *PLoS Comput. Biol.,* 8(5), e1002521.

Ranjan, R., Khazen, G., Gambazzi, L., Ramaswamy, S., Hill, S., Schürmann, F. and Markram, H. (2011) Channelpedia: an integrative and interactive database for ion channels. *Front. Neuroinform.,* 5.

Rao, C. V., Wolf, D. M. and Arkin, A. P. (2002) Control, exploitation and tolerance of intracellular noise. *Nature,* 420(6912), 231–237.

Rizzuto, R. (2001) Intracellular ca^{2+} pools in neuronal signalling. *Curr. Opin. Neurobiol.,* 11(3), 306–311.

Saarinen, A., Linne, M.-L. and Yli-Harja, O. (2006) Modeling single neuron behavior using stochastic differential equations. *Neurocomputing,* 69, 1091–1096.

Santello, M. and Volterra, A. (2010) Neuroscience: astrocytes as aide-memoires. *Nature,* 463(7278), 169–170.

Sarkisov, D. V. and Wang, S. S. (2008) Order-dependent coincidence detection in cerebellar Purkinje neurons at the inositol trisphosphate receptor. *J. Neurosci.,* 28(1), 133–142.

Schuster, S., Marhl, M. and Höfer, T. (2002) Modelling of simple and complex calcium oscillations. *Eur. J. Biochem.,* 269(5), 1333–1355.

Sharman, J. L., Benson, H. E., Pawson, A. J., Lukito, V., Mpamhanga, C. P., Bombail, V., Davenport, A. P., Peters, J. A., Spedding, M., Harmar, A. J. *et al.* (2013) Iuphar-db: updated database content and new features. *Nucleic acids research,* 41(D1), D1083–D1088.

Sharp, A., Nucifora Jr, F., Blondel, O., Sheppard, C., Zhang, C., Snyder, S., Russell, J., Ryugoand, D. and Ross, C. (1999) Differential cellular expression of isoforms of inositol 1,4,5-triphosphate receptors in neurons and glia in brain. *J. Comp. Neurol.,* 406(2), 207–220.

Shouval, H. Z., Wang, S. S.-H. and Wittenberg, G. M. (2010) Spike timing dependent plasticity: a consequence of more fundamental learning rules. *Front. Comput. Neurosci.,* 4.

Shuai, J. W. and Jung, P. (2002) Stochastic properties of Ca(2+) release of inositol 1,4,5-trisphosphate receptor clusters. *Biophys. J.,* 83(1), 87–97.

Shuai, J. W., Yang, D. P., E., P. J. and Rüdiger, S. (2009) An investigation of models of the IP_3R channel in Xenopus oocyte. *Chaos,* 19(3), 037105.

Siekmann, I., Wagner, L., Yule, D., Crampin, E. and Sneyd, J. (2012) A kinetic model for type I and II IP_3R accounting for mode changes. *Biophys. J.,* 103(4), 658–668.

Sivakumaran, S., Hariharaputran, S., Mishra, J. and Bhalla, U. S. (2003) The database of quantitative cellular signaling: management and analysis of chemical kinetic models of signaling networks. *Bioinformatics,* 19(3), 408–415.

Sjöström, P. J., Rancz, E. A., Roth, A. and Häusser, M. (2008) Dendritic excitability and synaptic plasticity. *Physiol. Rev.,* 88(2), 769–840.

Skupin, A., Kettenmann, H. and Falcke, M. (2010) Calcium signals driven by single channel noise. *PLoS Comp. Biol.,* 6(8), e1000870.

Skupin, A., Kettenmann, H., Winkler, U., Wartenberg, M., Sauer, H., Tovey, S. C., Taylor, C. W. and Falcke, M. (2008) How does intracellular ca_{2+} oscillate: by chance or by the clock? *Biophys. J.,* 94(6), 2404–2411.

Sneyd, J. and Dufour, J. (2002) A dynamic model of the type-2 inositol trisphosphate receptor. *Proc. Natl. Acad. Sci. U.S.A.,* 99(4), 2398–2403.

Sneyd, J. and Falcke, M. (2005) Models of the inositol trisphosphate receptor. *Prog. Biophys. Mol. Biol.,* 89, 207–245.

Sneyd, J., Falcke, M., Dufour, J. and Fox, C. (2004) A comparison of three models of the inositol trisphosphate receptor. *Prog. Biophys. Mol. Biol.,* 85(2-3), 121–140.

Southern, J., Pitt-Francis, J., Whiteley, J., Stokeley, D., Kobashi, H., Nobes, R., Kadooka, Y., Gavaghan, D. *et al.* (2008) Multi-scale computational modelling in biology and physiology. *Prog. Biophys. Mol. Biol.,* 96(1-3), 60.

Sugawara, T., Hisatsune, C., Le, T. D., Hashikawa, T., Hirono, M., Hattori, M., Nagao, S. and Mikoshiba, K. (2013) Type 1 Inositol trisphosphate receptor regulates cerebellar circuits by maintaining the spine morphology of Purkinje cells in adult mice. *J. Neurosci.,* 33(30), 12186–12196.

Swillens, S., Champeil, P., Combettes, L. and Dupont, G. (1998) Stochastic simulation of a single inositol 1,4,5-trisphosphate-sensitive Ca^{2+} channel reveals repetitive openings during 'blip-like' Ca^{2+} transients. *Cell calcium,* 23(5), 291–302.

Tanaka, M., Shih, P.-Y., Gomi, H., Yoshida, T., Nakai, J., Ando, R., Furuichi, T., Mikoshiba, K., Semyanov, A. and Itohara, S. (2013) Astrocytic ca^{2+} signals are required for the functional integrity of tripartite synapses. *Molecular brain,* 6, 1–13.

Tang, Y., Stephenson, J. and Othmer, H. (1996) Simplification and analysis of models of calcium dynamics based on IP_3-sensitive calcium channel kinetics. *Biophys. J.,* 70(1), 246–263.

Taufiq-Ur-Rahman, Skupin, A., Falcke, M. and Taylor, C. (2009) Clustering of $InsP_3$ receptors by $InsP_3$ retunes their regulation by $InsP_3$ and Ca^{2+}. *Nature,* 458(7238), 655–659.

Taylor, C. W., da Fonseca, P. C. and Morris, E. P. (2004) IP_3 receptors: the search for structure. *Trends Biochem. Sci.,* 29, 210–219.

Taylor, C. W. and Tovey, S. C. (2010) IP_3 receptors: Toward understanding their activation. *Cold Spring Harbor Perspect. Biol.,* 2(12).

The Protein Data Bank (PDB) (2013). http://www.rcsb.org/pdb, [Online], Accessed May 17, 2013.

The Protein Database (2013). http://www.ncbi.nlm.nih.gov/protein, [Online], Accessed May 17, 2013.

The STEPS developers (2013). Steps user manual and API references. http://steps.sourceforge.net/manual/manual_index.html, [Online], Accessed 16 Apr 2013.

Trappenberg, T. P. (2010) *Fundamentals of computational neuroscience.* Oxford University Press.

Turner, T. E., Schnell, S. and Burrage, K. (2004) Stochastic approaches for modelling in vivo reactions. *Comp. Biol. Chem.,* 28(3), 165–178.

Turrigiano, G. (2011) Too many cooks? Intrinsic and synaptic homeostatic mechanisms in cortical circuit refinement. *Ann. Rev. Neurosci.,* 34, 89–103.

Turrigiano, G. G. and Nelson, S. B. (2004) Homeostatic plasticity in the developing nervous system. *Nature Rev. Neurosci.,* 5(2), 97–107.

Ullah, G. and Jung, P. (2006) Modeling the statistics of elementary calcium release events. *Biophys. J.,* 90(10), 3485.

Walton, P. D., Airey, J. A., Sutko, J. L., Beck, C. F., Mignery, G. A., Südhof, T. C., Deerinck, T. J. and Ellisman, M. H. (1991) Ryanodine and inositol trisphosphate receptors coexist in avian cerebellar Purkinje neurons. *J. Cell Biol.,* 113(5), 1145–1157.

Wang, S. S.-H., Denk, W. and Häusser, M. (2000) Coincidence detection in single dendritic spines mediated by calcium release. *Nature Neurosci.,* 3(12), 1266–1273.

Watras, J., Bezprozvanny, I. and Ehrlich, B. (1991) Inositol 1,4,5-trisphosphate-gated channels in cerebellum: presence of multiple conductance states. *J. Neurosci.,* 11(10), 3239.

Wilkinson, D. (2007) Bayesian methods in bioinformatics and computational systems biology. *Brief. Bioinform.,* 8(2), 109.

Williams, G., Molinelli, E. and Smith, G. (2008) Modeling local and global intracellular calcium responses mediated by diffusely distributed inositol 1, 4, 5-trisphosphate receptors. *J. Theor. Biol.,* 253(1), 170–188.

Wils, S. and De Schutter, E. (2009) STEPS: modeling and simulating complex reaction-diffusion systems with Python. *Front. Neuroinform.,* 3(15), 165–178.

Wojda, U., Salinska, E. and Kuznicki, J. (2008) Calcium ions in neuronal degeneration. *IUBMB life,* 60(9), 575–590.

Zhao, H., Loessberg, P., Sachs, G. and Muallem, S. (1990) Regulation of intracellular Ca^{2+} oscillation in AR42J cells. *J. Biol. Chem.,* 265(34), 20856.

Publications

Publication I

Hituri K., Linne M.-L. (2013) Comparison of models for IP_3 receptor kinetics using stochastic simulations. PLoS ONE 8(4): e59618.

OPEN ACCESS Freely available online PLOS ONE

Comparison of Models for IP_3 Receptor Kinetics Using Stochastic Simulations

Katri Hituri*, Marja-Leena Linne*

Computational Neuroscience Laboratory, Department of Signal Processing, Tampere University of Technology, Tampere, Finland

Abstract

Inositol 1,4,5-trisphosphate receptor (IP_3R) is a ubiquitous intracellular calcium (Ca^{2+}) channel which has a major role in controlling Ca^{2+} levels in neurons. A variety of computational models have been developed to describe the kinetic function of IP_3R under different conditions. In the field of computational neuroscience, it is of great interest to apply the existing models of IP_3R when modeling local Ca^{2+} transients in dendrites or overall Ca^{2+} dynamics in large neuronal models. The goal of this study was to evaluate existing IP_3R models, based on electrophysiological data. This was done in order to be able to suggest suitable models for neuronal modeling. Altogether four models (Othmer and Tang, 1993; Dawson *et al.*, 2003; Fraiman and Dawson, 2004; Doi *et al.*, 2005) were selected for a more detailed comparison. The selection was based on the computational efficiency of the models and the type of experimental data that was used in developing the model. The kinetics of all four models were simulated by stochastic means, using the simulation software STEPS, which implements the Gillespie stochastic simulation algorithm. The results show major differences in the statistical properties of model functionality. Of the four compared models, the one by Fraiman and Dawson (2004) proved most satisfactory in producing the specific features of experimental findings reported in literature. To our knowledge, the present study is the first detailed evaluation of IP_3R models using stochastic simulation methods, thus providing an important setting for constructing a new, realistic model of IP_3R channel kinetics for compartmental modeling of neuronal functions. We conclude that the kinetics of IP_3R with different concentrations of Ca^{2+} and IP_3 should be more carefully addressed when new models for IP_3R are developed.

Citation: Hituri K, Linne M-L (2013) Comparison of Models for IP_3 Receptor Kinetics Using Stochastic Simulations. PLoS ONE 8(4): e59618. doi:10.1371/journal.pone.0059618

Editor: William W. Lytton, SUNY Downstate MC, United States of America

Received November 14, 2012; **Accepted** February 15, 2013; **Published** April 10, 2013

Funding: This work was supported by the Academy of Finland (project 129657, Finnish Programme for Centres of Excellence in Research 2006–2011) http://www.aka.fi; the Finnish Cultural Foundation, Pirkanmaa Regional fund http://www.skr.fi; Tampere University of Technology Graduate school http://www.tut.fi; and Tampere Doctoral Programme in Information Science and Engineering http://www.cs.tut.fi/tise/. The funders had no role in study design, data collection and analysis, decision to publish, or preparation of the manuscript.

Competing Interests: The authors have declared that no competing interests exist.

* E-mail: katri.hituri@tut.fi (KH); marja-leena.linne@tut.fi (M-LL)

Introduction

Inositol 1,4,5-trisphosphate receptor (IP_3R) is a ligand-gated calcium (Ca^{2+}) release channel typically expressed on the endoplasmic reticulum (ER) in neurons and many other cell types. It has a major role in intracellular Ca^{2+} dynamics which, in turn, is involved in many cellular processes such as muscle contraction, neurotransmitter release, vesicle secretion, fertilization, gene transcription, immunity, and apoptosis. In neurons, dynamical changes in Ca^{2+} concentration ($[Ca^{2+}]$) are involved, among others, in neuroplasticity and development (see recent reviews [1,2]), and in neurodegeneration (see [3,4]). Transient, repetitive changes in cytosolic Ca^{2+} concentration are crucial for synapse modification and plasticity, including long-term potentiation (LTP) and long-term depression (LTD) [5–8]. These phenomena constitute the biological basis for learning and memory formation in the brain [8,9]. Particularly in the cerebellum, IP_3Rs are relatively highly expressed in Purkinje cells [10]. Ca^{2+} release from ER has been shown to be a key mediator of cerebellar LTD [11].

The inositol 1,4,5-trisphosphate receptor is a tetrameric receptor-channel, consisting of four sub-units. In total, three different genes (ITPR1, ITPR2, and ITPR3) encode three different types (1, 2, and 3) of IP_3R and their splice variants from which homo- or heterotetramers can form [12]. IP_3R is activated and opened by both IP_3 and Ca^{2+}. Ca^{2+} can also act as the inhibitor of IP_3R in higher concentrations. IP_3 is produced from phosphatidylinositol 4,5-bisphosphate (PIP) by phospholipase C (PLC). After a cell is stimulated (for example by glutamate in neurons) certain G protein- or tyrosine kinase-linked receptors are activated. These, in turn, can activate PLC. ER acts as a Ca^{2+} store, and while open, IP_3R can release Ca^{2+} from ER lumen to the cytosol. Transient rises or oscillations in Ca^{2+} concentration can then activate various enzymes and even induce changes in the transcriptional level. IP_3Rs are known to be responsible for the phenomenon called Ca^{2+}-induced Ca^{2+} release (CICR), in addition to ryanodine receptors (RyRs) [13,14].

In order to develop models for ion channels and receptors detailed data on the structure and function of the modeled entity is required. The function of IP_3R has been studied with electrophysiological techniques. However, since IP_3Rs are prevalently located on the endoplasmic reticulum of a cell, performing the recordings is not straightforward. The first recordings performed

on IP_3Rs involved isolated microsomes from smooth muscle cells incorporated into artificial lipid bilayer [15]. Later, the same technique has been used, for example, for IP_3R in canine cerebellum [16–20], in mouse cerebellum [21], and in HEK cells [22] (IP_3R recombinantly expressed). IP_3Rs have also been recorded from the plasma membranes of DT40 cells [23] (IP_3R endogenously expressed (native)) and DT40-3KO cells [24,25] (stably expressed IP_3R construct, native IP_3R ablated). Since the nuclear membrane is a continuation of the ER, IP_3Rs have also been recorded from isolated nuclei of *Xenopus* oocytes (for example [26] (recombinantly expressed and native IP_3Rs), Purkinje neurons and granule cells [27,28] (IP_3R endogenously expressed), and DT40 cells [23,29]. These kind of data are of great value when developing a model for ion channel kinetics. However, the electrophysiological raw data on IP_3R is not available in any of the publicly available databases, but its statistics is described in publications. For example, the dependence of open probability on cytosolic Ca^{2+} or IP_3 concentrations is given ([16,19,20,29,30]). In some cases, the open and closed time distributions [18,20,22] or mean open time [17,18,22,29] are also reported. In an ideal case, the raw data would be publicly available in a database and a modeler could extract all needed statistical measures out of the data or use the raw data for automated estimation of model parameter values.

In addition to electrophysiological measurements, Ca^{2+} imaging and radioactive assays have also been used to study the behavior of IP_3R *in vitro*. For example, Fujiwara *et al.* [31] analyzed the kinetics of Ca^{2+} release via IP_3R in controlled cytoplasmic environment in permeabilized cerebellar Purkinje cells. In addition, superfusion and $^{45}Ca^{2+}$ release assay (radioactive assay) have been used for studying the Ca^{2+} release and inhibition of IP_3R by Ca^{2+} in hepatic microsomes [32–34]. These kind of studies give more detailed information on the IP_3R regulation by IP_3 and Ca^{2+} and their affinities than electrophysiological studies. In some cases, the data obtained from Ca^{2+} imaging studies or from radioactive assays has been used in modeling studies, for example Fujiwara *et al.* [31] by Doi *et al.* [32] and Dufour *et al.* [35] by Sneyd *et al.* [36].

In order to reach a better understanding of the dynamical behavior of IP_3R, as well as its involvement in various cellular processes, it is of interest to build models of IP_3R. Computational models are important for understanding the time evolution, dynamics, and regulation of ion channels and intracellular proteins and enzymes [37,38]. Several models have previously been proposed to describe the behavior of IP_3R (for a comprehensive review, see, for example [39]). There are models presented for different types of IP_3R (type 1, 2, and 3) [12] in different animals, tissues and cells (for example *Xenopus* oocyte [40], cerebellar cells [41], pancreatic acinar cells [42], and hepatic cells [32]). The first and most well-known model is the one by De Young and Keizer [41]. Some models for IP_3R have been compared either analytically or by means of simulation [36,43–45], and later reviewed [39,46].

The majority of the existing models is deterministic. Deterministic approaches, however, do not give biologically valid results and are not always capable of modeling the random behavior observed with small numbers of molecules [47–50]. Stochastic modeling is therefore more and more used for describing the dynamics of a biochemical system. The stochastic approach is always valid whenever the deterministic approach is valid, but when the deterministic is not, the stochastic might sometimes be valid [51]. Most commonly, deterministic methods and, in some cases, analytical methods are used to investigate the properties of IP_3R models (see, for example [43] or [52]). More rarely, stochastic methods are applied [53,54], even though it is known that the behavior of ion channels is stochastic.

Despite the wealth of IP_3R models the selection of a specific model for describing IP_3R related calcium dynamics or signaling is not straightforward. The models are seldom generic in nature and capable of describing all possible data obtained for a specific IP_3R or cell type. The reason for this is that the models are developed for some specific purpose, describe the behavior only in certain experimental conditions, or the dynamics are not fully analyzed to validate the model. This can be due to the limited access to experimental data. We therefore wanted to study the dynamics of existing models in detail and to specifically address their suitability in the context of complex neuronal models. In this work, the interest is set on the type 1 IP_3R because it is most commonly expressed in neurons [10]. After a preliminary study, we chose four models [35,55–57] for a more detailed analysis and comparison. Other models did not meet our criteria. The chosen models were originally developed by using data either from IP_3R in canine cerebellum or type 1 IP_3R. As the selected models are biophysically realistic and based on the law of mass action, they can be implemented to the stochastic simulation tool STEPS [58,59] used in this study. Additionally, we decided to concentrate on computationally inexpensive IP_3R models so that it would be possible to integrate them as part of larger model for calcium dynamics or synaptic plasticity. We validated the functionality of the models by comparing the statistical behavior of IP_3R channel kinetics (open probability curves, mean open times, and open and closed time distributions) to the equivalent obtained by electrophysiological recordings from IP_3Rs expressed in neurons.

Our results show firstly, that the behavior of the studied models varies in similar simulation conditions and, secondly, some models show quite unrealistic kinetic behavior. We therefore conclude that the kinetics of IP_3R (open and closed times and the open probability) with different concentrations of both Ca^{2+} and IP_3 should be more carefully addressed when new models for IP_3R are developed.

Materials and Methods

In our present work, after a preliminary review on existing IP_3R models, we selected four models [35,55–57] for comparison. The selection was based on the following criteria: (1) relative simpicity (i.e. the model should have less than 20 states), (2) development based on data obtained from neuronal or type 1 IP_3R, and (3) basis in the law of mass action (the reactions include binding and unbinding reaction and state transitions). As our ultimate goal is to find a model that can be an integral part of a larger model for Ca^{2+} dynamics or synaptic plasticity in neurons, it is an advantage to have a structurally simple model. The selected models are based on the law of mass action and can thus be implemented into the stochastic simulators such as STEPS [58].

Models

The model of Othmer and Tang. The model of Othmer and Tang [55] is one of the earliest and small- scaled models regarding the number of states. There is only four states, since the binding order of Ca^{2+} or IP_3 is not free, but sequential, opposite to the models of De Young and Keizer [41] or Bezprozvanny and Ehrlich [18]. Othmer and Tang [55] assume that IP_3 has to bind to its binding site before Ca^{2+} can bind and the channel can open, as well as the activating Ca^{2+} has to bind to its site before the inhibition by Ca^{2+} can occur. The schematic representation of the model of Othmer and Tang [55] in Figure 1A and the parameter

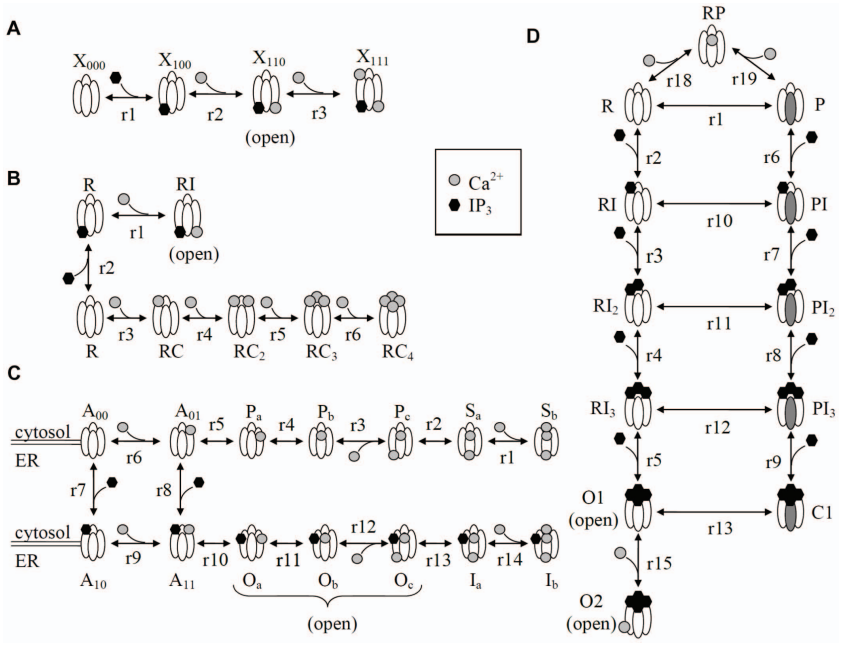

Figure 1. Schematic representation of the states and transitions of the IP_3R models. (A) Othmer and Tang [55] (forward direction of a reaction is to the right) (B) Doi *et al.* [35] (forward direction of a reaction is to the right or up), (C) Fraiman and Dawson [57] (forward direction of a reaction is to the right or down) (D) Dawson *et al.* [56] (forward direction of a reaction is the to the direction of binding a ligand or in the plain state transitions from left to the right).
doi:10.1371/journal.pone.0059618.g001

values in Table 1 were used in this study. The model of Othmer and Tang [55] has been used before as a part of a larger model for calcium dynamics, for example, by Mishra and Bhalla [60].

The model of Dawson *et al.* Dawson *et al.* [56] built a model for IP_3R, using a RyR model by Sachs *et al.* [61] as their starting point, to understand the adaptive and incremental behavior of IP_3R. The model of Dawson *et al.* [56] is applicable to type 1 and 2 IP_3Rs and with some modification to type 3. Dawson *et al.* [56] assume that IP_3R has two conformations, R and P. The conformation R can bind four IP_3 molecules rapidly, but with low affinity, to reach an open state. The conformation P, on the other hand, slowly binds four IP_3 molecules, but with high affinity, to reach a closed state where it is thereafter possible to reach the open state. In this work, Scheme 2 from the original paper was used with two exceptions: the flux through an open channel (reactions 14 and 16 in the original paper) and the diffusion of released Ca^{2+} (reaction 17) were not taken into account in order to make the model comparable with other models. This does not have an effect on the actual channel kinetics of the receptor as the removed reactions deal with Ca^{2+} flux and diffusion. Moreover, we used constant Ca^{2+} concentration and the simulated reactions happened in well-mixed system and in the present work only the kinetics of the IP_3R, not Ca^{2+} dynamics was studied. We used the the model presented in Figure 1D and the parameter values given in Table 2.

The model of Fraiman and Dawson. The IP_3R model of Fraiman and Dawson [57] was originally built to study the effects of different Ca^{2+} concentrations inside the ER to the kinetics of IP_3R. It is the only model included in the present study that has a Ca^{2+} binding site inside the ER in addition to the cytosolic binding sites. The state scheme of the model of Fraiman and Dawson [57] is presented in Figure 1C and the parameter values used in this work are in Table 3.

Originally, six states, O_a, O_b, O_c, P_a, P_b, and P_c, were considered open. However, it has been experimentally shown that

Table 1. Rate constants for IP_3R model of Othmer and Tang [55].

Reaction	k_f	k_b
r1	$12 \cdot 10^6 \frac{1}{\mu Ms}$	$8 \frac{1}{s}$
r2	$23.4 \cdot 10^6 \frac{1}{\mu Ms}$	$1.65 \frac{1}{s}$
r3	$2.81 \cdot 10^6 \frac{1}{\mu Ms}$	$0.21 \frac{1}{s}$

r1 to r3 refer to reactions represented in Figure 1A.
doi:10.1371/journal.pone.0059618.t001

Table 2. Rate constants for IP_3R model of Dawson *et al.* [56].

Reaction	k_f	k_b	Reaction	k_f	k_b
r1	$1\frac{1}{s}$	$100\frac{1}{s}$	r9	$100{\cdot}10^6\frac{1}{\mu Ms}$	$40\frac{1}{s}$
r2	$4000{\cdot}10^6\frac{1}{\mu Ms}$	$1000\frac{1}{s}$	r10	$1\frac{1}{s}$	$10\frac{1}{s}$
r3	$3000{\cdot}10^6\frac{1}{\mu Ms}$	$2000\frac{1}{s}$	r11	$1\frac{1}{s}$	$1\frac{1}{s}$
r4	$2000{\cdot}10^6\frac{1}{\mu Ms}$	$3000\frac{1}{s}$	r12	$10\frac{1}{s}$	$1\frac{1}{s}$
r5	$1000{\cdot}10^6\frac{1}{\mu Ms}$	$4000\frac{1}{s}$	r13	$10\frac{1}{s}$	$0.1\frac{1}{s}$
r6	$400{\cdot}10^6\frac{1}{\mu Ms}$	$10\frac{1}{s}$	r15	$100{\cdot}10^6\frac{1}{\mu Ms}$	$10\frac{1}{s}$
r7	$300{\cdot}10^6\frac{1}{\mu Ms}$	$20\frac{1}{s}$	r18	$1{\cdot}10^6\frac{1}{\mu Ms}$	$0.1\frac{1}{s}$
r8	$200{\cdot}10^6\frac{1}{\mu Ms}$	$30\frac{1}{s}$	r19	$10{\cdot}10^6\frac{1}{\mu Ms}$	$0.1\frac{1}{s}$

r1 to r19 refer to reactions presented in Figure 1D.
doi:10.1371/journal.pone.0059618.t002

IP_3R needs IP_3 to reach a stable open conformation [33,62]. For this reason, we neglected three of the original open states (i.e., they were considered closed) in the present work and only states O_a, O_b, and O_c were considered open. In addition, in the original publication [57], the rate constant of the transition from A_{10} to A_{00} is defined as 'detailed balance', with no given numerical value. In our study, it was mandatory to have a numerical value for the parameter and thus we fixed the parameter by testing three values with open probability simulations (data not shown). The parameter values of 0 s^{-1} and 200 s^{-1} produced identical results which were in accordance with the results in the original publication [57], while the value of 2000 s^{-1} slightly upraised the left side of the open probability curve. Based on these simulations we chose the value of 200 s^{-1} for the transition from A_{10} to A_{00} (reaction 7, k_b) and concluded that it was in the range of what was originally used.

Table 3. Rate constants for IP_3R model of Fraiman and Dawson [57], taken from [67].

Reaction	k_f	k_b
r1	$5000{\cdot}10^6\frac{1}{\mu Ms}$	$20\frac{1}{s}$
r2	$3000\frac{1}{s}$	$250\frac{1}{s}$
r3	$5000{\cdot}10^6\frac{1}{\mu Ms}$	$150\frac{1}{s}$
r4	$500\frac{1}{s}$	$100\frac{1}{s}$
r5	$0.3\frac{1}{s}$	$700\frac{1}{s}$
r6	$5000{\cdot}10^6\frac{1}{\mu Ms}$	$1\frac{1}{s}$
r7	$6670{\cdot}10^6\frac{1}{\mu Ms}$	$200\frac{1}{s}$
r8	$1540{\cdot}10^6\frac{1}{\mu Ms}$	$18\frac{1}{s}$
r9	$500{\cdot}10^6\frac{1}{\mu Ms}$	$667\frac{1}{s}$
r10	$1800\frac{1}{s}$	$330\frac{1}{s}$
r11	$133\frac{1}{s}$	$1500\frac{1}{s}$
r12	$70{\cdot}10^6\frac{1}{\mu Ms}$	$2000\frac{1}{s}$
r13	$630\frac{1}{s}$	$400\frac{1}{s}$
r14	$60{\cdot}10^6\frac{1}{\mu Ms}$	$16\frac{1}{s}$

r1 to r14 refer to reactions represented in Figure 1C.
doi:10.1371/journal.pone.0059618.t003

Table 4. Rate constants for IP_3R model of Doi *et al.* [35].

Reaction	k_f	k_b
r1	$8000{\cdot}10^6\frac{1}{\mu Ms}$	$2000\frac{1}{s}$
r2	$1000{\cdot}10^6\frac{1}{\mu Ms}$	$25800\frac{1}{s}$
r3	$8.889{\cdot}10^6\frac{1}{\mu Ms}$	$5\frac{1}{s}$
r4	$20{\cdot}10^6\frac{1}{\mu Ms}$	$10\frac{1}{s}$
r5	$40{\cdot}10^6\frac{1}{\mu Ms}$	$15\frac{1}{s}$
r6	$60{\cdot}10^6\frac{1}{\mu Ms}$	$20\frac{1}{s}$

r1 to r6 refer to reactions represented in Figure 1B.
doi:10.1371/journal.pone.0059618.t004

The model of Doi *et al.* The IP_3R model of Doi *et al.* [35] was originally published as part of a larger model for Ca^{2+} dynamics in the cerebellar Purkinje cell spine to investigate the role of IP_3Rs as a coincidence detector of two input signals. Doi *et al.* [35] constructed their model based on a conceptual model of Adkins and Taylor [34]. Doi *et al.* [35] used experimental data by Khodakhah and Ogden [63], Marchant and Taylor [33], and Fujiwara *et al.* [31] to define the structure and kinetics of the model and experimental data by Bezprozvanny *et al.* [16] to test how well the model can reproduce the bell-shaped curve. A schematic representation of the model is presented in Figure 1B and the rate constants for each reaction in Table 4. In the model of Doi *et al.* [35], IP_3R has seven states and the receptor needs to bind both IP_3 and Ca^{2+} to open and thus provide Ca^{2+} flux from ER lumen to cytosol. In this model, IP_3R has one open state, RIC.

Simulations and data analysis

In the present study, the simulations were designed to reproduce the data produced in experimental electrophysiological measurements from neuronal IP_3Rs. We used stochastic simulation approaches since deterministic approaches were not applicable due to the stochastic nature of ion channel gating. The simulated data was compared with experimental data available in literature. The four selected models were implemented according to the information presented in the original publications with some exceptions presented in the section 'Models'. Our work does not include parameter estimation (as, for example, [36]) since raw data on channel kinetics of IP_3Rs in neurons is not publicly available.

In this work, STEPS (STochastic Engine for Pathway Simulation) ([58,59]; http://steps.sourceforge.net/) version 1.1.2 was

used for simulation. With STEPS, it is possible to perform full stochastic simulation of reactions and diffusion of molecules in three dimensions and also deterministic simulations. For stochastic simulations, STEPS uses the stochastic simulation algorithm (SSA) described by Gillespie [64]. The model scripts are available at ModelDB (http://senselab.med.yale.edu/ModelDB/).

In our simulations, we assumed a well-mixed system. Our models had two compartments, cytosol and ER lumen, each having volume of 0.1 fl and a surface, ER, between them. The IP_3R was placed on the surface and the cytosolic concentrations of Ca^{2+} and IP_3 were kept constant in the simulations to mimic the buffered conditions in patch-clamp recording.

The simulations were run on a stand-alone Linux computer. For open probability curves, simulations were repeated, depending on the model, 750–12 000 times and averaged over the repetitions for each data point. To produce one such curve, the simulations lasted from an hour to several hours. Simulations for open and closed time distributions were run once for 10–5000 s to obtain sufficient number of events to get statistically significant results. These computations took from less than a second to a couple of seconds each. Analysis of the simulated data was performed and the figures were drawn with MATLAB [65].

Results

We compared four kinetic models previously developed for IP_3 receptor function by simulating them with the Gillespie stochastic simulation algorithm of STEPS simulator. The comparison was done by analyzing the steady-state behavior, such as the open probability, open and closed time distributions, and the mean open and closed time. Here we show that the behavior of the models varies and some models behave somewhat unrealistically.

Open probability

It has been experimentally shown that the open probability (P_o) of IP_3R is dependent on the cytosolic Ca^{2+} concentration and that the dependence is bell-shaped [16]. We repeated similar experiments by computational means and tested whether the selected four models are capable of expressing the bell-shaped curve. All the models except the model of Dawson *et al.* [56] produced the bell-shaped curve (see Figure 2A). Instead, the model of Dawson *et al.* [56] (blue in Figure 2A) produced an s-shaped curve similarly as in a previous comparison study by Sneyd *et al.* [36]. The model of Othmer and Tang [55] (green in Figure 2A) reaches the highest P_o ($P_o = 0.33$) at cytosolic Ca^{2+} concentration around 80 nM. The model of Doi *et al.* [35] (magenta in Figure 2A) and the model of Fraiman and Dawson[57] (red in Figure 2A) reach the highest P_o ($P_o = 0.15$ and $P_o = 0.38$, respectively) around $[Ca^{2+}]$ = 300 nM, which is closest to the experimentally obtained values ($[Ca^{2+}] = 250$ nM by Bezprozvanny *et al.* [16] and $[Ca^{2+}]$ = 200 nM by Kaznacheyeva *et al.* [22]). The absolute value of P_o obtained in simulations cannot be directly compared to the experimental data, because Bezprozvanny *et al.* [16] and Kaznacheyeva *et al.* [22] report only normalized values, not absolute values, for P_o.

The open probability of IP_3R is also dependent on cytosolic IP_3 concentration (see for example [17,27,29]). The open probability curves of the models obtained in simulations are shown in Figure 2B. All the models except the model of Dawson *et al.* [56] (blue in Figure 2B) follow the s-shape that is reported in experimental studies [17,27,29]. In their study on IP_3Rs on Purkinje cell nuclear membrane, Marchenko *et al.* [27] have shown that the P_o stays close to 0 until IP_3 concentration reaches 0.3 μM and keeps rising until IP_3 concentration is 3 μM ($[Ca^{2+}]$ = .25 μM). Watras *et al.* [17] have shown that the rise starts when IP_3 concentration is 0.03 μM and settles after 1 μM. The P_o in models of Dawson *et al.* [56] (blue in Figure 2B) and Doi *et al.* [35] (magenta in Figure 2B) starts rising approximately at the same IP_3 concentration as P_o in [27], but the elevation does not stop at the right concentrations. In the models of Othmer and Tang [55] (green in Figure 2B) and Fraiman and Dawson [57] (red in Figure 2B), P_o starts rising one or two orders of magnitude too low when compared to the experimental results.

Kaftan *et al.* [19] have shown in their experiments on cerebellar IP_3R that the bell-shaped Ca^{2+}-dependence curve moves upward and to the right when IP_3 concentration is increased. They used IP_3 concentration values of 0.02, 0.2, 2, and 180 μM. We used the same concentrations, in addition to their fivefold values, except 180 μM in our simulation for all the models (results in Figure 3). The model of Othmer and Tang [55] (Figure 3A) shows a shift upward and to the left, the model of Dawson *et al.* [56] (Figure 3B) upward, and the models of Fraiman and Dawson [57] (Figure 3C) and Doi *et al.* [35] (Figure 3D) upward and slightly to the left when IP_3 concentration increases. Similar trend has also been shown for the model of Othmer and Tang [55] by Diambra and Guisoni

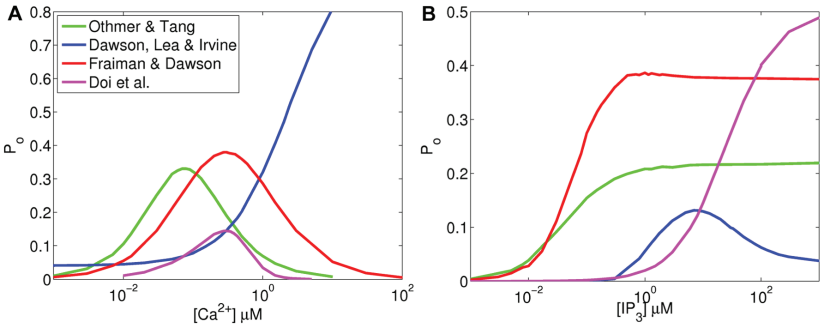

Figure 2. Open probability of IP_3R as a function of (A) cytosolic Ca^{2+} concentration (IP_3 = 10 μM) and (B) cytosolic IP_3 concentration (Ca^{2+} = 0.25 μM). Green: Othmer and Tang [55], Blue: Dawson *et al.* [56], Red: Fraiman and Dawson [57], Magenta: Doi *et al.* [35].
doi:10.1371/journal.pone.0059618.g002

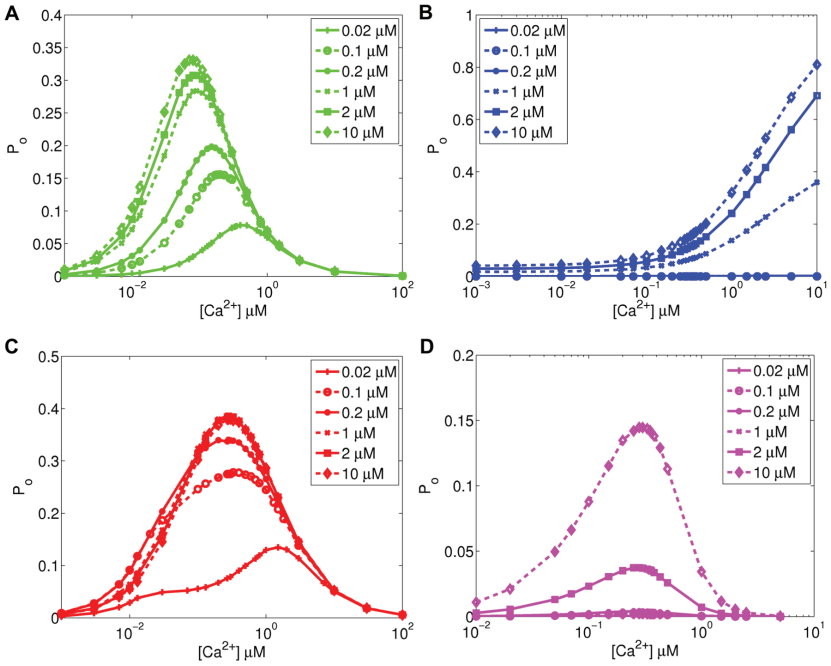

Figure 3. Open probability of IP_3R as a function of cytosolic Ca^{2+} concentration in different IP_3 concentrations. (A) Othmer and Tang [55] (B) Dawson *et al.* [56] (C) Fraiman and Dawson [57] (D) Doi *et al.* [35].
doi:10.1371/journal.pone.0059618.g003

[66] and Tang *et al.* [43]. None of the models reproduced the results presented by Kaftan *et al.* [19].

Mean open and closed times and distributions of open and closed times

Bezprozvanny and Ehrlich [18] reported that the mean open time of canine cerebellar IP_3R is 2.9 $\pm$ 0.2 ms and Kaznacheyeva *et al.* [22] that the mean open time of wild-type rat cerebellar IP_3R is 4.2 ± 0.5 ms and that the open and closed times have exponential distributions (black dashed line in Figure 4E and 4K) in certain experimental conditions (lipid bilayer experiments, $[IP_3] = 2\ \mu M$, $[Ca^{2+}] = 0.2\ \mu M$). We simulated the selected models in these same conditions (Sim 1, results in Table 5 and Figure 4A–F) and, in order to take into account the affinity difference [31], with five times greater IP_3 concentration (Sim 2, results in Table 5 and Figure 4G–L). The mean open times of the model of Fraiman and Dawson [57] are 2.5 ms (Sim 1) and 2.6 ms (Sim 2). These values are close to the experimentally obtained values. The mean open times obtained with the other models are an order of magnitude smaller (0.5 ms for Dawson *et al.* [56] and Doi *et al.* [35]) or significantly greater (460 ms, Othmer and Tang [55]). None of open time distributions of the selected models (Figures 4A-C and 4G-I) follow the experimental distribution by Kaznacheyeva *et al.* [22] fully, but all give, however, the exponential shape (see Figures 4B and 4K). The open time distribution of the model of Fraiman and Dawson [57] is the closest to experimentally [22] obtained distribution (see Figures 4B, 4H). The same applies also to the closed time distributions (see Figures 4E, 4K).

Moraru *et al.* [20] have presented open time distributions for canine cerebellar IP_3R in two different conditions (lipid bilayer experiments, $[Ca^{2+}] = 0.1$ and 0.01 μM, and $[IP_3] = 2\ \mu M$) (black dashed line in Figures 5 and 6). We simulated the behavior of the selected models in these same experimental conditions (Sim 3 and Sim 4, results in Table 5 and Figure 5) and also with fivefold IP_3 concentration (Sim 5 and Sim 6, results in Table 5 and Figure 6). The distributions in the wet-lab experiments are of exponential shape [18–20,22] and simulation results also show exponential shape for all the models. The only distributions that are also otherwise similar to the ones obtained in wet-lab experiments by Moraru *et al.* [20] are the distributions of the model of Fraiman and Dawson [57] (Figures 5B, 5H, 6B, and 6H). All the simulation conditions used are summarized in Table 6.

The Ca^{2+} concentrations used in the experiments by Moraru *et al.* [20] are unfortunately at the border or smaller than those observed in a neuron at resting level (i.e., Ca^{2+} used is 0.1 μM or less). As IP_3R is, however, known to have functional significance only above the resting level concentrations, more emphasis should be put on physiological conditions in experimental work in the future. In other words, experimental work should additionally be performed with Ca^{2+} concentrations above the known resting level.

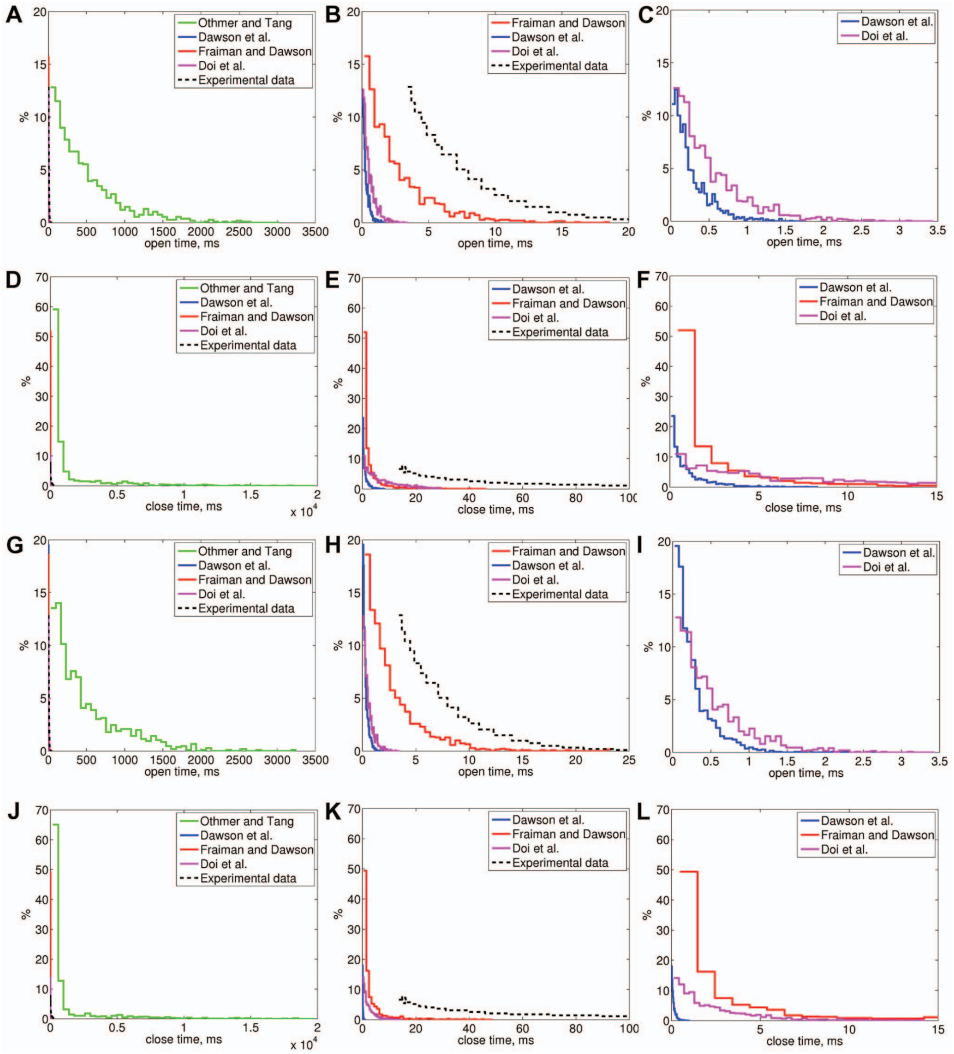

Figure 4. Distribution of IP_3 R open and closed times for all the selected models obtained in simulation conditions Sim 1 (A–F) and Sim 2 (G–L). (A) Open time distributions of all the models in conditions Sim 1, (B) Enlarged from A, (C) Enlarged from B, (D) Closed time distributions of all the models conditions Sim 1, (E) Enlarged from D, (F) Enlarged from E, (G) Open time distributions of all the models conditions Sim 2, (H) Enlarged from G, (I) Enlarged from H, (J) Closed time distributions of all the models conditions Sim 2, (K) Enlarged from J, (L) Enlarged from K. Experimental data is from [22]. In simulation conditions Sim 1 $[Ca^{2+}] = 0.2\ \mu M$, $[IP_3] = 2\ \mu M$ and Sim 2 $[Ca^{2+}] = 0.2\ \mu M$, $[IP_3] = 10\ \mu M$ (as shown in Table 6).

doi:10.1371/journal.pone.0059618.g004

Table 5. Mean open and closed times of IP_3R of the selected models.

	Model	mean open time (ms)	mean closed time (ms)	n	simulation time (s)
Sim 1	Othmer and Tang	451.19±423.06	12892563	1068	1 800
	Dawson *et al.*	0.59±5.46	10.33120.24	1797	20
	Fraiman and Dawson	2.45±2.52	4.0111.22	1535	10
	Doi *et al.*	0.470.46	11.2138.08	1711	20
Sim 2	Othmer and Tang	463.55463.96	12902793	1045	1 800
	Dawson *et al.*	0.524.70	9.38167.55	1897	20
	Fraiman and Dawson	2.572.76	4.9219.84	1391	10
	Doi *et al.*	0.470.46	3.7623.11	1501	6
Sim 3	Othmer and Tang	510.08526.46	1047±2074	1927	3 000
	Dawson *et al.*	0.465.90	8.83±97.56	2004	20
	Fraiman and Dawson	2.482.64	5.38±2.64	1293	10
	Doi *et al.*	0.530.53	19.00±29.60	1024	20
Sim 4	Othmer and Tang	509.68525.59	958.50±2073	2044	3 000
	Dawson *et al.*	0.6510.64	5.21±100.02	2063	10
	Fraiman and Dawson	2.512.67	5.50±15.55	1249	10
	Doi *et al.*	0.510.50	4.72±0.50	1866	10
Sim 5	Othmer and Tang	598.32598.68	3356±3384	1263	5 000
	Dawson *et al.*	0.250.25	12.60±129.80	1161	10
	Fraiman and Dawson	2.472.60	25.18±88.87	1446	40
	Doi *et al.*	0.470.47	107.37±123.06	1854	200
Sim 6	Othmer and Tang	596.98592.01	2712±2709	1509	5 000
	Dawson *et al.*	0.250.26	9.27±163.25	2098	20
	Fraiman and Dawson	2.492.61	27.54±95.62	1331	40
	Doi *et al.*	0.460.46	27.92±47.50	1407	40

The different simulation conditions (Sim 1 – Sim 6) are presented in Table 6.
doi:10.1371/journal.pone.0059618.t005

Discussion

In this work, four models of IP_3R [35,55–57] were selected among many to examine their steady-state and time series behavior and compare them with experimental data available in literature. We implemented and simulated the selected models using stochastic simulation software STEPS in order to obtain similar data as in single-channel patch-clamp recordings. The open probability curves and statistics, such as the mean open time and open and closed time distributions, were compared to experimental ones obtained in the same conditions. To our knowledge, this is the first detailed evaluation of IP_3R model kinetics with stochastic methods. Our comparative study shows significant differences in the behavior and kinetics of the studied models.

Based on our results, the statistical properties of the model of Fraiman and Dawson [57] seem to be the most similar to the ones obtained in wet-lab experiments. The properties of the model of Othmer and Tang [55] are very different when compared to the experimental data. All the models except the model of Dawson *et al.* [56] produce the bell-shaped open probability curve for Ca^{2+}-dependence and the s-shaped open probability curve for IP_3-dependence as seen in the electrophysiological experiments (for example [16,17,27]). However, none of the models reproduce the experimental finding presented by Kaftan *et al.* [19], which shows that Ca^{2+}-dependent open probability curve moves to the right and upward when IP_3 concentration increases. This kind of behavior is shown in the original article by Fraiman and Dawson [57]. The reason why the simulation of the same model in this study did not produce similar behavior might be the slight modification that we were forced to make to the model (defining a numerical value for the one parameter that was originally defined as 'detailed balance' and neglecting three of the six open states). It is also notable that there is an Errata [67] published for the original article [57] and that we used the parameter set in the Errata [67].

The simulated open and closed time distributions of all the models follow the exponential distribution as does the data from experiments [18–20,22]. However, the distributions are not similar apart from the distribution of Fraiman and Dawson [57]. The reason for this may be the relatively simple structure of the models, insufficiency of modeled states to reproduce the kinetics, and parameter values that do not fit the data.

According to our results, the mean open time of model of Doi *et al.* [35] is not congruent with the experimental findings. However, the shape and peak value of the open probability curve are in accordance with experimental data. As the model of Doi *et al.* [35] has originally been published as part of a larger signal transduction model for LTD induction, some inaccuracy in the behavior of the model could have been corrected by other parameters, such as the Ca^{2+} flux rate and thus the small mean open time does not invalidate the results in the original publication.

As our comparative study points out significant differences in the behavior and kinetics of the studied models, it is of interest to

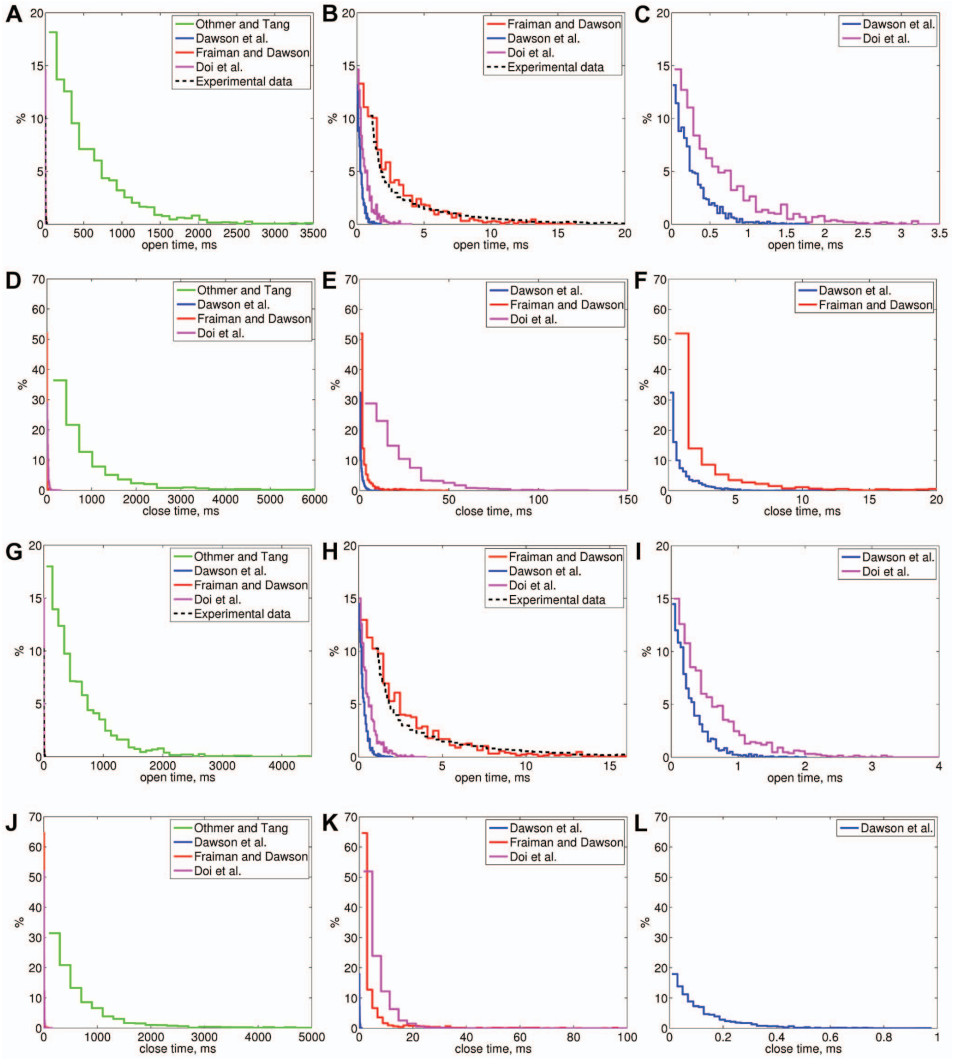

Figure 5. Distributions of IP_3R open and closed times for all the selected models obtained in simulation conditions Sim 3 (A–F) and Sim 4 (G–L). (A) Open time distributions of all the models in conditions Sim 3, (B) Enlarged from A, (C) Enlarged from B, (D) Closed time distributions of all the models in conditions Sim 3, (E) Enlarged from D, (F) Enlarged from E, (G) Open time distributions of all the models conditions Sim 4, (H) Enlarged from G, (I) Enlarged from H, (J) Closed time distributions of all the models conditions Sim 4, (K) Enlarged from J, (L) Enlarged from K. Experimental data is from [20]. In simulation conditions Sim 3 $[Ca^{2+}]=0.1$ μM, $[IP_3]=2$ μM and Sim 4 $[Ca^{2+}]=0.1$ μM, $[IP_3]=10$ μM (as shown in Table 6).
doi:10.1371/journal.pone.0059618.g005

consider reasons for it. We identify four major reasons why the selected models behave differently to each other: 1) the structure (i.e. the equations) and parameter values differ between the models, 2) experimental data that was used in the model development vary, 3) different data handling procedures have been used when developing the models, and 4) model developers

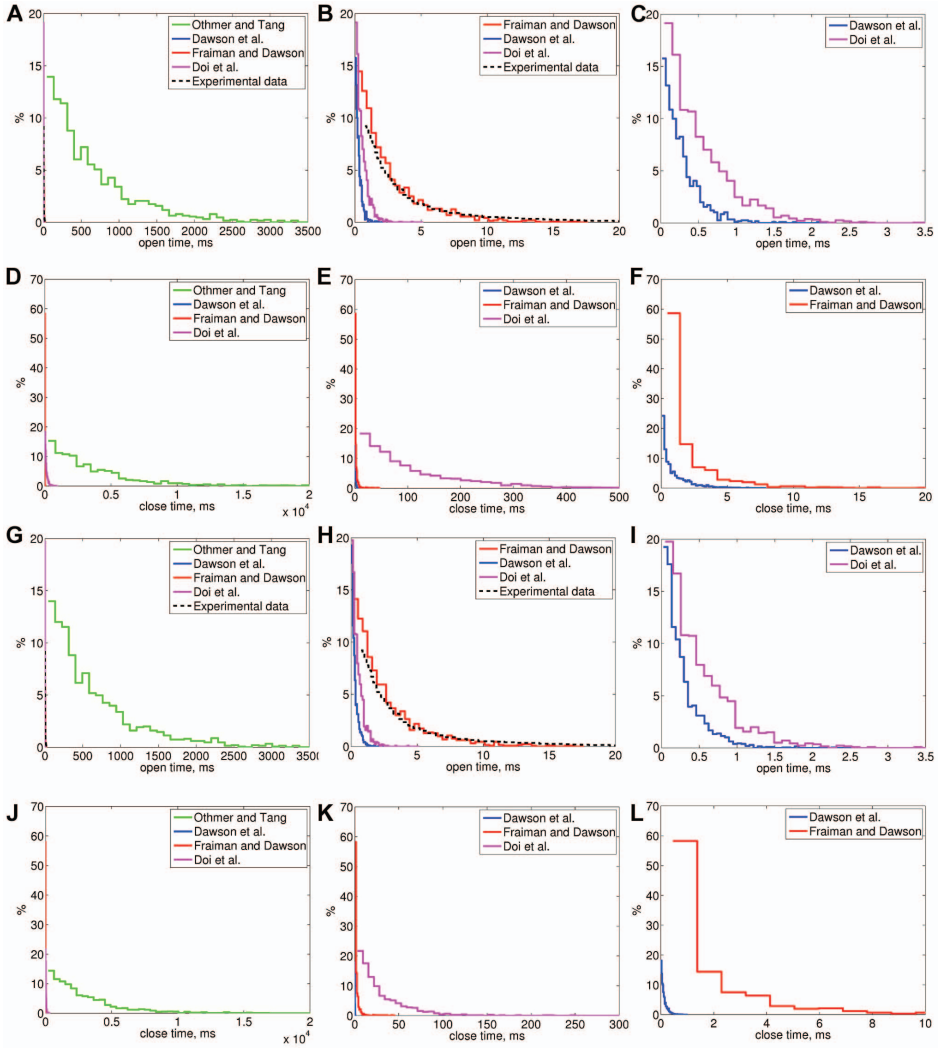

Figure 6. Distribution of IP_3R open and closed times for all the selected models obtained in simulation conditions Sim 5 (A–F) and Sim 6 (G–L). (A) Open time distributions of all the models conditions Sim 5, (B) Enlarged from A, (C) Enlarged from B, (D) Closed time distributions of all the models conditions Sim 5, (E) Enlarged from D, (F) Enlarged from E, (G) Open time distributions of all the models conditions Sim 6, (H) Enlarged from G, (I) Enlarged from H, (J) Closed time distributions of all the models conditions Sim 6, (K) Enlarged from J, (L) Enlarged from K. Experimental data is from [20]. In simulation conditions Sim 5 $[Ca^{2+}] = 0.01\ \mu M$, $[IP_3] = 2\ \mu M$ and Sim 6 $[Ca^{2+}] = 0.01\ \mu M$, $[IP_3] = 10\ \mu M$ (as shown in Table 6).
doi:10.1371/journal.pone.0059618.g006

did not use automated parameter estimation methods. Next, we will discuss each issue in detail.

Firstly, the most obvious reason for differences in the behavior of models is the structure and parameter values of the models. All the models studied here have different number of states, but this does not cause the differences as such. More importantly, different parameter values and thus the affinities of IP_3, as well as activating and inactivating Ca^{2+}, vary between the models. Since the models

Table 6. Ca^{2+} and IP_3 concentration used in different simulations for open and closed time distributions.

	$[Ca^{2+}]$ (μM)	$[IP_3]$ (μM)
Sim 1	0.2	2
Sim 2	0.2	10
Sim 3	0.1	2
Sim 4	0.1	10
Sim 5	0.01	2
Sim 6	0.01	10

The simulations were done in the same conditions as wet-lab experiments [20,22] and with five times greater IP_3 concentration in order to take into account the affinity difference between *in vivo* and lipid bilayer experiments [31].
doi:10.1371/journal.pone.0059618.t006

of Othmer and Tang [55] and Doi *et al.* [35] reproduce the correct shapes for the open probability curves, re-estimation of their parameters might improve the fitting of models to experimental data. As a general conclusion, all studies neither report the values of all parameters used in simulations nor make it evident which parameter set is used to produce specific results. This makes it difficult to reproduce results (see also discussion in [68]).

Secondly, another reason for the differences in the behavior of the models could be related to the variability in the use of experimental data when constructing the original model. Although the statistical properties of channel kinetics, such as the mean open time and the distributions of open times, are known to be important in properly reconstructing receptor-ion channel kinetics, they are relatively rarely used in developing or evaluating models for IP_3R. Furthermore, there exists a clear difference on how experimental data is used to construct (i.e., to define the structure, the number of states, and the number of parameter values in the model) and fine-tune the models (estimation of the unknown parameters). We have noticed that it is not always clear which data is used in modeling and, particularly, how it is used. In general, the models presented for IP_3R are constructed based on only some of the data or knowledge obtained from various animal species and experiments. Furthermore, data on kinetics of IP_3R have been obtained from various sources: native and recombinantly expressed receptors in cell lines and *Xenopus* oocytes, and from vertebrate cerebellum or hepatocytes.

Doi *et al.* [35] use the model of Adkins and Taylor [34] as their starting point and construct the model based on data by Marchant and Taylor [33] and use the open probability curve of Bezprozvanny *et al.* [16] to study the fitness of their model. The model of Othmer and Tang [55] is also shown to fit the data by Bezprozvanny *et al.* [16] in addition to data by Watras *et al.* [17] in [43], but this study does not take the difference in IP_3 affinity [31] into account as Doi *et al.* [35] or study the open or closed time distributions of the model. Fraiman and Dawson [57] and Dawson *et al.* [56] use several experimental observations when constructing their model, but they do not report using any data for actual fitting of the model parameters. The data that Dawson *et al.* [56] compare their model to is more dealing with temporal aspect of Ca^{2+} release and accumulation of Ca^{2+} to cytosol than actual channel kinetics.

Thirdly, the differences between the simulated and experimentally observed open time distributions and mean open times might also be due to differences in data handling procedures. Experimentally observed open time distributions can be biased due to the limitations and established practices regarding the temporal resolution in the patch-clamp recordings, while in the simulations in this study all the events are recorded exactly at the time they happen. Usually the time resolution in patch-clamp recordings is around 1 ms and thus any opening shorter than that would stay unnoticed or be merged with other channel openings.

Fourthly, to our knowledge, automated parameter estimation methods have not been used in the development of the four models here compared. Studies on IP_3R models consider, to some extent, the kinetic ion channel data to define the mathematical structure of the models. However, only a few previous studies use automated parameter estimation techniques and statistical data on ion channel kinetics to fine-tune the IP_3R models [36,69–72].

One of the major challenges in modeling the IP_3Rs is the lack of access to original raw data, for example from electrophysiological measurements, that could be used in quantitative modeling. This data is not currently available in any public database and as the years pass by it becomes extremely hard to acquire the data from its original sources. This problem is not new or limited just to measurements of ion channels but to all neuroscience data [73,74]. Some suggestions to improve the situation have been made. For instance, De Schutter [75] suggests that data publishing should be distinguished from paper publishing. Furthermore, Ranjan *et al.* [76] have established an information management framework for ion channel information, which hopefully will make IP_3R experimental data more accessible in the future.

Despite several shortcomings in the development and presentation of models, previous models on IP_3R, including the present comparative study on four stochastic IP_3R models, will give a good setting for constructing a new, realistic model of IP_3Rs for compartmental modeling of neuronal functions. It will be a challenge to develop computationally inexpensive models that can produce realistic stochastic behavior of an individual ion channel. A wealth of evidence indicates, however, an important role of randomly opening ion channels on the global behavior of cells. For example, in neurons the stochastic openings of single ion channels shape the integration of local signals in dendrites or spines [77], stochastic openings of voltage-gated ion channels have an important role in adjusting the transmembrane voltage dynamics [78–80], and the reliability of action potential propagation along thin axons is affected by the stochastic opening of voltage-gated ion channels [81]. Furthermore, molecular noise of single ion channel is shown to be translated into global cellular processes in astrocytes [82].

In summary, the development of new IP_3R models clearly calls for both steady-state and kinetic data. Fitting of the new computational models should be done using automated estimation techniques, possibly using Bayesian approaches [72,83–85]. Data for model construction and fine-tuning would ideally be acquired from the same neuronal type as the model is built for.

Acknowledgments

The authors thank Erik De Schutter and Stefan Wils for discussion and help in the use of STEPS in the early phase of the work.

Author Contributions

Conceived and designed the experiments: KH. Performed the experiments: KH. Analyzed the data: KH M-LL. Wrote the paper: KH. Revised the manuscript critically: M-LL.

References

1. Libersat F, Duch C (2004) Mechanisms of dendritic maturation. Mol Neurobiol 29: 303–320.
2. Michaelsen K, Lohmann C (2010) Calcium dynamics at developing synapses: mechanisms and functions. Eur J Neurosci 32: 218–223.
3. Banerjee S, Hasan G (2005) The $InsP_3$ receptor: its role in neuronal physiology and neurodegeneration. Bioessays 27: 1035–1047.
4. Foskett J (2010) Inositol trisphosphate receptor Ca^{2+} release channels in neurological diseases. Pflugers Arch Eur J Physiol 460: 481–494.
5. Bliss T, Collingridge G (1993) A synaptic model of memory: long-term potentiation in the hippocampus. Nature 361: 31–39.
6. Franks KM, Sejnowski TJ (2002) Complexity of calcium signaling in synaptic spines. BioEssays 24: 1130–1144.
7. Ogasawara H, Doi T, Kawato M (2008) Systems biology perspectives on cerebellar long-term depression. Neurosignals 16: 300–317.
8. Collingridge G, Peineau S, Howland J, Wang Y (2010) Long-term depression in the CNS. Nature Rev Neurosci 11: 459–473.
9. Citri A, Malenka R (2008) Synaptic plasticity: multiple forms, functions, and mechanisms. Neuropsychopharmacology 33: 18–41.
10. Sharp A, Nucifora Jr F, Blondel O, Sheppard C, Zhang C, et al. (1999) Differential cellular expression of isoforms of inositol 1,4,5-triphosphate receptors in neurons and glia in brain. J Comp Neurol 406: 207–220.
11. Ito M (2002) The molecular organization of cerebellar long-term depression. Nature Rev Neurosci 3: 896–902.
12. Foskett JK, White C, Cheung KH, Mak DOD (2007) Inositol trisphosphate receptor Ca^{2+} release channels. Physiol Rev 87: 593–658.
13. Llano I, DiPolo R, Marty A (1994) Calcium-induced calcium release in cerebellar Purkinje cells. Neuron 12: 663–673.
14. Barbara J (2002) IP_3-dependent calcium-induced calcium release mediates bidirectional calcium waves in neurones: functional implications for synaptic plasticity. Biochim Biophys Acta – Proteins & Proteomics 1600: 12–18.
15. Ehrlich B, Watras J (1988) Inositol 1,4,5-trisphosphate activates a channel from smooth muscle sarcoplasmic reticulum. Nature 336: 583–586.
16. Bezprozvanny I, Watras J, Ehrlich B (1991) Bell-shaped calcium-response curves of Ins(1,4,5)P_3- and calcium-gated channels from endoplasmic reticulum of cerebellum. Nature 351: 751–754.
17. Watras J, Bezprozvanny I, Ehrlich B (1991) Inositol 1,4,5-trisphosphate-gated channels in cerebellum: presence of multiple conductance states. J Neurosci 11: 3239.
18. Bezprozvanny I, Ehrlich B (1994) Inositol (1,4,5)-trisphosphate ($InsP_3$)-gated Ca channels from cerebellum: conduction properties for divalent cations and regulation by intraluminal calcium. J Gen Phys 104: 821–856.
19. Kaftan E, Ehrlich B, Watras J (1997) Inositol 1,4,5-trisphosphate ($InsP_3$) and calcium interact to increase the dynamic range of InsP3 receptor-dependent calcium signaling. J Gen Physiol 110: 529–538.
20. Moraru I, Kaftan E, Ehrlich B, Watras J (1999) Regulation of type 1inositol 1,4,5-trisphosphategated calcium channels by $InsP_3$ and calcium. Simulation of single shannel kinetics based on ligand binding and electrophysiological analysis. J Gen Physiol 113: 837–849.
21. Maeda N, Kawasaki T, Nakade S, Yokota N, Taguchi T, et al. (1991) Structural and functional characterization of inositol 1,4,5-trisphosphate receptor channel from mouse cerebellum. J Biol Chem 266: 1109–1116.
22. Kaznacheyeva E, Lupu VD, Bezprozvanny I (1998) Single-channel properties of inositol (1,4,5)- trisphosphate receptor heterologously expressed in HEK-293 cells. J Gen Physiol 111: 847–856.
23. Dellis O, Dedos S, Tovey S, Taufiq-Ur-Rahman, Dubel S, et al. (2006) Ca^{2+} entry through plasma membrane IP_3 receptors. Science 313: 229.
24. Wagner I, Larry E, Joseph S, Yule D (2008) Regulation of single inositol 1,4,5-trisphosphate receptor channel activity by protein kinase a phosphorylation. J Physiol 586: 3577–3596.
25. Wagner I, Larry E, Yule D (2012) Differential regulation of the $InsP_3$ receptor type-1 and -2 single channel properties by $InsP_3$, Ca^{2+} and ATP. J Physiol 590: 3245–3259.
26. Mak D, Foskett J (1994) Single-channel inositol 1,4,5-trisphosphate receptor currents revealed by patch clamp of isolated Xenopus oocyte nuclei. J Biol Chem 269: 29375–29378.
27. Marchenko S, Yarotskyy V, Kovalenko T, Kostyuk P, Thomas R (2005) Spontaneously active and $InsP_3$-activated ion channels in cell nuclei from rat cerebellar Purkinje and granule neurones. J Physiol 565: 897–910.
28. Marchenko S, Thomas R (2006) Nuclear Ca^{2+} signalling in cerebellar Purkinje neurons. The Cerebellum 5: 36–42.
29. Taufiq-Ur-Rahman, Skupin A, Falcke M, Taylor C (2009) Clustering of $InsP_3$ receptors by $InsP_3$ retunes their regulation by $InsP_3$ and Ca^{2+}. Nature 458: 655–659.
30. Mak D, McBride S, Foskett J (2001) ATP regulation of recombinant type 3 inositol 1, 4, 5- trisphosphate receptor gating. J Gen Physiol 117: 447–456.
31. Fujiwara A, Hirose K, Yamazawa T, Iino M (2001) Reduced IP_3 sensitivity of IP_3 receptor in Purkinje neurons. Neuroreport 12: 2647–2651.
32. Dufour J, Arias I, Turner T (1997) Inositol 1,4,5-trisphosphate and calcium regulate the calcium channel function of the hepatic inositol 1,4,5-trisphosphate receptor. J Biol Chem 272: 2675–2681.
33. Marchant JS, Taylor CW (1997) Cooperative activation of IP_3 receptors by sequential binding of IP_3 and Ca^{2+} safeguards against spontaneous activity. Curr Biol 7: 510–518.
34. Adkins C, Taylor C (1999) Lateral inhibition of inositol 1,4,5-trisphosphate receptors by cytosolic Ca^{2+}. Curr Biol 9: 1115–1118.
35. Doi T, Kuroda S, Michikawa T, Kawato M (2005) Inositol 1,4,5-trisphosphate-dependent Ca^{2+} threshold dynamics detect spike timing in cerebellar Purkinje cells. J Neurosci 25: 950–961.
36. Sneyd J, Falcke M, Dufour J, Fox C (2004) A comparison of three models of the inositol trisphosphate receptor. Prog Biophys Mol Biol 85: 121–140.
37. Eungdamrong N, Iyengar R (2004) Modeling cell signaling networks. Biol Cell 96: 355–362.
38. Hellgren Kotaleski J, Blackwell K (2010) Modelling the molecular mechanisms of synaptic plasticity using systems biology approaches. Nat Rev Neurosci 11: 239–251.
39. Sneyd J, Falcke M (2005) Models of the inositol trisphosphate receptor. Prog Biophys Mol Biol 89: 207–245.
40. Falcke M (2003) On the role of stochastic channel behavior in intracellular Ca^{2+} dynamics. Biophys J 84: 42–56.
41. De Young G, Keizer J (1992) A single-pool inositol 1,4,5-trisphosphate-receptor-based model for agonist-stimulated oscillations in Ca^{2+} concentration. Proc Natl Acad Sci USA 89: 9895–9899.
42. LeBeau A, Yule D, Groblewski G, Sneyd J (1999) Agonist-dependent phosphorylation of the inositol 1, 4, 5-trisphosphate receptor. J Gen Physiol 113: 851.
43. Tang Y, Stephenson J, Othmer H (1996) Simplification and analysis of models of calcium dynamics based on IP_3-sensitive calcium channel kinetics. Biophys J 70: 246–263.
44. Mak D,McBride S, Foskett J (2003) Spontaneous channel activity of the inositol 1,4,5-trisphosphate ($InsP_3$) receptor ($InsP_3R$). Application of allosteric modeling to calcium and $InsP_3$ regulation of $InsP_3R$ single-channel gating. J Gen Physiol 122: 583.
45. Shuai JW, Yang DP, Pearson JE, Rüdiger S (2009) An investigation of models of the IP_3R channel in Xenopus oocyte. Chaos 19: 037105.
46. Schuster S, Marhl M, Hofer T (2002) Modelling of simple and complex calcium oscillations. Eur J Biochem 269: 1333–1355.
47. Turner TE, Schnell S, Burrage K (2004) Stochastic approaches for modelling in vivo reactions. Comp Biol Chem 28: 165–178.
48. Barrio M, Burrage K, Leier A, Tian T (2006) Oscillatory regulation of Hes1: discrete stochastic delay modelling and simulation. PLOS Comp Biol 2: e117.
49. Hituri K, Achard P, Wils S, Linne ML, De Schutter E (2008) Stochastic modeling of inositol-1,4,5- trisphophate receptors in Purkinje cell spine. In: Proceedings of the 5th TICSP Workshop on Computation Systems Biology (WCSB 2008). Leipzig, Germany, pp. 57–60.
50. Choi T, Maurya M, Tartakovsky D, Subramaniam S (2010) Stochastic hybrid modeling of intracellular calcium dynamics. J Chem Phys 133: 165101.
51. Gillespie DT (1976) A general method for numerical simulating the stochastic time evolution of coupled chemical reactions. J Comp Phys 22: 403–434.
52. Sneyd J, Dufour J (2002) A dynamic model of the type-2 inositol trisphosphate receptor. Proc Natl Acad Sci USA 99: 2398–2403.
53. Swillens S, Champeil P, Combettes L, Dupont G (1998) Stochastic simulation of a single inositol 1,4,5-trisphosphate-sensitive Ca^{2+} channel reveals repetitive openings during 'blip-like' Ca^{2+} transients. Cell calcium 23: 291–302.
54. Haeri H, Hashemianzadeh S, Monajjemi M (2007) A kinetic Monte Carlo simulation study of inositol 1,4,5-trisphosphate receptor (IP_3R) calcium release channel. Comp Biol Chem 31: 99–109.
55. Othmer HG, Tang Y (1993) Oscillations and waves in a model of InsP3-controlled calcium dynamics, London: Plenum Press, volume 259 of Experimental and Theoretical Advances in Biological Pattern Formation. pp. 277–300.
56. Dawson A, Lea E, Irvine R (2003) Kinetic model of the inositol trisphosphate receptor that shows both steady-state and quantal patterns of Ca^{2+} release from intracellular stores. Biochem J 370: 621.
57. Fraiman D, Dawson SP (2004) A model of IP_3 receptor with a luminal calcium binding site: stochastic simulations and analysis. Cell Calcium 35: 403–413.
58. Wils S, De Schutter E (2009) STEPS: Modeling and simulating complex reaction-diffusion systems with Python. Front Neuroinform 3: 165–178.
59. Hepburn I, Chen W, Wils S, De Schutter E (2012) STEPS: efficient simulation of stochastic reaction-diffusion models in realistic morphologies. BMC Syst Biol 6: 1752–0509.
60. Mishra J, Bhalla U (2002) Simulations of inositol phosphate metabolism and its interaction with InsP3-mediated calcium release. Biophys J 83: 1298–1316.
61. Sachs F, Qin F, Palade P (1995) Models of Ca^{2+} release channel adaptation. Science 267: 2010–2011.
62. Taylor CW, da Fonseca PC, Morris EP (2004) IP_3 receptors: the search for structure. Trends Biochem Sci 29: 210–219.
63. Khodakhah K, Ogden D (1995) Fast activation and inactivation of inositol trisphosphate-evoked Ca^{2+} release in rat cerebellar Purkinje neurones. J Physiol 487: 343.
64. Gillespie DT (1977) Exact stochastic simulation of coupled chemical reactions. J Phys Chem 81: 2340–2361.

65. MATLAB (2011) version 7.13.0.564 (R2011b). Natick, Massachusetts: The MathWorks Inc.
66. Diambra L, Guisoni N (2005) Modeling stochastic Ca^{2+} release from a cluster of IP_3-sensitive receptors. Cell Calcium 37: 321–332.
67. Fraiman D, Dawson SP (2004) Erratum to "a model of IP_3 receptor with a luminal calcium binding site: stochastic simulations and analysis". Cell Calcium 36: 445.
68. De Schutter E (2008)Why are computational neuroscience and systems biology so separate? PLOS Comp Biol 4: e1000078.
69. Gin E, Falcke M, Wagner L, Yule D, Sneyd J (2009) Markov chain Monte Carlo fitting of singlechannel data from inositol trisphosphate receptors. J Theor Biol 257: 460–474.
70. Gin E, Falcke M, Wagner L, et al. (2009) A kinetic model of the inositol trisphosphate receptor based on single-channel data. Biophysical journal 96: 4053.
71. Gin E, Wagner L, Yule D, Sneyd J (2009) Inositol trisphosphate receptor and ion channel models based on single-channel data. Chaos 19: 037104.
72. Siekmann I, Wagner L, Yule D, Fox C, Bryant D, et al. (2011) MCMC estimation of Markov models for ion channels. Biophys J 100: 1919–1929.
73. Amari S, Beltrame F, Bjaalie J, Dalkara T, De Schutter E, et al. (2002) Neuroinformatics: the integration of shared databases and tools towards integrative neuroscience. J Integr Neurosci 1: 117–128.
74. Cannon R, Howell F, Goddard N, De Schutter E (2002) Non-curated distributed databases for experimental data and models in neuroscience. Network: Computation in Neural Systems 13: 415–428.
75. De Schutter E (2010) Data publishing and scientific journals: The future of the scientific paper in a world of shared data. Neuroinformatics : 1–3.
76. Ranjan R, Khazen G, Gambazzi L, Ramaswamy S, Hill S, et al. (2011) Channelpedia: an integrative and interactive database for ion channels. Front Neuroinform 5.
77. Cannon R, O'Donnell C, Nolan M (2010) Stochastic ion channel gating in dendritic neurons: Morphology dependence and probabilistic synaptic activation of dendritic spikes. PLOS Comp Biol 6: e1000886.
78. White J, Klink R, Alonso A, Kay A (1998) Noise from voltage-gated ion channels may influence neuronal dynamics in the entorhinal cortex. J Neurophysiol 80: 262.
79. Steinmetz P, Manwani A, Koch C, London M, Segev I (2000) Subthreshold voltage noise due to channel fluctuations in active neuronal membranes. J Comput Neurosci 9: 133–148.
80. Saarinen A, Linne ML, Yli-Harja O (2008) Stochastic differential equation model for cerebellar granule cell excitability. PLOS Comp Biol 4(2): e1000004.
81. Faisal A, Laughlin S (2007) Stochastic simulations on the reliability of action potential propagation in thin axons. PLOS Comp Biol 3: e79.
82. Skupin A, Kettenmann H, Falcke M (2010) Calcium signals driven by single channel noise. PLOS Comp Biol 6: e1000870.
83. Wilkinson D (2007) Bayesian methods in bioinformatics and computational systems biology. Brief Bioinform 8: 109.
84. Girolami M (2008) Bayesian inference for differential equations. Theor Comput Sci 408: 4–16.
85. PennyW, Stephan K, Daunizeau J, Rosa M, Friston K, et al. (2010) Comparing families of dynamic causal models. PLOS Comp Biol 6: e1000709.

Errata

Hituri K., Linne M.-L. (2013) Comparison of models for IP_3 receptor kinetics using stochastic simulations. PLoS ONE 8(4): e59618.

1. In Tables 1, 2, 3, and 4 the unit should be $(\mathrm{Ms})^{-1}$ instead of $(\mu\mathrm{Ms})^{-1}$.

2. Table 5 is misprinted in the final version of the publication. The correct table should be

Figure 5. Mean open and closed times of IP_3R of the selected models.

	Model	mean open time (ms)	mean closed time (ms)	n	simulation time (s)
Sim 1	Othmer and Tang	451.19 ± 423.06	1289 ± 2563	1068	1 800
	Dawson *et al.*	0.59 ± 5.46	10.33 ± 120.24	1797	20
	Fraiman and Dawson	2.45 ± 2.52	4.01 ± 11.22	1535	10
	Doi *et al.*	0.47 ± 0.46	11.21 ± 38.08	1711	20
Sim 2	Othmer and Tang	463.55 ± 463.96	1290 ± 2793	1045	1 800
	Dawson *et al.*	0.52 ± 4.70	9.38 ± 167.55	1897	20
	Fraiman and Dawson	2.57 ± 2.76	4.92 ± 19.84	1391	10
	Doi *et al.*	0.47 ± 0.46	3.76 ± 23.11	1501	6
Sim 3	Othmer and Tang	510.08 ± 526.46	1047 ± 2074	1927	3 000
	Dawson *et al.*	0.46 ± 5.90	8.83 ± 97.56	2004	20
	Fraiman and Dawson	2.48 ± 2.64	5.38 ± 2.64	1293	10
	Doi *et al.*	0.53 ± 0.53	19.00 ± 29.60	1024	20
Sim 4	Othmer and Tang	509.68 ± 525.59	958.50 ± 2073	2044	3 000
	Dawson *et al.*	0.65 ± 10.64	5.21 ± 100.02	2063	10
	Fraiman and Dawson	2.51 ± 2.67	5.50 ± 15.55	1249	10
	Doi *et al.*	0.51 ± 0.50	4.72 ± 0.50	1866	10
Sim 5	Othmer and Tang	598.32 ± 598.68	3356 ± 3384	1263	5 000
	Dawson *et al.*	0.25 ± 0.25	12.60 ± 129.80	1161	10
	Fraiman and Dawson	2.47 ± 2.60	25.18 ± 88.87	1446	40
	Doi *et al.*	0.47 ± 0.47	107.37 ± 123.06	1854	200
Sim 6	Othmer and Tang	596.98 ± 592.01	2712 ± 2709	1509	5 000
	Dawson *et al.*	0.25 ± 0.26	9.27 ± 163.25	2098	20
	Fraiman and Dawson	2.49 ± 2.61	27.54 ± 95.62	1331	40
	Doi *et al.*	0.46 ± 0.46	27.92 ± 47.50	1407	40

The different simulation conditions (Sim 1 – Sim 6) are presented in Table 6.

Publication II

Manninen T.*, Hituri K.*, Toivari E.*, Linne M.-L. (2011) Modeling signal transduction in synaptic plasticity: evaluation and comparison of five models. EURASIP Journal on Bioinformatics and Systems biology. Volume 2011, Article ID 797250. *Equal contribution

Hindawi Publishing Corporation
EURASIP Journal on Bioinformatics and Systems Biology
Volume 2011, Article ID 797250, 11 pages
doi:10.1155/2011/797250

Research Article

Modeling Signal Transduction Leading to Synaptic Plasticity: Evaluation and Comparison of Five Models

Tiina Manninen, Katri Hituri, Eeva Toivari, and Marja-Leena Linne

Department of Signal Processing, Tampere University of Technology, P.O. Box 553, 33101 Tampere, Finland

Correspondence should be addressed to Tiina Manninen, tiina.manninen@tut.fi

Received 1 November 2010; Revised 21 January 2011; Accepted 27 January 2011

Academic Editor: Carsten Wiuf

An essential phenomenon of the functional brain is synaptic plasticity which is associated with changes in the strength of synapses between neurons. These changes are affected by both extracellular and intracellular mechanisms. For example, intracellular phosphorylation-dephosphorylation cycles have been shown to possess a special role in synaptic plasticity. We, here, provide the first computational comparison of models for synaptic plasticity by evaluating five models describing postsynaptic signal transduction networks. Our simulation results show that some of the models change their behavior completely due to varying total concentrations of protein kinase and phosphatase. Furthermore, the responses of the models vary when models are compared to each other. Based on our study, we conclude that there is a need for a general setup to objectively compare the models and an urgent demand for the minimum criteria that a computational model for synaptic plasticity needs to meet.

1. Introduction

Neurons respond to variations in extracellular and intracellular environment by modifying their synaptic and intrinsic membrane properties. When a presynaptic neuron passes an electrical or chemical signal to a postsynaptic neuron, changes in the synapse occur. Long-term potentiation (LTP), also known as strengthening, and long-term depression (LTD), also known as weakening, of synapses are two forms of synaptic plasticity. Both LTP and LTD participate in storing information and inducing processes that are thought to ultimately lead to learning (see, e.g., [1]). The main focus in the research on synaptic plasticity in vertebrates has been on LTP and LTD in cornu ammonis 1 (CA1) region of the hippocampus [1] because hippocampus is especially important in the formation and retrieval of declarative memories. Several mechanisms have been shown to be the reason for changes in synaptic strength; for example, changes in neurotransmitter release, conductivityof receptors, numbers of receptors, numbers of active synapses, and structure of synapses [2].

At present, there are more than a hundred molecules found important in LTP/LTD, some of which are key components for LTP/LTD formation and others being able to modulate the ability to generate LTP/LTD [1]. Strong evidence supports the finding that calcium (Ca^{2+})/calmodulin (CaM)-dependent protein kinase II (CaMKII) meets the criteria for being the essential molecule to LTP [3]. Protein kinases add phosphates to proteins, and, on the other hand, protein phosphatases remove phosphates from proteins to activate or deactivate them. It is hence straightforward to consider that also the protein phosphatases, such as protein phosphatases 1, 2A, and 2B (PP1, PP2A, and PP2B, a.k.a. calcineurin (CaN)), have important roles in synaptic plasticity [4].

More than a hundred computational models, simple and more complex ones, have been developed to describe the mechanisms behind synaptic plasticity at the biochemical level (see, e.g., [5, 6]). Simplest models only have one reversible reaction (see, e.g., [7]) and most complicated ones several hundred reactions (see, e.g., [2]). The communities of researchers in computational systems biology and neuroscience are in a need for a general setup on how to evaluate and classify the models for synaptic plasticity (see also [5]). Because the statistical data from the models does not necessarily represent exactly the same phenomenon, mathematical methods, such as Bayesian methods [8–10], are not applicable to comparison of these synaptic

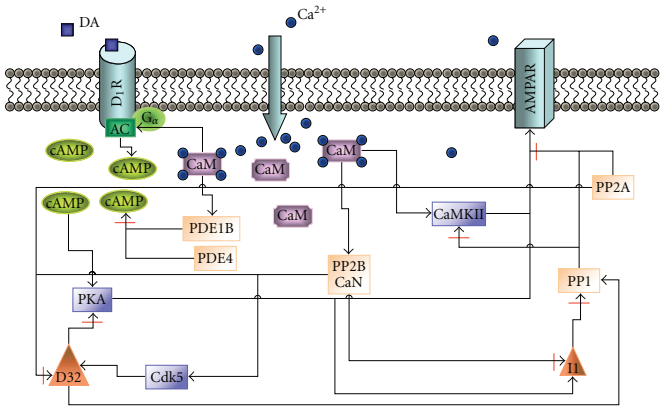

Figure 1: *Schematic representation of the postsynaptic mechanisms involved in signal transduction related to induction of LTP/LTD.* Intracellular calcium ions (Ca^{2+}) bind to calmodulin (CaM), which further affects the activation of protein phosphatase 2B (PP2B) a.k.a. calcineurin (CaN), CaM-dependent kinase II (CaMKII), adenylyl cyclase (AC, the catalyst of the reaction producing cyclic adenosine monophosphate (cAMP)), and phosphodiesterase type 1B (PDE1B). Dopamine (DA) increases cAMP concentration via AC activation. Together with PDE1B, also PDE type 4 (PDE4) degrades cAMP. cAMP-dependent protein kinase (PKA) phosphorylates α-amino-3-hydroxy-5-methylisoxazole-4-propionic acid receptor (AMPAR) and protein phosphatase 1 (PP1) inhibitor 1 (I1). In addition, protein phosphatase 2A (PP2A) and cyclin-dependent kinase 5 (Cdk5) affect PP1 regulatory subunit a.k.a. DA- and cAMP-regulated neuronal phosphoprotein of 32 kDa (D32).

plasticity models. Thus, some subjective selection of features describing the overall behavior of the modeled system and traditional simulation-based comparison are required. To enable the use of previous computational models for synaptic plasticity, minimum criteria for the models need to be set (see BioModels projects, e.g., [11, 12]).

The aim of this study is to provide the first comparison of synaptic plasticity models by computational means and to be the first step towards finding a general setup for comparison. The organization of this study is as follows. First, we shortly describe the biology behind synaptic plasticity by presenting five computational models selected for this evaluation. Second, the used simulation setups, including the second messenger Ca^{2+} and neurotransmitter dopamine (DA) inputs, as well as the total concentrations of protein kinase CaMKII and protein phosphatase PP1, are presented. Third, we show the comparative simulation results and evaluate the synaptic plasticity models. The comparison is made between the two models selected for the same neuron type, that is, between the two models for a hippocampal CA1 neuron and between the two models for a striatal medium spiny neuron. We also examine if a generic model is suitable for describing the behavior of either of the two neuron types and thus being a good computational representative of them. Lastly, we discuss our most important findings and provide some conclusions.

2. Models and Methods

2.1. Biological Background. Several types of LTP and LTD can occur in the brain depending on the neuron type and given input to the neuron. LTP can be divided into two main types: an early phase LTP (E-LTP), which lasts for 1 h-2 h, and a late phase LTP (L-LTP), which persists for several hours [1, 3]. Similar division can also be made for LTD. All types of plasticity involve three processes: induction, expression, and maintenance. The LTP/LTD phenomenon can be induced by introducing glutamatergic and dopaminergic inputs. Glutamatergic input causes the elevation of intracellular Ca^{2+} concentration in postsynaptic density, meaning a small volume linking postsynaptic membrane receptors, their signaling pathways, and the cytoskeleton, and in cytosol. Dopaminergic input activates the enzyme adenylyl cyclase (AC) on the cell membrane and thus increases the intracellular cyclic adenosine monophosphate (cAMP) concentration. This input can only be found in some neuron types, for example, in striatal medium spiny neurons. Ca^{2+} and cAMP serve as secondary messengers passing the glutamatergic and dopaminergic signals forward and activating downstream proteins. In this study, the elevations in Ca^{2+} and DA concentrations are used as model inputs (see details in Section 2.3).

Briefly, the signal transduction network leading to LTP/LTD phenomenon includes the following events (see Figure 1). Elevated Ca^{2+} concentration enables the binding of Ca^{2+} to CaM which further activates CaM-dependent kinase CaMKII. Then Ca^{2+}/CaM-CaMKII complex is able to proceed to autophosphorylation. Ca^{2+}/CaM also binds to protein phosphatase CaN. The effect of active CaN on protein phosphatase PP1 activity is bidirectional; CaN inhibits PP1 inhibitor 1 (I1) and activates cyclic-dependent kinase 5 (Cdk5). Both of these actions lead to activation

Table 1: *Characteristics of models*. Tabulated characteristics are the simulation environment and integration method, phases of long-term potentiation and long-term depression, model inputs, model outputs chosen for this study, and size of the model based on the number of different chemical species or other model variables. Used abbreviations are α-amino-3-hydroxy-5-methylisoxazole-4-propionic acid receptor (AMPAR), calcium ion (Ca^{2+}), Ca^{2+}/calmodulin-dependent protein kinase II (CaMKII), cyclic adenosine monophosphate (cAMP), dopamine (DA), DA- and cAMP-regulated neuronal phosphoprotein of 32 kDa (DARPP32), early phase LTP (E-LTP), induction (Ind.), Ca^{2+} influx via NMDARs (J_{NMDAR}), late phase LTP (L-LTP), long-term depression (LTD), long-term potentiation (LTP), N-methyl-D-aspartate receptor (NMDAR), and cAMP-dependent protein kinase (PKA).

Model	Simulation environment	Phases	Inputs	Outputs	Size
d'Alcantara et al. [16]	MATLAB, ode23 (explicit Runge-Kutta)	Ind. LTP/LTD	Ca^{2+}	AMPAR	14
Kim et al. [17]	XPPAUT, adaptive stiff integration method	Ind. L-LTP	Ca^{2+}, DA	CaMKII/PKA	49
Lindskog et al. [18]	XPPAUT, adaptive stiff integration method	Ind. E-LTP	Ca^{2+}, DA	DARPP32	89
Nakano et al. [19]	GENESIS/Kinetikit, exponential Euler	Ind. LTP/LTD	Ca^{2+}, DA	AMPAR	111
Hayer and Bhalla [2]	MATLAB, ode23s (based on Rosenbrock)	LTP/LTD	Ca^{2+}, cAMP, J_{NMDAR}	AMPAR	258

of PP1. However, active CaN is also able to deactivate PP1 regulatory subunit a.k.a. DA- and cAMP-regulated neuronal phosphoprotein of 32 kDa (DARPP32, D32 in Figure 1), which leads to deactivation of PP1. Active PP1 has a major role in dephosphorylating CaMKII and α-amino-3-hydroxy-5-methylisoxazole-4-propionic acid receptor (AMPAR). On the other hand, due to the DA input, cAMP activates cAMP-dependent protein kinase (PKA) which phosphorylates AMPAR (see synaptic plasticity mechanisms, e.g., in [1, 4]). In the ultimate end of the signaling cascade described in this study, protein kinases CaMKII and PKA, together with protein phosphatases PP1 and PP2A, act on AMPAR.

The phosphorylation and dephosphorylation of AMPAR subunits are crucial for the trafficking of AMPARs. Regulated AMPAR trafficking between intracellular, synaptic, and nonsynaptic membranes at the postsynaptic hippocampal neuron is found to provide a protein-level basis for controlling the amount of AMPARs on the plasma membrane and hence postsynaptic responsiveness [13, 14]. It is suggested that in the basal conditions, AMPARs are concentrated on the postsynaptic membrane but also exist abundantly in endosomal compartments, meaning the membranes inside the cell [15]. Some of the AMPAR subunits undergo constant recycling with membrane receptors in an activity-independent manner. However, the amount of AMPARs in the postsynaptic membrane shows only modest variation. Following the N-methyl-D-aspartate receptor (NMDAR) stimulation and CaMKII activation, exocytosis of AMPAR subunits from endosomal compartments to cell membrane is triggered, leading finally to the insertion of AMPARs into synapses [13]. On the contrary, in synaptic depression endocytotic mechanisms are activated and subunits of AMPARs are stored in endosomal compartments or degraded [13].

2.2. Selection of Models. We set our criteria for model selection to be the following: (1) the model for synaptic plasticity has to include adequate postsynaptic reactions and kinetics, (2) the model can be found in a database, (3) the model describes synaptic plasticity either in a hippocampal CA1 neuron or in a striatal medium spiny neuron, (4) the model uses Ca^{2+} as input, and (5) CaMKII and PP1 are included in the model.

We select the following models describing synaptic plasticity in a hippocampal CA1 neuron:

(i) model by d'Alcantara et al. [16],

(ii) model by Kim et al. [17].

In addition, we select the following models describing synaptic plasticity in a striatal medium spiny neuron:

(i) model by Lindskog et al. [18],

(ii) model by Nakano et al. [19].

Furthermore, we select one generic neuron model which is compared to models above:

(i) model by Hayer and Bhalla [2].

The characteristics and components of the selected models are tabulated in Tables 1 and 2 (see also [5]). In total, several protein kinases (CaMKII, Cdk5, and PKA) and protein phosphatases (CaN, PP1, and PP2A) are included in the models. The models have similar elements and are in some cases directly based on each other. Kim et al. [17] take the model by Lindskog et al. [18] as their base. This might be confusing since the models are made for neurons in different brain areas, but, on the other hand, they share similar pathways. Furthermore, the model by Kim et al. [17] takes into account the G protein-linked PKA activation. Within the models describing synaptic plasticity in a striatal medium spiny neuron, Nakano et al. [19] take some of the reactions from the earlier model by Lindskog et al. [18] and then use similar AMPAR trafficking model as the generic model by Hayer and Bhalla [2]. These selected models are also partly based on other published models, but we list here just how these selected models are based on each other. It should be noted that the models selected for this study as such can be considered as advanced models in the computational neuroscience community.

2.3. Simulation Setup. For all the models, the total simulation time is 2000 s and a four-train Ca^{2+} input is given at $t = 500$ s in which the basal concentration of Ca^{2+} is 0.1 μM and the pulse peak is 10 μM (see Figure 2(a)). A four-train

Table 2: *Model components*. Tabulated characteristics are the compartments, receptors, Ca^{2+} mechanisms, and signaling pathways modeled. Used abbreviations are adenylyl cyclase (AC), α-amino-3-hydroxy-5-methylisoxazole-4-propionic acid receptor (AMPAR), calmodulin (CaM), calcium/CaM-dependent protein kinase II (CaMKII), calcineurin (CaN), cyclin-dependent kinase 5 (Cdk5), dopamine receptor (D_1R), dopamine- and cyclic adenosine monophosphate-regulated neuronal phosphoprotein of 32 kDa (DARPP32), inhibitor 1 (I1), phosphodiesterase type 1 (PDE1), PDE type 1B (PDE1B), PDE type 2 (PDE2), PDE type 4 (PDE4), cyclic adenosine monophosphate-dependent protein kinase (PKA), protein phosphatase 1 (PP1), and protein phosphatase 2A (PP2A).

Model	Compartments	Receptors	Ca^{2+} mechanisms	Signaling pathways
d'Alcantara et al. [16]	1 postsynaptic	AMPAR	CaM buffer	CaM, CaMKII, CaN, I1, PP1
Kim et al. [17]	1 spine	D_1R	CaM buffer	CaM, CaMKII, CaN, G protein, I1, PDE1B, PDE4, PKA, PP1
Lindskog et al. [18]	1 spine	D_1R	CaM buffer	AC, CaM, CaMKII, CaN, DARPP32, PDE1, PDE4, PKA, PP1, PP2A
Nakano et al. [19]	1 spine	AMPAR, D_1R	CaM buffer	AC, CaM, CaMKII, CaN, Cdk5, DARPP32, I1, PDE1, PDE2, PKA, PP1, PP2A
Hayer and Bhalla [2]	1 dendritic, 1 postsynaptic, 1 spine-head	AMPAR	CaM buffer, 1-D diffusion of some of the molecules	AC, CaM, CaMKII, CaN, PKA, PP1

Table 3: Total concentrations of CaMKII and PP1 ($[CaMKII]_{tot}$, $[PP1]_{tot}$) and ratios of them used in different simulations.

Sim ID	$[CaMKII]_{tot}$ (μM)	$[PP1]_{tot}$ (μM)	Ratio
Sim1	0.5	2	0.25
Sim2	1	4	0.25
Sim3	2	4	0.5
Sim4	4	1	4
Sim5	20	5	4
Sim6	20	2	10

DA input (see Figure 2(b)), in addition to Ca^{2+} input, is given in the models that also model DA-related pathways, in other words to the models by Kim et al. [17], Lindskog et al. [18], and Nakano et al. [19]. Hayer and Bhalla [2] also use other inputs in addition to Ca^{2+} (see Table 1), and these other inputs are used similarly as presented in the original model.

Six simulations (Sim1–Sim6) with different total concentrations of CaMKII and PP1 are run for all the models with the same inputs (see Table 3). These total concentrations are selected based on the different values used in the original models. Otherwise, we use the parameter values and mostly the initial concentrations given in the original models. In Table 4, we list the actual values that have to be changed to reach the simulation conditions given in Table 3.

It is assumed that the original models have been tested against changes in the values of parameters and initial concentrations, and thus no detailed sensitivity analysis is performed in this study. It is beyond the scope of this study.

We want to emphasize that the purpose of this study is not to perform any detailed analysis of the used integration methods nor to implement the models using other integration methods. Instead, we use the model as it is presented in the model database and simulate it using the given simulation tool.

3. Results

3.1. Simulation Results. We evaluate and compare different computational models describing LTP and LTD phenomena based on the model outcomes. The comparison is made between the two models selected for the same neuron type; that is, two models are compared for a hippocampal CA1 neuron [16, 17] and two models for a striatal medium spiny neuron [18, 19]. In addition, we examine if a generic model [2] is a suitable approximation for hippocampal and striatal neurons in terms of reproducing the main LTP phenomenon. The model selection is justified upon the importance of AMPAR phosphorylation and dephosphorylation during synaptic plasticity. All the model outputs can be related to the phosphorylation and dephosphorylation of AMPARs. However, as the outputs of the models differ from each other, we also follow up the concentrations of active CaMKII and PP1, pivotal phosphorylating and dephosphorylating enzymes, respectively, in all the models. To compare the selected deterministic models [2, 16–19], we run simulations with several setups. Details of the simulation setups are given in Section 2.3.

3.1.1. Models Describing Synaptic Plasticity in a Hippocampal CA1 Neuron. The concentrations of active CaMKII (see Figures 3(a) and 3(d)) in simulations of the hippocampal CA1 neuron models by d'Alcantara et al. [16] and Kim et al. [17] depend completely on the total concentration of CaMKII; the higher the total concentration of CaMKII, the higher the concentration of active CaMKII. In the case of the same total concentration of CaMKII (20 μM in Sim5 and Sim6), the lower total concentration of PP1

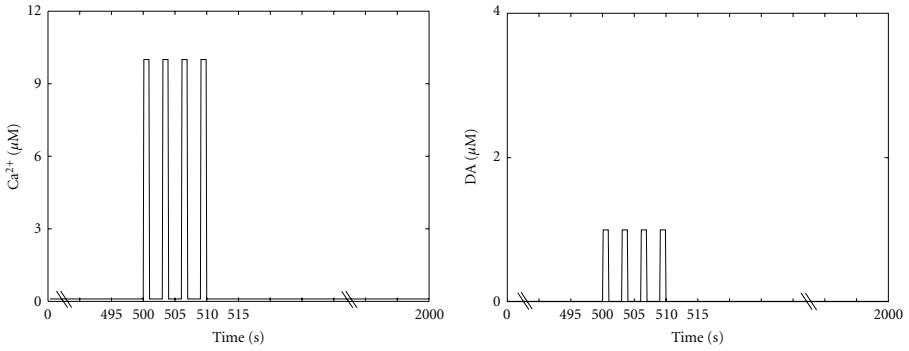

FIGURE 2: *Four-train (a) calcium (Ca^{2+}) and (b) dopamine (DA) inputs used in simulations.* 10 μM Ca^{2+} and 1 μM DA pulses are given for 1 s at time points $t = 500, 503, 506$, and 509 s. The duration of the basal plateau phases is thus 2 s. Before, between, and after the pulses a basal concentration of 0.1 μM for Ca^{2+} and 0.01 μM for DA is used.

TABLE 4: *Changed initial and total concentrations related to different states of CaMKII and PP1 to reach the total concentrations given in Table 3.* Other values used in the simulations are based on the original models. We use here the actual names of the variables and constants as given in the model code downloaded from a database. Values are given in units of μM.

Model	Sim1	Sim2	Sim3	Sim4	Sim5	Sim6
d'Alcantara et al. [16]	Naive states set to total, others zero	Naive states set to total, others zero	Naive states set to total, others zero	Naive states set to total, others zero	Naive states set to total, others zero	Naive states set to total, others zero
Kim et al. [17]	CK_ini = 0.5, pp1tot = 2, CKCaM = 0.01, CKpCaM = 0.01	CK_ini = 1, pp1tot = 4, CKCaM = 0.01, CKpCaM = 0.01	CK_ini = 2, pp1tot = 4	CK_ini = 4, pp1tot = 1	CK_ini = 20, pp1tot = 5	CK_ini = 20, pp1tot = 2
Lindskog et al. [18]	camkmax = 0.5, PP1tot = 2	camkmax = 1, PP1tot = 4	camkmax = 2, PP1tot = 4	camkmax = 4, PP1tot = 1	camkmax = 20, PP1tot = 5	camkmax = 20, PP1tot = 2
Nakano et al. [19]	CaMKII = 0.12, PP1_active = 0.87, PP1_I1_p = 0.60	CaMKII = 0.62, PP1_active = 1.87, PP1_I1_p = 1.60	CaMKII = 1.62, PP1_active = 1.87, PP1_I1_p = 1.60	CaMKII = 3.62, PP1_active = 0.29, PP1_I1_p = 0.18	CaMKII = 19.62, PP1_active = 2.37, PP1_I1_p = 2.10	CaMKII = 19.62, PP1_active = 0.87, PP1_I1_p = 0.60
Hayer and Bhalla [2]	basal_CaMKII_PSD = 0.5, PP1-active_PSD = 2	basal_CaMKII_PSD = 1, PP1-active_PSD = 4	basal_CaMKII_PSD = 2, PP1-active_PSD = 4	basal_CaMKII_PSD = 4, PP1-active_PSD = 1	basal_CaMKII_PSD = 20, PP1-active_PSD = 5	basal_CaMKII_PSD = 20, PP1-active_PSD = 2

produces higher concentration for active CaMKII. In this sense, simulations of the hippocampal CA1 neuron models by d'Alcantara et al. [16] and Kim et al. [17] show similar results for the concentrations of active CaMKII. Otherwise the model by Kim et al. [17] produces different responses for the concentration of active CaMKII compared to other models.

In the case of PP1 (see Figures 3(b) and 3(e)), the higher total concentration of PP1 produces higher concentration for PP1. Most models have only one unbound form of PP1 which concentration is plotted. Furthermore, the same total concentrations of PP1 (4 μM in Sim2 and Sim3 and 2 μM in Sim1 and Sim6) produce about the same concentrations for PP1.

The concentration of active PKA, which is the other output of the model by Kim et al. [17] in addition to the concentration of active CaMKII, varies very little due to the variation in total concentrations of CaMKII and PP1 (see Figure 3(f)). The simulations Sim1–Sim4, representing the ratios 0.25, 0.5, and 4 of the total concentrations of CaMKII and PP1, produce alike curves with peak concentrations of about 80 nM. In addition, the simulations Sim5 and

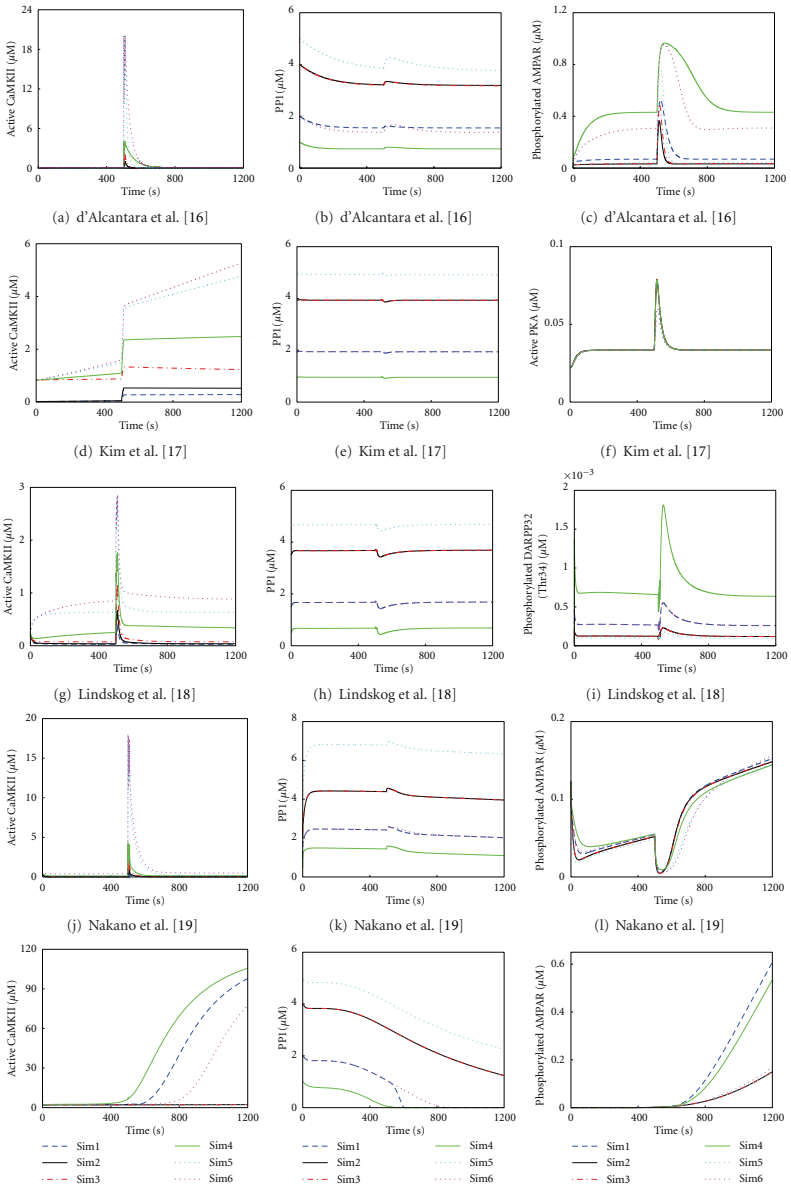

(a) d'Alcantara et al. [16] (b) d'Alcantara et al. [16] (c) d'Alcantara et al. [16]

(d) Kim et al. [17] (e) Kim et al. [17] (f) Kim et al. [17]

(g) Lindskog et al. [18] (h) Lindskog et al. [18] (i) Lindskog et al. [18]

(j) Nakano et al. [19] (k) Nakano et al. [19] (l) Nakano et al. [19]

(m) Hayer and Bhalla [2] (n) Hayer and Bhalla [2] (o) Hayer and Bhalla [2]

FIGURE 3: *Simulation results with different total concentrations of CaMKII and PP1*. First column presents active CaMKII, second column PP1 (most models have only one unbound form of PP1), and third column the selected output of each model. (a)–(o) show 1200 s of simulation time.

Sim6, representing the ratios 4 and 10, produce slightly different peak concentrations (about 60 nM) but otherwise similar curves with each other and with other ratios as well. However, the model by d'Alcantara et al. [16] does not produce as straightforward results for the output of the model. Figure 3(c) shows the concentration of phosphorylated AMPAR simulated by the model of d'Alcantara et al. [16]. This model does not follow any pattern related to changes in the total concentrations of CaMKII and PP1 or the ratio of them.

3.1.2. Models Describing Synaptic Plasticity in a Striatal Medium Spiny Neuron. The concentrations of active CaMKII and PP1 in simulations of the striatal medium spiny neuron models by Lindskog et al. [18] and Nakano et al. [19] follow similar behavior as the hippocampal CA1 neuron models (see Figures 3(g), 3(h), 3(j), and 3(k)). However, the actual concentrations vary even though the actual form of the curves can be similar. In this sense, simulations of the striatal medium spiny neuron models by Lindskog et al. [18] and Nakano et al. [19] show similar results for the concentrations of active CaMKII and PP1.

With the model by Lindskog et al. [18], the concentration of phosphorylated DARPP32 on threonine (Thr) 34 is plotted in Figure 3(i). Basically, this model output depends on the total concentration of PP1. If two simulations have the same total concentration of PP1, the concentrations of phosphorylated DARPP32 are the same. Furthermore, the lower the total concentration of PP1, the higher the concentration of phosphorylated DARPP32. However, the total concentrations of PP1 and CaMKII do not have a role for the concentration of phosphorylated DARPP32 on Thr75, thus it is about the same in all simulations (not shown). With the model by Nakano et al. [19], the concentration of phosphorylated AMPAR depends on the total concentration of PP1 before the input is given at 500 s (see Figure 3(l)). The lower the total concentration of PP1, the higher the concentration of phosphorylated AMPAR. However, after the input is given, the concentration of phosphorylated AMPAR does not follow any pattern related to changes in the total concentrations of CaMKII and PP1, or the ratio of them.

When simulating the model by Nakano et al. [19], we find out that the concentrations of active CaMKII and PP1 can reach higher than the total concentrations meaning they also appear elsewhere in the model. We have not found the reason for this even though we have marked all the initial concentrations related to them as zero. The problem is in the original model and not in the numerical integration. There is no easy way of debugging the code in Kinetikit either using the graphical user interface or modifying directly the model file.

3.1.3. Generic Neuron Model Describing Synaptic Plasticity. The concentration of active CaMKII from the model by Hayer and Bhalla [2] follows the total concentration of PP1 instead of the total concentration of CaMKII as in the other models (see Figure 3(m)). The lower the total concentration of PP1, the higher the concentration of active CaMKII. In the simulations Sim2 and Sim3, where the total concentration of PP1 is the same, the concentrations of active CaMKII stay on the same level. Earlier experimental results [20] have shown that CaMKII in the postsynaptic density can act as a stable switch, even in the presence of considerable phosphatase activity. Mullasseril et al. [20] justify the stability to be structural: CaMKII and PP1, both of which are in the postsynaptic density, are held in such a position that PP1 simply cannot reach the amino acid residue of CaMKII it is destined to dephosphorylate. This could be the experimental reasoning for the case in Figure 3(m), where the concentration of active CaMKII can rise high even though the total concentration of PP1 is considerably higher in respect to the total concentration of CaMKII (Sim1).

The concentration of PP1 follows similar behavior as the other models (see Figure 3(n)). The only exception is with Sim1, where the concentration of PP1 suddenly drops and does not behave similarly as in Sim6, as with the other models. The concentration of phosphorylated AMPAR does not follow any pattern related to changes in the total concentrations of CaMKII and PP1, or the ratio of them (see Figure 3(o)).

When simulating the model by Hayer and Bhalla [2], we set the total concentrations of CaMKII and PP1 only in the postsynaptic density. However, Hayer and Bhalla [2] also model diffusion of molecules between different compartments, being here between postsynaptic density and other compartments. Thus, the concentrations of active CaMKII and PP1 in the postsynaptic density can reach higher than the used total concentrations in the postsynaptic density.

3.1.4. Comparison of Models. For all the models, the peak concentrations of active CaMKII and PP1 are tabulated together with the concentrations at the end point 2000 s in Table 5. Furthermore, percentages from the maximum peak concentration are given separately for each model. The peak concentrations of active CaMKII vary the most in different models. Especially in Sim1, the percentage of the model by Hayer and Bhalla [2] is the opposite compared to the percentage of the other models. As a surprise, the models by d'Alcantara et al. [16] and Nakano et al. [19] produce similar peak concentrations for active CaMKII even though they are made for neurons in different brain areas, the structures of the models are different, and Nakano et al. [19] do not report using the model by d'Alcantara et al. [16] as their base. The same can be concluded for the models by Lindskog et al. [18] and Kim et al. [17], but this can be explained by Kim et al. [17] using the model by Lindskog et al. [18] as their base. The end point concentrations of active CaMKII with the models by Hayer and Bhalla [2] and Kim et al. [17] are much higher than with the other three models. The peak and end point concentrations of PP1 are quite similar in all the models. The only exception is basically the model by Hayer and Bhalla [2] that produces much lower end point concentrations.

3.2. User Experiences. The model by d'Alcantara et al. [16] is easy to implement in MATLAB, since all the

Table 5: *Concentrations of active CaMKII and PP1 in different simulations.* For all the models, the peak concentrations of active CaMKII and PP1 ($[\text{CaMKII}]_{\text{peak}}$, $[\text{PP1}]_{\text{peak}}$) are tabulated together with the concentrations at the end point 2000 s ($[\text{CaMKII}]_{\text{end}}$, $[\text{PP1}]_{\text{end}}$) in units of μM. Furthermore, percentages from the maximum peak concentration are given separately for each model.

Sim ID	Model	$[\text{CaMKII}]_{\text{peak}}$	$[\text{CaMKII}]_{\text{end}}$	$[\text{PP1}]_{\text{peak}}$	$[\text{PP1}]_{\text{end}}$
Sim1	d'Alcantara et al. [16]	0.4999 (3%)	0.0023	1.6276 (38%)	1.5507
	Kim et al. [17]	0.2912 (4%)[a]	0.2912	1.9634 (40%)	1.9440
	Lindskog et al. [18]	0.3617 (13%)	0.0251	1.7157 (36%)	1.6896
	Nakano et al. [19]	0.6707 (4%)	0.0173	2.5799 (37%)	1.7584
	Hayer and Bhalla [2]	117.9152 (99%)[a]	117.9152	2.0009 (40%)[a]	0.0002
Sim2	d'Alcantara et al. [16]	0.9998 (5%)	0.0030	3.3444 (78%)	3.1915
	Kim et al. [17]	0.5326 (8%)[a]	0.5174	3.9530 (80%)	3.9313
	Lindskog et al. [18]	0.6760 (24%)	0.0370	3.7155 (79%)	3.6893
	Nakano et al. [19]	1.1637 (6%)	0.0154	4.5621 (65%)	3.6606
	Hayer and Bhalla [2]	6.9027 (6%)[a]	6.9027	4.0004 (80%)[a]	0.1017
Sim3	d'Alcantara et al. [16]	1.9996 (10%)	0.0052	3.3480 (78%)	3.1744
	Kim et al. [17]	1.3295 (19%)[a]	1.1511	3.9524 (80%)	3.9295
	Lindskog et al. [18]	1.1739 (41%)	0.0737	3.7155 (79%)	3.6892
	Nakano et al. [19]	2.1318 (12%)	0.0286	4.5622 (65%)	3.6603
	Hayer and Bhalla [2]	6.9032 (6%)[a]	6.9032	4.0000 (80%)[a]	0.1017
Sim4	d'Alcantara et al. [16]	3.9996 (20%)	0.0341	0.8032 (19%)	0.7410
	Kim et al. [17]	2.5904 (37%)[a]	2.5904	0.9749 (20%)	0.9568
	Lindskog et al. [18]	1.7671 (61%)	0.3229	0.7160 (15%)	0.6890
	Nakano et al. [19]	4.0736 (23%)	0.2068	1.5902 (23%)	0.8950
	Hayer and Bhalla [2]	119.3471 (100%)[a]	119.3471	1.0006 (20%)[a]	0.0001
Sim5	d'Alcantara et al. [16]	19.9882 (100%)	0.0320	4.2702 (100%)	3.7504
	Kim et al. [17]	5.9959 (85%)[a]	5.9959	4.9522 (100%)	4.9102
	Lindskog et al. [18]	2.8245 (98%)	0.6318	4.7143 (100%)	4.6870
	Nakano et al. [19]	18.0171 (100%)	0.1727	6.9654 (100%)	6.0135
	Hayer and Bhalla [2]	20.0000 (17%)[a]	2.2876	5.0000 (100%)[a]	1.2884
Sim6	d'Alcantara et al. [16]	19.9933 (100%)	0.0686	1.6728 (39%)	1.3771
	Kim et al. [17]	7.0283 (100%)[a]	7.0283	1.9663 (40%)	1.9331
	Lindskog et al. [18]	2.8756 (100%)	0.8772	1.7143 (36%)	1.6862
	Nakano et al. [19]	18.0415 (100%)	0.5670	2.5900 (37%)	1.7571
	Hayer and Bhalla [2]	115.3967 (97%)[a]	115.3967	2.0000 (40%)[a]	0.0003

[a]The maximum value is given here because the data in Figure 3 does not show a peak.

necessary information is given in the original publication; the model can also be found in BioModels database (http://www.biomodels.net/, [12]) in Systems Biology Markup Language (SBML, http://sbml.org/) format.

The models by Kim et al. [17] and Lindskog et al. [18] can be found in ModelDB (http://senselab.med.yale.edu/modeldb/, [26, 27]) in XPPAUT format (http://www.math.pitt.edu/~bard/xpp/xpp.html, [21]). The codes are properly commented and divided into several subsections. Thus, it is easy to find the value one wants to change to modify the model. However, the use of XPPAUT requires some practise, because the menu is not intuitive for first-time users.

The model by Nakano et al. [19] can be found in Model DB in GENESIS/Kinetikit format (http://www.genesis-sim.org/GENESIS/, http://www.ncbs.res.in/node/350/, [22, 23]). In the database, the authors provide scripts for reproducing the figures in the original publication. As supplementary information of the original publication, they provide tables of initial concentrations and enzymatic and binding reactions. These tables are of great value when getting to know the model because the original model files are not commented and the language used for describing the model is not intuitive. Kinetikit provides a possibility to export an equation file which is also helpful. Unfortunately, the

file lacks the sum equations of molecular species. This is particularly inconvenient with the model by Nakano et al. [19] because many of the active enzymes, including CaMKII and PP1, are sums of many different forms of theirs. This causes the problem with excess CaMKII and PP1 mentioned in Section 3.1.2. Kinetikit can be used either from command line or from graphical user interface which is useful since many times different users prefer different ways of simulation.

The model by Hayer and Bhalla [2] can be found in database of quantitative cellular Signaling (DOQCS) (http://doqcs.ncbs.res.in/, [24]) in several formats from which we have used the MATLAB format. However, the MATLAB implementation of the model is hard to modify, since, for example, rate constants and reaction rates are not given as vectors, and stoichiometric constants are not given as a matrix. Thus, if the user wants to change one parameter value, one is required to change the value everywhere it is used in the code. This is time consuming. Despite this problem, we prefer the MATLAB format over the Kinetikit format because modifications required in this study are easily and reliably done in MATLAB.

4. Discussion and Conclusions

In this study, we provide the first computational comparison of models for synaptic plasticity. Five different models [2, 16–19] describing the phenomena of LTP and LTD were selected for comparison, mainly due to their availability in model databases. The models were evaluated according to the model outcomes and the obtained user experiences to modify and simulate the models in certain simulation tools. We carefully examined the input-output relationship of the models. For this examination, we ran for each model six different simulations that were in advance known to produce physiologically realistic results. Our study revealed that when using exactly the same input, models describing the LTP/LTD phenomenon in the very same neuron type produced different responses. This may partly be explained by the fact that some models had been constructed to ask relatively specific questions using a certain simulation tool. On the other hand, the models by d'Alcantara et al. [16] and Nakano et al. [19] produced similar kind of results even though they had been built for neurons in different brain areas, and Nakano et al. [19] did not report using the model by d'Alcantara et al. [16] as their base. Almost the same can be concluded to the hippocampal CA1 neuron model by Lindskog et al. [18] and the striatal medium spiny neuron model by Kim et al. [17], but this can be explained by Kim et al. [17] using the model by Lindskog et al. [18] as their base.

In our previous study, we sought to classify and analyze the features of all existing LTP and LTD models without performing time-consuming computational simulations [5]. After running the simulations in this study, we discovered that it is extremely difficult to compare the models to each other, since objective methods, such as Bayesian methods, are not applicable. With this study, we try to motivate the research community to make a step forward to find a general setup how to compare models for synaptic plasticity.

We propose that all models should (1) be formulated using common description language, (2) have adequate metadata related to model and experimental data used, (3) explain set of features describing the overall behavior of the modeled system, and (4) be compared to previous models. In other words, all new models should be constructed according to clearly defined general rules. The four points presented above can be called the minimum criteria that the models need to meet as also explained in different BioModels projects (see, e.g., [11, 12]) and by Manninen et al [5]. Similar ideas about combining unified experimental findings that the models should capture are presented by Lisman and Raghavachari [25]. Several model databases are also available to store models and metadata for future use, for example, the BioModels database [12], ModelDB [26, 27], and DOQCS [24]. In addition, an international initiative, NeuroML (http://www.neuroml.org/), to develop language for describing detailed models of neural systems [28] and a model description practice for realistic neuronal network models [29] have been presented. The NeuroML initiative, however, still requires solutions to properly link signal transduction pathways and subcellular phenomena with cellular phenomena. This is a clear problem in the case of LTP/LTD phenomenon which requires several scales to be represented in the model. Regardless of this development, many models are neither constructed nor validated based on previous models because most computational neuroscientists use the so-called rebuild-from-scratch (de novo) methodology in model formation, as described by Cannon et al. [30].

The field of computational neuroscience is moving forward with every hypothesis tested and verified with simulations. Despite the fact that many models are not well documented and reproducible, there exist several well-established models that are frequently used (for short-term plasticity, see, e.g. [31]). Similar models are clearly needed also for long-term plasticity in different brain areas [32]. The purpose of our study is to advance the field and not as such to judge the previous studies. We, here, strongly propose that evaluators of scientific publications should require testing the model in the context of minimum criteria to see that the new model behaves as it should. In the best case, this would enable truly incremental science. In addition, the establishment of compulsory policies from publishers would partly solve the difficulties in data sharing and deposit of data files into public databases and repositories [33, 34] as well as the lack of experimental metadata in neuroscience [35].

Acknowledgments

This study was supported by the Academy of Finland, application nos. 126556 and 129657 (Finnish Programme for Centres of Excellence in Research 2006–2011), as well as Emil Aaltonen Foundation, Finnish Concordia Fund, Finnish Foundation for Economic and Technology Sciences—KAUTE, Finnish Foundation for Technology Promotion, Otto A. Malm Foundation, Ulla Tuominen Foundation,

Tampere University of Technology Graduate School, and Tampere Doctoral Programme in Information Science and Engineering. Furthermore, the authors want to thank Dr. Juha Kesseli for fruitful discussions. T. Manninen, K. Hituri, and E. Toivari equally contributed to this work.

References

[1] A. Citri and R. C. Malenka, "Synaptic plasticity: multiple forms, functions, and mechanisms," *Neuropsychopharmacology*, vol. 33, no. 1, pp. 18–41, 2008.

[2] A. Hayer and U. S. Bhalla, "Molecular switches at the synapse emerge from receptor and kinase traffic," *PLoS Computational Biology*, vol. 1, no. 2, article e20, pp. 0137–0154, 2005.

[3] J. D. Sweatt, "Toward a molecular explanation for long-term potentiation," *Learning and Memory*, vol. 6, no. 5, pp. 399–416, 1999.

[4] D. G. Winder and J. D. Sweatt, "Roles of serine/threonine phosphatases in hippocampal synaptic plasticity," *Nature Reviews Neuroscience*, vol. 2, no. 7, pp. 461–474, 2001.

[5] T. Manninen, K. Hituri, J. Hellgren Kotaleski, K. T. Blackwell, and M.-L. Linne, "Postsynaptic signal transduction models for long-term potentiation and depression," *Frontiers in Computational Neuroscience*, vol. 4, Article ID 152, 2010.

[6] J. Hellgren Kotaleski and K. T. Blackwell, "Modelling the molecular mechanisms of synaptic plasticity using systems biology approaches," *Nature Reviews Neuroscience*, vol. 11, no. 4, pp. 239–251, 2010.

[7] B. Delord, H. Berry, E. Guigon, and S. Genet, "A new principle for information storage in an enzymatic pathway model," *PLoS Computational Biology*, vol. 3, no. 6, article e124, pp. 1123–1135, 2007.

[8] D. J. Wilkinson, "Bayesian methods in bioinformatics and computational systems biology," *Briefings in Bioinformatics*, vol. 8, no. 2, pp. 109–116, 2007.

[9] M. Girolami, "Bayesian inference for differential equations," *Theoretical Computer Science*, vol. 408, no. 1, pp. 4–16, 2008.

[10] W. D. Penny, K. E. Stephan, J. Daunizeau et al., "Comparing families of dynamic causal models," *PLoS Computational Biology*, vol. 6, no. 3, Article ID e1000709, 2010.

[11] N. Le Novère, A. Finney, M. Hucka et al., "Minimum information requested in the annotation of biochemical models (MIRIAM)," *Nature Biotechnology*, vol. 23, no. 12, pp. 1509–1515, 2005.

[12] N. Le Novère, B. Bornstein, A. Broicher et al., "BioModels Database: a free, centralized database of curated, published, quantitative kinetic models of biochemical and cellular systems," *Nucleic Acids Research*, vol. 34, pp. D689–D691, 2006.

[13] M. Sheng and S. H. Lee, "AMPA receptor trafficking and the control of synaptic transmission," *Cell*, vol. 105, no. 7, pp. 825–828, 2001.

[14] J. Boehm and R. Malinow, "AMPA receptor phosphorylation during synaptic plasticity," *Biochemical Society Transactions*, vol. 33, no. 6, pp. 1354–1356, 2005.

[15] H. W. Kessels and R. Malinow, "Synaptic AMPA receptor plasticity and behavior," *Neuron*, vol. 61, no. 3, pp. 340–350, 2009.

[16] P. d'Alcantara, S. N. Schiffmann, and S. Swillens, "Bidirectional synaptic plasticity as a consequence of interdependent Ca^{2+}-controlled phosphorylation and dephosphorylation pathways," *European Journal of Neuroscience*, vol. 17, no. 12, pp. 2521–2528, 2003.

[17] M. Kim, T. Huang, T. Abel, and K. T. Blackwell, "Temporal sensitivity of protein kinase A activation in late-phase long term potentiation," *PLoS Computational Biology*, vol. 6, no. 2, Article ID e1000691, 2010.

[18] M. Lindskog, M. Kim, M. A. Wikström, K. T. Blackwell, and J. Hellgren Kotaleski, "Transient calcium and dopamine increase PKA activity and DARPP-32 phosphorylation," *PLoS Computational Biology*, vol. 2, no. 9, article e119, pp. 1045–1060, 2006.

[19] T. Nakano, T. Doi, J. Yoshimoto, and K. Doya, "A kinetic model of dopamine- and calcium-dependent striatal synaptic plasticity," *PLoS Computational Biology*, vol. 6, no. 2, Article ID e1000670, 2010.

[20] P. Mullasseril, A. Dosemeci, J. E. Lisman, and L. C. Griffith, "A structural mechanism for maintaining the 'on-state' of the CaMKII memory switch in the post-synaptic density," *Journal of Neurochemistry*, vol. 103, no. 1, pp. 357–364, 2007.

[21] B. Ermentrout, *Simulating, Analyzing, and Animating Dynamical Systems: A Guide to XPPAUT for Researchers and Students*, SIAM, Philadelphia, PA, USA, 1st edition, 2002.

[22] U. S. Bhalla, "Use of Kinetikit and GENESIS for modeling signaling pathways," in *Methods in Enzymology*, J. D. Hildebrandt and R. Iyengar, Eds., vol. 345, pp. 3–23, Academic Press, San Diego, CA, USA, 2002.

[23] J. M. Bower and D. Beeman, *The Book of GENESIS: Exploring Realistic Neural Models with the GEneral NEural SImulation System*, Springer, New York, NY, USA, 2nd edition, 1998.

[24] S. Sivakumaran, S. Hariharaputran, J. Mishra, and U. S. Bhalla, "The database of quantitative cellular signaling: management and analysis of chemical kinetic models of signaling networks," *Bioinformatics*, vol. 19, no. 3, pp. 408–415, 2003.

[25] J. Lisman and S. Raghavachari, "A unified model of the presynaptic and postsynaptic changes during LTP at CA1 synapses," *Science's STKE*, vol. 2006, no. 356, p. re11, 2006.

[26] M. Migliore, T. M. Morse, A. P. Davison, L. Marenco, G. M. Shepherd, and M. L. Hines, "ModelDB: making models publicly accessible to support computational neuroscience," *Neuroinformatics*, vol. 1, no. 1, pp. 135–139, 2003.

[27] M. L. Hines, T. Morse, M. Migliore, N. T. Carnevale, and G. M. Shepherd, "ModelDB: a database to support computational neuroscience," *Journal of Computational Neuroscience*, vol. 17, no. 1, pp. 7–11, 2004.

[28] P. Gleeson, S. Crook, R. C. Cannon et al., "NeuroML: a language for describing data driven models of neurons and networks with a high degree of biological detail," *PLoS Computational Biology*, vol. 6, no. 6, Article ID e1000815, 2010.

[29] E. Nordlie, M. O. Gewaltig, and H. E. Plesser, "Towards reproducible descriptions of neuronal network models," *PLoS Computational Biology*, vol. 5, no. 8, Article ID e1000456, 2009.

[30] R. C. Cannon, M.-O. Gewaltig, P. Gleeson et al., "Interoperability of neuroscience modeling software: current status and future directions," *Neuroinformatics*, vol. 5, no. 2, pp. 127–138, 2007.

[31] M. Tsodyks, K. Pawelzik, and H. Markram, "Neural networks with dynamic synapses," *Neural Computation*, vol. 10, no. 4, pp. 821–835, 1998.

[32] M. Graupner and N. Brunel, "Mechanisms of induction and maintenance of spike-timing dependent plasticity in biophysical synapse models," *Frontiers in Computational Neuroscience*, vol. 4, Article ID 136, 2010.

[33] G. A. Ascoli, "The ups and downs of neuroscience shares," *Neuroinformatics*, vol. 4, no. 3, pp. 213–215, 2006.

[34] J. L. Teeters, K. D. Harris, K. J. Millman, B. A. Olshausen, and F. T. Sommer, "Data sharing for computational neuroscience," *Neuroinformatics*, vol. 6, no. 1, pp. 47–55, 2008.

[35] E. De Schutter, "Why are computational neuroscience and systems biology so separate?" *PLoS Computational Biology*, vol. 4, no. 5, Article ID e1000078, 2008.

Publication III

Manninen T., Hituri K., Hellgren Kotaleski J., Blackwell K.T., Linne M.-L. (2010) Postsynaptic signal transduction models for long-term potentiation and depression. Frontiers in Computational Neuroscience, 4:152.

frontiers in
COMPUTATIONAL NEUROSCIENCE

REVIEW ARTICLE
published: 13 December 2010
doi: 10.3389/fncom.2010.00152

Postsynaptic signal transduction models for long-term potentiation and depression

Tiina Manninen[1], Katri Hituri[1], Jeanette Hellgren Kotaleski[2,3], Kim T. Blackwell[4] and Marja-Leena Linne[1]*

[1] Department of Signal Processing, Tampere University of Technology, Tampere, Finland
[2] School of Computer Science and Communication, Royal Institute of Technology, Stockholm, Sweden
[3] Stockholm Brain Institute, Karolinska Institutet, Stockholm, Sweden
[4] Krasnow Institute for Advanced Study, George Mason University, Fairfax, VA, USA

Edited by:
Nicolas Brunel, Centre National de la Recherche Scientifique, France

Reviewed by:
Harel Z. Shouval, University of Texas Medical School at Houston, USA
Paul Miller, Brandeis University, USA

****Correspondence:***
Tiina Manninen, Computational Neuroscience Laboratory, Department of Signal Processing, Tampere University of Technology, P.O. Box 553, FI-33101 Tampere, Finland.
e-mail: tiina.manninen@tut.fi

More than a hundred biochemical species, activated by neurotransmitters binding to transmembrane receptors, are important in long-term potentiation (LTP) and long-term depression (LTD). To investigate which species and interactions are critical for synaptic plasticity, many computational postsynaptic signal transduction models have been developed. The models range from simple models with a single reversible reaction to detailed models with several hundred kinetic reactions. In this study, more than a hundred models are reviewed, and their features are compared and contrasted so that similarities and differences are more readily apparent. The models are classified according to the type of synaptic plasticity that is modeled (LTP or LTD) and whether they include diffusion or electrophysiological phenomena. Other characteristics that discriminate the models include the phase of synaptic plasticity modeled (induction, expression, or maintenance) and the simulation method used (deterministic or stochastic). We find that models are becoming increasingly sophisticated, by including stochastic properties, integrating with electrophysiological properties of entire neurons, or incorporating diffusion of signaling molecules. Simpler models continue to be developed because they are computationally efficient and allow theoretical analysis. The more complex models permit investigation of mechanisms underlying specific properties and experimental verification of model predictions. Nonetheless, it is difficult to fully comprehend the evolution of these models because (1) several models are not described in detail in the publications, (2) only a few models are provided in existing model databases, and (3) comparison to previous models is lacking. We conclude that the value of these models for understanding molecular mechanisms of synaptic plasticity is increasing and will be enhanced further with more complete descriptions and sharing of the published models.

Keywords: computational model, kinetic model, long-term depression, long-term potentiation, plasticity, postsynaptic signal transduction model

Abbreviations: 4E-BP, 4E-binding protein; AC, adenylyl cyclase; AKT, serine/threonine kinase; AMPAR, α-amino-3-hydroxy-5-methylisoxazole-4-propionic acid receptor; ATP, adenosine triphosphate; BDNF, brain-derived neurotrophic factor; BK_{Ca}, high-threshold Ca^{2+}- and voltage-gated K^+ channel; CA1, cornu ammonis 1; Ca^{2+}, calcium ion; CA3, cornu ammonis 3; Ca_L, high-threshold L-type Ca^{2+} channel; CaM, calmodulin; $CaMCa_1$, $CaM–1Ca^{2+}$ complex; $CaMCa_2$, $CaM–2Ca^{2+}$ complex; $CaMCa_3$, $CaM–3Ca^{2+}$ complex; $CaMCa_4$, $CaM–4Ca^{2+}$ complex; CaMK, Ca^{2+}/CaM-dependent protein kinase; CaMKII, CaMK type II; CaMKIII, CaMK type III; CaMKIV, CaMK type IV; cAMP, cyclic adenosine monophosphate; Ca_N, high-threshold N-type Ca^{2+} channel; CaN, calcineurin; Ca_Q, high-threshold P-type Ca^{2+} channel; Ca_T, low-threshold T-type Ca^{2+} channel; CD28k, calbindin; CG-1, Calcium-Green 1; cGMP, cyclic guanosine monophosphate; CICR, Ca^{2+}-induced Ca^{2+} release; CPEB1, cytoplasmic polyadenylation element binding protein; CRHR, corticotropin-releasing hormone receptor; ΔI_m, change in membrane current; ΔV_m, change in V_m; D, dimensional; D_1R, dopamine receptor; DA, dopamine; DARPP, cAMP-regulated phosphoprotein; DARPP32, DARPP of 32 kDa; DGC, dentate granule cell; DOQCS, Database of Quantitative Cellular Signaling; EGF, epidermal growth factor; EGFR, EGF receptor; E-LTD, early phase LTD; E-LTP, early phase LTP; ER, endoplasmic reticulum; ERK, extracellular signal-regulated kinase; ERKII, ERK type II; FF, Fura-FF; G, G protein; GABA, gamma-aminobutyric acid; $GABA_AR$, GABA receptor A; $GABA_BR$, GABA receptor B; GABAR, GABA receptor; g_{AMPAR}, AMPAR conductance; GC, guanylate cyclase; $g_{K_{Ca}}$, K_{Ca} channel conductance; Glu, glutamate; GluN, glutamatergic neuron; Gq, G protein type q; GrC, granule cell; Gs, G protein type s; g_{syn}, synaptic conductance; I1, inhibitor 1; I_{Ca}, Ca^{2+} current; IF, integrate-and-fire; I_{NMDAR}, Ca^{2+} current via NMDAR; IP_3, inositol trisphosphate; IP_3R, IP_3 receptor; I_{syn}, synaptic current; J_{Ca}, Ca^{2+} influx; J_{NMDAR}, Ca^{2+} influx via NMDAR; J_{VGCC}, Ca^{2+} influx via VGCC; K^+, potassium ion; $K2_{Ca}$, low-threshold K2-type Ca^{2+}-gated K^+ channel; K_A, transient A-type K^+ channel; K_{AHP}, after-hyperpolarization K^+ channel; K_{Ca}, Ca^{2+}- and voltage-gated K^+ channel; K_{DR}, delayed-rectifier K^+ channel; k_{fRaf}, activation rate for Raf; K_{GABA_AR}, $GABA_AR$-activated K^+ channel; K_{GABA_BR}, $GABA_BR$-activated K^+ channel; K_{IR}, inward-rectifier K^+ channel; K_M, muscarine-sensitive K^+ channel; K_{slow}, slow Ca^{2+}-independent tetraethylammonium-insensitive K^+ channel; L, large; LGIC, ligand-gated ion channel; LIF, leaky IF; L-LTD, late phase LTD; L-LTP, late phase LTP; LTD, long-term depression; LTP, long-term potentiation; Lyn, Lyn tyrosine kinase; M, medium; MAP2, microtubule-associated protein 2; MAPK, mitogen-activated protein kinase; MEK, MAPK kinase; MgGreen, Magnesium Green 1; mGluR, metabotropic glutamate receptor; MKKP, MEK phosphatase; MKP, MAPK phosphatase; MSN, medium spiny neuron; mTOR, mammalian target of rapamycin; N, neuron; Na^+, sodium ion; Na_{fast}, fast Na^+ channel; Na_p, recurrent Na^+ channel; Na_{slow}, non- or slowly inactivating Na^+ channel; Ng, neurogranin; NMDA, *N*-methyl-D-aspartate; NMDAR, NMDA receptor; NO, nitric oxide; OGB-1, Oregon Green BAPTA-1; PC, Purkinje cell; PDE, phosphodiesterase; PDE1, PDE type 1; PDE4, PDE type 4; PIP2, phosphatidylinositol biphosphate; PKA, cAMP-dependent protein kinase; PKC, protein kinase C; PKG, protein kinase G; PKM, atypical PKC isozyme; PKMζ, atypical PKC isozyme; PLA_2, phospholipase A_2; PLC, phospholipase C; PMCA, plasma membrane Ca^{2+}-ATPase; PN, pyramidal neuron; PP1, protein phosphatase 1; PP2A, protein phosphatase 2A; PSD, postsynaptic density; PV, parvalbumin; Raf, MEK kinase; S, small; S6K, 40S ribosomal protein S6 kinase; SBML, Systems Biology Markup Language; Ser, serine; SERCA, sarco/ER Ca^{2+}-ATPase; SoS, son of sevenless; STD, short-term depression; STDP, spike-timing-dependent plasticity; STP, short-term potentiation; Thr, threonine; TrkB, tropomyosin-receptor kinase B; VGCC, voltage-gated Ca^{2+} channel; VGIC, voltage-gated ion channel; V_m, membrane voltage.

1. INTRODUCTION

Synaptic plasticity is an activity-dependent change in the strength or efficacy of the synaptic connection between a pre- and postsynaptic neuron. It is induced with brief periods of synaptic activity, for example, using tetanic, high-frequency neuronal activity. Changes in synapses, in general, can last from milliseconds into years. These long-lasting changes, which require protein synthesis and gene transcription, are suggested to lead to learning and formation of memories.

The long-term activity-dependent strengthening and weakening of synapses are known as long-term potentiation (LTP; Bliss and Gardner-Medwin, 1973; Bliss and Lømo, 1973) and long-term depression (LTD; Ito et al., 1982; Ito, 1989; Dudek and Bear, 1992), respectively. Frequency-dependent LTP and LTD in the cornu ammonis 1 (CA1) region of the hippocampus, triggered by activation of *N*-methyl-D-aspartate (NMDA) receptors (NMDARs), are the most studied forms of long-term plasticity (see, e.g., Malenka and Bear, 2004; Citri and Malenka, 2008). In addition to hippocampal NMDAR-dependent LTP and LTD, diverse forms of LTP and LTD have been discovered in different brain regions. One example of non-NMDAR-dependent plasticity is cerebellar LTD. Some forms of LTP require neither the NMDA nor the non-NMDA ionotropic glutamate receptors (non-NMDARs include kainate receptors and α-amino-3-hydroxy-5-methylisoxazole-4-propionic acid receptors, AMPARs), but do require activation of metabotropic glutamate receptors (mGluRs). This form is found, for example, in the CA1 region of the hippocampus (Lanté et al., 2006). Despite the variation in NMDAR dependence, all forms of synaptic plasticity are calcium ion (Ca^{2+})-dependent; only the mechanisms for Ca^{2+} elevation vary.

Two broad types of computational models, phenomenological and biophysical models, have been developed to understand the pre- and postsynaptic events in LTP and LTD. Phenomenological models use abstract equations to describe a relationship between neuronal activity and synaptic plasticity. Biophysical models include electrophysiological models, biochemical models, and models that include both electrophysiological properties and biochemical reactions (signaling pathways) underlying the relationship between neuronal activity and synaptic plasticity, though even these include simplifications because all the mechanisms cannot be modeled in detail. The focus of the present study is on biophysical models which concentrate on postsynaptic biochemical reactions.

This review presents an overview of 117 postsynaptic signal transduction models, categorizes them so that similarities and differences are more readily apparent, and explains how these models can be used to identify key molecules and address questions related to mechanisms underlying LTP and LTD. Section 2 presents the biological background of synaptic plasticity, Section 3 classifies the computational postsynaptic signal transduction models, and Section 4 summarizes the directions and trends of this field.

2. SYNAPTIC PLASTICITY

Many different classification schemes for synaptic plasticity exist. Synaptic potentiation can be classified into three main types: short-term potentiation (STP), which lasts as long as 30–45 min; early phase LTP (E-LTP), which lasts for 1–2 h; and late phase LTP (L-LTP), which persists for considerably more than 2 h (Sweatt, 1999; Soderling and Derkach, 2000; Citri and Malenka, 2008). Synaptic depression, on the other hand, is typically classified into two types: short-term depression (STD) and LTD (Ito, 2001); though there appears to be an early and late phase LTD (E-LTD, L-LTD) also (Kauderer and Kandel, 2000). In addition, all types of plasticity involve three processes: induction, in which the mechanisms leading to plasticity are engaged; expression, which involves mechanisms allowing the plasticity to be exhibited and measured; and maintenance, which involves processes occurring after the induction phase is complete and allowing the plasticity to persist for long periods of time (Sweatt, 1999).

2.1. MECHANISMS TO TRIGGER SYNAPTIC PLASTICITY

Many different plasticity induction protocols have been developed. In general, potentiation is induced by a high-frequency stimulation and depression by a low-frequency stimulation of a chemical synapse, but there are variations in the experimental procedures depending on the cell type. Short-term plasticity is triggered typically by short trains of stimulation (Citri and Malenka, 2008). LTP is typically triggered with longer 1 s trains of high-frequency (100 Hz) stimulation (Citri and Malenka, 2008). One train triggers only E-LTP, whereas repetitive trains trigger L-LTP (Citri and Malenka, 2008). L-LTD is typically triggered with prolonged repetitive low-frequency (1 Hz) stimulation (Citri and Malenka, 2008). Theta stimulation consists of short bursts of trains repeated with 200 ms intervals and produces L-LTP, even though the number of pulses is more similar to that producing E-LTP. Spike-timing-dependent plasticity (STDP) is another protocol to trigger LTP as well as LTD. In STDP, pre- and postsynaptic neurons are stimulated independently and the timing between pre- and postsynaptic spikes determines whether potentiation or depression occurs (Markram et al., 1997; Bi and Poo, 1998; Bi and Rubin, 2005; Dan and Poo, 2006).

2.2. MOLECULAR MECHANISMS OF SYNAPTIC PLASTICITY

There are various mechanisms, both pre- and postsynaptic, that lead to changes in synaptic strength, for example changes in neurotransmitter release, conductance of receptors, numbers of receptors, numbers of active synapses, and structure of synapses (Hayer and Bhalla, 2005). Several reviews about the molecular mechanisms underlying synaptic plasticity have been published (see, e.g., Bliss and Collingridge, 1993; Malenka and Nicoll, 1999; Sweatt, 1999; Soderling and Derkach, 2000; Ito, 2002; Lisman et al., 2002; Malenka and Bear, 2004; Blitzer et al., 2005; Cooke and Bliss, 2006; Wang et al., 2006; Bruel-Jungerman et al., 2007; Citri and Malenka, 2008; Santos et al., 2009). Cytosolic Ca^{2+} is inarguably the most critical factor: chemical buffering of Ca^{2+} or pharmacological blocking of Ca^{2+} influx prevents both potentiation and depression. There are several sources of Ca^{2+}, depending on the brain region and the cell type. Influx through NMDARs is the most common source for LTP; influx through Ca^{2+}-permeable AMPARs, voltage-gated Ca^{2+} channels, or release from intracellular stores (triggered by mGluRs which are G protein-coupled receptors) are important in many cell types. Ca^{2+} can activate, both directly and indirectly, protein kinases and phosphatases leading to phosphorylation–dephosphorylation cycles and, ultimately, to LTP and LTD. The next paragraphs focus on the molecular mechanisms

behind NMDAR-dependent LTP and LTD, as well as cerebellar LTD, because these forms of plasticity have been studied the most both experimentally and computationally.

NMDAR-dependent potentiation is triggered by release of the neurotransmitter glutamate from the presynaptic neuron and subsequent binding to NMDARs on the postsynaptic neuron (Bliss and Collingridge, 1993; Malenka and Nicoll, 1999; Sweatt, 1999; Malenka and Bear, 2004; Citri and Malenka, 2008). After NMDARs are activated, Ca^{2+} can flow into the cell if the postsynaptic membrane is sufficiently depolarized to relieve the magnesium ion block from NMDAR. NMDAR-dependent LTP requires a large increase in postsynaptic Ca^{2+} concentration which triggers several events inside the cell. One of the most important events is Ca^{2+} binding to calmodulin, which then activates Ca^{2+}/calmodulin-dependent protein kinase II (CaMKII), leading to phosphorylation of AMPARs, increase in single-channel conductance of AMPARs, and incorporation of additional AMPARs into the postsynaptic density (Citri and Malenka, 2008). Ca^{2+} also binds to protein kinase C (PKC) which is involved in E-LTP in some cell types (Malinow et al., 1989; Klann et al., 1993). In the hippocampus, the calmodulin-$4Ca^{2+}$ complex ($CaMCa_4$) further activates adenylyl cyclase, leading to activation of cyclic adenosine monophosphate (cAMP)-dependent protein kinase (PKA) which is required for some forms of L-LTP (Woo et al., 2003).

Transcription and also somatic and dendritic protein synthesis are required for induction of L-LTP (Bradshaw et al., 2003b), but it is unclear whether protein synthesis is required for induction of E-LTP. These nuclear and somatic events involve Ca^{2+}/calmodulin-dependent protein kinase IV (CaMKIV), mitogen-activated protein kinase (MAPK, ERK), and PKA. For maintenance of L-LTP, the atypical PKC isozyme (PKMζ), which is an autonomously active form of PKC, is required in addition to local dendritic protein synthesis (Serrano et al., 2005).

NMDAR-dependent LTD needs only a modest increase in Ca^{2+} concentration (instead of the large Ca^{2+} increase for LTP). This modest increase in Ca^{2+} concentration leads to preferential activation of protein phosphatase 2B also known as calcineurin, because it has a much higher affinity for $CaMCa_4$ than CaMKII has. Activation of protein phosphatases leads to dephosphorylation and endocytosis of AMPARs located on the plasma membrane (Citri and Malenka, 2008), and thereby the expression of LTD. Protein translation may be needed for expression and maintenance of L-LTD (Citri and Malenka, 2008), but otherwise mechanisms behind maintenance of NMDAR-dependent LTD have not been studied extensively. Some forms of LTD also require Ca^{2+}-dependent production of endocannabinoids which travel retrogradely to produce changes in presynaptic release of neurotransmitters (Gerdeman and Lovinger, 2003).

Cerebellar LTD, the best studied form of non-NMDAR-dependent LTD, is observed at the parallel fiber to Purkinje cell synapse. Purkinje cells form synapses with several thousand parallel fibers and also receive many synaptic contacts from a single climbing fiber (Ito, 2002; Citri and Malenka, 2008). Cerebellar LTD is induced when parallel fibers and a climbing fiber are activated simultaneously. Glutamate released by parallel fibers activates mGluRs which in turn activate phospholipase C (Ito, 2002). Phospholipase C catalyzes the reaction producing diacylglycerol and inositol trisphosphate (IP_3). Diacylglycerol activates PKC, and IP_3 causes the release of Ca^{2+} from endoplasmic reticulum through IP_3 receptors (IP_3Rs). Phospholipase A_2, which is activated by an elevation in Ca^{2+} concentration, produces arachidonic acid which more persistently activates PKC that is transiently activated by diacylglycerol. PKC phosphorylates AMPARs and this leads to endocytosis of AMPARs from the plasma membrane. As in hippocampal LTP, protein synthesis is needed for L-LTD (Ito, 2001).

Given that Ca^{2+} activates multiple processes and enzymes, such as endocannabinoid production, calcineurin, and CaMKII, it is still not clear why some stimulation protocols produce depression and some produce potentiation. Non-linear interactions between multiple pathways make a quantitative understanding difficult solely from experiments. Computer modeling synthesizes information from myriad studies ranging from plasma membrane level phenomena to intracellular phenomena. Simulations therefore provide deeper insight into mechanisms underlying plasticity and this is why modeling studies have become more and more popular during the last 10 years.

3. COMPUTATIONAL MODELS

Many computational models have been developed to understand pre- and postsynaptic events in LTP and LTD. Several focused reviews that include models of a specific neural system or type of plasticity have appeared during the last 20 years (Brown et al., 1990; Neher, 1998; Hudmon and Schulman, 2002a,b; Bi and Rubin, 2005; Holmes, 2005; Wörgötter and Porr, 2005; Ajay and Bhalla, 2006; Klipp and Liebermeister, 2006; Zou and Destexhe, 2007; Morrison et al., 2008; Ogasawara et al., 2008; Bhalla, 2009; Ogasawara and Kawato, 2009; Tanaka and Augustine, 2009; Urakubo et al., 2009; Castellani and Zironi, 2010; Gerkin et al., 2010; Graupner and Brunel, 2010; Hellgren Kotaleski and Blackwell, 2010; Shouval et al., 2010); however, a comprehensive review on postsynaptic signal transduction models for LTP and LTD is lacking.

In this study, an analysis of altogether 117 postsynaptic signal transduction models published through the year 2009 is presented (see **Table 1**). We limit the present analysis to models of postsynaptic signal transduction pathways that are defined using several characteristics. First, the output of the model needs to be a postsynaptic aspect of the neuron. Second, some part of intracellular signaling is explicitly modeled. Thus, models in this review are required to include at least mechanisms for postsynaptic Ca^{2+} dynamics, Ca^{2+} buffers, phosphorylation–dephosphorylation cycles, LTP and LTD related enzymes, retrograde signals, or synaptic strength that depends on Ca^{2+} concentration. Alternatively, models that explicitly include the kinases and phosphatases underlying changes in AMPAR phosphorylation or synthesis of plasticity-related proteins are included. Models which have intracellular signaling pathways in neurons but do not address plasticity are excluded. Models of AMPAR and NMDAR activation alone, or models including only anchoring and scaffolding proteins as intracellular molecules are excluded. Lastly, purely phenomenological models of plasticity are excluded. These strict criteria are needed because of the large number of models. In addition, a few models published during 2010 are excluded (see, e.g., Clopath et al., 2010; Kim et al., 2010; Kubota and Kitajima, 2010; Nakano et al., 2010; Pepke et al., 2010; Qi et al., 2010; Rackham et al., 2010; Santamaria et al., 2010; Tolle and Le Novère, 2010a).

Table 1 | List of postsynaptic signal transduction models published each year.

Year	Models	No.
1985	Lisman (1985)	1
1987	Gamble and Koch (1987)	1
1988	Lisman and Goldring (1988a,b)	2
1989	Lisman (1989)	1
1990	Holmes (1990), Holmes and Levy (1990), Kitajima and Hara (1990), Zador et al. (1990)	4
1993	De Schutter and Bower (1993), Migliore and Ayala (1993)	2
1994	Gold and Bear (1994), Kötter (1994), Michelson and Schulman (1994)	3
1995	Matsushita et al. (1995), Migliore et al. (1995), Schiegg et al. (1995)	3
1996	Dosemeci and Albers (1996), Fiala et al. (1996)	2
1997	Coomber (1997), Holmes and Levy (1997), Kitajima and Hara (1997), Migliore et al. (1997)	4
1998	Coomber (1998a,b), Markram et al. (1998), Murzina and Silkis (1998)	4
1999	Bhalla and Iyengar (1999), Kötter and Schirok (1999), Kubota and Bower (1999), Migliore and Lansky (1999a,b), Volfovsky et al. (1999)	6
2000	Holmes (2000), Kitajima and Hara (2000), Li and Holmes (2000), Okamoto and Ichikawa (2000a,b), Zhabotinsky (2000)	6
2001	Castellani et al. (2001), Franks et al. (2001), Kubota and Bower (2001), Kuroda et al. (2001), Yang et al. (2001)	5
2002	Abarbanel et al. (2002), Bhalla (2002a,b), Hellgren Kotaleski and Blackwell (2002), Hellgren Kotaleski et al. (2002), Holthoff et al. (2002), Karmarkar and Buonomano (2002), Karmarkar et al. (2002), Saftenku (2002), Shouval et al. (2002a,b)	11
2003	Abarbanel et al. (2003), Bradshaw et al. (2003a), d'Alcantara et al. (2003), Dupont et al. (2003), Kikuchi et al. (2003)	5
2004	Ajay and Bhalla (2004), Holcman et al. (2004), Ichikawa (2004), Murzina (2004), Steuber and Willshaw (2004), Yeung et al. (2004)	6
2005	Abarbanel et al. (2005), Castellani et al. (2005), Doi et al. (2005), Hayer and Bhalla (2005), Hernjak et al. (2005), Miller et al. (2005), Naoki et al. (2005), Rubin et al. (2005), Saudargiene et al. (2005), Shouval and Kalantzis (2005)	10
2006	Badoual et al. (2006), Lindskog et al. (2006), Miller and Wang (2006), Shah et al. (2006), Smolen et al. (2006), Zhabotinsky et al. (2006)	6
2007	Ajay and Bhalla (2007), Cai et al. (2007), Cornelisse et al. (2007), Delord et al. (2007), Gerkin et al. (2007), Graupner and Brunel (2007), Ichikawa et al. (2007), Kubota et al. (2007), Ogasawara et al. (2007), Schmidt et al. (2007), Smolen (2007), Tanaka et al. (2007)	12
2008	Achard and De Schutter (2008), Brown et al. (2008), Canepari and Vogt (2008), Clopath et al. (2008), Helias et al. (2008), Keller et al. (2008), Kubota and Kitajima (2008), Kubota et al. (2008), Pi and Lisman (2008), Santucci and Raghavachari (2008), Smolen et al. (2008), Stefan et al. (2008), Urakubo et al. (2008), Yu et al. (2008)	14
2009	Aslam et al. (2009), Byrne et al. (2009), Castellani et al. (2009), Jain and Bhalla (2009), Kalantzis and Shouval (2009), Kitagawa et al. (2009), Ogasawara and Kawato (2009), Schmidt and Eilers (2009), Smolen et al. (2009)	9
All		117

Altogether 117 models have been published between the years 1985 and 2009. For chosen criteria, see the beginning of Section 3.

3.1. MAIN CHARACTERISTICS OF MODELS

The lists of LTP models (**Table 2**), LTD models (**Table 3**), and dual LTP and LTD models (**Table 4**) order the models alphabetically by the first author and by the publication month and year. Dual LTP and LTD models are able to simulate both forms of plasticity. Characteristics listed under the methods include the computational techniques: either deterministic ordinary and partial differential equations (Det.) or stochastic techniques (Stoch.) which include, for example, reaction algorithms such as the Gillespie stochastic simulation algorithm (Gillespie, 1976, 1977) and diffusion algorithms such as Brownian dynamics. A few studies also use so-called hybrid methods where different techniques are combined. The models are further classified according to the biochemical phenomena that are modeled: some models only describe reactions between chemical species (Reac.) and some also take into account the diffusion of at least some chemical species (Diff.). In addition to biochemical models, there are models which not only describe intracellular events associated with synaptic plasticity, but also take into account the associated plasma membrane and ion channel level phenomena by modeling the membrane voltage; these models are referred to as electrophysiological (Elect.). **Tables 2–4** indicate the simulation tool or programing language used when known, but this piece of information is not always given in the publications. Other characteristics included in **Tables 2–4** are the cell type of the model, which process of synaptic plasticity is modeled [induction (Ind.), expression (Expr.), or maintenance (Maint.)] according to the publications, time required for the dynamics of the model to reach a steady state, the model outputs used to demonstrate the change in synaptic strength, and the size of the model [less than 20 different chemical species or other model variables is defined as small (S), between 20 and 50 is medium (M), and more than 50 is large (L)]. If several different types of models are used in one publication, the size of the largest model is given. The time required for the dynamics of the model to reach a steady state is suggestive and it is not possible to compare all the models according to the time because different models use, for example, different inputs.

Table 2 | List of LTP models.

Model	Methods	Cell type	Phases	Time	Outputs	Size
Ajay and Bhalla (2004)	Det. Reac./GENESIS/Kinetikit[a]	Hippocampal CA1 N	Ind./Maint. LTP	60–80 min	ERKII	L
Ajay and Bhalla (2007)	Det. Reac. Diff. Elect./GENESIS/Kinetikit[a]	Hippocampal CA1 PN	Ind./Maint. LTP	1–4 h	ERKII	L
Aslam et al. (2009)	Det. Reac./MATLAB®	Generic	Ind./Maint. LLTP	100 min to 40 d	CaMKII	S
Bhalla and Iyengar (1999)	Det. Reac. Elect./GENESIS/Kinetikit[a]	Hippocampal CA1 N	Ind. E-LTP	30 min	CaMKII	L
Bhalla (2002a)	Det. Reac. Diff. Elect./GENESIS/Kinetikit[a]	Hippocampal CA1 N	Ind. E-LTP	50 min	CaMKII	L
Bhalla (2002b)	Det. Reac./GENESIS/Kinetikit[a]	Hippocampal CA1 N	Ind. E-LTP	15–60 min	CaMKII	L
Bradshaw et al. (2003a)	Det. Reac.	Hippocampal CA1 N	Ind. LTP		CaMKII	M
Canepari and Vogt (2008)	Det. Reac.	Cerebellar PC	Ind. LTP	0.01–0.25 s	Ca^{2+}	S
Cornelisse et al. (2007)	Det. Reac. Diff./CalC[b]	Visual cortical layer V PN	Ind. LTP	0.06–0.1 s	$CaMCa_1$	S
De Schutter and Bower (1993)	Det. Reac. Diff. Elect./GENESIS[c]	Hippocampal N	Ind. LTP	0.2 s	Ca^{2+}	L
Dupont et al. (2003)	Det. Reac.	Generic	LTP	10–100 s	CaMKII	S
Franks et al. (2001)	Det. Stoch. Reac. Diff. Elect./MCell[d], NEURON[e]	Neocortical PN	Ind. LTP	0.2–2 s	$CaMCa_4$	L
Gamble and Koch (1987)	Det. Reac. Diff. Elect.	Hippocampal PN	Ind. LTP	0.3 s	$CaMCa_4$	M
Gold and Bear (1994)	Det. Reac. Diff. Elect.	Hippocampal N	Ind. LTP	0.2–0.3 s	Ca^{2+}	M
Holmes and Levy (1990)	Det. Reac. Diff. Elect.	Hippocampal DGC	Ind. LTP	0.05–0.3 s	Ca^{2+}	L
Holmes (1990)	Det. Reac. Diff. Elect.	Hippocampal DGC	Ind. LTP	2 s	Ca^{2+}	L
Holmes and Levy (1997)	Det. Reac. Diff. Elect.	Hippocampal DGC	Ind. LTP	0.2 s	Ca^{2+}, $CaMCa_4$	L
Holmes (2000)	Det. Stoch. Reac. Diff. Elect./MCell[d]	Hippocampal DGC	Ind. LTP	2 s to 2 h	CaMKII	L
Kikuchi et al. (2003)	Det. Reac./E-Cell[f]	Hippocampal N	Ind. E-LTP	10–100 min	AMPAR	L
Kitagawa et al. (2009)	Det. Reac./GENESIS/Kinetikit[a]	Cerebellar PC	Ind./Expr./Maint. LTP	2–60 min	CaMKII	L
Kitajima and Hara (1990)	Det. Stoch. Reac. Elect.	Hippocampal PN	Ind./Maint. LTP	0.3 s	Ca^{2+}	S
Kubota and Bower (1999)	Stoch. Reac.	Generic	Ind. LTP	0.02 s	CaMKII	M
Kubota and Bower (2001)	Det. Reac./XPPAUT[g], MATLAB®	Generic	Ind. LTP		CaMKII	L
Kötter (1994)	Det. Reac.	Striatal MSN	LTP		DARPP, MAP2	S
Kötter and Schirok (1999)	Det. Reac./XPP[g]	Striatal MSN	LTP	1–2 s	cAMP	S
Li and Holmes (2000)	Det. Stoch. Reac. Diff. Elect./MCell[d]	Hippocampal DGC	Ind. LTP	1–35 s	CaMKII	L
Lindskog et al. (2006)	Det. Reac./XPPAUT[g]	Striatal MSN	Ind. E-LTP	3–30 min	DARPP32, PKA	L
Lisman (1985)	Det. Reac.	Generic	LTP		Kinase	S
Lisman and Goldring (1988b)	Det. Stoch. Reac.	Generic	LTP		CaMKII	M

(Continued)

Table 2 | *Continued*

Model	Methods	Cell type	Phases	Time	Outputs	Size
Lisman and Goldring (1988a)	Det. Stoch. Reac.	Generic	LTP		CaMKII	M
Lisman (1989)	Det. Reac.	Hippocampal N	LTP		CaMKII	S
Markram et al. (1998)	Det. Reac. Diff.	Neocortical layer V PN	STP/LTP	0.002–2 s	Buffered Ca^{2+}	L
Matsushita et al. (1995)	Det. Reac.	Generic	LTP	20 s to 60 min	CaMKII	M
Michelson and Schulman (1994)	Stoch. Reac.	Generic	LTP	10 s to 3 min	CaMK	L
Migliore and Ayala (1993)	Det. Reac.	Generic	Ind./Expr./Maint. STP/LTP		Postsyn. signal	S
Miller et al. (2005)	Det. Stoch. Reac.	Generic	Ind./Maint. LTP	2 s to 100 y	CaMKII	L
Miller and Wang (2006)	Stoch. Reac.	Generic	Ind./Maint. LTP	1–50 y	CaMKII	L
Okamoto and Ichikawa (2000b)	Det. Reac.	Generic	Ind. LTP		CaMKII	M
Okamoto and Ichikawa (2000a)	Det. Reac. Diff.	Hippocampal CA1 N	Ind. LTP	1–10 s	CaMKII	L
Santucci and Raghavachari (2008)	Det. Stoch. Reac. Diff. Elect.	Hippocampal CA1 PN	Ind. LTP	0.5–1 s	CaMKII	L
Schiegg et al. (1995)	Det. Reac. Diff. Elect.	Hippocampal CA1 PN	Ind. LTP	0.1–1.5 s	Ca^{2+}	L
Smolen et al. (2006)	Det. Reac./Java	Hippocampal CA1 N	Ind./Expr. LLTP	2–4 h	Synaptic strength	M
Smolen (2007)	Det. Reac.	Hippocampal CA1 N	Maint. LLTP	10 h to 3 mo	Synaptic strength	M
Smolen et al. (2008)	Det. Stoch. Reac./Java	Hippocampal CA1 or neocortical PN	Ind./Maint. LLTP	2 h to 8 d	MAPK	M
Smolen et al. (2009)	Det. Stoch. Reac./Java	Generic	Ind./Maint. LTP	1–6 h	CaMKII or MAPK	S
Volfovsky et al. (1999)	Det. Reac. Diff. Elect./FIDAP[n]	Hippocampal N	LTP	0.1–1.2 s	Ca^{2+}	L
Zador et al. (1990)	Det. Reac. Diff. Elect.	Hippocampal CA1 N	Ind. LTP	0.2–0.3 s	$CaMCa_4$	L
Zhabotinsky (2000)	Det. Reac.	Hippocampal N	Ind./Maint. LTP	2 s to 2 y	CaMKII	S

Models are in alphabetical order by the first author and according to the publication month and year. Tabulated characteristics are the method and model types (Det., Stoch., Reac., Diff., Elect., and simulation environment), cell type, phases of LTP, time required for the dynamics of the model to reach a steady state, model outputs, and size of the model based on the number of different chemical species or other model variables (less than 20 different chemical species or other model variables is defined as small (S), between 20 and 50 is medium (M), and more than 50 is large (L)). All abbreviations are given in the list of abbreviations.

[a]*GENESIS/Kinetikit (http://www.genesis-sim.org/GENESIS/; http://www.ncbs.res.in/index.php?option=com_content&task=view&id=307; Bower and Beeman, 1998; Bhalla, 2002c).*

[b]*CaIC (http://web.njit.edu/~matveev/calc.html; Matveev et al., 2002).*

[c]*GENESIS (http://www.genesis-sim.org/GENESIS/; Bower and Beeman, 1998).*

[d]*MCell (http://www.mcell.cnl.salk.edu/; Stiles and Bartol, 2001).*

[e]*NEURON (http://www.neuron.yale.edu/neuron/; Carnevale and Hines, 2006).*

[f]*E-Cell (http://www.e-cell.org; Tomita et al., 1999).*

[g]*XPP, XPPAUT (http://www.math.pitt.edu/~bard/xpp/xpp.html; Ermentrout, 2002).*

[h]*FIDAP (Engelman, 1982, 1996).*

Table 3 | List of LTD models.

Model	Methods	Cell type	Phases	Time	Outputs	Size
Achard and De Schutter (2008)	Det. Reac. Elect./GENESIS/ Kinetikit[a]	Cerebellar PC	Ind. LTD	1 s	Ca^{2+}	L
Brown et al. (2008)	Det. Reac. Diff./Virtual Cell[b]	Cerebellar PC	LTD	0.4–2 s	IP_3	M
Doi et al. (2005)	Det. Reac./GENESIS/ Kinetikit[a]	Cerebellar PC	Ind. LTD	0.2–1 s	Ca^{2+}	L
Fiala et al. (1996)	Det. Reac. Elect.	Cerebellar PC	Ind. LTD		$g_{K_{Ca}}$	M
Hellgren Kotaleski and Blackwell (2002)	Det. Reac. Diff./XPP[c]	Cerebellar PC	LTD	1–5 s	Ca^{2+}	S
Hellgren Kotaleski et al. (2002)	Det. Reac. Diff./XPP[c]	Cerebellar PC	Ind. LTD	5–30 s	PKC	M
Hernjak et al. (2005)	Det. Reac. Diff./Virtual Cell[b]	Cerebellar PC	Ind. LTD	0.1–4 s	Ca^{2+}	M
Holthoff et al. (2002)	Det. Reac. Diff. Elect./ MATLAB®	Neocortical layer V PN	Ind. LTD	0.5 s	Ca^{2+}	S
Kuroda et al. (2001)	Det. Reac./GENESIS/ Kinetikit[a]	Cerebellar PC	Ind. STD/E-,L-LTD	15–100 min	AMPAR	L
Murzina (2004)	Det. Reac. Diff. Elect.	Cerebellar PC	Ind. LTD		Kinase, receptor	M
Ogasawara et al. (2007)	Det. Reac. Diff. Elect.	Cerebellar PC	Ind./Expr./Maint. LTD	20–60 min	AMPAR	L
Ogasawara and Kawato (2009)	Det. Stoch. Reac.	Cerebellar PC	Ind./Maint. LTD	10 s to 70 min	Kinase	S
Schmidt et al. (2007)	Det. Reac. Diff./ Mathematica, FEMLAB	Cerebellar PC	Ind. LTD	0.2–4 s	Ca^{2+}, CaM	L
Schmidt and Eilers (2009)	Det. Reac. Diff./ Mathematica	Cerebellar PC	Ind. LTD	0.04–3 s	Ca^{2+}, CaM	S
Steuber and Willshaw (2004)	Det. Reac. Elect.	Cerebellar PC	Ind. LTD		$g_{K_{Ca}}$	S
Tanaka et al. (2007)	Det. Reac.	Cerebellar PC	Ind. LTD		AMPAR	M
Yang et al. (2001)	Det. Reac. Elect./GENESIS/ Chemesis[d]	Cerebellar PC	Ind. LTD	10–100 s	PKC	L

Models are in alphabetical order by the first author and according to the publication month and year. Tabulated characteristics are the method and model types (Det., Stoch., Reac., Diff., Elect., and simulation environment), cell type, phases of LTD, time required for the dynamics of the model to reach a steady state, model outputs, and size of the model based on the number of different chemical species or other model variables (S, M, L). All abbreviations are given in the list of abbreviations.
[a]GENESIS/Kinetikit (http://www.genesis-sim.org/GENESIS/; http://www.ncbs.res.in/index.php?option=com_content&task=view&id=307; Bower and Beeman, 1998; Bhalla, 2002c).
[b]Virtual Cell (http://vcell.org; Schaff et al., 1997; Slepchenko et al., 2003).
[c]XPP (http://www.math.pitt.edu/~bard/xpp/xpp.html; Ermentrout, 2002).
[d]GENESIS/Chemesis (http://www.genesis-sim.org/GENESIS/; http://krasnow.gmu.edu/CENlab/software.html; Bower and Beeman, 1998; Blackwell and Hellgren Kotaleski, 2002).

3.2. CATEGORIZATION OF MODELS

In this study, models are further categorized (**Figure 1**) into models for single pathways (**Table 5**), models for calcium mechanisms or simplified intracellular processes (**Table 6**), and models for signaling networks (**Table 7**). Models for single pathways involve at most one kinase as a model variable and do not include any receptors, ion channels, or pumps on the plasma membrane. Typically single pathways contain a pathway involving calmodulin and CaMKII and sometimes also phosphatases. Models for calcium mechanisms or simplified intracellular processes include postsynaptic Ca^{2+} buffers together with ion channels, receptors, or pumps, or simplified intracellular processes. The last group of models, consisting of signaling networks, takes into account interactions between at least two pathways and thus often have several protein kinases and phosphatases. These models can also include ion channels, receptors, and pumps. Several characteristics, such as model inputs, number and types of morphological compartments, molecules, ion channels, and receptors, are described for the models in the following sections. In some cases it is difficult to determine the model inputs based on the information given in the publications. For detailed biophysical models, the input is typically coupled with the plasma membrane level phenomena, such as membrane voltage. In these cases, we have indicated the change in membrane current (ΔI_m) or membrane voltage (ΔV_m) as the input. For more simplified models, a variety of mathematical equations are used to describe the model and the input. In these cases, we have indicated which physical property the input equation represents, such as synaptic stimulus (causing elevation in Ca^{2+} concentration). See also Section 4 for further comments on the presentation of input for models.

3.2.1. Models for single pathways

The models for single pathways typically focus on CaMKII (e.g., Dosemeci and Albers, 1996; Okamoto and Ichikawa, 2000a; Smolen et al., 2009), though one model for cAMP production (Kötter and

Table 4 | List of dual LTP and LTD models.

Model	Methods	Cell type	Phases	Time	Outputs	Size
Abarbanel et al. (2002)	Det. Reac. Elect.	Hippocampal GluN	Ind. LTP/LTD		Synaptic strength	S
Abarbanel et al. (2003)	Det. Reac. Elect.	Hippocampal CA1 PN	Ind. LTP/LTD		Synaptic strength	S
Abarbanel et al. (2005)	Det. Reac. Elect.	Hippocampal CA1 PN	Ind. LTP/LTD		Synaptic strength	M
Badoual et al. (2006)	Det. Reac. Diff. Elect./NEURON[a]	Cortical PN	Ind. LTP/LTD	0.05–0.25 s	Enzyme	S
Byrne et al. (2009)	Stoch. Reac. Diff./Java	Hippocampal CA1 PN	Ind. LTP/LTD	1–5 s	Ca^{2+}, CaM	L
Cai et al. (2007)	Det. Stoch. Reac. Elect./Java	Hippocampal or visual cortical N	Ind. LTP/LTD	100 s	Synaptic strength	S
Castellani et al. (2001)	Det. Reac. Elect.	Generic	Ind. LTP/LTD		AMPAR	S
Castellani et al. (2005)	Det. Reac.	Cortical N	Ind. LTP/LTD		AMPAR	M
Castellani et al. (2009)	Det. Stoch. Reac.	Generic	Ind./Maint. LTP/LTD		AMPAR	S
Clopath et al. (2008)	Det. Stoch. Reac. Elect./Python	Hippocampal CA1 PN	Ind./Maint. E_r, LLTP/LTD	3–5 h	Synaptic strength	L
Coomber (1997)	Det. Reac. Diff. Elect./GENESIS[a]	Neocortical PN	Ind./Maint. LTP/LTD	1 s	g_{AMPAR}	L
Coomber (1998a)	Det. Reac./C	Generic	Ind. LTP/LTD	5 s to 15 min	CaMKII	L
Coomber (1998b)	Det. Reac.	Generic	Ind. LTP/LTD	2–60 min	CaMKII	L
d'Alcantara et al. (2003)	Det. Reac./MATLAB[a]	Cerebral cortical or hippocampal CA1 N	Ind. LTP/LTD	20 s to 10 min	AMPAR	S
Delord et al. (2007)	Det. Stoch. Reac.	Generic	Ind./Maint. LTP/LTD	4 s to 4 mo	Substrate	S
Dosemeci and Albers (1996)	Stoch. Reac./FutureBASIC	Generic	Ind. LTP/LTD	20 s to 6 min	CaMKII	L
Gerkin et al. (2007)	Det. Reac.	Hippocampal N	Ind. LTP/LTD	5 s	Synaptic strength	S
Graupner and Brunel (2007)	Det. Reac. Elect./C++, XPPAUT[c]	Hippocampal N	Ind./Maint. LTP/LTD	1–3.5 min	CaMKII	M
Hayer and Bhalla (2005)	Det. Stoch. Reac. Diff./GENESIS/Kinetikit[d], GENESIS 3/MOOSE[e]	Generic	LTP/LTD	200 s to 30 h	AMPAR, CaMKII	L
Helias et al. (2008)	Det. Stoch. Reac. Elect./NEST	Cortical N	Ind. LTP/LTD		CaMKII	L
Holcman et al. (2004)	Stoch. Reac. Diff.	Generic	Ind. LTP/LTD	0.4–0.6 s	Ca^{2+}	L
Ichikawa (2004)	Det. Reac. Diff./A-Cell[b]	Generic	Ind. LTP/LTD		CaMKII	L
Ichikawa et al. (2007)	Det. Reac. Diff. Elect./A-Cell[b]	Hippocampal CA1 PN	Ind./Expr. LTP/LTD		CaMKII, CaN	M
Jain and Bhalla (2009)	Det. Reac./GENESIS/Kinetikit[d], GENESIS 3/MOOSE[e]	Hippocampal N	Ind. LTP/LTD	3 h	Protein	L
Kalantzis and Shouval (2009)	Det. Stoch. Reac. Diff. Elect.	Hippocampal CA1 PN	Ind. LTP/LTD	0.15 s	Synaptic strength	L
Karmarkar and Buonomano (2002)	Det. Reac. Elect./NEURON[a]	Hippocampal N	Ind. LTP/LTD		Synaptic strength	S
Karmarkar et al. (2002)	Det. Reac. Elect./NEURON[a]	Auditory cortical layer II/III PN	Ind. LTP/LTD		Synaptic strength	S
Keller et al. (2008)	Det. Stoch. Reac. Diff. Elect./MCell[h], NEURON[a]	Hippocampal CA1 PN	Ind. LTP/LTD	0.01–0.2 s	CaM	L
Kitajima and Hara (1997)	Det. Reac. Elect.	Generic	Ind./Expr. LTP/LTD	0.04–0.05 s	V_m	M
Kitajima and Hara (2000)	Det. Reac. Elect.	Generic	Ind. LTP/LTD		g_{AMPAR}	M
Kubota and Kitajima (2008)	Det. Stoch. Reac. Elect./C	Cortical PN	Ind. LTP/LTD	100 s to 80 min	Synaptic strength	L
Kubota et al. (2007)	Det. Stoch. Reac. Diff.	Hippocampal CA1 PN	Ind. LTP/LTD	0.05 s	CaM	L

Kubota et al. (2008)	Det. Reac. Elect.	Hippocampal CA1 PN	Ind. LTP/LTD	0.05–1 s	Synaptic strength	M
Migliore et al. (1995)	Det. Reac.	Hippocampal N	Ind./Expr./Maint. LTP/LTD		Postsyn. signal	S
Migliore et al. (1997)	Det. Reac.	Hippocampal N	Ind./Maint. LTP/LTD		Postsyn. signal	S
Migliore and Lansky (1998b)	Det. Reac. Elect./FORTRAN	Neocortical PN	Ind./Maint. LTP/LTD	20 s	Postsyn. signal	S
Migliore and Lansky (1998a)	Det. Reac./FORTRAN	Hippocampal N	Ind./Maint. LTP/LTD		Postsyn. signal	S
Murzina and Silkis (1998)	Det. Reac. Elect.	Hippocampal CA3 PN	Ind. LTP/LTD	0.1 s	V_m	M
Naoki et al. (2005)	Det. Reac. Diff./MATLAB®	Generic	Ind./Expr. LTP/LTD	0.5–10 s	$CaMCa_4$	L
Pi and Lisman (2008)	Det. Reac./MATLAB®	Generic	Ind./Maint. LTP/LTD, depotentiation, dedepression	3–8 s	AMPAR	S
Rubin et al. (2005)	Det. Reac. Diff. Elect./XPPAUT[c]	Hippocampal CA1 PN	Ind. LTP/LTD	10 s	Synaptic strength	M
Saftenku (2002)	Det. Reac. Elect./NEURON[a]	Cerebellar GrC	Ind. LTP/LTD	100 s	Postsyn. signal	L
Saudargiene et al. (2005)	Det. Reac. Elect.	Generic	Ind. LTP/LTD	0.06–0.1 s	Synaptic strength	S
Shah et al. (2006)	Det. Reac. Elect./Java, MATLAB®	Generic	Ind. LTP/STD/LTD		Synaptic strength	S
Shouval et al. (2002a)	Det. Reac. Elect.	Generic	Ind. LTP/LTD		Synaptic strength	S
Shouval et al. (2002b)	Det. Reac. Elect.	Generic	Ind. LTP/LTD		AMPAR	S
Shouval and Kalantzis (2005)	Det. Stoch. Reac. Elect.	Generic	Ind. LTP/LTD		Synaptic strength	S
Stefan et al. (2008)	Det. Reac./COPASI[f]	Generic	LTP/LTD		CaMKII, CaN	L
Urakubo et al. (2008)	Det. Reac. Diff. Elect./GENESIS/Kinetikit[d]	Visual cortical layer II/III PN	Ind. LTP/LTD	20 min	g_{syn}	L
Yeung et al. (2004)	Det. Reac. Elect.	Generic	Ind. LTP/LTD	2 h	Synaptic strength	L
Yu et al. (2008)	Det. Stoch. Reac. Elect.	Hippocampal place N	Ind. LTP/LTD		Synaptic strength	L
Zhabotinsky et al. (2006)	Det. Reac. Diff./XPPAUT[c]	Hippocampal CA1 N	Ind./Maint. E-, LLTP/LTD	10 s to 60 min	AMPAR	L

Models are in alphabetical order by the first author and according to the publication month and year. Tabulated characteristics are the method and model types (Det., Stoch., Reac., Diff., Elect., and simulation environment), cell type, phases of LTP/LTD, time required for the dynamics of the model to reach a steady state, model outputs, and size of the model based on the number of different chemical species or other model variables (S, M, L). All abbreviations are given in the list of abbreviations.

[a]*NEURON (http://www.neuron.yale.edu/neuron/; Carnevale and Hines, 2006).*

[b]*GENESIS (http://www.genesis-sim.org/GENESIS/; Bower and Beeman, 1998).*

[c]*XPP XPPAUT (http://www.math.pitt.edu/~bard/xpp/xpp.html; Ermentrout, 2002).*

[d]*GENESIS/Kinetikit (http://www.genesis-sim.org/GENESIS/; http://www.ncbs.res.in/index.php?option=com_content&task=view&id=307; Bower and Beeman, 1998; Bhalla, 2002c).*

[e]*GENESIS 3/MOOSE (http://www.genesis-sim.org/GENESIS/; http://moose.sourceforge.net/).*

[f]*NEST (http://www.nest-initiative.org/; Gewaltig and Diesmann, 2007).*

[g]*A-Cell (http://www.fujixerox.co.jp/crc/cng/A-Cell/; Ichikawa, 2001).*

[h]*MCell (http://www.mcell.cnl.salk.edu/; Stiles and Bartol, 2001; Kerr et al., 2008).*

COPASI (http://www.copasi.org/; Hoops et al., 2006).

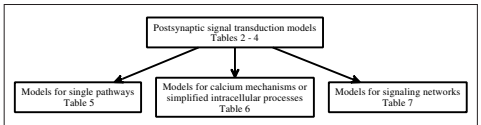

FIGURE 1 | Categorization of postsynaptic signal transduction models.

Schirok, 1999) exists and several models are focused on calmodulin activation (e.g., Kubota et al., 2007; Stefan et al., 2008). Most of these models use Ca^{2+} concentration as the input and include reaction kinetics of $CaMCa_4$ binding and unbinding to CaMKII subunits. Many of the models do not take into account the dodecameric structure of the CaMKII holoenzyme nor the spatial aspect of $CaMCa_4$-dependent autophosphorylation of CaMKII between adjacent subunits. Because of the importance of CaMKII in LTP, most of these single pathway models address the same issues of amplitude and frequency dependence of Ca^{2+}-bound calmodulin or CaMKII activation; subsequent models usually build on previous models and then advance the simulation technique (e.g., stochastic instead of deterministic simulations), or incorporate new experimental details on the CaMKII molecule.

Lisman (1985) presents one of the first models for LTP, which shows that a simple switch model has two stable states, one in which the kinase is dephosphorylated and the other in which it is almost completely phosphorylated. Switch-like behavior, important for memory formation, can be created even when reactions occur stochastically (Smolen et al., 2009), using fast and slow feedback loops. Another stochastic model (Miller et al., 2005) shows that the highly phosphorylated state of CaMKII can remain stable for years, another property which could be important for memory storage.

Okamoto and Ichikawa (2000a) demonstrate the crucial role of competition for calmodulin between spines by modeling several morphological compartments. They model CaMKII in a set of five spines connected to a dendrite and show that after autophosphorylation of CaMKII in a spine, calmodulin in the dendrite can diffuse into that spine for $CaMCa_4$ trapping, which leads to competition since there is a limited concentration of calmodulin. Most of calmodulin is taken by those spines that experience relatively large increases in Ca^{2+} concentration.

A few of the models contribute to understanding of CaMKII activation though they do not explicitly model CaMKII. Delord et al. (2007) use simple models for Ca^{2+}-controlled phosphorylation–dephosphorylation cycles with non-specific phosphoprotein substrates. Despite the simplicity of these models, the fraction of phosphorylated protein remains elevated for prolonged time periods after Ca^{2+} concentration returns to its basal level, representing a form of memory storage. Furthermore, the substrate phosphorylation persists in the presence of substrate turnover. Kubota et al. (2007) demonstrate that neurogranin regulates the spatiotemporal pattern of Ca^{2+}-bound calmodulin, which has important implications for CaMKII activation and spatial specificity, by modeling diffusion of single molecules in a spine using 3-D Brownian dynamics.

Several studies show the importance of phosphatases for persistence of synaptic plasticity. Kubota and Bower (2001) show that asymptotic Ca^{2+} frequency sensitivity of CaMKII depends on both CaMKII and protein phosphatase 1 (PP1). Matsushita et al. (1995) show that phosphatase concentration not only controls whether CaMKII remains phosphorylated, but also controls the intensity of the input required to switch on the persistently phosphorylated state. Lisman and Zhabotinsky (2001) revisit this issue, and show that the CaMKII and PP1 bistable switch activated during the induction of LTP remains active despite the protein turnover. The bistable switch allows CaMKII autophosphorylation to be maintained at low Ca^{2+} concentrations, even after considering the effect of phosphatases and protein turnover. On the other hand, Bradshaw et al. (2003a) show that the presence of PP1 transforms the CaMKII bistable switch into a reversible (ultrasensitive) switch because PP1 dephosphorylates CaMKII when Ca^{2+} concentration is lowered to a basal level. Coomber (1998a) studies autophosphorylation and dephosphorylation of CaMKII and includes autophosphorylation of an inhibitory site caused by low-frequency stimulation. In this manner, either LTP or LTD can occur. Though using different mechanisms, both Dosemeci and Albers (1996) and Coomber (1998a,b) show that the phosphorylation of CaMKII can be sensitive to the temporal pattern of Ca^{2+} pulses, and this may allow CaMKII in the postsynaptic density to act as synaptic frequency detectors. The large allosteric model for calmodulin activation in the postsynaptic density by Stefan et al. (2008) explains how different Ca^{2+} concentrations can trigger the activation of either CaMKII or calcineurin.

3.2.2. Models for calcium mechanisms or simplified intracellular processes

Models for calcium mechanisms or simplified intracellular processes are a diverse group of models which typically address the role of Ca^{2+} in producing changes in synaptic strength. Most of these models focus on mechanisms controlling Ca^{2+} dynamics, such as Ca^{2+} buffers, pumps, glutamate receptors, or Ca^{2+}-permeable ion channels. Another set of these models use more abstract equations representing intracellular processes and include an equation describing the Ca^{2+}-dependent change in synaptic strength, in order to evaluate whether LTP or LTD occurs with repeated patterns of stimulation.

One of the most compelling questions in the field of LTP is whether high-frequency stimulation increases the spine Ca^{2+} concentration more than low-frequency stimulation. This has been addressed using models of Ca^{2+} dynamics in spines alone (see, e.g., Gamble and Koch, 1987; Kitajima and Hara, 1990; Gold and Bear, 1994; Volfovsky et al., 1999; Franks et al., 2001) or spines that include NMDAR activation by electrical activity in models of an entire neuron (see, e.g., Holmes and Levy, 1990; Zador et al., 1990; Koch and Zador, 1993). Zador et al. (1990) further demonstrate that spines compartmentalize Ca^{2+} (i.e., the Ca^{2+} signal is limited to those spines that are stimulated), thus providing a mechanism for spatial specificity. Holmes and Levy (1990) show that the frequency sensitivity of LTP requires Ca^{2+} buffers in addition to NMDAR properties.

A variation of this question is the effect of spine geometry on Ca^{2+} concentration and synaptic plasticity. Both Volfovsky et al. (1999) and Schmidt and Eilers (2009) test different spine-neck lengths and show that a long neck isolates Ca^{2+} signaling and calmodulin activation to the spine while stubby spines have a strong coupling between spines and the dendrite. Cornelisse et al. (2007)

Table 5 | Characteristics of models for single pathways.

Type	Model	Inputs	Subunits/States/Residues	Ions and molecules
LTP	Bradshaw et al. (2003a)	Ca^{2+}	6/3[a]/Thr-286	Ca^{2+}, CaM, CaMKII, PP1
LTP	Dupont et al. (2003)	Ca^{2+}, CaM, $CaMCa_4$	[b]/5[c]/Thr-286	Ca^{2+}, CaM, CaMKII
LTP	Kubota and Bower (2001)	Ca^{2+}	2–4/5[d]/Thr-286, Thr-305/306	Ca^{2+}, CaM, CaMKII, PP1
LTP	Kötter and Schirok (1999)	Ca^{2+}	No	AC, ATP, Ca^{2+}, CaM, cAMP, PDE
LTP	Lisman (1985)	Kinase	1/2[e]	2 kinases, phosphatase[f]
LTP	Lisman and Goldring (1988b)	Ca^{2+}	[b]/3[g]	Ca^{2+}, CaMKII, phosphate ion
LTP	Lisman and Goldring (1988a)	Ca^{2+}	[b]/3[g]	Ca^{2+}, CaMKII, phosphate ion
LTP	Matsushita et al. (1995)	$CaMCa_4$	10/5[d]/Thr-286, Thr-305, Ser-314	ATP, Ca^{2+}, CaM, CaMKII, phosphatase, phosphate ion
LTP	Michelson and Schulman (1994)	Ca^{2+}	10/5[d]/Thr-286, Thr-305/306	Ca^{2+}, CaM, CaMK
LTP	Miller et al. (2005)	Ca^{2+}	12/2[e]/Thr-286/287	Ca^{2+}, CaM, CaMKII, CaN, I1, PKA, PP1
LTP	Miller and Wang (2006)	Ca^{2+}	12/2[e]/Thr-286/287	Ca^{2+}, CaM, CaMKII, PP1
LTP	Okamoto and Ichikawa (2000b)	Ca^{2+}	[b]/4[h]/Thr-286/287	Ca^{2+}, CaM, CaMKII
LTP	Okamoto and Ichikawa (2000a)	Ca^{2+}	10/4[h]/Thr-286/287	Ca^{2+}, CaM[i], $CaMCa_4$-binding protein, CaMKII
LTP	Smolen et al. (2009)	Ca^{2+}	1/2[e]	Ca^{2+}, CaMKII or MAPK
LTP	Zhabotinsky (2000)	Ca^{2+}	10/3/Thr-286	Ca^{2+}, CaM, CaMKII, CaN, I1, PKA, PP1
Dual	Byrne et al. (2009)	Ca^{2+}	12/6[k]	Ca^{2+}, CaM, CaMKII[l]
Dual	Coomber (1998a)	Ca^{2+}	5/7[m]/Thr-286	ATP, Ca^{2+}, CaM, CaMKII, phosphatase (CaN)
Dual	Coomber (1998b)	Ca^{2+}	4/12/Thr-286, Thr-305/306	ATP, Ca^{2+}, CaM, CaMKII, phosphatase (PP1)
Dual	Delord et al. (2007)	Ca^{2+}	1/2[e]	Ca^{2+}, kinase, phosphatase, substrate
Dual	Dosemeci and Albers (1996)	Ca^{2+}	10/4[n]/Thr-286, Thr-305/306	Ca^{2+}, CaM, CaMKII, phosphatase
Dual	Kubota et al. (2007)	Ca^{2+}	No	Ca^{2+}, CaM[o], Ng
Dual	Stefan et al. (2008)	Ca^{2+}	1/5[p]	Ca^{2+}, CaM, CaMKII, CaN

Models are in alphabetical order by the first author and according to the publication month and year. First all LTP models are listed and then all dual LTP and LTD models. Tabulated characteristics are the model inputs, number of CaMKII or kinase subunits, number of states for each subunit, specified threonine (Thr) and serine (Ser) residues of CaMKII that are phosphorylated, as well as ions and molecules whose interactions are modeled. Note that it is not always clear if all the subunits and number of states mentioned in the publications are actually modeled and simulated. Molecules that are modeled as constants are also listed. All abbreviations are given in the list of abbreviations.

[a]First three states of those mentioned under d below are modeled.

[b]It is not clearly stated in the publication how many CaMKII subunits are modeled.

[c]Inactive, bound with $CaMCa_4$, bound with $CaMCa_3$ and autophosphorylated, Ca^{2+} dissociated from CaM bound to the phosphorylated form (trapped), and CaM dissociated from the trapped form but remains phosphorylated (autonomous).

[d]Inactive, bound with $CaMCa_4$, bound with $CaMCa_3$ and autophosphorylated (trapped), $CaMCa_3$ dissociated from the trapped form but remains phosphorylated (autonomous), and autonomous state secondary autophosphorylated (capped).

[e]Inactive and phosphorylated.

[f]Ca^{2+} is not included in the model.

[g]Inactive, bound with Ca^{2+} and autophosphorylated, and Ca^{2+} dissociated but remains phosphorylated.

[h]First four states of those mentioned under d above are modeled.

[i]1-D CaM diffusion is modeled to five spines connected by a dendrite.

[l]Inactive, bound with $CaMCa_4$, and bound with $CaMCa_3$ and phosphorylated or autophosphorylated.

[k]Inactive and bound with CaM, $CaMCa_1$, $CaMCa_2$, $CaMCa_3$, or $CaMCa_4$.

[l]3-D CaM and CaMKII diffusion are modeled in a spine.

[m]Inactive, bound with $CaMCa_4$, bound with $CaMCa_3$ and autophosphorylated, and autophosphorylated on any 1–4 sites.

[n]Inactive, bound with $CaMCa_3$ and autophosphorylated, autophosphorylated, and secondary phosphorylated.

[o]3-D CaM diffusion is modeled in a spine.

[p]Inactive and bound with $CaMCa_1$, $CaMCa_2$, $CaMCa_3$, or $CaMCa_4$.

investigate the role of spine geometry compared to the dendrite. In particular, they demonstrate that the surface area to volume does not completely explain the difference in Ca^{2+} decay between a spine and dendrite. Instead, a lower buffer capacity of the spine is required to explain the experimental data.

Another important question is the role of various Ca^{2+} buffers in controlling Ca^{2+} dynamics. Many models of Ca^{2+} dynamics have only one or two Ca^{2+}-binding proteins, instead of the many types found in real neurons. Markram et al. (1998) show that competition among Ca^{2+}-binding proteins of various speeds and affinities influences the differential activation of intracellular targets. Models of Ca^{2+} dynamics permit tight coupling between experiments and models, but require the use of both intrinsic buffers, such as calbindin and parvalbumin, as well as Ca^{2+} indicators, such as Fura-FF, which themselves are fast, highly diffusible buffers. Other models have shown that buffer saturation is a crucial factor producing supralinear increases in Ca^{2+} concentration (Hellgren Kotaleski and Blackwell, 2002; Hernjak et al., 2005; Canepari and Vogt, 2008).

Table 6 | Characteristics of models for calcium mechaniems or simplified intracellular processes.

Type	Model	Inputs	Compartments	VGICs	LGICs	Molecules and mechanisms
LTP	Canepari and Vogt (2008)	I_{Ca}	1 dendritic	No	No	CD28k, FF, and PV buffers, PMCA pump
LTP	Cornelisse et al. (2007)	J_{VGCC}	Several dendritic and spine compartments	No	No	CaM, CD28k, OGB-1, and PV buffers, 1-D diffusion of Ca^{2+} and some of the buffers, PMCA pump
LTP, Elect.	De Schutter and Bower (1993)	ΔI_m or ΔV_m	Neuron with 1192 compartments	No	NMDAR, non-NMDAR	Buffer, 1-D Ca^{2+} diffusion, PMCA pump
LTP, Elect.	Franks et al. (2001)	ΔI_m or ΔV_m	1 spine	Ca_L, Ca_T	NMDAR	CaM and other buffers, 3-D Ca^{2+} diffusion, PMCA pump
LTP, Elect.	Gamble and Koch (1987)	I_{syn}	1 dendritic, 2 spine-head, 2 spine-neck	Ca^{2+}, K_M	No	CaM buffer, CaN, 1-D Ca^{2+} diffusion, PMCA pump
LTP, Elect.	Gold and Bear (1994)	ΔI_m or ΔV_m	1 dendritic, 4 spine-head, 3 spine-neck	No	NMDAR	Buffer, 1-D Ca^{2+} diffusion, PMCA pump
LTP, Elect.	Holmes and Levy (1990)	ΔI_m or ΔV_m	Neuron with several 4-compartment dendrites, 4304 spines with 4 spine-head and 3 spine-neck, 1–115 synapses	No	NMDAR, non-NMDAR	Buffer, 1-D Ca^{2+} diffusion, PMCA pump
LTP, Elect.	Holmes (1990)	ΔI_m or ΔV_m	Neuron with several 4-compartment dendrites, 3 spines with 5 spine-head and 3 spine-neck, 96 synapses	No	NMDAR, non-NMDAR	Buffer, 1-D Ca^{2+} diffusion, PMCA pump
LTP, Elect.	Holmes and Levy (1997)	ΔI_m or ΔV_m	Neuron with several 12-compartment dendrites, several spines with 4 spine-head and 4 spine-neck, several synapses, 1 axonal, 1 somatic	Ca^{2+}, K_X, K_{Ca}, Na_{fast}	$GABA_AR$, NMDAR, non-NMDAR	CaM and other buffers, 1-D Ca^{2+} diffusion, PMCA pump
LTP, Elect.	Holmes (2000)	ΔI_m or ΔV_m	Neuron with several 12-compartment dendrites, several spines with 4 spine-head and 4 spine-neck, several synapses, 1 axonal, 1 somatic	Ca^{2+}, K_X, K_{Ca}, Na_{fast}	NMDAR, non-NMDAR	CaM buffer, CaMKII[a], CaN, 1-D Ca^{2+} diffusion, PMCA pump
LTP, Elect.	Kitajima and Hara (1990)	ΔI_m or ΔV_m	1 somatic, 1 spine-head, 1 spine-neck	No	NMDAR, non-NMDAR	CaM buffer, CaMKII[b]
LTP, Elect.	Li and Holmes (2000)	ΔI_m or ΔV_m	Neuron with several 12-compartment dendrites, several spines with 4 spine-head and 4 spine-neck, several synapses, 1 axonal, 1 somatic	Ca^{2+}, K_X, K_{Ca}, Na_{fast}	NMDAR, non-NMDAR	CaM buffer, CaMKII[a], CaN, 1-D–3-D Ca^{2+} and Glu diffusion, PMCA pump
LTP	Markram et al. (1998)	I_{Ca}	1 or 25 dendritic	No	No	Buffer, 1-D Ca^{2+} diffusion, PMCA pump
LTP	Migliore and Ayala (1993)	Presyn. stimulus	1 pre-, 1 postsynaptic	No	No	Simplified intracellular processes[c]
LTP, Elect.	Santucci and Raghavachari (2008)	ΔI_m or ΔV_m	1 pre-, 1 postsynaptic	No	AMPAR, NMDAR	CaM buffer, CaMKII[a], CaN, 3-D Glu diffusion, I1, PKA, PP1, 2 vesicles
LTP, Elect.	Schiegg et al. (1995)	ΔI_m or ΔV_m	Neuron with 8 dendritic, 1 somatic, 3 spine-head, 3 spine-neck	No	AMPAR, NMDAR	CaM buffer, CaN, CICR, 1-D Ca^{2+} diffusion, Na^+/Ca^{2+} exchanger, PMCA pump, Ca^{2+} store
LTP, Elect.	Volfovsky et al. (1999)	J_{Ca}, ΔI_m or ΔV_m	Several multi-compartment spines and dendrites	Ca^{2+}	No	CaM and CG-1 buffers, CaN, CICR, 3-D Ca^{2+} and CG-1 diffusion, PMCA and SERCA pumps, Ca^{2+} store
LTP, Elect.	Zador et al. (1990)	ΔI_m or ΔV_m	Neuron with 28 compartments	No	NMDAR, non-NMDAR	CaM buffer, 1-D Ca^{2+} diffusion, 2 PMCA pumps

LTD	Hellgren Kotaleski and Blackwell (2002)	Ca^{2+}	1 spine	No	IP_3R	Buffer, 1-D Ca^{2+} diffusion, IP_3, PMCA pump	
LTD	Hemjak et al. (2005)	J_{Ca}	1–32 1-compartment spines, 2 dendritic	No	IP_3R	CD28k, CG-1, and PV buffers, 1-D and 2-D diffusion of all molecules, IP_3, PMCA and SERCA pumps, Ca^{2+} store	
LTD, Elect.	Holthoff et al. (2002)	ΔI_m or ΔV_m	1 dendritic, 1 spine-head, 1 spine-neck	Ca_L	No	CG-1 and other buffers, 1-D Ca^{2+} diffusion, PMCA and SERCA pumps	
LTD	Schmidt et al. (2007)	I_{Ca}	1 or 7 1-compartment spines, 1 or 7 dendritic	No	No	CaM, CD28k, OGB-1, and PV buffers, 1-D–3-D diffusion of all molecules, PMCA pump	
LTD	Schmidt and Eilers (2009)	I_{Ca}	1 spine, 1 dendritic	No	No	CaM, CD28k, OGB-1, and PV buffers, 1-D diffusion of all molecules, PMCA pump	
Dual, Elect., STDP	Abarbanel et al. (2002)	Synaptic stimulus	1 pre-, 1 postsynaptic	No[e]	Simplified processes	Simplified intracellular processes[c]	
Dual, Elect., STDP	Abarbanel et al. (2003)	ΔI_m or ΔV_m	Neuron with 1 compartment	Ca_v, K^+, Na^+	AMPAR, NMDAR	Phosphorylation, dephosphorylation	
Dual, Elect., STDP	Abarbanel et al. (2005)	ΔI_m or ΔV_m	2 neurons with 1 presynaptic and 1 2-compartment postsynaptic	Ca^{2+}, K^+, K_v, K_M, Na^+	AMPAR, NMDAR	Phosphorylation, dephosphorylation	
Dual, Elect., STDP	Badoual et al. (2006)	ΔI_m or ΔV_m	Neuron with 1 spine, 1 axonal, 1 dendritic, 1 somatic	Ca_L, K_{Ca}, K_{DR}, K_M, Na^+	AMPAR, NMDAR	1-D Ca^{2+} diffusion, PMCA pump, 3 enzymes	
Dual, Elect., STDP	Cai et al. (2007)	Synaptic stimulus	1 pre-, 1 postsynaptic	No	NMDAR	Simplified intracellular processes, vesicle	
Dual, Elect.	Castellani et al. (2001)	ΔI_m or ΔV_m	1 spine	No	AMPAR, NMDAR	2 kinases, 2 phosphatases	
Dual	Castellani et al. (2009)	CaMKII	1 postsynaptic	No	AMPAR	CaMKII, PKA, PP1[c]	
Dual, Elect.	Clopath et al. (2008)	ΔI_m	Neuron with 1 compartment, 100 synapses	No[f]	Simplified processes	Protein synthesis[c]	
Dual, Elect.	Coomber (1997)	ΔI_m or ΔV_m	Neuron with 149 compartments	Ca_L, K_v, K_{AHP}, K_{Ca}, K_{DR}, K_M, Na^+	AMPAR, NMDAR	Buffer, 1-D Ca^{2+} diffusion, PMCA pump	
Dual, STDP	Gerkin et al. (2007)	Synaptic stimulus	1 pre-, 1 postsynaptic	No	No	Simplified intracellular processes[c]	
Dual, Elect., STDP	Hellas et al. (2008)	Synaptic stimulus	Neuron with 1 compartment, max 10000 synapses	No[g]	NMDAR	CaMKII	
Dual	Holcman et al. (2004)	J_{NMDAR}	4-compartment spine	No	No	CaM buffer, CaN, 2-D Ca^{2+} diffusion, PMCA pump	
Dual	Ichikawa (2004)	J_{NMDAR}	3112-compartment spine	No	No	CaM buffer, CaMKII, CaN, 3-D diffusion of all molecules	

(Continued)

Table 6 | *Continued*

Type	Model	Inputs	Compartments	VGICs	LGICs	Molecules and mechanisms
Dual, Elect.	Ichikawa et al. (2007)	ΔI_m or ΔV_m	1 spine, 1 dendritic	No	AMPAR, NMDAR	CaM and other buffers, CaMKII, CaN, 1-D Ca^{2+} diffusion, PMCA pump
Dual, Elect., STDP	Kalantzis and Shouval (2009)	ΔV_m	6 spine-head, 10 spine-neck	No	NMDAR	Buffer, 1-D Ca^{2+} diffusion, PMCA pump
Dual, Elect., STDP	Karmarkar and Buonomano (2002)	Synaptic stimulus	2 1-compartment neurons	Ca^{2+h}	AMPAR, NMDAR	Simplified intracellular processes
Dual, Elect.	Karmarkar et al. (2002)	Synaptic stimulus	2 1-compartment neurons	No[h]	AMPAR, NMDAR	Simplified intracellular processes
Dual, Elect.	Keller et al. (2008)	ΔI_m or ΔV_m	1 dendritic, 1 extracellular, 1 presynaptic, 1 spine-head	Ca^{2+}	AMPAR, NMDAR	CaM, CD28k, OGB-1, and other buffers, 3-D diffusion of all molecules, Na^+/Ca^{2+} exchanger, PMCA pump
Dual, Elect.	Kitajima and Hara (1997)	Presyn. stimulus	Several spines with 1 spine-head and 1 spine-neck, 3 dendritic, 1 presynaptic	Ca^{2+}	AMPAR, GABAR, NMDAR	Kinase, phosphatase, PMCA pump, vesicle
Dual, Elect.	Kitajima and Hara (2000)	ΔI_m or ΔV_m	Neuron with 2 1-8-compartment dendrites, 1 spine, 1 axonal, 1 somatic	Ca_L, Ca_N, Ca_T, K_A, K_{DR}, Na^+	AMPAR, NMDAR	Phosphorylation, dephosphorylation
Dual, Elect., STDP	Kubota and Kitajima (2008)	ΔI_m or ΔV_m	Neuron with 2 44-7-compartment dendrites, 1 spine, 4800 synapses, 1 somatic	K_A, K_{AHP}, $Na_{fast}{}^i$	AMPAR, GABAR, NMDAR	Simplified intracellular processes
Dual, Elect.	Kubota et al. (2008)	ΔI_m or ΔV_m	1 spine	No	NMDAR	CaM buffer, Ng
Dual	Migliore et al. (1996)	Presyn. stimulus	1 pre-, 1 postsynaptic	No	No	Simplified intracellular processes[c]
Dual	Migliore et al. (1997)	Presyn. stimulus	Several synapses with 1 pre- and 1 postsynaptic	No	No	Simplified intracellular processes[c]
Dual, Elect.	Migliore and Lansky (1999b)	Presyn. stimulus	1 pre-, 1 postsynaptic	No[i]	No	Simplified intracellular processes[c]
Dual	Migliore and Lansky (1999a)	Presyn. stimulus	1 pre-, 1 postsynaptic	No	No	Simplified intracellular processes[c]
Dual	Naoki et al. (2005)	I_{NMDAR}	15-compartment spine	No	No	CaM and other buffers, 1-D diffusion of all molecules, Na^+/Ca^{2+} exchanger, PMCA and SERCA pumps
Dual	Pi and Lisman (2008)	J_{NMDAR}	1 spine	No	AMPAR	Buffer, CaMKII, PP2A, AMPAR trafficking
Dual, Elect., STDP	Rubin et al. (2005)	ΔI_m or ΔV_m	Neuron with 1 spine (dendritic), 1 somatic	Ca_L, K_A, K_{AHP}, K_{DR}, Na^+	AMPAR, NMDAR	Buffer, Ca^{2+} detectors, 1-D Ca^{2+} diffusion
Dual, Elect.	Saftenku (2002)	ΔI_m or ΔV_m	Neuron with several compartments	BK_{Ca}, Ca_N, K_A, K_{DR}, K_{IR}, K_{slow}, Na_{fast}, Na_p, Na_{slow}	AMPAR, NMDAR	Simplified intracellular processes

Dual, Elect., STDP	Saudargiene et al. (2005)	ΔI_m or ΔV_m	1 dendritic	No	AMPAR, NMDAR	Simplified intracellular processes
Dual, Elect., STDP	Shah et al. (2006)	Synaptic stimulus	1 pre-, 1 postsynaptic	No	NMDAR	Simplified intracellular processes
Dual, Elect., STDP	Shouval et al. (2002a)	Synaptic stimulus	1 synaptic	No	NMDAR	Simplified intracellular processes
Dual, Elect., STDP	Shouval et al. (2002b)	Synaptic stimulus	1 pre-, 1 postsynaptic	No	AMPAR, NMDAR	2 kinases, 2 phosphatases
Dual, Elect., STDP	Shouval and Kalantzis (2005)	Synaptic stimulus	1 synaptic	No	NMDAR	Simplified intracellular processes
Dual, Elect., STDP	Yeung et al. (2004)	Synaptic stimulus	Neuron with 1 compartment, 120 synapses	No[g]	NMDAR	Simplified intracellular processes
Dual, Elect., STDP	Yu et al. (2008)	Synaptic stimulus	Neuron with 1 compartment, 1000 synapses	No[i]	NMDAR	Simplified intracellular processes

Models are in alphabetical order by the first author and according to the publication month and year. First all LTP models are listed, then all LTD models, and finally all dual LTP and LTD models. Furthermore, electrophysiological (Elect.) models taking into account membrane voltage and spike-timing-dependent plasticity (STDP) models are indicated in the first column. Tabulated characteristics are the model inputs, compartments, voltage-gated ion channels (VGICs), ligand-gated ion channels (LGICs), as well as molecules and Ca^{2+} mechanisms modeled. I_{ca} denotes in this study the Ca^{2+} current but dependency in membrane voltage is not modeled. I_{NMDAR} denotes in this study the Ca^{2+} current via NMDARs but dependency in membrane voltage and NMDAR kinetics are not modeled. I_{syn} denotes the synaptic current. J_{ca} denotes the Ca^{2+} influx, J_{VGCC} denotes the Ca^{2+} influx via VGCC, and J_{NMDAR} denotes the Ca^{2+} influx via NMDARs. For complex CaMKII models, number of CaMKII subunits, number of states for each subunit, and specified threonine (Thr) residues of CaMKII that are phosphorylated are given. Molecules that are modeled as constants are also listed. All abbreviations are given in the list of abbreviations.

[a]Ten CaMKII subunits/Thr-286, Thr-305/306 with five states: inactive, bound with $CaMCa_2$, bound with $CaMCa_4$ and autophosphorylated (trapped), $CaMCa_4$ dissociated from the trapped form but remains phosphorylated (autonomous), and autonomous state secondary phosphorylated (capped).

[b]It is not clearly stated in the publication how many CaMKII subunits are modeled but they have two states: inactive and phosphorylated.

[c]Ca^{2+} is not included in the model.

[d]Model is by Miller et al. (2005), 12 CaMKII subunits/Thr286/287 with two states: inactive and phosphorylated.

[e]Pre- and postsynaptic membrane voltage are modeled.

[f]Postsynaptic neuron is described using adaptive exponential IF neuron model.

[g]Postsynaptic neuron is described using IF neuron model.

[h]Pre- and postsynaptic neurons are described using IF neuron model.

[i]Postsynaptic neuron is described using LIF neuron model.

[j]Postsynaptic membrane voltage is modeled.

Table 7 | Characteristics of models for signaling networks.

Type	Model	Inputs	Compartments	VGICs	LGICs	Other	Mechanisms	Pathways
LTP	Ajay and Bhalla (2004)	Glu, J_{NMDAR}	1 postsynaptic	No	No	EGFR, mGluR	CaM and other buffers	AC, CaM, CaMKII*, CaN, Gq, MAPK, MKP, PKA, PKC, PKMζ, PLA_2, PLC, PP1, Ras, SoS
LTP, Elect.	Ajay and Bhalla (2007)	Ca^{2+}, ΔI_m or ΔV_m, J_{Ca}	Neuron with 1–324 compartments	Ca^{2+}, K_A, K_{AHP}, K_{Ca}, K_{DR}, Na^+	AMPAR, NMDAR	No	CaM buffer, 1-D diffusion of all molecules, PMCA pump, transport of all molecules	CaM, MAPK, PKC, PKM, PLA_2, Ras
LTP	Aslam et al. (2009)	$CaMCa_4$	1 postsynaptic	No	No	No	CaM buffer	CaMKII, CPEB1
LTP, Elect.	Bhalla and Iyengar (1999)	ΔI_m or ΔV_m, EGF, Glu	Neuron with several compartments	Ca^{2+}, K_A, K_{AHP}, K_{Ca}, K_{DR}, Na^{2+}	AMPAR, IP_3R, NMDAR	EGFR, mGluR	CaM buffer, PMCA pump, Ca^{2+} store	AC, CaM, CaMKII*, CaN, Gq, MAPK, PKA, PKC, PLA_2, PLC, PP1, Ras, SoS
LTP, Elect.	Bhalla (2002a)	ΔI_m or ΔV_m, EGF, Glu, hormone	Neuron with 24 dendritic, 1 somatic, 4 spine-head, 3 spine-neck	Ca^{2+}, K_A, K_{AHP}, K_{Ca}, K_{DR}, Na^+	AMPAR, IP_3R, NMDAR	EGFR, mGluR	CaM and other buffers, 1-D Ca^{2+} diffusion, PMCA and SERCA pumps, Ca^{2+} store	AC, CaM, CaMKII*, CaN, Gq, Gs, MAPK, PKA, PKC, PLA_2, PLC, PP1, Ras, SoS
LTP	Bhalla (2002b)	EGF, Glu, hormone, J_{Ca}	1 extracellular, 1 intracellular, 1 store	No	IP_3R	EGFR, mGluR	CaM buffer, PMCA and SERCA pumps, Ca^{2+} store	AC, CaM, CaMKII*, CaN, Gq, Gs, MAPK, PKA, PKC, PLA_2, PLC, PP1, Ras, SoS
LTP	Kikuchi et al. (2003)	Glu, J_{NMDAR}	1 postsynaptic	No	AMPAR, IP_3R	mGluR	CaM buffer, Ca^{2+} store	AC, CaM, CaMKII, CaN, Gq, I1, MAPK, MEK, MKP, PKA, PKC, PLA_2, PLC, PP1, PP2A, Raf, Ras
LTP	Kitagawa et al. (2009)	Ca^{2+}, $GABA_BR$	1 postsynaptic	No	$GABA_AR$	$GABA_BR$	CaM buffer	AC, CaM, CaMKII*, cAMP, CaN, DARPP32, PDE1, PDE4, PKA, PP1
LTP	Kubota and Bower (1999)	Ca^{2+}	1 spine-head	No	AMPAR	No	CaM buffer, Ca^{2+} transport	AC, CaM, CaMKII*, cAMP, CaN, I1, MAPK, PDE, PKA, PP1, Ras
LTP	Kötter (1994)	Ca^{2+}, DA	1 postsynaptic	No	No	No	Buffer	AC, CaMKII, cAMP, CaN, DARPP, MAP2, PDE, PKA, PP1
LTP	Lindskog et al. (2006)	Ca^{2+}, DA	1 spine	No	No	D_1R	CaM buffer	AC, CaM, CaMKII, CaN, DARPP32, PDE1, PDE4, PKA, PP1, PP2A
LTP	Lisman (1989)	Ca^{2+}	1 postsynaptic	No	No	No	CaM buffer	AC, CaM, CaMKII, cAMP, CaN, I1, PDE, PKA, PP1
LTP	Smolen et al. (2006)	Ca^{2+}, cAMP, k_{Raf}	1 nucleus, 1 somatic, 1 synaptic	No	No	No	Buffer	CaMKII, CaMKIV, MAPK, PKA, gene expression
LTP	Smolen (2007)	Ca^{2+}	1–5 synapses	No	No	No	Buffer	CaMKII, CaMKIV, MAPK, PKA, gene expression

LTP	Smolen et al. (2008)	Raf	1 spine	No	No	No	No	ERK, MEK, MKKP, MKP, Raf[4]
LTD, Elect.	Achard and De Schutter (2008)	ΔI_m or ΔV_m	Neuron with 1600 compartments, 1 cytosolic, 1 ER, 1 PSD	BK_{Ca}, Ca_P, Ca_T, $K2_{Ca}$, K_A, K_{DR}, K_{IR}, K_M, Na_{fast}, Na_{slow}	AMPAR, IP_3R	mGluR	CD28k, MgGreen, PV, and other buffers, Na^+/Ca^{2+} exchanger, PMCA and SERCA pumps, Ca^{2+} store	Gq, IP_3 3-kinase, IP_3 5-phosphatase, PLC
LTD	Brown et al. (2008)	PIP2, PLC	1 or several 1-compartment spines, 1 dendritic	No	No	No	Buffers, 1-D and 3-D diffusion of all molecules	PIP2, PLC
LTD	Doi et al. (2005)	Glu, J_{Ca}	1 cytosolic, 1 ER, 1 PSD	No	IP_3R	mGluR	CD28k, MgGreen, PV, and other buffers, Na^+/Ca^{2+} exchanger, PMCA and SERCA pumps, Ca^{2+} store	Gq, IP_3 3-kinase, IP_3 5-phosphatase, PLC
LTD, Elect.	Fiala et al. (1996)	cGMP, Glu	1 cytosolic, 1 ER, 1 extracellular	K_{Ca}	IP_3R	mGluR	Na^+/Ca^{2+} exchanger, SERCA pump, Ca^{2+} store	CaN, G, PKC, PLC
LTD	Hellgren Kotaleski et al. (2002)	Ca^{2+}, Glu	1 spine-head, 2 spine-neck	No	IP_3R	mGluR	2 buffers, 1-D Ca^{2+} diffusion, Ca^{2+} store	G, PKC, PLA_2, PLC
LTD	Kuroda et al. (2001)	Ca^{2+}, Glu, NO	1 postsynaptic	No	AMPAR	CRHR, mGluR	No	cGMP, Gq, Lyn, MAPK, MEK, PKC, PLA_2, PLC, Raf
LTD, Elect.	Murzina (2004)	ΔV_m, Glu	Neuron with 2 1-compartment spines, 5 dendritic, 1 somatic	Ca^{2+}, K^+, K_{Ca}, $K_{GABA_A}R$, Na^+	AMPAR, $GABA_AR$	$GABA_BR$, mGluR	CaM buffer, 1-D diffusion of NO	CaM, CaMKII, CaN, cGMP, G, GC, PKC, PKG, PP1
LTD, Elect.	Ogasawara et al. (2007)	ΔI_m or ΔV_m, Glu, NO	1350 1-compartment spines, 30 dendritic	BK_{Ca}, Ca_P	AMPAR, IP_3R	mGluR	CD28k, MgGreen, PV, and other buffers, 3-D diffusion of NO, PMCA and SERCA pumps, Ca^{2+} store	cGMP, Gq, MAPK, MEK, PKC, PLA_2, PLC, Raf
LTD	Ogasawara and Kawato (2009)	Generic	1 postsynaptic	No	No	No	No	4 kinases[4]
LTD, Elect.	Steuber and Willshaw (2004)	cGMP, Glu	0 or 10 dendritic, 1 somatic	K_{Ca}	IP_3R	mGluR	Buffer, Na^+/Ca^{2+} exchanger, SERCA pump, Ca^{2+} store	CaN, G, PKC, PLC
LTD	Tanaka et al. (2007)	Ca^{2+}	1 postsynaptic	No	AMPAR	No	No	MAPK, MEK, PKC, PLA_2, Raf
LTD, Elect.	Yang et al. (2001)	Ca^{2+}	Neuron with 1600 compartments	BK_{Ca}, Ca_P, Ca_T, $K2_{Ca}$, K_A, K_{DR}, K_{IR}, K_M, Na_{fast}, Na_{slow}	AMPAR, IP_3R	mGluR	Ca^{2+} store	Gq, PKC, PLA_2, PLC
Dual	Castellani et al. (2005)	Ca^{2+}	1 postsynaptic	No	AMPAR	No	CaM buffer	CaM, CaMKII, cAMP, CaN, I1, PKA, PP1
Dual	d'Alcantara et al. (2003)	Ca^{2+}	1 postsynaptic	No	AMPAR	No	CaM buffer	CaM, CaMKII, CaN, I1, PP1

(Continued)

Table 7 | *Continued*

Type	Model	Inputs	Compartments	VGICs	LGICs	Other	Mechanisms	Pathways
Dual, Elect., STDP	Graupner and Brunel (2007)	ΔI_m	1 spine	Ca_L, K_{DR}, Na^+	AMPAR, NMDAR	No	Simplified, CaM and other buffers	CaM, CaMKII[a], I1, PP1
Dual	Hayer and Bhalla (2005)	Ca^{2+}, cAMP, J_{NMDAR}	1 dendritic, 1 PSD, 1 spine-head	No	AMPAR	No	CaM buffer, 1-D diffusion of some of the molecules	AC, CaM, CaMKII[a], CaN, PKA, PP1
Dual	Jain and Bhalla (2009)	BDNF, J_{NMDAR}, MAPK	1 postsynaptic	No	No	TrkB	CaM buffer	40S, 4E-BP, AKT, CaM, CaMKIII, MAPK, mTOR, PKC, Ras, S6K, SoS
Dual, Elect.	Murzina and Silkis (1998)	ΔI_m or ΔV_m	Neuron with several compartments	Ca^{2+}, K^+, $K_{GABA(f)}$, Na^+	AMPAR, $GABA_A$R, NMDAR	$GABA_B$R, mGluR	Buffer, Ca^{2+} store	AC, CaMKII, cAMP, PKA, PKC
Dual, Elect., STDP	Urakubo et al. (2008)	ΔI_m or ΔV_m	Neuron with 2-compartment spine, 20 dendritic, 1 somatic	Ca_L, K_A, K_{DR}, Na^+, Na_{slow}	AMPAR, NMDAR	No	CaM buffer, 1-D diffusion of most of the molecules, PMCA pump, AMPAR trafficking	CaM, CaMKII, CaN, cAMP, I1, PKA, PP1, PP2A
Dual	Zhabotinsky et al. (2006)	J_{NMDAR}	1 spine, 1 dendritic, 1 cell body	No	AMPAR	No	CaM buffer, 1-D diffusion of some of the molecules, AMPAR trafficking	CaM, CaMKII[a], CaN, I1, Ng, PKA, PP1, PP2A

Models are in alphabetical order by the first author and according to the publication month and year. First all LTP models are listed, then all LTD models, and finally all dual LTP and LTD models. Furthermore, electrophysiological (Elect.) models taking into account membrane voltage and spike-timing-dependent plasticity (STDP) models are indicated in the first column. Tabulated characteristics are the model inputs, compartments, voltage-gated ion channels (VGICs), ligand-gated ion channels (LGICs), other receptors, Ca^{2+} mechanisms, and signaling pathways modeled. J_{Ca} denotes the Ca^{2+} influx and J_{NMDAR} denotes the Ca^{2+} influx via NMDARs. For complex CaMKII models, number of CaMKII subunits, number of states for each subunit, and specified threonine (Thr) residues of CaMKII that are phosphorylated are given. All abbreviations are given in the list of abbreviations.

[a]One CaMKII subunit/Thr-286, Thr-306 with six states: inactive, bound with CaM/Ca_4, bound with CaM/Ca_4 and autophosphorylated (trapped), CaM/Ca_4 dissociated from the trapped form but remains phosphorylated (autonomous), autonomous state secondary phosphorylated (capped), and capped state dephosphorylated.

[b]It is not clearly stated in the publication how many CaMKII subunits are modeled. CaMKII subunits/Thr-286/287,Thr-305/306 with six states: inactive, bound with CaM/Ca_4, and autophosphorylated (trapped), CaM/Ca_4 dissociated from the trapped form but remains phosphorylated (autonomous), autonomous state secondary phosphorylated (capped), and capped state dephosphorylated.

[c]It is not clearly stated in the publication how many CaMKII subunits are modeled. CaMKII subunits/Thr-286, Thr-305/306 with five states: inactive, bound with CaM/Ca_4, and autophosphorylated (trapped), CaM/Ca_4 dissociated from the trapped form but remains phosphorylated (autonomous), and autonomous state secondary phosphorylated (capped).

[d]Ca^{2+} is not included in the model.

[e]Two to eight CaMKII subunits/Thr-286 with four states: inactive, bound with CaM/Ca_4, and autophosphorylated, and autophosphorylated only.

[f]One CaMKII subunit/Thr-286 with several states: inactive, bound with CaM, CaM/Ca_2, CaM/Ca_3, CaM/Ca_4, or CaM/Ca_4, and dissociated but remains phosphorylated.

[g]Two models. Model 1 is one CaMKII subunit/Thr-286 with seven states: inactive, bound with CaM/Ca_2, bound with two CaM/Ca_2, bound with two CaM/Ca_3, and autophosphorylated, CaM/Ca_4-dissociated but remains phosphorylated, two CaM/Ca_4 dissociated but remains phosphorylated, and autophosphorylated. Model 2 is by Miller et al. (2005), 12 CaMKII subunits/Thr-286/287 with two states: inactive and phosphorylated.

Improvements in Ca^{2+} imaging techniques have been accompanied by the development of sophisticated models that investigate mechanisms underlying Ca^{2+} microdomains. Naoki et al. (2005) take into account buffering by Ca^{2+}-binding proteins and show that the diffusion coefficient of calmodulin has a strong effect on calmodulin activation in the microdomain near NMDARs. Kubota et al. (2008) investigate the Ca^{2+}-binding protein neurogranin which increases Ca^{2+} dissociation from calmodulin. Their results show that with no Ca^{2+} extrusion mechanism, neurogranin increases the steady state concentration of Ca^{2+}; however, in the presence of Ca^{2+} extrusion mechanisms, neurogranin instead enhances the decay rate of Ca^{2+}. Keller et al. (2008) use MCell (Stiles and Bartol, 2001; Kerr et al., 2008) to develop one of the most advanced models of Ca^{2+} dynamics in a spine, including Ca^{2+} pumps, and both voltage-gated Ca^{2+} channels and NMDA-type of glutamate receptors. The voltage-dependent activation of the channels is coupled to a NEURON (Carnevale and Hines, 2006) simulation of membrane voltage. Keller et al. (2008) show that the Ca^{2+} gradient and calmodulin activation in the postsynaptic density depend on the order of glutamate release and action potential, and thus may explain the results of STDP experiments.

Just as recent models of Ca^{2+} dynamics include additional biophysical details, other models explore how biophysical processes related to, for example, glutamate receptors modulate LTP induction. Santucci and Raghavachari (2008) study the role of different types of NMDAR NR2 subunits on subsequent CaMKII activation. They show that though NR2B subunits have a more prolonged time course, the higher open probability of NR2A subunits leads to greater Ca^{2+} influx and CaMKII activation. The model of Li and Holmes (2000) shows that the variability in NMDAR opening, the spine-head Ca^{2+} concentration, and levels of CaMKII activation can play an important role in LTP induction. The spine model by Schiegg et al. (1995) includes calcineurin and Ca^{2+} release from stores, for example through IP_3Rs, in the spine head. This study shows that the inclusion of calcineurin alone, which is a Ca^{2+} sensitive protein phosphatase important for synaptic depression, eliminates LTP; further inclusion of Ca^{2+} release from stores is required to restore LTP induction. Pi and Lisman (2008) study the role of AMPAR trafficking, modeled by inserting and removing AMPARs in the postsynaptic membrane with a rate that depends on phosphorylated CaMKII and dephosphorylated protein phosphatase 2A (PP2A). Pi and Lisman (2008) show that CaMKII activity is high during LTP, PP2A activity remains high during LTD, and neither activity is high during a basal state; thus, LTD is not a reversal of previous LTP, rather a distinct phenomenon. Clopath et al. (2008) focus on synaptic tagging, an experimental concept important for synaptic specificity of protein synthesis-dependent LTP. The model includes production of plasticity-related proteins which can be captured by tagged synapses. Non-tagged synapses can be tagged stochastically in either a high or low state. They show that synapses share protein synthesis processes which have an effect on the stabilization of potentiated synapses during the transition from E-LTP to L-LTP.

As with all computational models, verification by direct comparison with experimental data strengthens the ability to make experimental predictions and resolve conflicting experimental evidence. The study by Santucci and Raghavachari (2008) is an excellent example on developing a computationally realistic model from good quality data, using the model to resolve conflicting experimental evidence, and then making further experimental predictions. Other examples of direct comparison with experiments include studies by Markram et al. (1998), Volfovsky et al. (1999), Cornelisse et al. (2007), and Schmidt and Eilers (2009). In addition, the prediction that PP2A is critical for LTD induction has been confirmed experimentally (Nicholls et al., 2008). Cai et al. (2007) demonstrate that including the stochastic properties of synaptic transmission significantly affects the form of STDP curves, and indeed is required to explain the experimental data.

3.2.3. Models for signaling networks

Many LTP models for signaling networks are extensions of the single pathway CaMKII models. The model by Lisman (1989) is a landmark because it is one of the first to show that synaptic strength stored by CaMKII could be bidirectionally modified by physiological activity according to the postsynaptic Ca^{2+} concentration. Kubota and Bower (1999) predict that the CaMKII activity can be sensitive to small changes in the timing of presynaptic signal to the spine head and that CaMKII can exhibit temporal sensitivity even in the presence of PP1. Kitagawa et al. (2009) evaluate the effect of inhibitory G protein-coupled gamma-aminobutyric acid (GABA) B receptor ($GABA_BR$) activation on LTP. They show that a transient increase in Ca^{2+} concentration induces long-term activation of CaMKII, which is attenuated by $GABA_BR$ activation due to inhibition of PKA. They further show a role for a novel positive feedback loop – one involving CaMKII-mediated downregulation of phosphodiesterase type 1.

Bhalla and Iyengar (1999), Bhalla (2002a,b), Ajay and Bhalla (2004, 2007), and Hayer and Bhalla (2005) have modeled pathways for several protein kinases and phosphatases to investigate information processing. The first study (Bhalla and Iyengar, 1999) uses synaptic stimulation of a compartmental neuron model (Holmes and Levy, 1990; Traub et al., 1991; De Schutter and Bower, 1993) to determine the Ca^{2+} concentration that is the input to signaling network models. Simulations show that several properties not present in individual pathways, such as feedback loops, thresholds, and sensitivity to signal strength and duration, can emerge from the interaction of pathways. Feedback loops and thresholds can give rise to bistability, offering the possibility that information can be stored within biochemical reactions in the signaling network. The role of temporal sensitivity is further explored (Bhalla, 2002a). This study shows that different input patterns are processed differently by the signaling network, thus giving rise to different outputs (input pattern discrimination). The role of the feedback loop involving MAPK and PKC is further explored in additional studies that integrate experiments and modeling (Bhalla, 2002b). The signaling network models are further refined to include $PKM\zeta$ (Ajay and Bhalla, 2004, 2007), diffusional processes (Ajay and Bhalla, 2007), and electrical activity (Ajay and Bhalla, 2007) to explore mechanisms underlying MAPK activation in LTP. Ajay and Bhalla (2007) show that extracellular signal-regulated kinase (ERK, MAPK) type II (ERKII) activation after an LTP-inducing stimuli is not explained with reaction–diffusion alone but requires a distributed synaptic input and activation of voltage-gated Ca^{2+} channels. The model by

Hayer and Bhalla (2005) shows that CaMKII and AMPAR phosphorylation form distinct bistable switches, allowing for multiple stable states of the system.

The models of striatal medium spiny neurons (Kötter, 1994; Lindskog et al., 2006) focus on integration of dopamine and glutamate signals, and explore mechanisms which are important for striatal learning. The model by Kötter (1994) is the first to investigate signaling pathways underlying plasticity in the striatum, and shows that, with Ca^{2+}-activated adenylyl cyclase, dopamine and Ca^{2+} synergistically activate PKA. The model by Lindskog et al. (2006) includes the striatal adenylyl cyclase type 5, which is inhibited by Ca^{2+}, and shows that separate transient dopamine or Ca^{2+} elevations each may increase the phosphorylation of cAMP-regulated phosphoprotein (DARPP32), due to Ca^{2+} activation of PP2A. Through this mechanism, paired stimuli yield increased PKA activation and DARPP32 phosphorylation compared to dopamine alone, in contrast to the effect of prolonged stimuli in which Ca^{2+} decreases DARPP32 phosphorylation. Fernandez et al. (2006) study the functions of DARPP32 with a detailed signaling network model but they do not address plasticity, thus this study is not included in **Table 7**. However, their study may be used as a valuable model to build on for future modeling efforts studying plasticity.

More recently models have been constructed to investigate mechanisms underlying L-LTP, by incorporating molecules such as CaMKIV, transcription factors, or the translation factor cytoplasmic polyadenylation element binding protein (CPEB1). Smolen (2007) shows that long periods of decreased activity reset synaptic strength to a low value, whereas episodic activity with short inactive periods maintains strong synapses. Smolen et al. (2008) implement a stochastic model to show that the feedback loop from MAPK to MAPK kinase kinase (Raf) increases the robustness of both stable states of MAPK activity to stochastic fluctuations. Aslam et al. (2009) show that the positive feedback loop between CaMKII and CPEB1 forms a bistable switch accounting for the protein synthesis dependence of L-LTP. In addition, Jain and Bhalla (2009) are interested in protein synthesis dependence of L-LTP, and thus investigate how the synaptic input pattern affects dendritic protein synthesis. These types of models are likely to increase because behavioral memories require protein synthesis.

Long-term depression is predominant for synapses in the cerebellum; thus, most models of LTD describe signaling networks in cerebellar Purkinje cells. Kuroda et al. (2001) investigate the mechanism producing persistent phosphorylation of AMPARs, required for LTD. Simulations show that the initial phase of phosphorylation of AMPARs depends on the activation of PKC by arachidonic acid, Ca^{2+}, and diacylglycerol, whereas a later phase depends on the activation of a positive feedback loop and especially phospholipase A_2 and arachidonic acid. Tanaka et al. (2007) further demonstrate that disrupting the positive feedback loop between several protein kinases can affect Ca^{2+} triggering of LTD. Brown et al. (2008) present an elaborate three-dimensional model of a Purkinje cell dendrite with spines to investigate the issue of whether sufficient phosphatidylinositol biphosphate (PIP2) is available in a single spine to achieve the experimentally estimated concentrations of IP_3 required for Ca^{2+} release and subsequent LTD. They elegantly show that a relatively novel mechanism, namely stimulated synthesis of PIP2, is required to account for experimental results. Three of the LTD models (Yang et al., 2001; Ogasawara et al., 2007; Achard and De Schutter, 2008) use the multi-compartment, multi-channel Purkinje cell model by De Schutter and Bower (1994a,b) to simulate electrical activity leading to Ca^{2+} influx through synaptic and voltage-gated ion channels. Ogasawara et al. (2007) show that the nitric oxide concentration is critical for induction of LTD and for its input specificity. Achard and De Schutter (2008) re-evaluate the importance of conjunctive parallel fiber and climbing fiber inputs. They show that both inputs are required to produce a sufficient Ca^{2+} elevation to trigger LTD.

Because of the role of the cerebellum in eyeblink classical conditioning, several signaling network models investigate whether temporal characteristics of classical conditioning can be explained by temporal characteristics of LTD in single Purkinje cells. Fiala et al. (1996) have developed the first model to explain adaptive timing of the eyeblink response in classical conditioning. They use a biochemical variant of spectral timing for their parallel fiber inputs, and also include the effect of Ca^{2+}-gated potassium channel activation on membrane voltage. They show that the phosphorylation state of target proteins responsible for LTD depends on the timing between climbing fiber and parallel fiber stimulation. Hellgren Kotaleski et al. (2002) include production of PKC activators by parallel fiber and climbing fiber stimulation in order to evaluate the relationship between LTD and behavior. Both Hellgren Kotaleski et al. (2002) and Doi et al. (2005) show that IP_3-dependent Ca^{2+} dynamics are sensitive to temporal interval between parallel fiber and climbing fiber stimulation. Hellgren Kotaleski et al. (2002) further demonstrate that PKC activation is sensitive to temporal interval between parallel fiber and climbing fiber inputs (which is analogous to classical conditioning being sensitive to temporal interval). The importance of conjunctive parallel fiber and climbing fiber inputs for Ca^{2+} elevation is confirmed using a multi-compartment, multi-channel Purkinje cell model by Ogasawara et al. (2007) which more accurately simulates Ca^{2+} influx through synaptic and voltage-gated ion channels. Steuber and Willshaw (2004) show that replacing the spectral timing mechanism with Ca^{2+}-dependent phosphorylation of mGluRs allows a single Purkinje cell to learn the adaptive timing of the eyeblink response.

More recent dual LTP and LTD models evaluate signaling network activation using spike-timing-dependent protocols (Graupner and Brunel, 2007; Urakubo et al., 2008). Urakubo et al. (2008) show that Ca^{2+} influx through NMDARs does not vary with spike timing (contrary to expectations) without suppression of NMDARs by Ca^{2+}-bound calmodulin. Graupner and Brunel (2007) have constructed models for Ca^{2+}/CaM-dependent autophosphorylation of CaMKII and PP1-dependent dephosphorylation of CaMKII. Graupner and Brunel (2007) show that CaMKII plays a central role in LTD because it is dephosphorylated during induction of LTD. More importantly, their bistable model can reproduce plasticity in response to STDP and high-frequency stimulation, without requiring abnormally low Ca^{2+} concentrations for dephosphorylation.

4. ANALYSIS AND DISCUSSION

This study provides an extensive overview of 117 computational models for postsynaptic signal transduction pathways in synaptic plasticity developed over the past 25 years through 2009. Our purpose is to categorize the models so that similarities and differences

are more readily apparent. Due to the large number of models, many models, though valuable, are excluded since they do not reach our criteria given in the beginning of Section 3. Some of the models included in this study are very simplified biochemical models meaning that a specific phenomenon is expressed using only a couple of reactions (see, e.g., Delord et al., 2007; Pi and Lisman, 2008). In the other extreme are the complex biophysical models that include detailed reaction–diffusion systems coupled to neuronal electrical activity (see, e.g., Bhalla, 2002a; Urakubo et al., 2008). Though model complexity has been increasing (**Figures 2 and 3**),

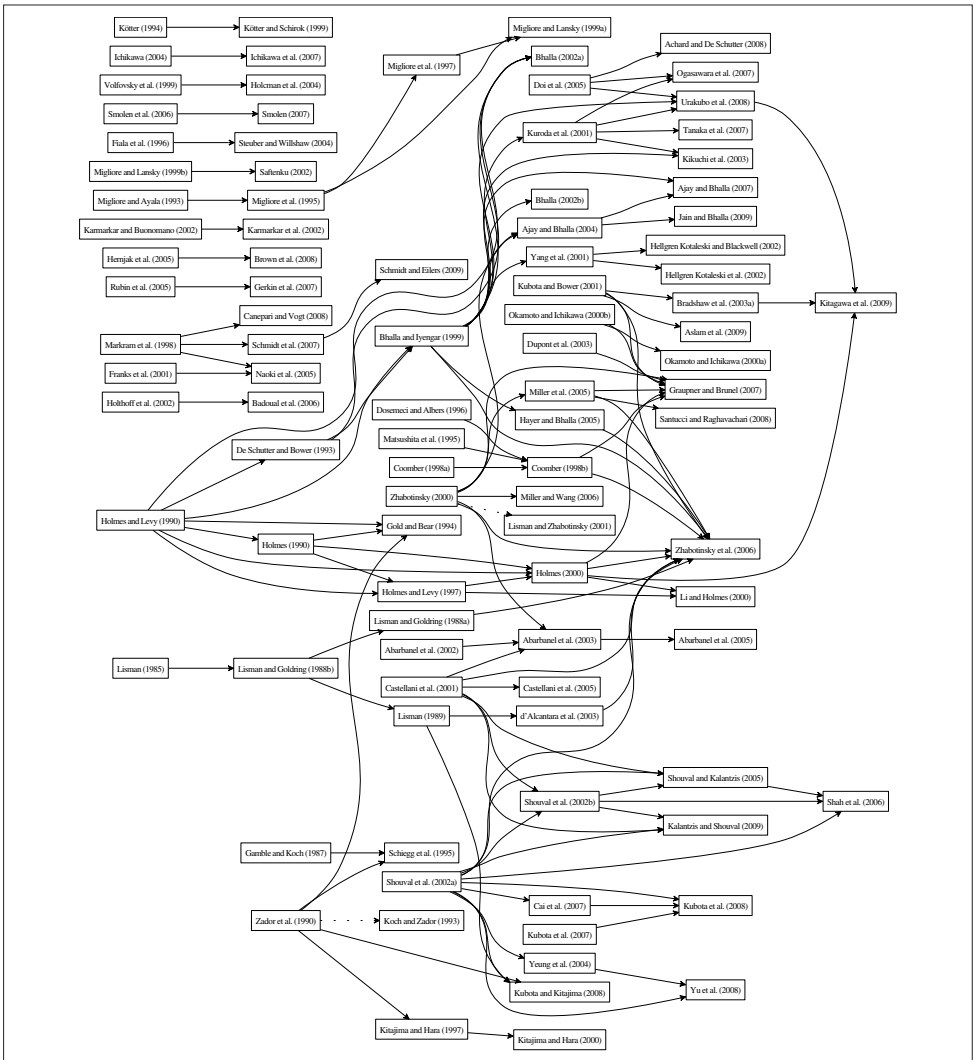

FIGURE 2 | Evolution of postsynaptic signal transduction models from 1985 to 2009. The starting point of an arrow represents the model which is used by the latter model indicated as the arrowhead. A dotted line in the arrow means that the two studies use exactly the same model (the latter study is not presented in **Tables 1–9**).

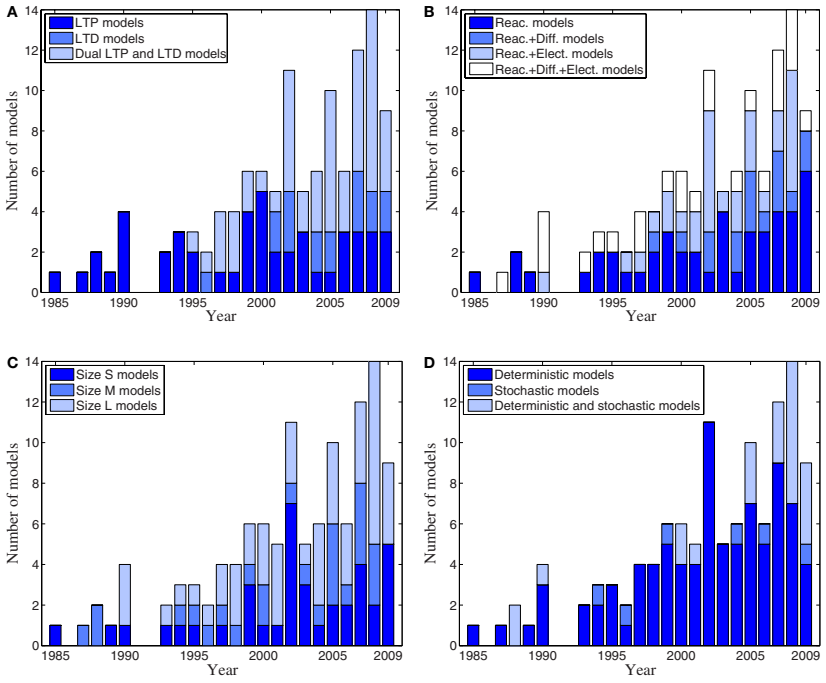

FIGURE 3 | Numbers of published postsynaptic signal transduction models per year from 1985 to 2009. (A) Numbers of LTP, LTD, and dual LTP and LTD models. **(B)** Numbers of reaction, reaction and diffusion, reaction and electrophysiological, as well as reaction, diffusion, and electrophysiological models. **(C)** Numbers of different size (S, M, and L) models. **(D)** Numbers of deterministic, stochastic, and deterministic and stochastic models.

the simpler biochemical models remain a valuable approach. They are relatively easy to construct, and the number of parameters to be fine-tuned is small. Not only are they computationally efficient, but they allow theoretical analysis and identification of which pathway, or combination of pathways, produces which property. On the other hand, models with detailed mechanisms are ideal for investigating which of several candidate molecules and mechanisms control or modulate a particular response. Furthermore, the direct correspondence between a detailed model and real neuron allows specific model predictions to be tested experimentally.

In our study, the emphasis is more on evaluating the model components and on the significance of the models rather than on comparison of the actual model responses. The comparison of model responses is not trivial because all models would need to be implemented and simulated before a comparative analysis could be performed (see also Pettinen et al., 2005). Indeed, this is not only time consuming, but impossible since many of the models are neither described in sufficient detail nor provided in model databases or by other open-access means (see **Table 8**). Even qualitative comparison is difficult since only a few publications provide a graphical illustration of the model components and in many cases it is difficult to interpret the model input or stimulus. These observations serve also as guidelines for reviewers evaluating future publications and models: (1) all models should be described in sufficient detail including equations, inputs, outputs, compartments, variables, constants, parameters, and initial conditions; (2) graphical illustration of the model should include only those model components that actually participate in simulations; (3) the simulation tool or programing language should be specified; and (4) the model should be provided in a model database. Nordlie et al. (2009) propose a good model description practice for neuronal network models. A similar description practice is needed for signal transduction models and our study is one step toward this, as is the BioModels Database project (Le Novère et al., 2006).

Every computational model needs to be stimulated to study evoked activity even though this aspect is not always clearly indicated in the publications. In other words, an input similar to the one given in experimental wet-lab studies or as in the physiological *in vivo* state is required. In many cases, however, it is a challenge to mimic the input used in experiments. The construction of input stimulus is quite straightforward in cases where biophysically detailed models and a high-frequency stimulation protocol are

Table 8 | Models provided in databases or by other open-access means.

Model	Simulation environment	Databases
Ajay and Bhalla (2004)	GENESIS/Kinetikit[a], MATLAB®, SBML[b]	DOQCS[c]
	SBML[b]	BioModels Database[d]
Ajay and Bhalla (2007)	GENESIS/Kinetikit[a], MATLAB®, SBML[b]	DOQCS[c]
	SBML[b]	BioModels Database[d]
Aslam et al. (2009)	MATLAB®	Supplementary material by Aslam et al. (2009)
Badoual et al. (2006)	NEURON[e]	ModelDB[f]
Bhalla and Iyengar (1999)	GENESIS/Kinetikit[a], MATLAB®, SBML[b]	DOQCS[c]
	SBML[b]	BioModels Database[d]
	SBML[b]	CellML[g]
Bhalla (2002b)	GENESIS/Kinetikit[a], MATLAB®, SBML[b]	DOQCS[c]
Brown et al. (2008)	Virtual Cell[h]	Virtual Cell[h]
Clopath et al. (2008)	Python	ModelDB[f]
Cornelisse et al. (2007)	CalC[i]	ModelDB[f]
d'Alcantara et al. (2003)	SBML[b]	BioModels Database[d]
Doi et al. (2005)	GENESIS/Kinetikit[a]	ModelDB[f]
Gerkin et al. (2007)	IGOR Pro[j]	ModelDB[f]
Graupner and Brunel (2007)	XPPAUT[k]	ModelDB[f]
Hayer and Bhalla (2005)	GENESIS/Kinetikit[a], GENESIS 3/MOOSE[l],	DOQCS[c]
	MATLAB®, SBML[b]	
Hernjak et al. (2005)	MathSBML[m]	Virtual Cell[h]
	MathSBML[m]	BioModels Database[d]
Ichikawa (2004)	A-Cell[n]	http://www.his.kanazawa-it.ac.jp/ –ichikawa/
		EnglishTop.html
Ichikawa et al. (2007)	A-Cell[n]	http://www.his.kanazawa-it.ac.jp/ –ichikawa/
		EnglishTop.html
Jain and Bhalla (2009)	GENESIS/Kinetikit[a], GENESIS 3/MOOSE[l]	DOQCS[c]
	XML	Supplementary material by Jain and Bhalla (2009)
Kitagawa et al. (2009)	SBML[b]	Supplementary material by Kitagawa et al. (2009)
Kuroda et al. (2001)	GENESIS/Kinetikit[a], MATLAB®, SBML[b]	DOQCS[c]
	GENESIS/Kinetikit[a]	http://www.cns.atr.jp/neuroinfo/kuroda/
	SBML[b]	BioModels Database[d]
Lindskog et al. (2006)	XPPAUT[k]	ModelDB[f]
Migliore and Lansky (1999b)	QuickBASIC	ModelDB[f]
Saftenku (2002)	NEURON[e]	ModelDB[f]
Schmidt and Eilers (2009)	Mathematica	Supplementary material by Schmidt and Eilers (2009)
Stefan et al. (2008)	BioPAX[o], CellML[g], SBML[b], Scilab[p],	BioModels Database[d]
	Virtual Cell[h], XPP[k]	
Urakubo et al. (2008)	GENESIS/Kinetikit[a]	ModelDB[f]
	GENESIS/Kinetikit[a]	http://www.bi.s.u-tokyo.ac.jp/kuroda-lab/info/
		STDP/index.html

[a]*GENESIS/Kinetikit (http://www.genesis-sim.org/GENESIS/; http://www.ncbs.res.in/index.php?option=com_content&task=view&id=307; Bower and Beeman, 1998; Bhalla, 2002c).*
[b]*SBML (http://sbml.org/).*
[c]*DOQCS (http://doqcs.ncbs.res.in/; Sivakumaran et al., 2003).*
[d]*BioModels Database (http://www.biomodels.net/; Le Novère et al., 2006).*
[e]*NEURON (http://www.neuron.yale.edu/neuron/; Carnevale and Hines, 2006).*
[f]*ModelDB (http://senselab.med.yale.edu/modeldb/; Migliore et al., 2003; Hines et al., 2004).*
[g]*CellML (http://www.cellml.org; Lloyd et al., 2008).*
[h]*Virtual Cell (http://vcell.org; Schaff et al., 1997; Slepchenko et al., 2003).*
[i]*CalC (http://web.njit.edu/–matveev/calc.html; Matveev et al., 2002).*
[j]*IGOR Pro (http://www.wavemetrics.com/).*
[k]*XPP, XPPAUT (http://www.math.pitt.edu/–bard/xpp/xpp.html; Ermentrout, 2002).*
[l]*GENESIS 3/MOOSE (http://www.genesis-sim.org/GENESIS/; http://moose.sourceforge.net/).*
[m]*MathSBML (http://sbml.org/Software/MathSBML).*
[n]*A-Cell (http://www.fujixerox.co.jp/crc/cng/A-Cell/; Ichikawa, 2001, 2005).*
[o]*BioPAX (http://www.biopax.org/; Luciano and Stevens, 2007).*
[p]*Scilab (http://www.scilab.org/; Gomez, 1999).*

used. In the other extreme are the models which use some function mimicking synaptic stimulus. This input type is not adequately described in many of the publications analyzed in the present study. This makes the reproduction of simulation results and the comparison of the models impossible. Therefore, the description of input stimuli should be taken into account when developing specific description language solutions for computational neuroscience and neuroinformatics.

Testing sensitivity to changes in parameter values is very important because many of the model parameters are not sufficiently constrained by experimental data. **Table 9** highlights the models that evaluate whether the simulation results are sensitive to changes in parameter values. In this study, small-scale testing means that values for 10 parameters or less (for example rate constants) are varied, and large-scale testing means that values for greater than 10 parameters are varied. **Table 9** shows that only a few models employ the large-scale testing of sensitivity to changes in parameter values. Publications that only test sensitivity to changes in input parameter values or do parameter estimation to fit experimental data, without analyzing the different model responses, are not included in **Table 9**.

In order to predict the future direction of the field, trends regarding the development of models of postsynaptic signal transduction pathways underlying LTP and LTD are illustrated (**Figures 2 and 3**). **Figure 2** shows how different models reviewed in this study have evolved from each other. Two models are connected in **Figure 2** if the publication either states directly that other models are used or the publication uses a subset of the exact same equations appearing in the older publications by the same authors. Models are excluded from **Figure 2** if there is no clear evidence that they have used some other model as the basis, or if they are only based on models not reviewed in this study. **Figure 2** shows that the models by Holmes and Levy (1990), Bhalla and Iyengar (1999), and Shouval et al. (2002a) are most often used as a starting point when developing new models. Zhabotinsky et al. (2006) and Graupner and Brunel (2007) cite the largest number of models when developing their models, but, on the other hand, they do not clearly state which parts of their model are taken from which other models.

Though LTP models appeared first, most of the new models are dual LTP and LTD models (**Figure 3A**), suggesting that these are being developed to investigate which characteristics of synaptic input patterns lead to LTP versus LTD. Despite limiting the review to models of signaling pathways, the models are extremely diverse in scope, with less than half including only reactions. Other models combine reactions and diffusion, or reactions and electrophysiological phenomena; about one-fifth have all three (**Figure 3B**). About one-third of the models are size small, meaning that there are less than 20 different chemical species or other model variables, and about half of the models are size large meaning that there are more than 50 different chemical species or other model variables (**Figure 3C**). The trend is toward increasing numbers of large models, reflecting both the increase in computational power and increasing knowledge of the biochemical pathways. Nonetheless, the continued development of small models reflects their utility in theoretical analysis. Most of the models are still deterministic even though stochastic methods have been developed more and more recently (**Figure 3D**). The scarcity of stochastic models compared to large models may reflect the availability of software modeling tools and analytic tools. However, several stochastic reaction–diffusion simulation tools have appeared recently (see, e.g., Kerr et al., 2008; Wils and De Schutter, 2009; Andrews et al., 2010; Byrne et al., 2010; Oliveira et al., 2010; Tolle and Le Novère, 2010b). Stochastic methods are important because very small numbers of molecules can have a dramatic effect on either strengthening or weakening the synapses and these effects should be taken into account. Another possibility is to develop and use so-called hybrid simulation methods where specific events are modeled as stochastic and others as deterministic. Though not illustrated graphically, only about one-fourth of the reviewed publications specify the simulation tool or programing language used. Most often the simulation tool used is GENESIS/Kinetikit (Bower and Beeman, 1998; Bhalla, 2002c), XPPAUT (Ermentrout, 2002), and NEURON (Carnevale and Hines, 2006). Programing languages most often used are Java and MATLAB®.

The trends in **Figure 3** lead to several predictions about the future of signaling pathway modeling. The first prediction is that both the number of large models and the size of the largest model will continue to increase. Thus, existing models will be expanded to include additional signaling pathways, in parallel with the increase in experimental data of additional molecular mechanisms. Second, the trend in **Figure 3D** suggests that increasing number of models will be implemented stochastically or using hybrid deterministic–stochastic

Table 9 | Models testing sensitivity to changes in parameter values.

Testing	Models
Small-scale	Holmes (1990, 2000), Holmes and Levy (1990), Gold and Bear (1994), Matsushita et al. (1995), Migliore et al. (1995), Schiegg et al. (1995), Dosemeci and Albers (1996), Fiala et al. (1996), Coomber (1998a,b), Volfovsky et al. (1999), Okamoto and Ichikawa (2000b), Zhabotinsky (2000), Kuroda et al. (2001), Hellgren Kotaleski et al. (2002), Karmarkar and Buonomano (2002), Shouval et al. (2002a,b), Abarbanel et al. (2003, 2005), d'Alcantara et al. (2003), Kikuchi et al. (2003), Hayer and Bhalla (2005), Hernjak et al. (2005), Miller et al. (2005), Naoki et al. (2005), Rubin et al. (2005), Lindskog et al. (2006), Smolen et al. (2006, 2008), Zhabotinsky et al. (2006), Cai et al. (2007), Cornelisse et al. (2007), Delord et al. (2007), Graupner and Brunel (2007), Ogasawara et al. (2007), Smolen (2007), Brown et al. (2008), Kubota and Kitajima (2008), Urakubo et al. (2008), Yu et al. (2008), Aslam et al. (2009), Castellani et al. (2009), Jain and Bhalla (2009), Kalantzis and Shouval (2009)
Large-scale	Bhalla and Iyengar (1999), Doi et al. (2005), Achard and De Schutter (2008), Kitagawa et al. (2009)

Small-scale testing means that values for 10 parameters or less (for example rate constants) are varied, and large-scale testing means that values for greater than 10 parameters are varied.

methods. The stochastic part of the models in particular may focus on events in the postsynaptic density and other multi-protein complexes. The third prediction is that the scope of the models will expand, with more models of dual LTP and LTD phenomena, in part because both phenomena have been measured in most cell types, and in part because the increase in size of the models is expanding to include signaling pathways for both phenomena. Related to the increase in scope of the models, more will blend reactions with diffusion or electrophysiological phenomena in order to study spatial aspects of signaling and also to better relate to experiments. In particular, modeling reactions alone is not sufficient for understanding synaptic plasticity but also electrophysiological phenomena needs to be taken into account by modeling neuronal networks (Hellgren Kotaleski and Blackwell, 2010). Further development of simulation tools (Pettinen et al., 2005; Alves et al., 2006) together with improvements in parallel computing should help in this endeavor.

Though the trend is toward larger and more complex models, this does not imply that all larger models are better than simpler models. As explained above, the quality of a model depends on many factors. Probably the most important criteria is whether the model can address a question of general scientific interest. For this reason, we have tried to organize our description of the models in order to highlight the questions addressed. Another related criteria is whether a model can make verifiable, i.e. falsifiable, predictions. Using these two criteria, models incorporating more biochemical details often appear superior, but only if the parameters can be adequately constrained. However, models which simplify the equations describing intracellular signaling pathways are more easily integrated with whole neuron electrophysiological models or able to simulate longer time frames. From this perspective they may excel for investigating whether different stimulation patterns change synaptic strength differently. It is important to note that earlier models may have been groundbreaking at the time of publication, yet their perceived quality decreases as more is learned about the interactions of intracellular molecules. Only a couple of studies reduce complex models to simpler ones and show comparative simulation results between the models (see, e.g., Hayer and Bhalla, 2005; Smolen, 2007). The reduction of model complexity will be an important research area in the future because simplified models that can capture relevant aspects of dynamics could be embedded, for example, into biologically-inspired neuronal network models when the activity of individual neurons is modeled in more detail.

To fully understand synaptic plasticity, many different characteristics of signaling pathways need to be considered. Temporal and spatial aspects of signaling are crucially important because they relate the cellular phenomenon of plasticity to the behavioral phenomenon of learning. Not only do theoreticians and modelers need to incorporate experimental findings, but also experimental progress can be enhanced by using model simulations to select the most promising experiments. Careful attention to these issues should improve the utility of modeling approaches for investigating molecular mechanisms of synaptic plasticity. The ultimate future goal of LTP and LTD modeling is to find such models for different brain regions and cells that can explain all the phases of synaptic plasticity, and then use these models to explain the differences in plasticity between brain regions or cell types. Many of the modeling studies have so far concentrated on only one type of synaptic plasticity. We believe that an analysis like the one provided by us will help in this endeavor to make more predictive models for synaptic plasticity in the future.

ACKNOWLEDGMENTS

This work was partly supported by research project grants from Academy of Finland [106030 and 124615 (Marja-Leena Linne), 126556 (Tiina Manninen), and 129657 (Finnish Programme for Centres of Excellence in Research 2006–2011)], Swedish Research Council (Jeanette Hellgren Kotaleski), the Parkinson's Foundation (Jeanette Hellgren Kotaleski), HFSP programme (Kim T. Blackwell), and the joint NSF-NIH CRCNS programme through NIH grant R01 AA16022 and R01 AA18060 (Kim T. Blackwell). Additional support was obtained from Finnish Foundation for Economic and Technology Sciences – KAUTE (Tiina Manninen), Otto A. Malm Foundation (Tiina Manninen and Katri Hituri), Emil Aaltonen Foundation (Katri Hituri), Finnish Foundation for Technology Promotion (Katri Hituri), and two graduate schools (Tampere University of Technology Graduate School and Tampere Doctoral Programme in Information Science and Engineering) (Katri Hituri).

REFERENCES

Abarbanel, H. D. I., Gibb, L., Huerta, R., and Rabinovich, M. I. (2003). Biophysical model of synaptic plasticity dynamics. *Biol. Cybern.* 89, 214–226.

Abarbanel, H. D. I., Huerta, R., and Rabinovich, M. I. (2002). Dynamical model of long-term synaptic plasticity. *Proc. Natl. Acad. Sci. U.S.A.* 99, 10132–10137.

Abarbanel, H. D. I., Talathi, S. S., Gibb, L., and Rabinovich, M. I. (2005). Synaptic plasticity with discrete state synapses. *Phys. Rev. E* 72, 031914.

Achard, P., and De Schutter, E. (2008). Calcium, synaptic plasticity and intrinsic homeostasis in Purkinje neuron models. *Front. Comput. Neurosci.* 2:8. doi: 10.3389/neuro.10.008.2008

Ajay, S. M., and Bhalla, U. S. (2004). A role for ERKII in synaptic pattern selectivity on the time-scale of minutes. *Eur. J. Neurosci.* 20, 2671–2680.

Ajay, S. M., and Bhalla, U. S. (2006). Synaptic plasticity in vitro and in silico: insights into an intracellular signaling maze. *Physiology* 21, 289–296.

Ajay, S. M., and Bhalla, U. S. (2007). A propagating ERKII switch forms zones of elevated dendritic activation correlated with plasticity. *HFSP J.* 1, 49–66.

Alves, R., Antunes, F., and Salvador, A. (2006). Tools for kinetic modeling of biochemical networks. *Nat. Biotechnol.* 24, 667–672.

Andrews, S. S., Addy, N. J., Brent, R., and Arkin, A. P. (2010). Detailed simulations of cell biology with Smoldyn 2.1. *PLoS Comput. Biol.* 6, e1000705. doi: 10.1371/journal.pcbi.1000705

Aslam, N., Kubota, Y., Wells, D., and Shouval, H. Z. (2009). Translational switch for long-term maintenance of synaptic plasticity. *Mol. Syst. Biol.* 5, 284.

Badoual, M., Zou, Q., Davison, A. P., Rudolph, M., Bal, T., Fregnac, Y., and Destexhe, A. (2006). Biophysical and phenomenological models of multiple spike interactions in spike-timing dependent plasticity. *Int. J. Neural Syst.* 16, 79–97.

Bhalla, U. S. (2002a). Biochemical signaling networks decode temporal patterns of synaptic input. *J. Comput. Neurosci.* 13, 49–62.

Bhalla, U. S. (2002b). Mechanisms for temporal tuning and filtering by postsynaptic signaling pathways. *Biophys. J.* 83, 740–752.

Bhalla, U. S. (2002c). "Use of Kinetikit and GENESIS for modeling signaling pathways," in *Methods in Enzymology*, Vol. 345, eds J. D. Hildebrandt and R. Iyengar (San Diego: Academic Press), 3–23.

Bhalla, U. S. (2009). "Molecules, networks, and memory," in *Systems Biology: The Challenge of Complexity*, 1st Edn., eds S. Nakanishi, R. Kageyama, and D. Watanabe (Tokyo: Springer), 151–158.

Bhalla, U. S., and Iyengar, R. (1999). Emergent properties of networks of biological signaling pathways. *Science* 283, 381–387.

Bi, G.-Q., and Poo, M.-M. (1998). Synaptic modifications in cultured hippocampal neurons: dependence on spike timing, synaptic strength, and postsynaptic cell type. *J. Neurosci.* 18, 10464–10472.

Bi, G.-Q., and Rubin, J. (2005). Timing in synaptic plasticity: from detection to integration. *Trends Neurosci.* 28, 222–228.

Blackwell, K. T., and Hellgren Kotaleski, J. (2002). "Modeling the dynamics of second messenger pathways," in *Neuroscience Databases: A Practical Guide*, ed. R. Kötter (Norwell, MA: Kluwer Academic Publishers), 63–80.

Bliss, T. V. P., and Collingridge, G. L. (1993). A synaptic model of memory: long-term potentiation in the hippocampus. *Nature* 361, 31–39.

Bliss, T. V. P., and Gardner-Medwin, A. R. (1973). Long-lasting potentiation of synaptic transmission in the dentate area of the unanaesthetized rabbit following stimulation of the perforant path. *J. Physiol.* 232, 357–374.

Bliss, T. V. P., and Lømo, T. (1973). Long-lasting potentiation of synaptic transmission in the dentate area of the anaesthetized rabbit following stimulation of the perforant path. *J. Physiol.* 232, 331–356.

Blitzer, R. D., Iyengar, R., and Landau, E. M. (2005). Postsynaptic signaling networks: cellular cogwheels underlying long-term plasticity. *Biol. Psychiatry* 57, 113–119.

Bower, J. M., and Beeman, D. (1998). *The Book of GENESIS: Exploring Realistic Neural Models with the GEneral NEural SImulation System*, 2nd Edn. New York: Telos/Springer-Verlag.

Bradshaw, J. M., Kubota, Y., Meyer, T., and Schulman, H. (2003a). An ultrasensitive Ca^{2+}/calmodulin-dependent protein kinase II-protein phosphatase 1 switch facilitates specificity in postsynaptic calcium signaling. *Proc. Natl. Acad. Sci. U.S.A.* 100, 10512–10517.

Bradshaw, K. D., Emptage, N. J., and Bliss, T. V. P. (2003b). A role for dendritic protein synthesis in hippocampal late LTP. *Eur. J. Neurosci.* 18, 3150–3152.

Brown, S.-A., Morgan, F., Watras, J., and Loew, L. M. (2008). Analysis of phosphatidylinositol-4,5-bisphosphate signaling in cerebellar Purkinje spines. *Biophys. J.* 95, 1795–1812.

Brown, T. H., Kairiss, E. W., and Keenan, C. L. (1990). Hebbian synapses: biophysical mechanisms and algorithms. *Annu. Rev. Neurosci.* 13, 475–511.

Bruel-Jungerman, E., Davis, S., and Laroche, S. (2007). Brain plasticity mechanisms and memory: a party of four. *Neuroscientist* 13, 492–505.

Byrne, M. J., Putkey, J. A., Waxham, M. N., and Kubota, Y. (2009). Dissecting cooperative calmodulin binding to CaM kinase II: a detailed stochastic model. *J. Comput. Neurosci.* 27, 621–638.

Byrne, M. J., Waxham, M. N., and Kubota, Y. (2010). Cellular dynamic simulator: an event driven molecular simulation environment for cellular physiology. *Neuroinformatics* 8, 63–82.

Cai, Y., Gavornik, J. P., Cooper, L. N., Yeung, L. C., and Shouval, H. Z. (2007). Effect of stochastic synaptic and dendritic dynamics on synaptic plasticity in visual cortex and hippocampus. *J. Neurophysiol.* 97, 375–386.

Canepari, M., and Vogt, K. E. (2008). Dendritic spike saturation of endogenous calcium buffer and induction of postsynaptic cerebellar LTP. *PLoS ONE* 3, e4011. doi: 10.1371/journal.pone.0004011

Carnevale, T., and Hines, M. (2006). *The NEURON Book*, 1st Edn. Cambridge, UK: Cambridge University Press.

Castellani, G. C., Bazzani, A., and Cooper, L. N. (2009). Toward a microscopic model of bidirectional synaptic plasticity. *Proc. Natl. Acad. Sci. U.S.A.* 106, 14091–14095.

Castellani, G. C., Quinlan, E. M., Bersani, F., Cooper, L. N., and Shouval, H. Z. (2005). A model of bidirectional synaptic plasticity: from signaling network to channel conductance. *Learn. Mem.* 12, 423–432.

Castellani, G. C., Quinlan, E. M., Cooper, L. N., and Shouval, H. Z. (2001). A biophysical model of bidirectional synaptic plasticity: dependence on AMPA and NMDA receptors. *Proc. Natl. Acad. Sci. U.S.A.* 98, 12772–12777.

Castellani, G. C., and Zironi, I. (2010). "Biophysics-based models of LTP/LTD," in *Hippocampal Microcircuits: A Computational Modeler's Resource Book*, eds V. Cutsuridis, B. Graham, S. Cobb, and I. Vida (New York: Springer), 555–570.

Citri, A., and Malenka, R. C. (2008). Synaptic plasticity: multiple forms, functions, and mechanisms. *Neuropsychopharmacology* 33, 18–41.

Clopath, C., Büsing, L., Vasilaki, E., and Gerstner, W. (2010). Connectivity reflects coding: a model of voltage-based STDP with homeostasis. *Nat. Neurosci.* 13, 344–352.

Clopath, C., Ziegler, L., Vasilaki, E., Büsing, L., and Gerstner, W. (2008). Tag-trigger-consolidation: a model of early and late long-term-potentiation and depression. *PLoS Comput. Biol.* 4, e1000248. doi: 10.1371/journal.pcbi.1000248

Cooke, S. F., and Bliss, T. V. P. (2006). Plasticity in the human central nervous system. *Brain* 129, 1659–1673.

Coomber, C. (1997). A model of associative long-term potentiation and long-term depression in a compartmental reconstruction of a neuron. *Neurocomputing* 16, 189–205.

Coomber, C. (1998a). Current theories of neuronal information processing performed by Ca^{2+}/calmodulin-dependent protein kinase II with support and insights from computer modelling and simulation. *Comput. Chem.* 22, 251–263.

Coomber, C. J. (1998b). Site-selective autophosphorylation of Ca^{2+}/calmodulin-dependent protein kinase II as a synaptic encoding mechanism. *Neural Comput.* 10, 1653–1678.

Cornelisse, L. N., van Elburg, R. A. J., Meredith, R. M., Yuste, R., and Mansvelder, H. D. (2007). High speed two-photon imaging of calcium dynamics in dendritic spines: consequences for spine calcium kinetics and buffer capacity. *PLoS ONE* 2, e1073. doi: 10.1371/journal.pone.0001073

d'Alcantara, P., Schiffmann, S. N., and Swillens, S. (2003). Bidirectional synaptic plasticity as a consequence of interdependent Ca^{2+}-controlled phosphorylation and dephosphorylation pathways. *Eur. J. Neurosci.* 17, 2521–2528.

Dan, Y., and Poo, M.-M. (2006). Spike timing-dependent plasticity: from synapse to perception. *Physiol. Rev.* 86, 1033–1048.

Delord, B., Berry, H., Guigon, E., and Genet, S. (2007). A new principle for information storage in an enzymatic pathway model. *PLoS Comput. Biol.* 3, e124. doi: 10.1371/journal.pcbi.0030124

De Schutter, E., and Bower, J. M. (1993). Sensitivity of synaptic plasticity to the Ca^{2+} permeability of NMDA channels: a model of long-term potentiation in hippocampal neurons. *Neural Comput.* 5, 681–694.

De Schutter, E., and Bower, J. M. (1994a). An active membrane model of the cerebellar Purkinje cell. I. Simulation of current clamps in slice. *J. Neurophysiol.* 71, 375–400.

De Schutter, E., and Bower, J. M. (1994b). An active membrane model of the cerebellar Purkinje Cell. II. Simulation of synaptic responses. *J. Neurophysiol.* 71, 401–419.

Doi, T., Kuroda, S., Michikawa, T., and Kawato, M. (2005). Inositol 1,4,5-trisphosphate-dependent Ca^{2+} threshold dynamics detect spike timing in cerebellar Purkinje cells. *J. Neurosci.* 25, 950–961.

Dosemeci, A., and Albers, R. W. (1996). A mechanism for synaptic frequency detection through autophosphorylation of CaM kinase II. *Biophys. J.* 70, 2493–2501.

Dudek, S. M., and Bear, M. F. (1992). Homosynaptic long-term depression in area CA1 of hippocampus and effects of *N*-methyl-D-aspartate receptor blockade. *Proc. Natl. Acad. Sci. U.S.A.* 89, 4363–4367.

Dupont, G., Houart, G., and De Koninck, P. (2003). Sensitivity of CaM kinase II to the frequency of Ca^{2+} oscillations: a simple model. *Cell Calcium* 34, 485–497.

Engelman, M. S. (1982). FIDAP (A Fluid Dynamics Analysis Program). *Adv. Eng. Softw.* (1978) 4, 163–166.

Engelman, M. S. (1996). *FIDAP Theoretical Manual*, Version 7.5. Evanston, IL: Fluid Dynamics Inc.

Ermentrout, B. (2002). *Simulating, Analyzing, and Animating Dynamical Systems: A Guide to XPPAUT for Researchers and Students*, 1st Edn. Philadelphia: Society for Industrial and Applied Mathematics (SIAM).

Fernandez, É., Schiappa, R., Girault, J.-A., and Le Novère, N. (2006). DARPP-32 is a robust integrator of dopamine and glutamate signals. *PLoS Comput. Biol.* 2, e176. doi: 10.1371/journal.pcbi.0020176

Fiala, J. C., Grossberg, S., and Bullock, D. (1996). Metabotropic glutamate receptor activation in cerebellar Purkinje cells as substrate for adaptive timing of the classically conditioned eye-blink response. *J. Neurosci.* 16, 3760–3774.

Franks, K. M., Bartol, T. M., and Sejnowski, T. J. (2001). An MCell model of calcium dynamics and frequency-dependence of calmodulin activation in dendritic spines. *Neurocomputing* 38–40, 9–16.

Gamble, E., and Koch, C. (1987). The dynamics of free calcium in dendritic spines in response to repetitive synaptic input. *Science* 236, 1311–1315.

Gerdeman, G. L., and Lovinger, D. M. (2003). Emerging roles for endocannabinoids in long-term synaptic plasticity. *Br. J. Pharmacol.* 140, 781–789.

Gerkin, R. C., Bi, G.-Q., and Rubin, J. E. (2010). "A phenomenological calcium-based model of STDP," in *Hippocampal Microcircuits: A Computational Modeler's Resource Book*, eds V. Cutsuridis, B. Graham, S. Cobb, and I. Vida (New York: Springer), 571–591.

Gerkin, R. C., Lau, P.-M., Nauen, D. W., Wang, Y. T., and Bi, G.-Q. (2007). Modular competition driven by NMDA receptor subtypes in spike-timing-dependent plasticity. *J. Neurophysiol.* 97, 2851–2862.

Gewaltig, M. O., and Diesmann, M. (2007). NEST (neural simulation tool). *Scholarpedia* 2, 1430.

Gillespie, D. T. (1976). A general method for numerically simulating the stochastic time evolution of coupled chemical reactions. *J. Comput. Phys.* 22, 403–434.

Gillespie, D. T. (1977). Exact stochastic simulation of coupled chemical reactions. *J. Phys. Chem.* 81, 2340–2361.

Gold, J. I., and Bear, M. F. (1994). A model of dendritic spine Ca^{2+} concentration exploring possible bases for a sliding synaptic modification threshold. *Proc. Natl. Acad. Sci. U.S.A.* 91, 3941–3945.

Gomez, C. (Ed.). (1999). Engineering, and Scientific Computing with Scilab. Boston: Birkhäuser.

Graupner, M., and Brunel, N. (2007). STDP in a bistable synapse model based on CaMKII and associated signaling pathways. *PLoS Comput. Biol.* 3, e221. doi: 10.1371/journal.pcbi.0030221

Graupner, M., and Brunel, N. (2010). Mechanisms of induction and maintenance of spike-timing dependent plasticity in biophysical synapse models. *Front. Comput. Neurosci.* 4:136. doi:10.3389/fncom.2010.00136

Hayer, A., and Bhalla, U. S. (2005). Molecular switches at the synapse emerge from receptor and kinase traffic. *PLoS Comput. Biol.* 1, e20. doi: 10.1371/journal.pcbi.0010020

Helias, M., Rotter, S., Gewaltig, M.-O., and Diesmann, M. (2008). Structural plasticity controlled by calcium based correlation detection. *Front. Comput. Neurosci.* 2:7. doi: 10.3389/neuro.10.007.2008

Hellgren Kotaleski, J., and Blackwell, K. T. (2002). Sensitivity to interstimulus interval due to calcium interactions in the Purkinje cell spines. *Neurocomputing* 44–46, 13–18.

Hellgren Kotaleski, J., and Blackwell, K. T. (2010). Modelling the molecular mechanisms of synaptic plasticity using systems biology approaches. *Nat. Rev. Neurosci.* 11, 239–251.

Hellgren Kotaleski, J., Lester, D., and Blackwell, K. T. (2002). Subcellular interactions between parallel fibre and climbing fibre signals in Purkinje cells predict sensitivity of classical conditioning to interstimulus interval. *Integr. Physiol. Behav. Sci.* 37, 265–292.

Hernjak, N., Slepchenko, B. M., Fernald, K., Fink, C. C., Fortin, D., Moraru, I. I., Watras, J., and Loew, L. M. (2005). Modeling and analysis of calcium signaling events leading to long-term depression in cerebellar Purkinje cells. *Biophys. J.* 89, 3790–3806.

Hines, M. L., Morse, T., Migliore, M., Carnevale, N. T., and Shepherd, G. M. (2004). ModelDB: a database to support computational neuroscience. *J. Comput. Neurosci.* 17, 7–11.

Holcman, D., Schuss, Z., and Korkotian, E. (2004). Calcium dynamics in dendritic spines and spine motility. *Biophys. J.* 87, 81–91.

Holmes, W. R. (1990). Is the function of dendritic spines to concentrate calcium? *Brain Res.* 519, 338–342.

Holmes, W. R. (2000). Models of calmodulin trapping and CaM kinase II activation in a dendritic spine. *J. Comput. Neurosci.* 8, 65–86.

Holmes, W. R. (2005). "Calcium signaling in dendritic spines," in *Modeling in the Neurosciences: From Biological Systems to Neuromimetic Robotics*, 2nd Edn., eds G. N. Reeke, R. R. Poznanski, K. A. Lindsay, J. R. Rosenberg, and O. Sporns (Boca Raton: CRC Press), 25–60.

Holmes, W. R., and Levy, W. B. (1990). Insights into associative long-term potentiation from computational models of NMDA receptor-mediated calcium influx and intracellular calcium concentration changes. *J. Neurophysiol.* 63, 1148–1168.

Holmes, W. R., and Levy, W. B. (1997). Quantifying the role of inhibition in associative long-term potentiation in dentate granule cells with computational models. *J. Neurophysiol.* 78, 103–116.

Holthoff, K., Tsay, D., and Yuste, R. (2002). Calcium dynamics of spines depend on their dendritic location. *Neuron* 33, 425–437.

Hoops, S., Sahle, S., Gauges, R., Lee, C., Pahle, J., Simus, N., Singhai, M., Xu, L., Mendes, P., and Kummer, U. (2006). COPASI – a complex pathway simulator. *Bioinformatics* 22, 3067–3074.

Hudmon, A., and Schulman, H. (2002a). Neuronal Ca^{2+}/calmodulin-dependent protein kinase II: the role of structure and autoregulation in cellular function. *Annu. Rev. Biochem.* 71, 473–510.

Hudmon, A., and Schulman, H. (2002b). Structure-function of the multifunctional Ca^{2+}/calmodulin-dependent protein kinase II. *Biochem. J.* 364(Pt 3), 593–611.

Ichikawa, K. (2001). A-Cell: graphical user interface for the construction of biochemical reaction models. *Bioinformatics* 17, 483–484.

Ichikawa, K. (2004). Localization of activated Ca^{2+}/calmodulin-dependent protein kinase II within a spine: modeling and computer simulation. *Neurocomputing* 58–60, 443–448.

Ichikawa, K. (2005). A modeling environment with three-dimensional morphology, A-Cell-3D, and Ca^{2+} dynamics in a spine. *Neuroinformatics* 3, 49–63.

Ichikawa, K., Hoshino, A., and Kato, K. (2007). Induction of synaptic depression by high-frequency stimulation in area CA1 of the rat hippocampus: modeling and experimental studies. *Neurocomputing* 70, 2055–2059.

Ito, M. (1989). Long-term depression. *Annu. Rev. Neurosci.* 12, 85–102.

Ito, M. (2001). Cerebellar long-term depression: characterization, signal transduction, and functional roles. *Physiol. Rev.* 81, 1143–1195.

Ito, M. (2002). The molecular organization of cerebellar long-term depression. *Nat. Rev. Neurosci.* 3, 896–902.

Ito, M., Sakurai, M., and Tongroach, P. (1982). Climbing fiber induced depression of both mossy fiber responsiveness and glutamate sensitivity of cerebellar Purkinje cells. *J. Physiol.* 324, 113–124.

Jain, P., and Bhalla, U. S. (2009). Signaling logic of activity-triggered dendritic protein synthesis: an mTOR gate but not a feedback switch. *PLoS Comput. Biol.* 5, e1000287. doi: 10.1371/journal.pcbi.1000287

Kalantzis, G., and Shouval, H. Z. (2009). Structural plasticity can produce metaplasticity. *PLoS ONE* 4, e8062. doi: 10.1371/journal.pone.0008062

Karmarkar, U. R., and Buonomano, D. V. (2002). A model of spike-timing dependent plasticity: one or two coincidence detectors? *J. Neurophysiol.* 88, 507–513.

Karmarkar, U. R., Najarian, M. T., and Buonomano, D. V. (2002). Mechanisms and significance of spike-timing dependent plasticity. *Biol. Cybern.* 87, 373–382.

Kauderer, B. S., and Kandel, E. R. (2000). Capture of a protein synthesis-dependent component of long-term depression. *Proc. Natl. Acad. Sci. U.S.A.* 97, 13342–13347.

Keller, D. X., Franks, K. M., Bartol, Jr., T. M., and Sejnowski, T. J. (2008). Calmodulin activation by calcium transients in the postsynaptic density of dendritic spines. *PLoS ONE* 3, e2045. doi: 10.1371/journal.pone.0002045

Kerr, R. A., Bartol, T. M., Kaminsky, B., Dittrich, M., Chang, J.-C. J., Baden, S. B., Sejnowski, T. J., and Stiles, J. R. (2008). Fast Monte Carlo simulation methods for biological reaction–diffusion systems in solution and on surfaces. *SIAM J. Sci. Comput.* 30, 3126–3149.

Kikuchi, S., Fujimoto, K., Kitagawa, N., Fuchikawa, T., Abe, M., Oka, K., Takei, K., and Tomita, M. (2003). Kinetic simulation of signal transduction system in hippocampal long-term potentiation with dynamic modeling of protein phosphatase 2A. *Neural Netw.* 16, 1389–1398.

Kim, M. S., Huang, T., Abel, T., and Blackwell, K. T. (2010). Temporal sensitivity of protein kinase A activation in late-phase long term potentiation. *PLoS Comput. Biol.* 6, e1000691. doi: 10.1371/journal.pcbi.1000691

Kitagawa, Y., Hirano, T., and Kawaguchi, S.-Y. (2009). Prediction and validation of a mechanism to control the threshold for inhibitory synaptic plasticity. *Mol. Syst. Biol.* 5, 280.

Kitajima, T., and Hara, K. (1990). A model of the mechanisms of long-term potentiation in the hippocampus. *Biol. Cybern.* 64, 33–39.

Kitajima, T., and Hara, K. (2000). A generalized Hebbian rule for activity-dependent synaptic modifications. *Neural Netw.* 13, 445–454.

Kitajima, T., and Hara, K.-I. (1997). An integrated model for activity-dependent synaptic modifications. *Neural Netw.* 10, 413–421.

Klann, E., Chen, S. J., and Sweatt, J. D. (1993). Mechanism of protein kinase C activation during the induction and maintenance of long-term potentiation probed using a selective peptide substrate. *Proc. Natl. Acad. Sci. U.S.A.* 90, 8337–8341.

Klipp, E., and Liebermeister, W. (2006). Mathematical modeling of intracellular signaling pathways. *BMC Neurosci.* 7(Suppl. 1), S10.

Koch, C., and Zador, A. (1993). The function of dendritic spines: devices subserving biochemical rather than electrical compartmentalization. *J. Neurosci.* 13, 413–422.

Kötter, R. (1994). Postsynaptic integration of glutamatergic and dopaminergic signals in the striatum. *Prog. Neurobiol.* 44, 163–196.

Kötter, R., and Schirok, D. (1999). Towards an integration of biochemical and biophysical models of neuronal information processing: a case study in the nigro-striatal system. *Rev. Neurosci.* 10, 247–266.

Kubota, S., and Kitajima, T. (2008). A model for synaptic development regulated by NMDA receptor subunit expression. *J. Comput. Neurosci.* 24, 1–20.

Kubota, S., and Kitajima, T. (2010). Possible role of cooperative action of NMDA receptor and GABA function in developmental plasticity. *J. Comput. Neurosci.* 28, 347–359.

Kubota, Y., and Bower, J. M. (1999). Decoding time-varying calcium signals by the postsynaptic biochemical network: computer simulations of molecular kinetics. *Neurocomputing* 26–27, 29–38.

Kubota, Y., and Bower, J. M. (2001). Transient versus asymptotic dynamics of CaM kinase II: possible roles of phosphatase. *J. Comput. Neurosci.* 11, 263–279.

Kubota, Y., Putkey, J. A., Shouval, H. Z., and Waxham, M. N. (2008). IQ-motif proteins influence intracellular free Ca^{2+} in hippocampal neurons through their interactions with calmodulin. *J. Neurophysiol.* 99, 264–276.

Kubota, Y., Putkey, J. A., and Waxham, M. N. (2007). Neurogranin controls the

spatiotemporal pattern of postsynaptic Ca^{2+}/CaM signaling. *Biophys. J.* 93, 3848–3859.

Kuroda, S., Schweighofer, N., and Kawato, M. (2001). Exploration of signal transduction pathways in cerebellar long-term depression by kinetic simulation. *J. Neurosci.* 21, 5693–5702.

Lanté, F., de Jésus Ferreira, M.-C., Guiramand, J., Récasens, M., and Vignes, M. (2006). Low-frequency stimulation induces a new form of LTP, metabotropic glutamate ($mGlu_5$) receptor- and PKA-dependent, in the CA1 area of the rat hippocampus. *Hippocampus* 16, 345–360.

Le Novère, N., Bornstein, B., Broicher, A., Courtot, M., Donizelli, M., Dharuri, H., Li, L., Sauro, H., Schilstra, M., Shapiro, B., Snoep, J. L., and Hucka, M. (2006). BioModels Database: a free, centralized database of curated, published, quantitative kinetic models of biochemical and cellular systems. *Nucleic Acids Res.* 34, D689–D691.

Li, Y., and Holmes, W. R. (2000). Comparison of CaMKinase II activation in a dendritic spine computed with deterministic and stochastic models of the NMDA synaptic conductance. *Neurocomputing* 32–33, 1–7.

Lindskog, M., Kim, M., Wikström, M. A., Blackwell, K. T., and Hellgren Kotaleski, J. (2006). Transient calcium and dopamine increase PKA activity and DARPP-32 phosphorylation. *PLoS Comput. Biol.* 2, e119. doi: 10.1371/journal.pcbi.0020119

Lisman, J. (1989). A mechanism for the Hebb and the anti-Hebb processes underlying learning and memory. *Proc. Natl. Acad. Sci. U.S.A.* 86, 9574–9578.

Lisman, J., and Goldring, M. A. (1988a). Evaluation of a model of long-term memory based on the properties of the Ca^{2+}/calmodulin-dependent protein kinase. *J. Physiol. (Paris)* 83, 187–197.

Lisman, J. E., and Goldring, M. A. (1988b). Feasibility of long-term storage of graded information by the Ca^{2+}/calmodulin-dependent protein kinase molecules of the postsynaptic density. *Proc. Natl. Acad. Sci. U.S.A.* 85, 5320–5324.

Lisman, J., Schulman, H., and Cline, H. (2002). The molecular basis of CaMKII function in synaptic and behavioural memory. *Nat. Rev. Neurosci.* 3, 175–190.

Lisman, J. E. (1985). A mechanism for memory storage insensitive to molecular turnover: a bistable autophosphorylating kinase. *Proc. Natl. Acad. Sci. U.S.A.* 82, 3055–3057.

Lisman, J. E., and Zhabotinsky, A. M. (2001). A model of synaptic memory: a CaMKII/PP1 switch that potentiates transmission by organizing an AMPA receptor anchoring assembly. *Neuron* 31, 191–201.

Lloyd, C. M., Lawson, J. R., Hunter, P. J., and Nielsen, P. F. (2008). The CellML model repository. *Bioinformatics* 24, 2122–2123.

Luciano, J. S., and Stevens, R. D. (2007). e-Science and biological pathway semantics. *BMC Bioinformatics* 8(Suppl. 3), S3.

Malenka, R. C., and Bear, M. F. (2004). LTP and LTD: an embarrassment of riches. *Neuron* 44, 5–21.

Malenka, R. C., and Nicoll, R. A. (1999). Long-term potentiation – a decade of progress? *Science* 285, 1870–1874.

Malinow, R., Schulman, H., and Tsien, R. W. (1989). Inhibition of postsynaptic PKC or CaMKII blocks induction but not expression of LTP. *Science* 245, 862–866.

Markram, H., Lübke, J., Frotscher, M., and Sakmann, B. (1997). Regulation of synaptic efficacy by coincidence of postsynaptic APs and EPSPs. *Science* 275, 213–215.

Markram, H., Roth, A., and Helmchen, F. (1998). Competitive calcium binding: implications for dendritic calcium signaling. *J. Comput. Neurosci.* 5, 331–348.

Matsushita, T., Moriyama, S., and Fukai, T. (1995). Switching dynamics and the transient memory storage in a model enzyme network involving Ca^{2+}/calmodulin-dependent protein kinase II in synapses. *Biol. Cybern.* 72, 497–509.

Matveev, V., Sherman, A., and Zucker, R. S. (2002). New and corrected simulations of synaptic facilitation. *Biophys. J.* 83, 1368–1373.

Michelson, S., and Schulman, H. (1994). CaM kinase: a model for its activation and dynamics. *J. Theor. Biol.* 171, 281–290.

Migliore, M., Alicata, F., and Ayala, G. F. (1995). A model for long-term potentiation and depression. *J. Comput. Neurosci.* 2, 335–343.

Migliore, M., Alicata, F., and Ayala, G. F. (1997). Possible roles of retrograde messengers on LTP, LTD, and associative memory. *Biosystems* 40, 127–132.

Migliore, M., and Ayala, G. F. (1993). A kinetic model of short- and long-term potentiation. *Neural Comput.* 5, 636–647.

Migliore, M., and Lansky, P. (1999a). Computational model of the effects of stochastic conditioning on the induction of long-term potentiation and depression. *Biol. Cybern.* 81, 291–298.

Migliore, M., and Lansky, P. (1999b). Long-term potentiation and depression induced by a stochastic conditioning of a model synapse. *Biophys. J.* 77, 1234–1243.

Migliore, M., Morse, T. M., Davison, A. P., Marenco, L., Shepherd, G. M., and Hines, M. L. (2003). ModelDB: making models publicly accessible to support computational neuroscience. *Neuroinformatics* 1, 135–139.

Miller, P., and Wang, X.-J. (2006). Stability of discrete memory states to stochastic fluctuations in neuronal systems. *Chaos* 16, 026109.

Miller, P., Zhabotinsky, A. M., Lisman, J. E., and Wang, X.-J. (2005). The stability of a stochastic CaMKII switch: dependence on the number of enzyme molecules and protein turnover. *PLoS Biol.* 3, e107. doi: 10.1371/journal.pbio.0030107

Morrison, A., Diesmann, M., and Gerstner, W. (2008). Phenomenological models of synaptic plasticity based on spike timing. *Biol. Cybern.* 98, 459–478.

Murzina, G. B. (2004). Mathematical simulation of the induction of long-term depression in cerebellar Purkinje cells. *Neurosci. Behav. Physiol.* 34, 115–121.

Murzina, G. B., and Silkis, I. G. (1998). Studies of long-term potentiation and depression of inhibitory transmission by mathematical modeling of postsynaptic processes. *Neurosci. Behav. Physiol.* 28, 121–129.

Nakano, T., Doi, T., Yoshimoto, J., and Doya, K. (2010). A kinetic model of dopamine- and calcium-dependent striatal synaptic plasticity. *PLoS Comput. Biol.* 6, e1000670. doi: 10.1371/journal.pcbi.1000670

Naoki, H., Sakumura, Y., and Ishii, S. (2005). Local signaling with molecular diffusion as a decoder of Ca^{2+} signals in synaptic plasticity. *Mol. Syst. Biol.* 1, 2005.0027.

Neher, E. (1998). Usefulness and limitations of linear approximations to the understanding of Ca^{2+} signals. *Cell Calcium* 24, 345–357.

Nicholls, R. E., Alarcon, J. M., Malleret, G., Carroll, R. C., Grody, M., Vronskaya, S., and Kandel, E. R. (2008). Transgenic mice lacking NMDAR-dependent LTD exhibit deficits in behavioral flexibility. *Neuron* 58, 104–117.

Nordlie, E., Gewaltig, M.-O., and Plesser, H. E. (2009). Towards reproducible descriptions of neuronal network models. *PLoS Comput. Biol.* 5, e1000456. doi: 10.1371/journal.pcbi.1000456

Ogasawara, H., Doi, T., Doya, K., and Kawato, M. (2007). Nitric oxide regulates input specificity of long-term depression and context dependence of cerebellar learning. *PLoS Comput. Biol.* 3, e179. doi: 10.1371/journal.pcbi.0020179

Ogasawara, H., Doi, T., and Kawato, M. (2008). Systems biology perspectives on cerebellar long-term depression. *Neurosignals* 16, 300–317.

Ogasawara, H., and Kawato, M. (2009). "Computational models of cerebellar long-term memory," in *Systems Biology: The Challenge of Complexity*, 1st Edn., eds S. Nakanishi, R. Kageyama, and D. Watanabe (Tokyo: Springer), 169–182.

Okamoto, H., and Ichikawa, K. (2000a). A model for molecular mechanisms of synaptic competition for a finite resource. *Biosystems* 55, 65–71.

Okamoto, H., and Ichikawa, K. (2000b). Switching characteristics of a model for biochemical-reaction networks describing autophosphorylation versus dephosphorylation of Ca^{2+}/calmodulin-dependent protein kinase II. *Biol. Cybern.* 82, 35–47.

Oliveira, R. F., Terrin, A., Di Benedetto, G., Cannon, R. C., Koh, W., Kim, M., Zaccolo, M., and Blackwell, K. T. (2010). The role of type 4 phosphodiesterases in generating microdomains of cAMP: large scale stochastic simulations. *PLoS ONE* 5, e11725. doi: 10.1371/journal.pone.0011725

Pepke, S., Kinzer-Ursem, T., Mihalas, S., and Kennedy, M. B. (2010). A dynamic model of interactions of Ca^{2+}, calmodulin, and catalytic subunits of Ca^{2+}/calmodulin-dependent protein kinase II. *PLoS Comput. Biol.* 6, e1000675. doi: 10.1371/journal.pcbi.1000675

Pettinen, A., Aho, T., Smolander, O.-P., Manninen, T., Saarinen, A., Taattola, K.-L., Yli-Harja, O., and Linne, M.-L. (2005). Simulation tools for biochemical networks: evaluation of performance and usability. *Bioinformatics* 21, 357–363.

Pi, H. J., and Lisman, J. E. (2008). Coupled phosphatase and kinase switches produce the tristability required for long-term potentiation and long-term depression. *J. Neurosci.* 28, 13132–13138.

Qi, Z., Miller, G. W., and Voit, E. O. (2010). The internal state of medium spiny neurons varies in response to different input signals. *BMC Syst. Biol.* 4, 26.

Rackham, O. J. L., Tsaneva-Atanasova, K., Ganesh, A., and Mellor, J. R. (2010). A Ca^{2+}-based computational model for NMDA receptor-dependent synaptic plasticity at individual post-synaptic spines in the hippocampus. *Front. Syn. Neurosci.* 2:31. doi: 10.3389/fnsyn.2010.00031

Rubin, J. E., Gerkin, R. C., Bi, G.-Q., and Chow, C. C. (2005). Calcium time course as a signal for spike-timing-dependent plasticity. *J. Neurophysiol.* 93, 2600–2613.

Saftenku, E. E. (2002). A simplified model of long-term plasticity in cerebellar

mossy fiber-granule cell synapses. *Neurophysiology* 34, 216–218.

Santamaria, F., Gonzalez, J., Augustine, G. J., and Raghavachari, S. (2010). Quantifying the effects of elastic collisions and non-covalent binding on glutamate receptor trafficking in the post-synaptic density. *PLoS Comput. Biol.* 6, e1000780. doi: 10.1371/journal.pcbi.1000780

Santos, S. D., Carvalho, A. L., Caldeira, M. V., and Duarte, C. B. (2009). Regulation of AMPA receptors and synaptic plasticity. *Neuroscience* 158, 105–125.

Santucci, D. M., and Raghavachari, S. (2008). The effects of NR2 subunit-dependent NMDA receptor kinetics on synaptic transmission and CaMKII activation. *PLoS Comput. Biol.* 4, e1000208. doi: 10.1371/journal.pcbi.1000208

Saudargiene, A., Porr, B., and Wörgötter, F. (2005). Synaptic modifications depend on synapse location and activity: a biophysical model of STDP. *Biosystems* 79, 3–10.

Schaff, J., Fink, C. C., Slepchenko, B., Carson, J. H., and Loew, L. M. (1997). A general computational framework for modeling cellular structure and function. *Biophys. J.* 73, 1135–1146.

Schiegg, A., Gerstner, W., Ritz, R., and van Hemmen, J. L. (1995). Intracellular Ca^{2+} stores can account for the time course of LTP induction: a model of Ca^{2+} dynamics in dendritic spines. *J. Neurophysiol.* 74, 1046–1055.

Schmidt, H., and Eilers, J. (2009). Spine neck geometry determines spino-dendritic cross-talk in the presence of mobile endogenous calcium binding proteins. *J. Comput. Neurosci.* 27, 229–243.

Schmidt, H., Kunerth, S., Wilms, C., Strotmann, R., and Eilers, J. (2007). Spino-dendritic cross-talk in rodent Purkinje neurons mediated by endogenous Ca^{2+}-binding proteins. *J. Physiol.* 581, 619–629.

Serrano, P., Yao, Y., and Sacktor, T. C. (2005). Persistent phosphorylation by protein kinase Mζ maintains late-phase long-term potentiation. *J. Neurosci.* 25, 1979–1984.

Shah, N. T., Yeung, L. C., Cooper, L. N., Cai, Y., and Shouval, H. Z. (2006). A biophysical basis for the inter-spike interaction of spike-timing-dependent plasticity. *Biol. Cybern.* 95, 113–121.

Shouval, H. Z., Bear, M. F., and Cooper, L. N. (2002a). A unified model of NMDA receptor-dependent bidirectional synaptic plasticity. *Proc. Natl. Acad. Sci. U.S.A.* 99, 10831–10836.

Shouval, H. Z., Castellani, G. C., Blais, B. S., Yeung, L. C., and Cooper, L. N. (2002b). Converging evidence for a simplified biophysical model of synaptic plasticity. *Biol. Cybern.* 87, 383–391.

Shouval, H. Z., and Kalantzis, G. (2005). Stochastic properties of synaptic transmission affect the shape of spike time-dependent plasticity curves. *J. Neurophysiol.* 93, 1069–1073.

Shouval, H. Z., Wang, S. S. H., and Wittenberg, G. M. (2010). Spike timing dependent plasticity: a consequence of more fundamental learning rules. *Front. Comput. Neurosci.* 4:19. doi: 10.3389/fncom.2010.00019

Sivakumaran, S., Hariharaputran, S., Mishra, J., and Bhalla, U. S. (2003). The Database of Quantitative Cellular Signaling: management and analysis of chemical kinetic models of signaling networks. *Bioinformatics* 19, 408–415.

Slepchenko, B. M., Schaff, J. C., Macara, I., and Loew, L. M. (2003). Quantitative cell biology with the Virtual Cell. *Trends Cell Biol.* 13, 570–576.

Smolen, P. (2007). A model of late long-term potentiation simulates aspects of memory maintenance. *PLoS ONE* 2, e445. doi: 10.1371/journal.pone.0000445

Smolen, P., Baxter, D. A., and Byrne, J. H. (2006). A model of the roles of essential kinases in the induction and expression of late long-term potentiation. *Biophys. J.* 90, 2760–2775.

Smolen, P., Baxter, D. A., and Byrne, J. H. (2008). Bistable MAP kinase activity: a plausible mechanism contributing to maintenance of late long-term potentiation. *Am. J. Physiol. Cell Physiol.* 294, C503–C515.

Smolen, P., Baxter, D. A., and Byrne, J. H. (2009). Interlinked dual-time feedback loops can enhance robustness to stochasticity and persistence of memory. *Phys. Rev. E* 79, 031902.

Soderling, T. R., and Derkach, V. A. (2000). Postsynaptic protein phosphorylation and LTP. *Trends Neurosci.* 23, 75–80.

Stefan, M. I., Edelstein, S. J., and Le Novère, N. (2008). An allosteric model of calmodulin explains differential activation of PP2B and CaMKII. *Proc. Natl. Acad. Sci. U.S.A.* 105, 10768–10773.

Steuber, V., and Willshaw, D. J. (2004). A biophysical model of synaptic delay learning and temporal pattern recognition in a cerebellar Purkinje cell. *J. Comput. Neurosci.* 17, 149–164.

Stiles, J. R., and Bartol, T. M. (2001). "Monte Carlo methods for simulating realistic synaptic microphysiology using MCell," in *Computational Neuroscience: Realistic Modeling for Experimentalists*, ed. E. De Schutter (Boca Raton: CRC Press), 87–127.

Sweatt, J. D. (1999). Toward a molecular explanation for long-term potentiation. *Learn. Mem.* 6, 399–416.

Tanaka, K., and Augustine, G. J. (2009). "Systems biology meets single-cell physiology: role of a positive-feedback signal transduction network in cerebellar long-term synaptic depression," in *Systems Biology: The Challenge of Complexity*, 1st Edn., eds S. Nakanishi, R. Kageyama, and D. Watanabe (Tokyo: Springer), 159–168.

Tanaka, K., Khiroug, L., Santamaria, F., Doi, T., Ogasawara, H., Ellis-Davies, G. C. R., Kawato, M., and Augustine, G. J. (2007). Ca^{2+} requirements for cerebellar long-term synaptic depression: role for a postsynaptic leaky integrator. *Neuron* 54, 787–800.

Tolle, D. P., and Le Novère, N. (2010a). Brownian diffusion of AMPA receptors is sufficient to explain fast onset of LTP. *BMC Syst. Biol.* 4, 25.

Tolle, D. P., and Le Novère, N. (2010b). Meredys, a multi-compartment reaction–diffusion simulator using multistate realistic molecular complexes. *BMC Syst. Biol.* 4, 24.

Tomita, M., Hashimoto, K., Takahashi, K., Shimizu, T. S., Matsuzaki, Y., Miyoshi, F., Saito, K., Tanida, S., Yugi, K., Venter, J. C., and Hutchison III, C. A. (1999). E-CELL: software environment for whole-cell simulation. *Bioinformatics* 15, 72–84.

Traub, R. D., Wong, R. K., Miles, R., and Michelson, H. (1991). A model of a CA3 hippocampal pyramidal neuron incorporating voltage-clamp data on intrinsic conductances. *J. Neurophysiol.* 66, 635–650.

Urakubo, H., Honda, M., Froemke, R. C., and Kuroda, S. (2008). Requirement of an allosteric kinetics of NMDA receptors for spike timing-dependent plasticity. *J. Neurosci.* 28, 3310–3323.

Urakubo, H., Honda, M., Tanaka, K., and Kuroda, S. (2009). Experimental and computational aspects of signaling mechanisms of spike-timing-dependent plasticity. *HFSP J.* 3, 240–254.

Volfovsky, N., Parnas, H., Segal, M., and Korkotian, E. (1999). Geometry of dendritic spines affects calcium dynamics in hippocampal neurons: theory and experiments. *J. Neurophysiol.* 82, 450–462.

Wang, H., Hu, Y., and Tsien, J. Z. (2006). Molecular and systems mechanisms of memory consolidation and storage. *Prog. Neurobiol.* 79, 123–135.

Wils, S., and De Schutter, E. (2009). STEPS: modeling and simulating complex reaction–diffusion systems with Python. *Front. Neuroinform.* 3:15. doi: 10.3389/neuro.11.015.2009

Woo, N. H., Duffy, S. N., Abel, T., and Nguyen, P. V. (2003). Temporal spacing of synaptic stimulation critically modulates the dependence of LTP on cyclic AMP-dependent protein kinase. *Hippocampus* 13, 293–300.

Wörgötter, F., and Porr, B. (2005). Temporal sequence learning, prediction, and control: a review of different models and their relation to biological mechanisms. *Neural Comput.* 17, 245–319.

Yang, K.-H., Hellgren Kotaleski, J., and Blackwell, K. T. (2001). The role of protein kinase C in the biochemical pathways of classical conditioning. *Neurocomputing* 38–40, 79–85.

Yeung, L. C., Shouval, H. Z., Blais, B. S., and Cooper, L. N. (2004). Synaptic homeostasis and input selectivity follow from a calcium-dependent plasticity model. *Proc. Natl. Acad. Sci. U.S.A.* 101, 14943–14948.

Yu, X., Shouval, H. Z., and Knierim, J. J. (2008). A biophysical model of synaptic plasticity and metaplasticity can account for the dynamics of the backward shift of hippocampal place fields. *J. Neurophysiol.* 100, 983–992.

Zador, A., Koch, C., and Brown, T. H. (1990). Biophysical model of a Hebbian synapse. *Proc. Natl. Acad. Sci. U.S.A.* 87, 6718–6722.

Zhabotinsky, A. M. (2000). Bistability in the Ca^{2+}/calmodulin-dependent protein kinase-phosphatase system. *Biophys. J.* 79, 2211–2221.

Zhabotinsky, A. M., Camp, R. N., Epstein, I. R., and Lisman, J. E. (2006). Role of the neurogranin concentrated in spines in the induction of long-term potentiation. *J. Neurosci.* 26, 7337–7347.

Zou, Q., and Destexhe, A. (2007). Kinetic models of spike-timing dependent plasticity and their functional consequences in detecting correlations. *Biol. Cybern.* 97, 81–97.

Conflict of Interest Statement: The authors declare that the research was conducted in the absence of any commercial or financial relationships that could be construed as a potential conflict of interest.

Received: 15 July 2010; paper pending published: 26 August 2010; accepted: 22 November 2010; published online: 13 December 2010.

*Citation: Manninen T, Hituri K, Hellgren Kotaleski J, Blackwell KT and Linne M-L (2010) Postsynaptic signal transduction models for long-term potentiation and depression. Front. Comput. Neurosci. **4**:152. doi: 10.3389/fncom.2010.00152*

Publication IV

Hituri, K., Achard, P., Wils, S., Linne, M.-L., De Schutter, E. (2008) Stochastic modeling of inositol-1,4,5-trisphosphate receptors in Purkinje cell spine. In Proceedings of 5^{th} International Workshop on Computational Systems Biology (WCSB08), Ahdesmäki, M., Strimmer, K., Radde, N., Rahnenführer, J., Klemm, K., Lähdemäki, H., Yli-Harja, O. (eds.), pp. 57–60, Leipzig, Germany.

STOCHASTIC MODELING OF INOSITOL-1,4,5-TRISPHOSPHATE RECEPTORS IN PURKINJE CELL SPINE

Katri Hituri[1], *Pablo Achard*[2], *Stefan Wils*[2,3], *Marja-Leena Linne*[1], *and Erik De Schutter*[2,3]

[1]Department of Signal Processing, Tampere University of Technology,
P.O. Box 553, FI-33101 Tampere, Finland
[2]Theoretical Neurobiology Laboratory, University of Antwerp, Belgium
[3]Computational Neuroscience Unit, Okinawa Institute of Science and Technology, Japan
katri.hituri@tut.fi

ABSTRACT

Transient rises in cytosolic calcium concentration play a crucial role in initiating long-term depression (LTD) of synaptic activity. Calcium release from endoplasmic reticulum is particularly important in LTD. In Purkinje cells, the release is mediated by inositol-1,4,5-trisphosphate (IP_3) receptors (IP_3Rs) that are highly expressed in dendritic spines. The small volume of spine and the small number of molecules involved increase stochasticity in biochemical processes. We studied the effects of stochasticity by comparing stochastic and deterministic simulations for two different IP_3R models. We found a significant difference between the responses when using small initial concentration of calcium or IP_3. Deterministic simulations of IP_3R activation do not produce realistic results under all conditions.

1. INTRODUCTION

Transient rises in the cytosolic Ca^{2+} concentration have an important functional role in neurons. In cerebellar Purkinje cell (PC) dendritic spines, they are essential for generation of LTD of synaptic strength [1, 2]. These temporary rises are due to Ca^{2+} entry from the extracellular space and Ca^{2+} release from intracellular stores such as endoplasmic reticulum (ER). In PC spines, IP_3Rs are responsible for the Ca^{2+} release from the ER and are relatively highly expressed.

Mathematical modeling is one of the important tools when trying to understand the complex behavior of proteins within networks and pathways. Several models have been proposed to describe the behavior of IP_3R (for a comprehensive review, see, for example, [3]). All the IP_3R models and simulations were deterministic until recent years. Deterministic models show the average behavior of the system, i.e. do not include any kind of randomness. However, when biochemical reactions occur in very small volumes, such as in dendritic spines, the number of molecules is low even with fairly large concentrations. The small number of molecules increases the possibility for stochastic effects in reactions. Both the randomness of molecular encounters and the fluctuations in the transitions between the conformational states of proteins become relevant. Given the small volume of the PC spine, it is of interest to test the stochastic nature of the system and to take the stochasticity into account to obtain biologically realistic simulations. Even though the deterministic approach is adequate in some cases, it fails to reflect the detailed nature of the biological system.

The aim of this work was to study the concentration levels at which the effects of stochasticity on the function of IP_3R can not be ignored. Among many mathematical models of IP_3R two recent ones were chosen as test cases. The models were implemented into two different software, GENESIS/Kinetikit [4, 5] for deterministic simulations and STEPS [6] for stochastic simulations, to perform two types of simulations, open probability simulations and dynamic simulations.

2. MATERIALS AND METHODS

2.1. IP_3R models

2.1.1. Model of Doi et al.

The IP_3R model of Doi et al.[7] was originally published as a part of a larger model for Ca^{2+} dynamics in the cerebellar PC spine and parameter values of this model were determined based on experimental data from Purkinje cells [7]. The model was originally implemented as deterministic. A schematic representation of the model is shown in Figure 1a.

All the reactions and their rate constants can be found in Supplemental material of the original article [7]. Briefly, in this model IP_3R needs to bind both IP_3 and Ca^{2+} to open and thus provide Ca^{2+} flux from ER lumen to cytosol. IP_3R has only one open state, RIC, in this model.

2.1.2. Model of Fraiman and Dawson

The IP_3R model of Fraiman and Dawson [8] (see Figure 1b) is the only model that has a Ca^{2+} binding site inside the ER in addition to the cytosolic binding sites found in other models. The parameter values used in this work can be found in Errata for the original article [8]. This model was originally simulated stochastically, as a Markov process.

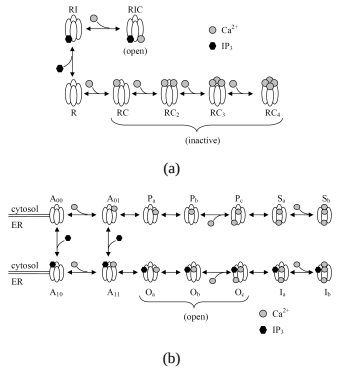

Figure 1. Schematic representation of the states and transitions of the IP_3R models. (a) Doi et al. (b) Fraiman and Dawson.

Originally, the six states, O_a, O_b, O_c, P_a, P_b, and P_c, are considered as open. However, IP_3R needs IP_3 to reach a stable open conformation [9, 10]. For this reason, three of the original open states were neglected in the present work and only states O_a, O_b, and O_c were considered as open. Also in the original article [8], the rate constant of the transition from A_{10} to A_{00} is defined as 'detailed balance'. We fixed the parameter by testing three values with deterministic open probability simulations (data not shown). Simulations were done as described in Section 2.3.1. The parameter values of 0 s^{-1} and 200 s^{-1} produced identical results while the value of 2000 s^{-1} slightly upraised the left side of the open probability curve. Based on these test simulations the value of 200 s^{-1} was chosen.

2.2. Simulation software

2.2.1. Genesis/Kinetikit

The GENESIS (GEneral NEural SImulation System) [4] simulation environment can be extended with Kinetikit [5] that is an extension for simulating reaction kinetics in well-mixed conditions. GENESIS/Kinetikit can be used to model and simulate the behavior of molecular networks and pathways. In this work, GENESIS version 2.2.1 for Cygwin and Kinetikit version 10 were used to obtain deterministic simulation results. Deterministic versions of the IP_3R models used are based on the law of mass action. The differential equation system was numerically solved (simulated) with the Exponential Euler method [4].

2.2.2. STEPS

STEPS (STochastic Engine for Pathway Simulation) [6] performs full stochastic simulation of reactions and diffusion of molecules in three dimensions. It extends the stochastic simulation algorithm (SSA) described by Gillespie [11]. In this work, STEPS developmental version 0.1.3 was used. Simulations were run both on a computer cluster and in a Cygwin environment on a standalone machine.

In the SSA, all reactions must be unidirectional. For this reason forward and backward parts of reversible reactions are defined as two separate reactions in the STEPS input file. In this early version of the software, the compartments of the modeled system are geometrically modeled as cubic shapes that are then discretized into small voxels. It is possible to define walls or surfaces between voxels that belong to different compartments. This enables modeling of surface bound molecules, such as ion channels, in their natural location.

2.3. Simulations

2.3.1. Open probability simulations

It has been experimentally shown that the open probability of IP_3R is dependent on the cytosolic Ca^{2+} concentration ($[Ca^{2+}]$) [12]. This dependence is bell-shaped with logarithmic x-axis. Originally, both models were built to reproduce this dependency.

In the deterministic open probability simulations, the behavior of a single IP_3R is simulated in an environment with constant $[Ca^{2+}]$ (several points, see Figure 2) and $[IP_3]$ (10 μM) until steady-state is achieved. The cytosol and also the ER had a volume of 0.1 μm^3 which is an experimentally defined average volume for PC spine cytosol [13]).

Deterministic simulations, using GENESIS/Kinetikit, were run for 5 or 15 s with a time step of 1 μs. The open probability of IP_3R was obtained at the end of simulation. In stochastic simulations with STEPS the models were simulated for 20 s using a sampling frequency of 0.1 s. In stochastic simulations the steady-state was achieved before 10 s time. For each initial Ca^{2+} concentration, 100 simulations were run with different seed values for the random number generator. The open probability was calculated as an average of the open IP_3Rs for the time interval 10-20 s over the 100 iterations.

2.3.2. Dynamic simulations

A cell is a constantly evolving dynamic system. It is therefore important to study the dynamic behavior of intracellular functions in addition to steady-state properties. In this work, we studied the cytosolic Ca^{2+} concentration as a function of time. In the dynamic simulations, the Ca^{2+} flux through the open IP_3R was modeled in addition to IP_3R state transitions. In GENESIS/Kinetikit, the flux is modeled using the *kchan* entity which describes a ligand-gated channel. The equation for flux behind *kchan* is not published, but it is known to depend on the concentration gradient over the membrane and the rate of the flux is controlled with a parameter defined by the user. In STEPS, the flux is also dependent on the concentration gradient. Based on test simulations (data not shown) the equations for the flux are almost identical in GENESIS/Kinetikit and in STEPS.

Rate parameters of the flux were estimated for both simulators separately. It is estimated that 5400 Ca^{2+} ions go through open IP_3R during one opening and that the

Table 1. Initial conditions for dynamic simulations.

Species	Value
Number of IP_3Rs (naive state)	16
$[IP_3]$	0.1 μM, 0.2 μM, 0.5 μM, 1.0 μM, 5.0 μM
$[Ca^{2+}]_{cyt}$	0.01 μM, 0.05 μM, 0.1 μM, 0.2 μM, 0.5 μM, 1 μM
$[Ca^{2+}]_{ER}$	150 μM

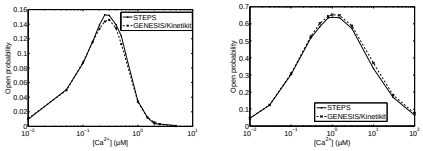

(a) (b)

Figure 2. Results of open probability simulations. (a) Doi et al. (b) Fraiman and Dawson.

mean open time of IP_3R is 3.7 ms in physiological conditions [14]. The estimated parameter values for flux functions were 595 (unit not known) for GENESIS/Kinetikit and $5.8{\cdot}10^8$ $M^{-1}s^{-1}$ for STEPS.

The compartments in these dynamic simulations had the same volume as in open probability simulations and the volumes were considered as well-mixed (i.e diffusion was not taken into account). The initial conditions used in dynamic simulations are given in Table 1. The average number of IP_3Rs in a PC spine has been estimated to be 16 (see Supplemental material of [7]). There are five different initial concentrations for IP_3 and six for cytosolic Ca^{2+}. All combinations of the initial concentrations were used in simulations. A deterministic simulation response and 100 stochastic simulation responses were obtained for each situation. Data analysis was done with MATLAB®.

3. RESULTS

3.1. Open probability simulations

The results from open probability simulations are presented in Figure 2. The open probability curves obtained from deterministic (GENESIS/Kinetikit) and stochastic simulations (STEPS) are consistent. This expected result shows that both models were correctly implemented in both simulation environments.

3.2. Dynamic simulations

To study the dynamic behavior of the two IP_3R models, cytosolic $[Ca^{2+}]$ was followed as a function of time. Examples of simulation results with both IP_3R models are shown in Figure 3. The 100 individual stochastic iterations are shown as thin gray curves, their mean as thick solid curve, and the deterministic curve as dashed line for comparison. The variation in stochastic simulations increases, i.e. the gray curves are more spread out, when initial $[IP_3]$ and $[Ca^{2+}]$ are decreased.

The data was examined in two ways. First, the maximum Ca^{2+} concentration reached during simulations was measured as a function of the initial $[IP_3]$ and initial cytosolic $[Ca^{2+}]$ (data not shown) for the deterministic and for the mean of the stochastic cases. Second, the time at which half of the maximum cytosolic Ca^{2+} concentration was reached was measured as a function of the initial $[IP_3]$ and initial cytosolic $[Ca^{2+}]$. This is a convenient way to compare the curve slopes at the steepest region.

The maximum cytosolic Ca^{2+} concentration attained in the deterministic simulations with both models is dependent only on initial $[IP_3]$, not on initial $[Ca^{2+}]$. The latter might be due to the quick response to the rising $[Ca^{2+}]$. $[Ca^{2+}]$ rises when the channel opens and so the initial concentration does not have much influence on the maximum concentration. In the stochastic simulations, the results are similar to the deterministic ones above initial cytosolic $[Ca^{2+}]$ of 0.1 μM. Below this concentration value, the maximum $[Ca^{2+}]$ might be also dependent on the initial $[Ca^{2+}]$. This concentration threshold is identical for both models.

The time at which half of the maximum cytosolic Ca^{2+} concentration was reached is dependent on the initial $[IP_3]$ in deterministic and stochastic simulations. However, in the deterministic simulations, only a minor dependence on the initial $[Ca^{2+}]$ can be seen, whereas, in stochastic simulations, dependence on the initial $[Ca^{2+}]$ is more emphasized. In stochastic simulations, the dependence on both $[IP_3]$ and $[Ca^{2+}]$ is evidently seen. These results are consistent in both models.

To study the difference between deterministic and stochastic simulation results in times at which half of the maximum cytosolic Ca^{2+} concentration was reached the deterministic plots were subtracted from the stochastic plots for both models. The difference between stochastic and deterministic simulation results is shown in Figure 4. Furthermore, a threshold, below which the effect of stochasticity seems to be significant, can be determined from these plots. In the case of IP_3R model of the Doi et al. the thresholds for the initial $[IP_3]$ is around 1.0 μM and for the initial cytosolic $[Ca^{2+}]$ between 0.1 μM and 0.2 μM. In the case of the IP_3R model of Fraiman and Dawson the thresholds are slightly lower, namely 0.5 μM for $[IP_3]$ and 0.1 μM for $[Ca^{2+}]$. Our work implies that there is a difference when having 100 or less molecules. An important thing to notice is that the thresholds for $[Ca^{2+}]$ are close to the resting level of Ca^{2+} concentration, 70 ± 29 nM, if we apply results from hippocampal pyramidal neuron [15] to PC spines.

4. CONCLUSIONS

In this work, the importance of stochasticity in simulation of IP_3 receptor function was determined. The stochastic simulation algorithm gives more realistic results than the deterministic one because it takes random fluctuations

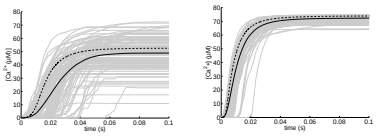

(a) (b)

Figure 3. Examples of dynamic simulations. Results from deterministic simulations (dashed) and the mean value (solid) of 100 stochastic simulations (thin gray) are shown. Initial concentrations: $[IP_3]$ = 0.2 μM, $[Ca^{2+}]$ = 0.1 μM. (a) Doi et al. (b) Fraiman and Dawson.

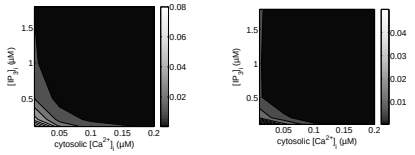

(a) (b)

Figure 4. Difference (gray scale) between deterministic and stochastic simulation results as a function of initial $[IP_3]$ and $[Ca^{2+}]$. (a) Doi et al. (b) Fraiman and Dawson.

into account. Based on dynamic simulation results of both models, we evaluated that there exists a threshold for initial IP_3 and cytosolic Ca^{2+} concentrations below which the effect can not be neglected. The threshold for Ca^{2+} concentration is close to the resting level of Ca^{2+} concentration in spines and thus it corresponds to the resting state of a spine before Ca^{2+} signals are induced. The present study strongly advocates for stochastic modeling and simulation of protein function.

5. ACKNOWLEDGMENTS

This work was supported by the Academy of Finland, project No. 213462 (Finnish Centre of Excellence program, 2006 - 2011). Tampere University of Technology Graduate school, Tampere Graduate school in Information Science and Engineering, and Finnish Cultural Foundation are acknowledged.

6. REFERENCES

[1] A. Konnerth, J. Dreessen, and G. J. Augustine, "Brief dendritic calcium signals initiate long-lasting synaptic depression in cerebellar Purkinje cells," *PNAS*, vol. 89, pp. 7051–7055, Aug 1992.

[2] M. Ito, "Cerebellar long-term depression: characterization, signal transduction, and functional roles," *Physiol. Rev.*, vol. 81, pp. 1143–1195, Jul 2001.

[3] J. Sneyd and M. Falcke, "Models of the inositol trisphosphate receptor," *Prog. Biophys. Mol. Biol.*, vol. 89, pp. 207–245, Nov 2005.

[4] J. M. Bower and D. Beeman, *The book of GENESIS: Exploring realistic neural models with the GEneral NEural SImulation System*, Springer-Verlag, New York, 1998.

[5] U. Bhalla, *Methods in Enzymology*, chapter Use of Kinetikit and GENESIS for modeling signaling pathways, pp. 3–23, Academic Press, New York, 2002.

[6] S. Wils and E. De Schutter, "STEPS: Stochastic simulation of reaction-diffusion in complex 3-D environment.," in *Abstract book of 15th Annual Meeting of the Organization for Computational Neurosciences CNS*2006*, Edinburgh, UK, July 2006.

[7] T. Doi, S. Kuroda, T. Michikawa, and M. Kawato, "Inositol 1,4,5-trisphosphate-dependent Ca^{2+} threshold dynamics detect spike timing in cerebellar Purkinje cells," *J. Neurosci.*, vol. 25, pp. 950–961, Jan 2005.

[8] D. Fraiman and S. P. Dawson, "A model of IP_3 receptor with a luminal calcium binding site: stochastic simulations and analysis," *Cell Calcium*, vol. 35, pp. 403–413, May 2004.

[9] J. S. Marchant and C. W. Taylor, "Cooperative activation of IP_3 receptors by sequential binding of IP_3 and Ca^{2+} safeguards against spontaneous activity," *Curr. Biol.*, vol. 7, pp. 510–518, Jul 1997.

[10] C. W. Taylor, P. C. da Fonseca, and E. P. Morris, "IP_3 receptors: the search for structure," *Trends Biochem. Sci.*, vol. 29, pp. 210–219, Apr 2004.

[11] D. T. Gillespie, "Exact stochastic simulation of coupled chemical reactions," *J. Phys. Chem.*, vol. 81, pp. 2340 – 2361, 1977.

[12] I. Bezprozvanny, J. Watras, and B. E. Ehrlich, "Bell-shaped calcium-response curves of Ins(1,4,5)P_3- and calcium-gated channels from endoplasmic reticulum of cerebellum," *Nature*, vol. 351, pp. 751–754, Jun 1991.

[13] K. M. Harris and J. K. Stevens, "Dendritic spines of rat cerebellar Purkinje cells: serial electron microscopy with reference to their biophysical characteristics," *J. Neurosci.*, vol. 8, pp. 4455–4469, Dec 1988.

[14] I. Bezprozvanny and B. E. Ehrlich, "Inositol (1,4,5)-trisphosphate ($InsP_3$)-gated Ca channels from cerebellum: conduction properties for divalent cations and regulation by intraluminal calcium," *J. Gen. Phys.*, vol. 104, pp. 821–856, Nov 1994.

[15] B. L. Sabatini, T. G. Oertner, and K. Svoboda, "The life cycle of Ca^{2+} ions in dendritic spines," *Neuron*, vol. 33, pp. 439–452, Jan 2002.

Publication V

Intosalmi J., Manninen T., Hituri K., Ruohonen K., and Linne M.-L. Modeling of IP_3 receptor function using stochastic approaches. In Proceedings of 5^{th} International Workshop on Computational Systems Biology (WCSB08), Ahdesmäki, M., Strimmer, K., Radde, N., Rahnenführer, J., Klemm, K., Lähdemäki, H., Yli-Harja, O. (eds.), pp. 69–72, Leipzig, Germany.

MODELING IP_3 RECEPTOR FUNCTION USING STOCHASTIC APPROACHES

Jukka Intosalmi[1,2], Tiina Manninen[1,2], Katri Hituri[2], Keijo Ruohonen[1], and Marja-Leena Linne[2]

[1]Department of Mathematics, Tampere University of Technology,
[2]Department of Signal Processing, Tampere University of Technology,
P.O. Box 553, FI-33101 Tampere, Finland
jukka.intosalmi@tut.fi

ABSTRACT

The time evolution of chemical systems is traditionally modeled using deterministic ordinary differential equations. Chemical reactions, however, are random in nature, and the deterministic approach is valid only for a restricted class of systems. Stochastic models take random fluctuations into account and are thus more realistic. In this work, we simulate an inositol trisphosphate receptor model using ordinary differential equations, stochastic differential equations, and the Gillespie stochastic simulation algorithm. The main goal of this work is to study the applicability of these methods for a system containing small numbers of molecules and ions. We concentrate especially on the SDE approach and investigate how well it models systems with small numbers of chemical species.

1. INTRODUCTION

Biochemical reactions can be modeled stochastically using numerous different methods [1, 2]. An ideal model would have the following three important properties. First, the model should be as realistic as possible, second, the mathematical method should be easily implementable as a computer algorithm, and third, the algorithm should be computationally effective. Some realistic modeling approaches can be derived directly from chemical kinetics without making any approximations. Such approaches are called exact. A good example of an exact modeling approach is the stochastic simulation algorithm (SSA) developed by Gillespie [3, 4]. The SSA is applicable when the molecular populations in the system are small, but it becomes computationally inefficient when the numbers of molecules increase [4].

In order to construct stochastic models that can be effectively simulated, new mathematical approaches have to be explored. As an approximate method also stochastic differential equations (SDEs) have been considered a promising way to model biochemical reactions stochastically [5]. The SDE approach is attractive especially if we consider a system for which the SSA is computationally inefficient and the traditional deterministic ordinary differential equation (ODE) approach cannot be used as a good approximation.

In this study, we simulate the inositol trisphosphate receptor (IP_3R) model containing small numbers of chemical species. The SSA is evidently the most efficient modeling approach in this case. However, our goal is rather to study the typical characteristics of different approaches. This kind of knowledge is extremely valuable when the modeling approaches are applied for larger systems.

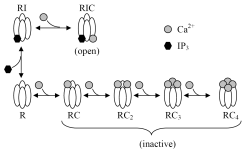

Figure 1. States and transitions of the IP_3R model.

2. SYSTEM AND METHODS

Several models have been proposed for the IP_3 receptor (for a review, see, e.g. [6]). In this study, we use the model of Doi et al. [7] which was originally published as a part of a larger model for calcium ion (Ca^{2+}) dynamics in the cerebellar Purkinje cell spine. The graphical illustration of the model is given in Figure 1. The transitions between the states are described by reversible chemical reactions of the form

$$\mathrm{A} + \mathrm{B} \underset{k_b}{\overset{k_f}{\rightleftharpoons}} \mathrm{C}, \tag{1}$$

where A, B, and C are chemical species, and k_f and k_b are *rate constants* for forward and backward reactions, respectively. The reactions of the model are given in Table 1. The rate constants of these reactions have been determined from experimental data [7]. The used volume of cytosol is $0.1\ \mu\mathrm{m}^3$. In the following, [X] denotes the concentration of species X.

The IP_3R model involves one open state (i.e. RIC). Once the IP_3R channel structure is open, Ca^{2+} flux from the endoplasmic reticulum (ER) to the cytosol starts. In this study, we model the Ca^{2+} flux using the differential equation

$$\begin{aligned} \frac{d[\mathrm{Ca}^{2+}]_{\mathrm{cyt}}}{dt} &= -\frac{d[\mathrm{Ca}^{2+}]_{\mathrm{ER}}}{dt} \\ &= k[\mathrm{RIC}]([\mathrm{Ca}^{2+}]_{\mathrm{ER}} - [\mathrm{Ca}^{2+}]_{\mathrm{cyt}}), \\ &\quad \text{when } [\mathrm{Ca}^{2+}]_{\mathrm{ER}} - [\mathrm{Ca}^{2+}]_{\mathrm{cyt}} > 0, \text{otherwise } 0, \end{aligned} \tag{2}$$

Table 1. Reversible reactions, reaction rates, and rate constants for the IP_3R model of Doi et al. [7]

	Reaction	Reaction rate	k_f	k_b
R_1	RI + Ca^{2+} $\underset{k_b^{R_1}}{\overset{k_f^{R_1}}{\rightleftharpoons}}$ RIC	$v_{R_1} = k_f^{R_1}[RI][Ca^{2+}]_{cyt} - k_b^{R_1}[RIC]$	$8 \times 10^9 \frac{1}{Ms}$	$2000 \frac{1}{s}$
R_2	R + IP_3 $\underset{k_b^{R_2}}{\overset{k_f^{R_2}}{\rightleftharpoons}}$ RI	$v_{R_2} = k_f^{R_2}[R][IP_3] - k_b^{R_2}[RI]$	$10^9 \frac{1}{Ms}$	$25800 \frac{1}{s}$
R_3	R + Ca^{2+} $\underset{k_b^{R_3}}{\overset{k_f^{R_3}}{\rightleftharpoons}}$ RC	$v_{R_3} = k_f^{R_3}[R][Ca^{2+}]_{cyt} - k_b^{R_3}[RC]$	$8.889 \times 10^6 \frac{1}{Ms}$	$5 \frac{1}{s}$
R_4	RC + Ca^{2+} $\underset{k_b^{R_4}}{\overset{k_f^{R_4}}{\rightleftharpoons}}$ RC_2	$v_{R_4} = k_f^{R_4}[RC][Ca^{2+}]_{cyt} - k_b^{R_4}[RC_2]$	$2 \times 10^7 \frac{1}{Ms}$	$10 \frac{1}{s}$
R_5	RC_2 + Ca^{2+} $\underset{k_b^{R_5}}{\overset{k_f^{R_5}}{\rightleftharpoons}}$ RC_3	$v_{R_5} = k_f^{R_5}[RC_2][Ca^{2+}]_{cyt} - k_b^{R_5}[RC_3]$	$4 \times 10^7 \frac{1}{Ms}$	$15 \frac{1}{s}$
R_6	RC_3 + Ca^{2+} $\underset{k_b^{R_6}}{\overset{k_f^{R_6}}{\rightleftharpoons}}$ RC_4	$v_{R_6} = k_f^{R_6}[RC_3][Ca^{2+}]_{cyt} - k_b^{R_6}[RC_4]$	$6 \times 10^7 \frac{1}{Ms}$	$20 \frac{1}{s}$

where k is rate parameter, [RIC] is the concentration of open channels, and Ca^{2+} denotes calcium ions passing through the open channel. For k, we use the value $5.8 \times 10^8 \frac{1}{Ms}$, and the initial value for $[Ca^{2+}]_{ER}$ is 150 μM (cf. [8]).

2.1. Ordinary differential equation modeling

A set of chemical reactions can be modeled deterministically using the law of mass action and ODEs. According to the law of mass action, we can determine the *reaction rate* v of the reaction in Equation 1 by means of the equation

$$v = -\frac{d[A]}{dt} = -\frac{d[B]}{dt} = \frac{d[C]}{dt} = k_f[A][B] - k_b[C]. \quad (3)$$

If we consider a system of n species X_i, $i = 1, \ldots, n$, and m reactions R_j, $j = 1, \ldots, m$, the time evolution of the ith species is described by the equation

$$\frac{d[X_i]}{dt} = \sum_{j=1}^{m} s_{ij} v_j, \quad (4)$$

where s_{ij} is the stoichiometric coefficient and v_j is the reaction rate of the jth reaction. The stoichiometric coefficient $s_{ij} \in \mathbb{Z}$ describes how many molecules of a certain kind are involved in a certain reaction. It is positive if the amount of the molecule is increasing, negative if the amount is decreasing, and 0, if the amount is not changing in the reaction.

We now have a set of coupled ordinary differential equations that can be written in the form

$$\frac{d\mathbf{X}(t)}{dt} = \mathbf{S}\mathbf{v}(\mathbf{K}, \mathbf{X}(t)), \quad (5)$$

where $\mathbf{X}(t) : [0, \infty) \longrightarrow \mathbb{R}^n$ consists of the concentrations of the chemical species $X_i, i = 1, \ldots, n$, $\mathbf{v}(\mathbf{K}, \mathbf{X}) : \mathbb{R}^n \longrightarrow \mathbb{R}^m$ describes the reaction rates, $\mathbf{S} \in \mathbb{R}^{n \times m}$ is the stoichiometric matrix including the stoichiometric constants, and $\mathbf{K}$ is a vector including the rate constants.

2.2. Stochastic differential equation modeling

SDE modeling is based on the theory of stochastic integration. If we consider the n-dimensional deterministic ODE model introduced in Subsection 2.1, we can obtain an SDE model by incorporating an Itô integrable stochastic term in Equation 5. As a result, we have the equation

$$d\mathbf{X}(t) = \mathbf{S}\mathbf{v}(\mathbf{K}, \mathbf{X}(t))dt + \mathbf{S}\mathbf{P}\mathbf{V}(\mathbf{X}(t))d\mathbf{B}(t), \quad (6)$$

where $\mathbf{B}(t) \sim N(\mathbf{0}, t\mathbf{I})$ is the m-dimensional Brownian motion, $\mathbf{P} \in \mathbb{R}^{m \times m}$ is a diagonal matrix describing the parameters, $\mathbf{V} : \mathbb{R}^n \longrightarrow \mathbb{R}^{m \times m}$ is a diagonal matrix including reaction rates without rate constants, and $\mathbf{X}, \mathbf{S}$, and $\mathbf{v}$ are as in the ODE model described by Equation 5 [5]. If we want to incorporate randomness in each reaction rate constant separately, we just consider one reversible reaction as two separate non-reversible reactions and use the same technique as described above.

Equation 6, describing a stochastic process, can also be written in the form

$$\mathbf{X}(t) = \mathbf{X}_0 + \int_0^t \mathbf{S}\mathbf{v}ds + \int_0^t \mathbf{S}\mathbf{P}\mathbf{V}d\mathbf{B}(s), \quad (7)$$

where $\mathbf{X}_0$ is the initial state, the first integral is the Riemann integral, and the second integral is the Itô integral [9]. The expected value and the variance of this process are usually difficult to solve. Simulation studies are thus needed. Parameters included in $\mathbf{P}$ should be estimated using some estimation algorithm.

2.3. Stochastic simulation algorithm

The stochastic simulation algorithm (SSA) is a Monte Carlo procedure, which is used to generate numerically the time evolution of a chemically reacting system [3]. It treats chemical species discretely and simulates every reaction one at a time [3, 4]. In the following, the basic idea of the SSA is presented.

Let us consider the system of n species and m reactions introduced earlier in Subsections 2.1 and 2.2, and let $\mathbf{X}(t) : [0, \infty) \longrightarrow \mathbb{Z}^n$ be a vector containing the numbers of molecules of each species at time t. Each reaction R_j, $j = 1, \ldots, m$, in the system can be characterized by a *propensity function* $a_j(\mathbf{X})$ which depends on the current state of the system. A *state change vector* $\mathbf{v}_j \in \mathbb{Z}^n$ describes the stoichiometry of the reaction R_j. In the simulation algorithm, the propensity functions are used for determining the distributions of the next reaction to happen (j) and the time to the next reaction (τ). These distributions are then sampled and the state of the system is updated by state change vector. The SSA consists of the following steps:

1. Initialize the time $t = t_0$ and the state of the system $\mathbf{X}(t) = \mathbf{X}_0$.
2. Evaluate $a_j(\mathbf{X}(t)), j = 1, \ldots, m$, and $a_0(\mathbf{X}(t)) = \sum_{k=1}^{m} a_k(\mathbf{X}(t))$.
3. Generate two uniformly distributed random variables r_1 and r_2 and take $\tau = (1/a_0(\mathbf{X}(t))) \ln(1/r_1)$ and j such that $\sum_{k=1}^{j-1} a_k(\mathbf{X}(t)) < r_2 a_0(\mathbf{X}(t)) \leq \sum_{k=1}^{j} a_k(\mathbf{X}(t))$.
4. Replace $\mathbf{X}(t + \tau) = \mathbf{X}(t) + \mathbf{v}_j$ and $t = t + \tau$.
5. Return to step 2 or end the simulation.

3. RESULTS

We simulate the IP_3R model using ODEs, SDEs, and the SSA. All simulatios are run in MATLAB®. The Ca^{2+} flux described by Equation 2 is modeled simply as a part of the set of differential equations in the ODE and SDE implementations. In the SSA simulations, the flux is described as a forward reaction for which the propensity function is determined by the number of open channels and by the number of Ca^{2+} ions in the cytosol and ER.

3.1. ODE and SSA

When modeling biochemical systems, the selection of the model plays an important role. The model should describe the natural phenomenon as rigorously as possible, but ignore the details that are not essential for system level behavior. After a proper model has been selected, the next step is to choose the formalism to describe the model and find out how to implement the model as an algorithm.

Previous computational studies considering the IP_3R model show that the traditional ODE approach provides us with a satisfactory approximation only in the case in which the concentrations are relatively large (see e.g. [8]). When the numbers of chemical species are small, the relative amount of random fluctuations in the system is greater. In this case, we have to use modeling methods that are capable of taking these fluctuations into account. In the following, we concentrate on the cases in which stochastic methods are needed.

When the IP_3R model is simulated stochastically using the SSA, the results differ notably from the results of the ODE simulations (Figure 2(a)). The main reason for this is that the SSA simulation quite often leads to a closed receptor state. This means that there is no open channel for Ca^{2+} flux from the ER and thus the number of Ca^{2+} ions in the cytosol does not increase. The SSA simulations also support the intuitive assumption that the two reactions leading to the open state of the receptor are the most essential when the stochastic nature of the model is concerned.

It is clear that the SSA is the most efficient approach when it comes to computational time if the numbers of chemical species are small. However, it is also useful to study approximative methods in order to learn about their properties and behavior. It is clear that many continuous time approximations of the SSA cannot be applied. For example, the use of the chemical Langevin equation (CLE) requires certain conditions to be fulfilled [4]. First, several reactions must occur during one time step, and second, the time step should be small enough. When we take a closer look at our SSA simulations, we observe that both of these conditions cannot be satisfied at the same time.

3.2. SDE

In biological systems, the concentrations of chemical species are often very small and the SDE modeling is thus challenging. The possibility of negative concentrations and the risk of an unstable model are always present. This means that although the model would be mathematically correct, it might not be biologically realistic. Therefore, the type of the SDE model, the model parameters, and the numerical method for solving the SDE have to be chosen carefully.

The SDE models tested in this study are built on the basis of the results obtained from the SSA simulations. As mentioned already in Subsection 3.1, the two reactions leading to the open state of the IP_3 receptor (R_1 and R_2 in Table 1) are the most significant when we study the Ca^{2+} levels in the system. When the SDE model is tuned so that randomness is incorporated only in these two reactions, the model is incabable of producing similar results as the SSA. The problem is that in order to avoid negative concentrations, we have to adjust the model parameters and the time step so that variance in the rate constants is very small. Thus, the system is always driven towards the open state and consequently the Ca^{2+} concentration in the cytosol increases. The same result is obtained if randomness is incorporated in all rate constants.

In addition to the two reactions leading to the open state, also the Ca^{2+} flux has an essential role in the model. When the whole model is constructed using the SDE, we are able to allow a greater variance of the fluctuations in the rate parameter of the flux. The drawback of this approach is that random fluctuations in the flux overpower the fluctuations in the other rate constants. This shows that the same results can be obtained using an SDE model in which randomness is incorporated only in the flux.

In order to illustrate the results, we show in Figure 2(a) the sample mean of $[Ca^{2+}]$ from thousand SSA and SDE model (randomness only in the flux) runs, and the deterministic ODE model response. In the simulations, the initial concentrations for Ca^{2+}, IP_3, and R were 0.05

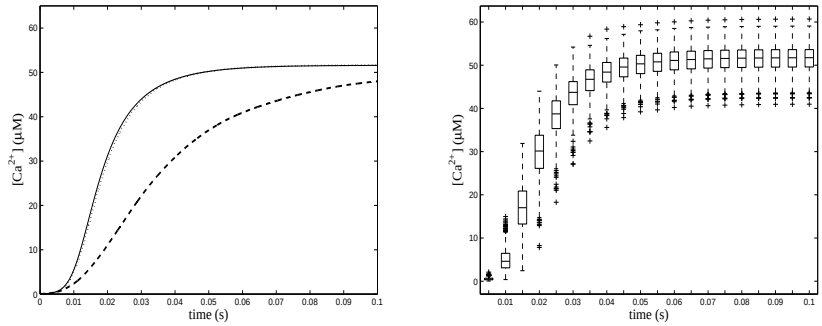

(a) Sample mean of Ca^{2+} concentration.

(b) Boxplot illustration of the distribution of SDE paths.

Figure 2. (a) Sample mean of Ca^{2+} concentration in IP_3R model simulated with SDE ($\cdots$) and SSA ($--$), and deterministic response of the ODE (—). (b) Boxplot illustration of the distribution of SDE paths.

μM, 0.2 μM, and 0.2657 μM, respectively. Other initial concentrations were equal to zero. We see clearly that the SSA differs from the deterministic response, whereas the SDE model converges to it. Figure 2(b) illustrates the distribution of the solution of the SDE model. Similar analysis for the SSA reveals the great variance of the SSA paths (not shown). The deterministic response is solved numerically using the Euler method with time step 2×10^{-6} s and the SDE model is simulated using the Euler-Maruyama method with the same time step.

4. CONCLUSION

In this study, three approaches to the modeling of chemically reacting systems are introduced. The modeling approaches, namely the deterministic differential equation modeling, stochastic differential equation modeling, and the stochastic simulation algorithm, are then applied in the modeling of an IP_3 receptor model. The simulations show that when the numbers of molecules in the system are small, realistic results can be obtained only using stochastic modeling approaches. In addition, it is concluded that stochastic differential equation modeling might lead to an unstable model when the numbers of molecules are small.

5. ACKNOWLEDGMENTS

This work was supported by the Academy of Finland, project nos 213462 (Finnish Programme for Centres of Excellence in Research 2006-2011), 106030, and 124615, as well as Tampere Graduate School in Information Science and Engineering (TISE) and Tampere University of Technology Graduate School.

6. REFERENCES

[1] T. E. Turner, S. Schnell, and K. Burrage, "Stochastic approaches for modelling in vivo reactions," *Comput. Biol. Chem.*, vol. 28, pp. 165–178, 2004.

[2] T. Manninen, *Stochastic methods for modeling intracellular signaling*, Ph.D. thesis, Department of Science and Engineering, Tampere University of Technology, Tampere, Finland, 2007.

[3] D. T. Gillespie, "A general method for numerically simulating the stochastic time evolution of coupled chemical reactions," *J. Comput. Phys.*, vol. 22, no. 4, pp. 403–434, 1976.

[4] D. T. Gillespie, "Stochastic chemical kinetics," in *Handbook of Materials Modeling*, S. Yip, Ed., pp. 1735–1752. Springer, Dordrecht, 2005.

[5] T. Manninen, M.-L. Linne, and K. Ruohonen, "Developing Itô stochastic differential equation models for neuronal signal transduction pathways," *Comput. Biol. Chem.*, vol. 30, no. 4, pp. 280–291, 2006.

[6] J. Sneyd and M. Falcke, "Models of the inositol trisphosphate receptor," *Prog. Biophys. Mol. Biol.*, vol. 89, pp. 207–245, 2005.

[7] T. Doi, S. Kuroda, T. Michikawa, and M. Kawato, "Inositol 1,4,5-trisphosphate-dependent Ca^{2+} threshold dynamics detect spike timing in cerebellar Purkinje cells," *J. Neurosci.*, vol. 25, no. 4, pp. 950–961, 2005.

[8] K. Hituri, "Simulation of IP_3 receptor function in cerebellar Purkinje cell dendritic spine: Importance of stochasticity," M.S. thesis, Faculty of Medicine, Institute of Medical Technology, University of Tampere, Tampere, Finland, 2007.

[9] B. Øksendal, *Stochastic Differential Equations: an Introduction with Applications*, Springer-Verlag, Berlin, 6th edition, 2007.

Publication VI

Mäkiraatikka E., Manninen T., Saarinen A., Ylipää A., Teppola H., Hituri K., Pettinen A., Yli-Harja O., and Linne M.-L. (2007) Stochastic simulation tools for cell signaling: Survey, evaluation and quantitative analysis. Proceedings of the 2^{nd} Conference on the Foundations of Systems Biology in Engineering (FOSBE2007), Allgöwer, F. and Reuss, M. (eds.), pp. 171–176, Stuttgart, Germany.

STOCHASTIC SIMULATION TOOLS FOR CELLULAR SIGNALING: SURVEY, EVALUATION AND QUANTITATIVE ANALYSIS

Eeva Mäkiraatikka *, **Tiina Manninen**, **Antti Saarinen**, **Antti Ylipää**, **Heidi Teppola**, **Katri Hituri**, **Antti Pettinen**, **Olli Yli-Harja**, **and Marja-Leena Linne** *

* *Corresponding authors, eeva.makiraatikka@tut.fi, marja-leena.linne@tut.fi*
Institute of Signal Processing, Tampere University of Technology, P.O. Box 553, FI-33101 Tampere, Finland

Abstract: Several stochastic simulation tools have been developed recently for studying cellular signaling systems. These systems consist of reactions involving minute quantities of molecules. Therefore, the dynamic time-series behavior of these signaling systems needs to be studied by stochastic means. We evaluate and compare simulation tools which utilize stochastic simulation algorithms. The current state of development in this area is then studied by simulation of a test case. As a test case we use gene expression/protein function hybrid model. The model describes the expression of the gene coding luciferase and the function of the enzyme. First, existing simulation tools are examined superficially. Then, freely downloadable stochastic simulation tools which support SBML, are chosen for closer evaluation. The results show that only few of the tools are capable of simulating the selected test case which is in SBML format. In addition, the usage of the tools varies in user-friendliness and applicability. This study will help cell and molecular biologists, as well as computer scientists, in using and developing stochastic simulation tools.

Keywords: Cellular signaling, Comparative evaluation, Gillespie stochastic simulation algorithm, Luciferase, SBML, Simulation tool

1. INTRODUCTION

To get an idea about the current state of development of simulation tools for cellular signaling we chose to trawl through the tools supporting SBML (Systems Biology Markup Language). Also to support the aims of our research group's interest (Manninen *et al.*, 2006*b*) we were interested in implementing a model which includes transcription of genes, translation of mRNA, and functionality of proteins. We implemented the model of our choice (described in Section 3) to a simulation tool and exported it to the SBML level 2 format. Then the resulting SBML file was imported to as many simulation tools as possible. With these tools we simulated the time-series behavior of the model species. Finally, the simulation results were compared to one another using a statistical method. To further verify the simulation results, we simulated the model with our own implementation of the Gillespie stochastic simulation algorithm (Gillespie, 1976; Gillespie, 1977) in MATLAB.

Table 1. Free tools supporting SBML and having stochastic simulation algorithm.

Toolname	Operating system	Web site address	References
BASIS	Linux	http://www.basis.ncl.ac.uk/	(Gillespie *et al.*, 2006)
BioNetGen	Linux/Windows/OSX	http://bionetgen.lanl.gov/	(Blinov *et al.*, 2004)
Bio-SPICE	Linux/Windows/OSX	http://biocomp.ece.utk.edu/	(Kumar and Feidler, 2003*b*) (Kumar and Feidler, 2003*a*) (Garvey *et al.*, 2003)
COPASI	Linux/Windows/OSX	http://www.copasi.org/tiki-index.php	(Hoops *et al.*, 2006)
Cyto-Sim	Linux/Windows/OSX	http://www.cosbi.eu/Rpty_Soft_CytoSim.php	(Cavaliere and Sedwards, 2006)
Dizzy	Linux/Windows	http://magnet.systemsbiology.net/software/Dizzy/	(Ramsey *et al.*, 2005)
E-CELL	Linux/Windows	http://www.e-cell.org/software/e-cell-system	(Tomita *et al.*, 1999)
Narrator	Linux/Windows	http://narrator-tool.org/	(Mandel *et al.*, 2004)
SmartCell	Linux/Windows/OSX	http://smartcell.embl.de/	(Ander *et al.*, 2004) (Elf and Ehrenberg, 2004)
StochKit	Unix	http://www.engineering.ucsb.edu/∼cse/StochKit/	(Cao *et al.*, 2005)
STOCKS	Linux/Windows	http://www.sysbio.pl/stocks/	(Kierzek, 2002)
XPPAUT	Linux/Windows/OSX	http://www.math.pitt.edu/∼bard/xpp/xpp.html	(Ermentrout, 2002)

In this study, we report the current status of the field of simulation tools for cellular signaling. We have tested simulation tools before (Pettinen *et al.*, 2005; Manninen *et al.*, 2006*a*), but the perspective has been very different.

We start by listing the most common stochastic simulation tools available. Simulation tools which were selected for the closer evaluation had to be freely downloadable. In addition, they had to support SBML and include the possibility for stochastic simulation using the Gillespie algorithm. Unfortunately, it was not possible to import the selected model in SBML format into all of the 12 tools mentioned in Table 1 and Fig. 1. We were able to simulate the model in only three simulation tools: Dizzy, Narrator, and XPPAUT. In addition, MATLAB implementation was used as a control.

Then we move on to enumerating properties of the tools we considered important for the end-user. Moreover, we concentrate on evaluating the tools from the user's perspective. This includes the ease of installation, general usability, instruction manual, comprehensiveness of properties, and user interfaces. The simulation results are also reported for each tool. This study will help cell and molecular biologists, as well as computer scientists, in using and developing stochastic simulation tools. We would like to remind the reader that this study is more like a guide for researchers who tend to run stochastic simulations rather than a comprehensive study. For more details about tools for kinetic modeling, see e.g. (Kim *et al.*, 2006; Alves *et al.*, 2006).

2. SIMULATION TOOLS

2.1 Tool selection

The tools listed on the SBML webpage *http://sbml.org/* are screened for the properties we choose as the selection criteria for this study. All freely downloadable tools with the support for the SBML format and Gillespie stochastic simulation algorithm are selected for further study. Even though there are numerous different simulation tools available, only few of them meet our criteria. More often than not, a simulation tool only partially supports SBML format. Moreover, certain tools do not support both level 1 and level 2 versions of the SBML format. [1]

It was found out that most of the tools are made for some specific case. We could not find a universal tool for several purposes. The selected stochastic simulation tools are listed in Table 1. A total of 12 tools (BASIS, BioNetGen, Bio-SPICE, COPASI, Cyto-Sim, Dizzy, E-CELL, Narrator, SmartCell, StochKit, STOCKS, XPPAUT) are selected. After a closer survey, we find out that out of 12 tools only 7 support both SBML import and export. Some of the most important properties from the user's perspective are shown in Fig. 1.

2.2 Benefits and drawbacks

Dizzy provides a collection of simulation algorithms for solving the time-series behavior of a dynamic system. Both stochastic and deterministic algorithms are available. The installation of Dizzy is straighforward and the syntax used to implement the model is very simple. As Dizzy imports only level 1 SBML, our model had to be modified manually. In case of a typo in the implementation, message about the error appears. The error messages in general were not informative enough. The user interface is clear and the use of the software is easy even for a beginner. In addition, a clear benefit for Dizzy is fast simulation. In comparison to Narrator, Dizzy is able to simulate the selected model hundred times faster.

[1] We would like to remind the reader that even though all the SBML constructs of level 1 can be mapped to level 2, the levels still remain distinct. A valid SBML level 1 document is not a valid SBML level 2 document and vice versa.

Toolname	SBML import	SBML export	Stand alone	Web application	Editable list of all parameters/initial conditions	Time-dependent input as an equation or as a file	Deterministic differential equation solver	Stochastic differential equation solver	Gillespie stochastic simulation algorithm	Sensitivity analysis	Parameter estimation	Commandline	GUI
BASIS	x	x		x				x	x			x	x
BioNetGen		x	x		x		x	x	x			x	x
Bio-SPICE	x	x	x				x		x	x	x		x
COPASI	x	x	x		x		x	x	x	x	x		x
Cyto-Sim		x		x				x	x				x
Dizzy	x	x	x		x	x	x	x	x				x
E-CELL	x	x	x		x	x	x	x	x			x	x
Narrator	x	x	x	x		x	x	x	x				x
SmartCell		x	x				x	x	x				x
StochKit	x		x						x			x	
STOCKS	x	x	x					x	x			x	
XPPAUT	x		x		x	x	x	x	x	x	x		x

Fig. 1. Comparing the properties of simulation tools for cellular signaling. SBML (Systems Biology Markup Language), GUI Graphical User Interface.

Narrator's installation and the import of the SBML level 2 model takes only a few minutes. The instruction manual includes the most important tasks the user has to complete to get started. A minor thing but worth mentioning is that the visualization of the imported model is poor. Unexperienced user gets confused about NaN simulation values. This problem is caused by the default time step which is too large for simulating our model deterministically. Although Narrator seemed at first to be the perfect tool for stochastic simulation, there also were problems. The way Narrator handles memory usage is poor. Our model can not be simulated for more than about 350,000 time points. Furthermore, consecutive simulation runs can not be done automatically.

XPPAUT provides an easy installation package for Windows. It is a multifunctional tool but it comes with the cost of inconsistency. Thus, the time it takes to understand how to use this tool is longer than with the tools that can only be used for simulation. A separate program for converting an SBML to XPPAUT format model can be found on the XPPAUT webpage. However, some changes needed to be made to the converter so that it worked. Furthermore, some parameters need to be added to the output file of the converter to make it compatible with the Gillespie stochastic simulation algorithm.

In general, there were various problems related to the model import and simulation. Next, we explain the problems that prevented us from using other tools than Dizzy, Narrator, and XPPAUT. Also we point out the benefits and drawbacks of the tools we were not able to use for some reason.

The installation of **E-CELL** was very easy to complete. However, the use of **E-CELL**, as well as **BASIS** and **STOCKS**, requires skills in computer science. The model import and simulation were not at all straightforward. E-CELL supports SBML import and export, but the graphical user interface designed to help the SBML import is not intuitive. The SBML file has to be imported using command line. This method is not suitable for simulation tools designed for biologists. Instead, the GUI should be fully functional. Despite the great effort, we were not able to run the simulations with the imported model in E-CELL. E-CELL uses the Gibson-Bruck stochastic algorithm (Gibson and Bruck, 2000) and, in this context, it is regarded as a variation of Gillespie stochastic simulation algorithm. The major drawback of **StochKit** due to our criteria is that it does not support SBML level 2 import. Further, for stochastic simulations all the chemical reactions in the model have to be irreversible. Although the model was implemented and exported with only irreversible reactions, **COPASI** mistook some of the reac-

tions for reversible and could not run stochastic simulation. Apparently the changes have to be made manually. The error messages in **BioSPICE** are not informative enough.

3. TEST CASE

Photon producing reactions have long been used to quantify reaction kinetics, e.g. the consumption of adenosine triphosphate (ATP) (see related reviews, e.g. (Schwiebert and Zsembery, 2003; Stanley, 1989)). If along with a product molecule a photon is produced, the amount of product molecules can easily be counted by counting the photons emitted. Usually in the reaction system there is only one reaction emitting light, so the photons can be counted with a light-sensitive apparatus such as luminometer or modified optical microscope. The measurement system is simple and easy to use.

In luminescent reactions light is produced by the oxidation of luciferin, i.e., chemical energy is converted to light energy. The phenomenon of light production in organisms is called bioluminescence. As most of the reactions in nature, bioluminescence is highly regulated and requires the presence of enzymes and cofactors (cations Ca^{2+}, Mg^{2+} and ATP). A generic name for enzymes commonly used in nature in bioluminescent reactions is luciferase.

In addition to our present work on evaluating simulation software, we try to achieve a better understanding in quantification of the following biological phenomena: I. Gene expression (binding of RNA polymerase, transcription, binding of ribosomes to ribosome binding sites (RBS), initiation of translation, elongation, termination of translation); II. The function of a transcription product (here luciferase enzyme); III. Calculation of emitted photons. Photons are byproducts of the reaction catalyzed by luciferase and emitted photons can be calculated. Furthermore gene expression can be evaluated quantitatively. With the model we aim to simulate the states I.-III. *in silico*.

Table 2. Initial values for the reactants of the model. The values are given as the number of molecules.

Reactant		Reactant	
AAs	0	E.P1	0
elRIB	0	E.Pin	0
ElRNAP	0	E.S1	0
nucleotides	0	E.S1.S2	0
Promoter	1	E.S1.S2in	0
E	0	E.S1in	0
PRNAP	0	E.S2	0
RBS	0	E.S2in	0
Ribosome	351	Ein	0
RibRBS	0	P	0
RNAP	35	hν	0
TrRNAP	0	S1(=ATP)	602214
AMP	0	S2(=LH2)	60221
E.P	0		

Table 3. Reactions and rate constants (k) of the model.

Reaction	k (1/s)
Promoter + RNAP → PRNAP	0.16605
PRNAP → Promoter + RNAP	10
PRNAP → TrRNAP	1.0
TrRNAP → RBS + Promoter + ElRNAP + RNAP	1.0
Ribosome + RBS → RibRBS	0.16605
RibRBS → Ribosome + RBS	2.25
RibRBS → elRIB + RBS	0.5
RBS → nucleotides	0.3
ElRNAP → nucleotides	0.3
elRIB → Ribosome + E	0.015
E → AAs	0.0001
E + S1 → E.S1	$3.32108 \cdot 10^{-5}$
E.S1 → E + S1	6
E.S1 + S2 → E.S1.S2	$1.66054 \cdot 10^{-3}$
E.S1.S2 → E.S1 + S2	10
E + S2 → E.S2	$1.66054 \cdot 10^{-3}$
E.S2 → E + S2	10
E.S2 + S1 → E.S1.S2	$3.32108 \cdot 10^{-5}$
E.S1.S2 → E.S2 + S1	6
E.S1.S2 → E.P1 + AMP	30
E.P1 → E.P + hν	10
E.P → P + E	0.1
P + E → E.P	$1.66054 \cdot 10^{-3}$
E.S1 → E.S1in	$2.6 \cdot 10^{-5}$
E → Ein	$2.6 \cdot 10^{-5}$
E.S2 → E.S2in	$2.6 \cdot 10^{-5}$
E.S1.S2 → E.S1.S2in	$2.6 \cdot 10^{-5}$
E.P → E.Pin	0.0003

The model we used to describe the production and emission of light is modified from the models introduced by two groups (Kierzek *et al.*, 2001; Brovko *et al.*, 1994). These models can be found from the DOQCS database *(http://doqcs.ncbs.res.in/)*. We combined the models into a model which includes transcription of genes, translation of mRNA, and functionality of a protein. It is assumed that a DNA promoter region, ribosomes, RNA polymerases, ATP, and luciferin molecules are present in quantities given in Table 2. The model describes the expression of the gene coding luciferase and the function of the enzyme. The initial number of molecules for reactants [2], reactions, and rate constants are listed in Tables 2 and 3. Rate constants are in units of 1/s since the simulations are run using the number of molecules.

[2] amino acid residues (AAs), ribosome elongating protein chain (elRIB), polymerase elongating mRNA (ElRNAP), promoter region in DNA (Promoter), product of the expression of the gene of interest is luciferase (E), promoter-polymerase complex (PRNAP), ribosome binding site (RBS), ribosome bound with RBS (RibRBS), RNA polymerase (RNAP), polymerase transcribing RNA (TrRNAP), adenosine monophosphate (AMP), product of enzyme reaction is oxyluciferin (P), photon (hν), ATP (S1), luciferin (S2)

4. SIMULATION RESULTS AND ANALYSIS

It is important that simulation tools produce similar results when simulating the same model. In this section we test the simulation of the model described above in four different simulation tools (i.e. Dizzy, MATLAB, Narrator, and XPPAUT). In the stochastic simulation framework one realization of the system is not enough to fully understand the dynamics of the model. Therefore, we simulate the model 20 times for 700 s in each of the selected simulation tools. The simulation time was limited due to Narrator's capabilities: in this simulation tool the model could not be simulated for more than about 700 s.

By doing so, we are able to get samples from the joint probability distribution describing the state of the system at the time point of 700 s. To continue, we test the similarity of these probability distributions by selecting three components (i.e. enzyme (E), product (P), and photon (hν)) to which we perform the Kolmogorov-Smirnov test for equal cumulative functions.

Table 4. Mean and standard deviation for samples from enzyme (E), product (P), and photon (hν) distributions at the time point of 700 s generated with different simulation tools.

	Dizzy	MATLAB	Narrator	XPPAUT
E_{mean}	1.35	1.90	2.05	2.35
P_{mean}	36686.00	37258.65	37267.90	37012.85
$h\nu_{mean}$	38724.75	39336.90	39351.10	39082.05
E_{std}	1.3	1.4	1.3	1.6
P_{std}	1184.5	1094.4	1182.1	836.5
$h\nu_{std}$	1274.3	1172.9	1240.2	871.0

Table 5. p-values from the Kolmogorov-Smirnov test. Four simulation tools are tested using three components of the system, i.e. enzyme (E), product (P), and photon (hν). In the table the upper value in each intersection is the p-value for the similarity of the distributions of P, the middle the p-value for the distribution of E, and lower the p-value for the distribution of hν.

	MATLAB	Narrator	XPPAUT	
Dizzy	0.2753	0.1349	0.4973	P
	0.2753	0.4973	0.2753	E
	0.2753	0.4973	0.2753	hν
MATLAB	1	0.9999	0.7710	P
	1	0.7710	0.2753	E
	1	0.4973	0.2753	hν
Narrator		1	0.9655	P
		1	0.4973	E
		1	0.4973	hν

Basic statistical characteristics of the samples are presented in Table 4. As there are on average only one or two enzyme molecules at the time point 700 s it is essential to simulate the model with stochastic simulation algorithm.

Table 5 presents the p-values obtained from the Kolmogorov-Smirnov test. Based on this testing, the simulation tools produce similar results at the selected time point. The lowest risk-level is obtained from the test where results for P are compared in Dizzy and in Narrator implementations. This level is, however, over 13% so it cannot be argued that the distributions have different cumulative functions.

5. CONCLUSIONS

The results show that only few tools are capable of simulating the selected test case. In addition, the usage of the tools varies greatly in user-friendliness and applicability. In this study we report the current state of the field of stochastic simulation tools. We selected tools that have SBML support, Gillespie stochastic simulation algorithm, and are freely downloadable. Further, we implemented a gene expression/protein function hybrid model. We also list properties of the tools we considered important for the user's perspective. The simulation results are similar based on the p-values obtained from the Kolmogorov-Smirnov test. As the outcome of the simulations does not differ between the simulation tools the user can freely select the tool according to the properties one wishes the simulation tool to have. Usually in the expence of user-friendliness one can also select the tool with multiple properties. This, of course, comes with the demand that the user has experience of computer science. We have informed the developers about some of the drawbacks in their tools. With this study we wish to contribute to developing better modeling and simulation tools for the use of both biologists and computer scientists.

6. ACKNOWLEDGEMENT

This work was supported by the Academy of Finland, No. 213462 (Finnish Programme for Centres of Excellence in Research 2006-2011), 104508, 106030, and 107694, Tampere University of Technology Graduate School, and Tampere Graduate School in Information Science and Engineering (TISE).

REFERENCES

Alves, R., F. Antunes and A. Salvador (2006). Tools for kinetic modeling of biochemical networks. *Nature Biotechnol.* **24**, 667–672.

Ander, M., P. Beltrao, B. Di Ventura, J. Ferkinghoff-Borg, M. Foglierini, A. Kaplan, C. Lemerle, I. Tomas-Oliveira and L. Serrano (2004). SmartCell, a framework

to simulate cellular processes that combines stochastic approximation with diffusion and localisation: analysis of simple networks. *Syst. Biol.* **1**, 129–138.

Blinov, M.L., J.R. Faeder, B. Goldstein and W.S. Hlavacek (2004). BioNetGen: software for rule-based modeling of signal transduction based on the interactions of molecular domains. *Bioinformatics* **20**, 3289–3291.

Brovko, L.Yu., O.A. Gandel'man, T.E. Polenova and N.N. Ugarova (1994). Kinetics of bioluminescence in the firefly luciferin-luciferase. *Biochem. (Moscow)* **59**, 195–201.

Cao, Y., A. Hall, H. Li, S. Lampoudi and L. Petzold (2005). User's guide for StochKit. *http://www.engineering.ucsb.edu/∼cse/StochKit/StochKitUserGuide.pdf*.

Cavaliere, M. and S. Sedwards (2006). Modelling cellular processes using membrane systems with peripheral and integral proteins. *Technical Report, The Microsoft Research - University of Trento Centre for Computational and Systems Biology. http://www.cosbi.eu/Rpty_Soft_CytoSim.php*.

Elf, J. and M. Ehrenberg (2004). Spontaneous separation of bi-stable biological systems into spatial domains of opposite phases. *Syst. Biol.* **2**, 230–236.

Ermentrout, B. (2002). *Simulating, Analyzing, and Animating Dynamical Systems: A Guide to XPPAUT for Researchers and Students*. Society for Industrial & Applied Mathematics (SIAM), Philadelphia, USA.

Garvey, T.D., P. Lincoln, C.J. Pedersen, D. Martin and M. Johnson (2003). BioSPICE: Access to the most current computational tools for biologists. *OMICS: A Journal of Integrative Biology* **7**, 411–420.

Gibson, M. A. and J. Bruck (2000). Efficient exact stochastic simulation of chemical systems with many species and many channels. *J. Phys. Chem. A* **104**, 1876–1889.

Gillespie, C.S., D.J. Wilkinson, D.P. Shanley, C.J. Proctor, R.J. Boys and T.B.L. Kirkwood (2006). BASIS: an internet resource for network modelling. *Journal of Integrative Bioinformatics* **3**, 2:26.

Gillespie, D. T. (1976). A general method for numerically simulating the stochastic time evolution of coupled chemical reactions. *J. Comput. Phys.* **22**, 403–434.

Gillespie, D. T. (1977). Exact stochastic simulation of coupled chemical reactions. *J. Phys. Chem.* **81**, 2340–2361.

Hoops, S., S. Sahle, R. Gauges, C. Lee, J. Pahle, N. Simus, M. Singhal, L. Xu, P. Mendes and U. Kummer (2006). COPASI - a complex pathway simulator. *Bioinformatics* **22**, 3067–3074.

Kierzek, A.M. (2002). STOCKS: STOChastic Kinetic Simulations of biochemical systems with Gillespie algorithm. *Bioinformatics* **18**, 470–481.

Kierzek, A.M., J. Zaim and P. Zielenkiewicz (2001). The effect of transcription and translation initiation frequencies on the stochastic fluctuations in procaryotic gene expression. *J. Biol. Chem.* **276**, 8165–8172.

Kim, J.S., H. Yun, H.U. Kim, H.S. Choi, T.Y. Kim, H.M. Woo and S.Y. Lee (2006). Resources for systems biology research. *J. Microbiol. Biotechnol.* **16**, 832–848.

Kumar, S.P. and J.C. Feidler (2003*a*). BioSPICE, 2: A computational infrastructure for integrative biology. *OMICS: A Journal of Integrative Biology* **7**, 335–335.

Kumar, S.P. and J.C. Feidler (2003*b*). BioSPICE: A computational infrastructure for integrative biology. *OMICS: A Journal of Integrative Biology* **7**, 225–226.

Mandel, J., N. Palfreyman, J. Lopez and W. Dubitzky (2004). Representing bioinformatics causality. *Briefings in Bioinformatics (Henry Stewart Publications)* **5**, 270–283.

Manninen, T., E. Mäkiraatikka, A. Ylipää, A. Pettinen, K. Leinonen and M.-L. Linne (2006*a*). Discrete stochastic simulation of cell signaling: comparison of computational tools. *Proceedings of the 28th Annual International Conference of the IEEE Engineering in Medicine and Biology Society, EMBC 2006, New York, USA* pp. 2013–2016.

Manninen, T., M.-L. Linne and K. Ruohonen (2006*b*). Developing Itô stochastic differential equation models for neuronal signal transduction pathways. *Comput. Biol. Chem.* **30**, 280–291.

Pettinen, A., T. Aho, O. Smolander, T. Manninen, A. Saarinen, K. Taattola, O. Yli-Harja and M.-L. Linne (2005). Simulation tools for biochemical networks: evaluation of performance and usability. *Bioinformatics* **21**, 357–363.

Ramsey, S., D. Orrell and H. Bolouri (2005). Dizzy: Stochastic simulation of large-scale genetic regulatory networks. *J. Bioinform. Comput. Biol.* **3**, 415–436.

Schwiebert, E.M. and A. Zsembery (2003). Extracellular ATP as a signaling molecule for epithelial cells. *Biochim Biophys Acta* **1615**, 7–32.

Stanley, P.E. (1989). A review of bioluminescent ATP techniques in rapid microbiology. *J. Biolumin. Chemilumin.* **4**, 375–380.

Tomita, M., K. Hashimoto and K. Takahashi (1999). E-CELL: software environment for whole-cell simulation. *Bioinformatics* **15**, 72–84.

Tampereen teknillinen yliopisto
PL 527
33101 Tampere

Tampere University of Technology
P.O.B. 527
FI-33101 Tampere, Finland

ISBN 978-952-15-3163-7
ISSN 1459-2045